A Thesis submitted for the degree of Doctor of Philosophy

Relativistic Coupled Cluster Theory – in Molecular Properties and in Electronic Structure

Avijit Shee

Université Toulouse III – Paul Sabatier

Contents

Acknowledgements

First and foremost, I would like to thank my supervisor Trond Saue. I would like to mention his help to settle me down in this very much 'french' country, will remember several nights of watching sports together, going for lunch among many other instances, in the non-scientific side. On the scientific side, I learnt from him what sort of theoretical rigour one should follow. Other than that his programming tips, even latex tips were very helpful.

Next I like to thank Debashis Mukherjee, with whom I started working in electronic structure theory back in Kolkata, India. Countless hours of discussion with him taught me very basic to very sophisticated aspects of that domain, and that teaching has not finished yet.

I like to thank Luuk Visscher to be a collaborator in the gradient project. Several Skype sessions with him was not only helpful in terms of technicalities, but also it gave me hope, confidence and enthusiasm to finish that project.

I like to thank Sangita Sen. We started working on a MRCC project together, which was successful on the one hand, but on the other it has not been exploited to its full capacity so far. Hopefully, there will be time to make the full use of that theory. Apart from that, several hours of 'inexperienced' scientific discussion with her helped me to gain a lot of experiences, taught me several things which are otherwise difficult to grasp.

From the DIRAC family I would like to thank specially Stefan Knecht, for his collaboration in one article and, Radovan Bast for technical advices and for his ideas about modern coding practice. Very friendly and lively atmosphere of our annual DIRAC meeting always makes me feel that science can also be a joyous experience. Fantastic people associated with it help to create that atmosphere. Thanks to all of them.

I will like to thank all the past and present members of the LCPQ group, specially to Adel and Nathaniel for their patience to help me in french language related sufferings.

Also, I like to thank the members of my previous group in IACS - Rahul Maitra, Debalina Sinha, Shubhrodeep Pathak, Avijit Sen, Pradipta Samanta, for giving me memories to cherish.

I will like to mention the names of few other scientists, short term work or discussions with whom were very enlightening - Daniel Crawford, Ed Valeev, Marcel Nooijen, Toru Shiozaki, Lan Cheng, Matthias Hanauer among few others.

Thanks to Ranajoy, Pratyay, Jishnu, Anjan, Vivek, Biplab, my friends back in India (though a few of them are living in abroad). Life always feels better around them.

Last but not the least I want to mention my younger brother, elder sister and my parents for their silent support and help. There are no words to thank them.

1. Introduction

"You see, we're in a funny position: It's not that we're looking for the theory, we've got the theory – a good, good candidate – but we're in the step in the science that we need to compare the theory to experiment by seeing what the consequences are and checking it. We're stuck in seeing what the consequences are, and it's my aim, it's my desire to see if I can work out a way to work out what the consequences of this theory are (LAUGHS). It's a kind of a crazy position to be in, to have a theory that you can't work out the consequences of ... I can't stand it, I have to figure it out. Someday, maybe. **Let George Do It***". ....Richard P. Feynman in 'The Pleasure of Finding Things Out'*

With the crowning success in explaining some enigmatic behaviour of heavy element chemistry [50], relativity made firm its foothold in electronic structure theory in the early 1980s. Nowadays it has widespread application, for instance, in the domain of lanthanide and actinide chemistry - for the studies of single molecule magnets, luminescent complexes etc. Lanthanide and actinide compounds normally consist of several open-shells, which is considered as a strong correlation problem. The effect of relativity and correlation is certainly not additive [77], and one needs to develop a correlation method within the framework of relativity (meaning based on the Dirac equation). But, the overwhelming computational cost of a relativistic correlation method precludes the routine use of them, which has made its application domain somewhat limited. It is therefore necessary not only to develop new methodology and computational techniques, but also to study the existing methodologies for the challenging problems. This thesis includes studies of such kind along with implementation and use of new methods.

In the first part of this thesis I will provide some background of relativistic electronic structure theory. I will mostly be focusing on the intricacies pertaining to the domains which are not really present in the non-relativistic version. Hamiltonians and different methodologies - starting from the mean field theory to the sophisticated most recent correlation theories will be touched upon. Thereby, one will be able to see the breadth and scope of this field. I will emphasize the theoretical details of the Coupled Cluster theory, since a large part of the discussions in this thesis will revolve around that method.

In the next chapter, I will first discuss why relativistic theories are so much more expensive and what measures had been undertaken to deal with that problem. Nonetheless, as already discussed, it is of paramount interest to study relativity and correlation together and we will get into the business of studying problems where both of them have major roles to play. We have studied the problem of heavy and superheavy rare gas dimers. This study has provided benchmark spectroscopic constants for these systems. Moreover, it has shown at least one example where the interplay between the Gaunt interaction and correlation can be very dramatic indeed. We have continued our study

of this effect on a different problem, namely the simulation of X-ray spectroscopy for actinides. As X-ray spectroscopy probes the core-region of a molecule, relativity has to be considered from the outset. Besides, one needs to carefully treat open-shells present in such problems since they lead to various physical effects e.g, Auger shifts and the Coester-Kronig effect. We have implemented Relativistic Single Reference Open Shell Møller-Plesset perturbation theory for this purpose.

Another important aspect of relativistic theories is that they provide the most natural framework for studying electromagnetic interactions, especially for magnetic properties.

In the second part of this thesis we will move into the discussion of molecular properties. In the first chapter of this part we will theoretically analyze the role of spin-orbit coupling in various molecular properties. This analysis helped us to conclude that Spin Orbit Coupling (SOC) has a great deal to do in both magnetic and electric properties. While in the case of magnetic properties the origin of the problem lies fundamentally in the nature of the interaction, for electric properties it hinges on the change of bonding behaviour with and without the consideration of spin-orbit coupling. In numerous situation SOC is not at all a perturbation, and then one should include SOC at the zeroth order of the Hamiltonian. The effect of Spin-Orbit coupling is ubiquitous in nature. Therefore various approximate ways of treating it has been tried over the years. But, very few of them really consider SOC at the variational level. In the present work our approach is to treat SOC at the variational level. Moreover, for the study of molecular properties a very accurate density of a particular state is necessary, which is possible to obtain only through a high accuracy correlation method. Coupled Cluster theory is known to provide the best accuracy with compromisable computational cost. Therefore, our effort has been to develop and implement the first coupled cluster analytic gradient code which incorporates SOC from the start.

The implementation of the Coupled Cluster theory requires a few words. Overwhelming success of this theory has driven people to implement this method with very sophisticated computer technology, modern algorithms etc. Apart from the efficiency aspect, the major thrust in those works has been to provide a sufficiently robust framework, where one can implement various realizations of the theory in different contexts. We have tried to build one such framework (where the efficiency issue has not been addressed so far), which will be discussed first in chapter 6 (principle) and then again in section 6.3 (details).

To show that this theory really meets our expectation about the accuracy of predicting molecular properties, we will demonstrate a few pilot applications. We have in this thesis studied electric field gradient of molecules at the nuclear position of the heavier atom, as well as the parity violation energy shift of chiral molecules.

At the very end, I have shown a work where core-spectroscopy was studied with multi-reference coupled cluster theory. Promising results of that work prompted us to extend it to the relativistic domain. Work in that direction is underway.

2. Publication List

1. A theoretical benchmark study of the spectroscopic constants of the very heavy rare gas dimers., A.Shee, S. Knecht and T. Saue. *Physical Chemistry Chemical Physics* ***17(16)****, 10978-10986 (2015).*

2. Theoretical X-ray Spectroscopy of the Actinides : study with UO_2^{2+}, UNO^{+1} and UN_2, C. South, A. Shee, A.K. Wilson and T. Saue *(manuscript).*

3. Analytic Gradient at the 4-component Relativistic Coupled Cluster Level with Inclusion of Spin-Orbit Coupling, A. Shee, L. Visscher, T. Saue *(manuscript prepared for J. Chem. Phys.)*

   An additional paper from my non-relativistic works.

4. A study of the ionisation and excitation energies of core electrons using a unitary group adapted state universal approach, S.Sen, A.Shee and D.Mukherjee, *Mol. Phys.* ***111****, 2477(2013).*
   We are working on the relativistic extension of it.

Part I.

Electronic Structure

3. Brief Overview of Relativistic Electronic Structure Theory

3.1. Relativistic Molecular Hamiltonian

The dynamics of a particle in quantum mechanics is represented by the time-dependent Schrödinger equation:

$$i\hbar\frac{\partial\psi(r,t)}{\partial t} = H\psi \tag{3.1}$$

which is understandable from the classical mechanical energy momentum relationship of a free particle: $E = \frac{p^2}{2m}$, with the heuristic replacement of E and p by the quantum mechanical operators $i\hbar\frac{\partial}{\partial t}$ and $-i\hbar\vec{\nabla}$.

However, in the relativistic case the energy momentum relationship is somewhat complicated

$$E^2 = p^2c^2 + m^2c^4, \tag{3.2}$$

meaning energy appears as a quadratic term. Naive replacement of E and p by the quantum mechanical operators as stated above will give us the equation:

$$-\hbar^2\frac{\partial^2\psi(r,t)}{\partial t^2} = (-\hbar^2c^2\nabla^2 + m^2c^4)\psi(r,t) \equiv H\psi(r,t), \tag{3.3}$$

which is quadratic in time derivative unlike the Schrödinger equation. By an attempt to maintain the linear time derivative form, Dirac reached the very famous equation:

$$i\hbar\frac{\partial\psi(r,t)}{\partial t} = (c\vec{\alpha}.\vec{p} + \beta mc^2)\psi(r,t) \tag{3.4}$$

with the introduction of the abstract quantities $\vec{\alpha}$ and β. They must obey certain relationships:

$$\alpha_i\alpha_j + \alpha_j\alpha_i = 2\delta_{ij}\mathbf{1} \tag{3.5}$$

$$\alpha_i\beta + \beta\alpha_i = 0 \tag{3.6}$$

$$\alpha_i^2 = \beta^2 = \mathbf{1} \tag{3.7}$$

It can be deduced that the explicit form of $\vec{\alpha}$ and β which satisfy all the above relationships are given by the following quantities:

$$\alpha_i = \begin{pmatrix} 0 & \sigma_i \\ \sigma_i & 0 \end{pmatrix}; \beta = \begin{pmatrix} 1 & 0 \\ 0 & -1 \end{pmatrix} \tag{3.8}$$

here, σ_is are the Pauli spin matrices. If we plug the wave function in Schrödinger picture : $\psi(r,t) = \psi(r)e^{-\frac{iEt}{\hbar}}$ to the Equation 3.4, we get

$$H_D\psi = E\psi. \tag{3.9}$$

In the above equation we have dropped the r dependence of the wave function. We will not carry this label from now on.

Expanding Equation 3.9 with the help of Equation 3.8 we get :

$$\begin{pmatrix} mc^2 & -c(\vec{\sigma}.\vec{p}) \\ -c(\vec{\sigma}.\vec{p}) & -mc^2 \end{pmatrix} \begin{pmatrix} \Psi^L \\ \Psi^S \end{pmatrix} = E \begin{pmatrix} \Psi^L \\ \Psi^S \end{pmatrix} \tag{3.10}$$

where we have written $\psi = \begin{pmatrix} \Psi^L \\ \Psi^S \end{pmatrix}$ on purpose, which will be clear in the following section.

The solutions of Equation 3.10 are given by:

$$E_\pm = \pm\sqrt{p^2 + mc^2} \equiv \pm E \tag{3.11}$$

$$\Psi^S = \frac{c(\vec{\sigma}.\vec{p})}{mc^2 \pm E}\Psi^L \tag{3.12}$$

We have got two solutions which differ only in the Ψ^S part through the explicit dependence on energy E. If we shift the energy scale by separating out the rest mass term: $E \to E' = E + mc^2$, we can see that for ψ_+, $\Psi^S \sim O(c^{-1})\Psi^L$ since $mc^2 \gg E'$. That justifies the label L as large and S as small for the ψ_+ branch of the solutions. However, for ψ_- the role of Ψ^L and Ψ^S are exactly reverse [1]. The total wave function of the particle will be the linear superposition of ψ_+ and ψ_-. The energy difference between these two branches is $\sim 2mc^2$. ψ_+ and ψ_- are called the positive-energy solution and the negative-energy solutions respectively. Here, we should look back and can see that we were aiming for a single particle wave function and we have ended up getting two solutions! Dirac interpreted the negative-energy solution as like having a filled vacuum state which prevents the transition of a particle from the positive-energy branch to the lower energy negative-energy one. That gives a stabilized description of the positive-energy branch. We can also notice that had the particle been boson type we could have filled in the energy states with arbitrary number of particles, leading to an infinitely stabilized vacuum, which does not make sense. However, for the fermions, fortunately

[1] The large and small nomenclature is a bit confusing. But, we identify ψ_+ as the electronic part of the solution and that is the important solution for our later discussion. Therefore, we will not be bothered much about the ψ_- and keep the same nomenclature.

enough the situation is different i.e, we can fill up each state by only one particle, which does not lead to infinite energy problem. This Dirac Hamiltonian constitutes the one-electronic part of our many-electron Hamiltonian.

In a molecule we consider the electrons moving in a clamped nuclei potential (the Born-Oppenheimer approximation). The effect of the external potential is accounted for by the principle of "minimal coupling" [25]:

$$\vec{p} \rightarrow \vec{p} - q\vec{A}; E \rightarrow E - q\phi. \tag{3.13}$$

By substituting electronic charge (q=-e) to the above equation we get

$$\vec{p} \rightarrow \vec{p} + e\vec{A}; E \rightarrow E + e\phi. \tag{3.14}$$

We will neglect the effect of internal magnetic moment of the nucleus since that contribution is very tiny ($O(c^{-2})$). This substitution completes the description of our one-electronic Hamiltonian:

$$H_{1-e} = c(\vec{\alpha}.\vec{p}) + \beta mc^2 + v \tag{3.15}$$

where, $v = -e\phi$.

Now we shall describe the two-electronic part of the Hamiltonian. The derivation of the Hamiltonian follows the same principle as above. The scalar and the vector potential for the electron-electron interaction are in Coulomb gauge expressed as

$$\phi(\vec{r}, t) = \int \frac{\rho(\vec{r'}, t)}{|r - r'|} d\tau' \tag{3.16}$$

$$\vec{A}(\vec{r}, t) = \frac{4\pi}{c^2} \int \frac{j_\perp(\vec{r'}, t_r)}{|r - r'|} d\tau'. \tag{3.17}$$

Here, we notice that the $\phi(\vec{r}, t)$ is equivalent to the instantaneous Coulomb interaction. On the other hand, for the vector potential we have a retarded time. Retarded time can be understood from a heuristic argument that, in electrodynamics source is also moving, therefore the signal which matters has been left at an earlier time, more precisely at $t_r = t - (r - r')/c$, where t is the present time. That means we need to know the position r' of the other electron at a retarded time. $j_\perp$ is the solenoidal or divergence free part of the current. In the quantum domain the description of two-electronic term requires full machinery of QED. Here we will use only two lowest order (order of $\frac{1}{c^2}$) terms :

$$H_{2-e}^{Coulomb} = \frac{I_4.I_4}{r_{ij}} \tag{3.18}$$

$$H_{2-e}^{Breit} = -\frac{e^2}{c^2}\{\frac{(c\alpha_i).(c\alpha_j)}{2r_{ij}} + \frac{(c\alpha_i r_{ij})(c\alpha_j r_{ij})}{2r_{ij}^3})\}. \tag{3.19}$$

With a little manipulation of the Breit term we get

$$H_{2-e}^{Gaunt} = -\frac{1}{c^2}\frac{(ec\alpha_i).(ec\alpha_j)}{r_{ij}} \tag{3.20}$$

which represents a current-current interaction. And,

$$H_{2-e}^{Gauge} = \frac{(ec\alpha_i.\vec{\nabla}_i)(ec\alpha_j.\vec{\nabla}_j)r_{ij}}{2c^2} \tag{3.21}$$

The most common choice is to use only the Coulomb term as the two-electronic part i.e, the zeroth-order term. The total Hamiltonian then is called the Dirac-Coulomb (DC) Hamiltonian. When the other terms are also included, we call them the Dirac-Coulomb-Gaunt (DCG) or the Dirac-Coulomb-Breit (DCB) accordingly. In the present work the DC Hamiltonian has been used predominantly.

3.1.1. Elimination of Spin

The molecular Hamiltonian we have discussed so far includes spin from the outset. In this section we will show how we can separate the Hamiltonian into an explicit spin-dependent and spin-independent part. This analysis is particularly important because it reveals various physical contributions "hidden" within the Dirac-Coulomb-Breit Hamiltonian. Moreover, this helps us to identify the order of appearance of various terms, thereby we can make systematic approximations about the inclusion of them. We will follow the approach as advocated by Dyall [17].

One Electronic Hamiltonian:

Before starting the derivation we will set the zero of energy to $+mc^2$, which amounts to replacing β in Equation 3.15 by $(\beta - 1_{4\times4})$. We align the relativistic and non-relativistic energy scale through this procedure. With this modification we rewrite Equation 3.15 as

$$v\psi^L + c(\vec{\sigma}.\vec{p})\psi^S = E\psi^L \tag{3.22}$$

$$c(\vec{\sigma}.\vec{p})\psi^L + (v - 2mc^2)\psi^S = E\psi^S. \tag{3.23}$$

From Equation 3.23 we get :

$$\psi^S = \frac{1}{2mc^2}\left(1 + \frac{E-v}{2mc^2}\right)^{-1} c(\vec{\sigma}.\vec{p})\psi^L. \tag{3.24}$$

From there we define a pseudo-large component (ϕ^L) as follows:

$$\psi^S = \frac{1}{2mc}\,(\vec{\sigma}.\vec{p})\,\phi^L. \tag{3.25}$$

In the non-relativistic limit the pseudo-large component is the large component for a positive-energy E and non-singular v (Equation 3.24).

Now, substitution of ψ^S from Equation 3.25 into Equation 3.22 and Equation 3.23, and premultiplying Equation 3.23 by $\frac{1}{2mc}(\vec{\sigma}.\vec{p})$ leads us to :

$$\left[\begin{pmatrix} v & \frac{p^2}{2m} \\ \frac{p^2}{2m} & \frac{1}{4m^2c^2}(\vec{p}v.\vec{p}) - \frac{p^2}{2m} \end{pmatrix} + \begin{pmatrix} O & O \\ O & \frac{1}{4m^2c^2} i\vec{\sigma}.(\vec{p}v \times \vec{p}) \end{pmatrix}\right] \begin{pmatrix} \Psi^L \\ \phi^L \end{pmatrix} = \begin{pmatrix} I & O \\ O & \frac{p^2}{4mc^2} \end{pmatrix} \begin{pmatrix} \Psi^L \\ \phi^L \end{pmatrix} \tag{3.26}$$

Equation 3.26 is called the modified Dirac Equation [17]. The Hamiltonian now is clearly separated into a spin-free and a spin-dependent term. We have not considered any approximation in deriving this equation. Therefore we will not miss out any contribution from the original Dirac equation by this dressing. The spin-dependent part obtained by the spin-separation has dependence on the external potential v. For the point nucleus v is given by $-\frac{Z}{r_i}$. With this substitution the spin-dependent term gives :

$$i\sigma.\vec{p}v \times \vec{p} = +\frac{2Z}{r_i^3} s_i.l_i \tag{3.27}$$

which we can identify as Spin-Orbit Coupling (SOC) contribution.

Two Electronic Hamiltonian

The spin-separation of the two-electronic part of the Hamiltonian is possible by carrying out the same analysis as above. Instead of showing the explicit derivation we will only mention all the terms involved in the Hamiltonian. For the derivation we will refer to the book by Dyall and Fægri [20]. The spin-free part of the two electronic Coulomb term gives the non-relativistic Coulomb type repulsion term and the Darwin term. The spin-dependent part gives a contribution of the following kind :

$$H_{2-el}^{sd,coul} = \vec{p_i}\frac{1}{r_{ij}}.\vec{p_i} + \hbar\Sigma_i.(\vec{\nabla}_i\frac{1}{r_{ij}}) \times \vec{p_i} \tag{3.28}$$

where,

$$\Sigma_i = \begin{pmatrix} \sigma_i & 0 \\ 0 & \sigma_i \end{pmatrix} \tag{3.29}$$

By using the relation

$$\vec{\nabla}_i\frac{1}{r_{ij}} = -\frac{\vec{r_i}}{r_{ij}} \tag{3.30}$$

to the second term of Equation 3.28

$$\hbar\Sigma_i.(\vec{\nabla}_i\frac{1}{r_{ij}}) \times \vec{p_i} = -\frac{2}{r_{ij}^3} s_i.l_{ij} \tag{3.31}$$

This term contains the information about the interaction of spin of electron i with its angular momentum generated due to the rotation around another electron j. This contribution is called the spin-same-orbit (SSO) interaction. It can further be shown by the

decomposition of the Gaunt term that there is another spin-orbit coupling contribution namely the spin-other-orbit (SOO) coupling.

In DIRAC [1], the use of quaternion algebra allows us to separate the spin-free part of the Hamiltonian very conveniently, just by considering the term associated with the real quaternion unit [81].

3.1.2. 4-component to 2-component

In chemistry we are mostly interested in the electronic part of the wave function, which consists of both positive-energy and negative-energy orbitals. It is therefore reasonable to think of eliminating the negative-energy from the positive-energy part to get an electron-only equation, for the majority of the chemical applications. This amounts to going from a 4-component picture to the 2-component one. This picture change is possible by block-diagonalizing the Hamiltonian into an upper and lower block. That has been tried in various ways, to name a few: the Foldy-Wouthuysen (FW) [23], the Douglas-Kroll-Hess (DKH) [16, 28, 27], the Barysz-Sadlej-Snijders [11] transformations, the Zeroth Order Regular Approximation (ZORA) [14, 72], the Infinite Order Two Component (IOTC) [31] approach etc. Fortunately consensus has been reached for one particular approach which goes by the name eXact two component (X2C) Hamiltonian. Here, we will schematically present all the steps involve in deriving the Hamiltonian:

1. Using a finite basis construct the one-electronic part of the Dirac Hamiltonian in matrix form.

2. Diagonalize that matrix by a unitary transformation matrix U:

$$U^\dagger h U = \begin{pmatrix} h^{++} & O \\ O & h^{--} \end{pmatrix} \tag{3.32}$$

3. The h^{++} block of Equation 3.32 is regarded as the X2C Hamiltonian. The eigenvector from above transformation is given by:

$$c' = U^\dagger \begin{pmatrix} c_L \\ c_S \end{pmatrix} = \begin{pmatrix} c^+ \\ c^- \end{pmatrix} \tag{3.33}$$

   The choice of U ensures that $c^- = 0$ therefore c^+ as the corresponding eigenvector of the X2C Hamiltonian.

If we now transform the two-electron part of the Hamiltonian (to be consistent with the usual notation, H_{2-e} will be called V, from now on) by the same U as obtained above we get:

$$(U(1) \otimes U(2))^\dagger V (U(1) \otimes U(2)) = \begin{pmatrix} \tilde{V}^{++}_{++} & \tilde{V}^{+-}_{++} & \tilde{V}^{-+}_{++} & \tilde{V}^{--}_{++} \\ \tilde{V}^{++}_{+-} & \tilde{V}^{+-}_{+-} & \tilde{V}^{-+}_{+-} & \tilde{V}^{--}_{+-} \\ \tilde{V}^{++}_{-+} & \tilde{V}^{+-}_{-+} & \tilde{V}^{-+}_{-+} & \tilde{V}^{--}_{-+} \\ \tilde{V}^{++}_{--} & \tilde{V}^{+-}_{--} & \tilde{V}^{-+}_{--} & \tilde{V}^{--}_{--} \end{pmatrix} \tag{3.34}$$

This matrix consists of complicated transformed terms. The calculation of all these terms is more expensive than the full-blown 4-component calculation. Therefore we will approximate the transformed 2-electron Hamiltonian as the $\tilde{V}_{++}^{++}$ block i.e, the (1,1) element from the above matrix. By neglecting the remaining terms we exclude the possibility of including the spin-same-orbit contribution in the DC Hamiltonian and additionally spin-other-orbit coupling contribution in the DCG Hamiltonian. Often the error is amended by the so-called AMFI [29, 61] approach, where we add the mean-field atomic contribution from the SOO and SSO terms at the second order DKH level to the Hamiltonian. However, the full picture change transformation has been tried also [46]. In an alternative approach proposed by Sikkema *et al.* [66] mean field one-electronic matrix i.e, the Fock matrix is diagonalized to get the decoupling transformation (U). Therefore the treatment of SSO and SOO coupling is exact at the mean-field level. Only the fluctuation potential part of the Hamiltonian remains untransformed. This Hamiltonian is called the X2C-molecular mean field (mmf) Hamiltonian. We have used this Hamiltonian in one of our works presented in the next section.

3.2. Relativistic Mean Field Theory

In the problems of many-body physics, the first approach in most of the cases is to consider that each particle is moving in an average or mean field of others. In non-relativistic molecular theory, this mean-field approach is the well-known Hartree-Fock (HF) method. That leads us to a single Slater determinant of indistinguishable fermions as a molecular wave function. When it was tried to adapt for relativistic theories (or many Dirac-particle problem), several challenges were faced in the early stage of development. Mostly because of the involvement of the negative-energy orbitals, it was very difficult to get a stable bound state solution. Through continuous effort of several groups most of the issues were settled down in early 1980s. It was needed to invoke new techniques for the construction of basis sets, to obtain numerical stability of the self consistent field equations etc. In this section I will describe briefly the very essentials of those developments, mostly pointing at the departures from the non-relativistic version. The relativistic HF method will be called the Dirac Hartree Fock (DHF) method.

A Dirac spinor is composed of the large and small components :

$$\Psi = \begin{pmatrix} \psi^L \\ \psi^S \end{pmatrix} \tag{3.35}$$

A Roothan type solution of the DHF equation requires suitable basis set expansion of the spinors ψ^L and ψ^S. Any arbitrary expansion of them usually results in "variational collapse". One has to obey the fact that they are related by the Dirac equation. A major breakthrough came when that has been considered approximately by the "kinetic balance" condition [67]. It is defined as : to reproduce correct kinetic energy for the positive-energy branch of the solution, in the non-relativistic limit, the small component bases has to be expressed in terms of the large component bases:

$$\chi^S = N(\vec{\sigma}.\vec{p})\chi^L \tag{3.36}$$

where, χ is the basis functions and N is the normalization constant. If the basis functions do not satisfy this condition, it can be shown that the error in the non-relativistic kinetic energy is of the order of $c^{(0)}$ [21].

The 2-spinor representation in Equation 3.35 therefore needs different expansion of the large and small components. They are clearly not the same as non-relativistic ones, they have to be separately optimized, also evaluation of integrals in terms of them is a separate task. Although there are attempts to devise basis sets along that line [55, 87], it is more practical to think of using standard non-relativistic scalar basis functions, so that one can utilize the advantage of previous developments in that domain. That leads to a 4-component expansion of the wave function:

$$\Psi = \begin{pmatrix} \psi^{L^\alpha} \\ \psi^{L^\beta} \\ \psi^{S^\alpha} \\ \psi^{S^\beta} \end{pmatrix} \tag{3.37}$$

where, both ψ^{L^α} and ψ^{L^β} are expanded in terms of standard non-relativistic basis functions, with different expansion coefficients. The choice of standard non-relativistic basis sets for the light to the medium-heavy elements are reasonably good but, the heavier elements have stronger effect of orbital contraction, spin-orbit coupling etc. Therefore the exponents for them should be determined by using relativistic Hamiltonian. The small components are generated with the kinetic balance condition and expanded with different expansion coefficients for α and β. Each component of Equation 3.37 can be written as:

$$\psi^{X^\mu} = \sum_{k=1,N_X} C_k^{X^\mu} \chi_k^{X^\mu} \tag{3.38}$$

where, X=L,S ; $\mu = \alpha, \beta$. Note that, as the number of large and small component bases may differ (please see the discussion below) we have introduced N_X, which keeps track of the number of them.

In terms of the choice of basis set, Gaussian functions are always preferred because of their convenient analytical integrability. A Cartesian Gaussian basis function is expressed as:

$$\chi_k = N_k^{i+j+k} x^i y^j z^k e^{-\zeta(x^2+y^2+z^2)} \tag{3.39}$$

where, i+j+k = l (angular momentum), $x^2 + y^2 + z^2 = r^2$ and N is the normalization constant. They are the choice for large component basis with suitably optimized exponents. The small component basis, on the other hand, is generated by the operation $(\vec{\sigma}.\vec{p})\chi_k^L$, which involves a term like $\nabla\chi_k^L$. That will generally give rise to functions of angular momentum (l+1) and (l-1). As a result, there will be small component basis functions of certain angular momentum as a combination of large component bases of different angular momentum. One can choose the specific combination of them to generate the small component basis function, which is called the Restricted Kinetic Balance

(RKB) condition. Also one can take a set of functions which is the union of (l+1) and (l-1) functions, named as the Unrestricted Kinetic Balance (UKB) condition. Though construction of small component set with RKB and UKB requires the same computational effort, at the DHF step UKB is more expensive. Also, UKB generates few unphysical solution vector for the DHF calculations, which should be removed. Another issue is that UKB generates a lot of linearly dependent small component functions, which can be realized as - a small component function of fixed angular momentum can come from the large component functions of different angular momentum. For RKB the problem of linear dependence is somewhat lesser, the reason has been well-explained in [20]. The use of contracted basis function poses some inconveniences for the use of RKB, as pointed out by Visscher *et.al* [76]. The way around is to solve the uncontracted DHF type equation for the atoms we are interested in, that will generate contracted and kinetically balanced large and small component basis sets with the exact connection between them. This procedure is termed as the atomic balance [76]. In DIRAC [1] we work with the scalar basis functions, for which employing uncontracted basis set is the logical choice since, if we consider the example of p function, combination of same scalar p_x, p_y, p_z function span both j functions ($p_{1/2}$,$p_{3/2}$) of a relativistic p orbital. UKB is also natural choice for the scalar basis functions. In DIRAC [1] the RKB is restored at the solution step of DHF equation, where the AO overlap matrix is diagonalized. We multiply the metric from the modified Dirac equation (Equation 3.25) to the overlap matrix, prior to the diagonalization [81]. As an aside we should also note that, kinetic balance condition takes care of the non-relativistic limit of kinetic energy for the positive-energy solutions not for the negative-energy part. Therefore they are somewhat ill-defined in terms of the above description. They might create problem when the negative-energy branch of the solution is also important, for example, in the case of magnetic properties. There has been effort to solve this problem by means of dual kinetic balance [63, 13] and very recently by dual atomic balance [19].

With the one-electron basis at our disposal, we can proceed to the solution of the DHF equation. The HF equation is customarily solved through the following steps: (1) build a Fock matrix with the help of guessed density matrix ; (2) diagonalize it to obtain solution vectors, from which construct new density matrix (3) rebuild the Fock matrix with the new density matrix and check convergence upon the new density matrix. With the DC Hamiltonian the Fock matrix can be concisely written in 2-spinor basis as:

$$F = \begin{pmatrix} f^{LL} & f^{LS} \\ f^{SL} & f^{SS} \end{pmatrix} \tag{3.40}$$

where,

$$f^{LL} = v^{LL} + J^{LL} - K^{LL} \tag{3.41}$$

$$f^{LS} = c(\vec{\sigma}.\vec{p})^{LS} - K^{LS} \tag{3.42}$$

$$f^{SL} = c(\vec{\sigma}.\vec{p})^{SL} - K^{SL} \tag{3.43}$$

$$f^{SS} = v^{SS} - 2mc^2 S^{SS} + J^{SS} - K^{SS} \tag{3.44}$$

J and K are the direct and exchange integrals; S is the overlap matrix. J and K depend on the various components of density matrix, where those components are given by:

$$D_{\mu\nu}^{XY} = \sum_{i=N_{occ}} C_{i\mu}^{X} C_{i\nu}^{Y*}; X, Y \in L, S \tag{3.45}$$

μ and ν are the labels for atomic orbitals and N_{occ} is the number of occupied orbitals.

Diagonalization of Equation 3.40 generates the solution vectors both for the positive-energy orbitals and the negative-energy orbitals. The negative-energy orbitals lie below the positive-energy orbitals with a large energy gap of $\sim 2mc^2$. Therefore, effort to minimize the energy with the variation of orbital rotation parameter pe-pe and pe-ne kind, will bring us to a solution within negative-energy domain. However, we are looking for a solution of the state which is minimum in the positive-energy spectrum, in other words a maximum of the negative-energy spectrum, therefore a minimax problem [69]. It has been resolved by Mittleman [47], by defining a projection operator for the positive-energy orbital, which eliminates the negative-energy orbitals at every iterative step of the SCF solution. The negative-energy orbital, as a consequence, changes its description at every iterative step depending on the positive-energy eigenvectors. This is the "floating vacuum" interpretation of the negative-energy orbitals. In practice, instead of defining any explicit projector, we occupy the positive-energy orbitals following the aufbau principle, at the density matrix (Equation 3.45) construction step in each iteration. That implicitly takes care of the projection. Due to the large separation between the pe and ne states, solution of a DHF equation does not suffer from numerical instability.

For the relativistic wave-function spin is not a good number. However, according to the Kramer's theorem one electronic wave-function will still remain doubly degenerate in the absence of external magnetic field. Instead of spin-partner, those functions are called time-reversal partner or Kramer's pair. It has the implication that in the relativistic domain also we can use the benefit analogous to the use of spatial orbital in non-relativistic cases. This has been done most elegantly by introducing quaternion algebra. We will not go into the details of that approach, but refer to the original work by Saue *et al.* [59]. In DIRAC [1], the quaternion scheme as advocated by Saue *et al.* is employed.

3.3. Relativistic Correlation Methods

The starting point of the discussion for relativistic correlation method is how to include electronic interaction to the Hamiltonian beyond the mean-field approximation. Due to the involvement of the negative-energy orbitals, one can conceive of a situation where electrons make a transition from the positive-energy orbitals to the negative-energy one, thereby creates a configuration, in which the difference of energy due to this transition gets cancelled by the opposite sign of energy for the negative- and positive-energy orbitals. It results in a configuration of equal energy. There is a possibility of creating many such configurations, which form a continuum. Therefore it is difficult to get a bound state solution. This problem is called the continuum dissolution [68] or Brown-

Ravenhall disease [2]. In the literature, it has been argued that this problem is an artefact of the description of relativistic Hamiltonian in configuration space [42]. This is typically avoided by introducing "no-pair" projection operator :

$$H^{NP} = \sum_{i=1,n} \Lambda(i)^+ h_i \Lambda(i)^+ + \frac{1}{2} \sum_{i,j=1,n} \Lambda(i)^+ \Lambda(j)^+ V_{ij} \Lambda(i)^+ \Lambda(j)^+ \tag{3.46}$$

where Λ^+ is an operator to project out all the negative-energy orbitals. Several choices of this operator have been reported over the literature [39]. The major difference between them lies in the choice of external potential.

It is worthwhile to reinterpret the "no-pair" projection in terms of the Fock-Space Hamiltonian. We should first recall that in second quantized formalism the electronic Hamiltonian is written as:

$$H = \int \psi^\dagger(1') h(1) \psi(1') d1' + \frac{1}{2} \int \psi^\dagger(1') \psi^\dagger(2') V(1,2) \psi(2') \psi(1') d1' d2' \tag{3.47}$$

where ψ and $\psi^\dagger$ are the field operators. In the relativistic theory, a field operator is expanded in terms of suitably chosen eigenvectors (χ) of electron and positron (charge conjugated negative-energy orbitals),

$$\psi = \sum_p b_p \chi_p \tag{3.48}$$

$$\psi^\dagger = \sum_p b_p^\dagger \chi_p^\dagger \tag{3.49}$$

Here, p runs over both electronic and positronic degrees of freedom. 'b' and '$b^\dagger$' are defined in the spirit of quasi-particle creation and annihilation operators:

$$\left.\begin{aligned} b_p &= a_p \\ b_p^\dagger &= a_p^\dagger \end{aligned}\right\} \; electron \tag{3.50}$$

$$\left.\begin{aligned} b_p^\dagger &= a_p \\ b_p &= a_p^\dagger \end{aligned}\right\} \; positron \tag{3.51}$$

where, 'a', '$a^\dagger$' are the particle creation, annihilation operators in traditional sense. This choice is motivated from the fact that annihilation of a negative-energy electron can be considered as a creation of a positron.

Substituting Equation 3.48 and Equation 3.49 in to Equation 3.47 we get

$$H = \sum_{p,q} h_p^q b_q^\dagger b_p + \frac{1}{2} \sum_{p,q,r,s} V_{pq}^{rs} b_r^\dagger b_s^\dagger b_q b_p \; . \tag{3.52}$$

Now, by applying Wick's theorem one gets [2]

[2] Wick's theorem states the relationship between an ordinary product and normal-ordered product of a string of operators : $AB = \{AB\} + \{AB\}_c$, where c indicates operator A and B are contracted.

$$\{H\} = \sum_{p,q} h'^{q}_{p}\{b^{\dagger}_{q}b_{p}\} + \frac{1}{2}\sum_{p,q,r,s} V^{rs}_{pq}\{b^{\dagger}_{r}b^{\dagger}_{s}b_{q}b_{p}\}, \tag{3.53}$$

where, {..} is the symbol of normal ordered product. h' is the modified one electronic part (one can recall the definition of a Fock matrix for h', though, the interpretation of it follows from the QED picture). Normal ordering in 'H' ensures that all the vacuum expectation value terms are cancelled. This is the Fock Space definition of the Hamiltonian. We will drop the {..} symbol from H for simplicity, and will (try to) stick to the normal ordered form of the Hamiltonian.

Now, if we analyze the one-electronic part in Equation 3.53 it consists of two parts:

$$\sum_{p,q} h^{q}_{p}\{b^{\dagger}_{q}b_{p}\} = \sum_{p,q} h'^{q++}_{p}\{b^{\dagger}_{q}b_{p}\} - h'^{q--}_{p}\{a^{\dagger}_{q}a_{p}\} \tag{3.54}$$

$$= \sum_{p,q} \epsilon^{++}_{p} a^{\dagger}_{p}a_{p} - \sum_{p} \epsilon^{--}_{p} a^{\dagger}_{p}a_{p} + \langle vac|h'^{q--}_{p}|vac\rangle \tag{3.55}$$

In the above equation the range of p and q is dictated by the sign of the h'^{q}_{p} term. When it is +ve, p and q run over the positive-energy orbitals, otherwise the negative-energy orbitals. In the final normal-ordered Hamiltonian the vacuum expectation value term will go away.

Let us introduce $N_e = -e(a^{\dagger}_{q}a_{p})$ as electronic (p and q restricted to positive-energy orbitals) and $N_p = +e(a^{\dagger}_{q}a_{p})$ as positronic (p,q restricted to negative-energy orbitals) charge operator. We can see that the energy of those two states are of the same sign since the charge of them is of opposite sign, which is in contradiction to the configuration space description.[3]

The contribution ϵ^{--}_{p} (there will be similar terms from the two-electronic part of the Hamiltonian as well) from Equation 3.55 can be very large and they don't represent the energy of the electronic states either. It is therefore reasonable to exclude them from the Hamiltonian. A convenient way is to define a new normal ordering with respect to the whole negative-energy orbital as vacuum. In accordance with our previous discussion if we consider the vacuum as 'empty', then the new normal ordering precludes any rotation between the positive and negative-energy orbitals. The Hamiltonian will then reduce to :

$$H = \sum_{p,q=1,n_e} h'^{q}_{p}\{b^{\dagger}_{q}b_{p}\} + \frac{1}{4}\sum_{p,q,r,s=1,n_e} V^{rs}_{pq}\{b^{\dagger}_{r}b^{\dagger}_{s}b_{q}b_{p}\}, \tag{3.56}$$

Now the question is : what will be the choice of basis set by which the field operators will be expanded? It is reasonable to choose the HF basis in this purpose. One can however choose a better basis set, for instance, MCSCF basis set. This choice defines the previously mentioned projection operator. Accordingly, we can call them as HF

[3]Interesting point to note here is that neither N_e nor N_p commutes with the Hamiltonian. But, the electronic charge operator $Q = -e(N_e - N_p)$ commutes, meaning that for the relativistic Hamiltonian total charge of the system is a conserved quantity not the individual number of particles.

projector, MCSCF projector etc. This is precisely the reason why there is no "exact" relativistic correlation energy. Nevertheless, in DIRAC [1] HF projector is used for all the correlation modules. Notice that the choice of projector for the correlation method is different from the HF method, here vacuum is "fixed" not "floating". Possibly, this is embedded in the Fock space description of the Hamiltonian.

Furthermore, we can employ the 'Fermi Vacuum' or 'HF Vacuum' to the Equation 3.56 exactly like in the non-relativistic theory. Redefining the creation and annihilation operator in terms of the standard hole-particle picture is still valid since we have excluded all the positronic label only the particle type labels from the previous definition exists. We can safely replace 'h'' by F also. The final Hamiltonian is therefore :

$$H = \sum_{p,q=1,n_e} F_p^q \{b_q^\dagger b_p\} + \frac{1}{4} \sum_{p,q,r,s=1,n_e} V_{pq}^{rs} \{b_r^\dagger b_s^\dagger b_q b_p\}, \tag{3.57}$$

where, the new normal-ordering cancels the HF total energy term. In the above form the Hamiltonian is exactly equivalent to the non-relativistic one. A difference lies in the fact that the Fock matrix and V matrix now is in terms of the complex 4-spinor orbitals and symmetry structure of them is also different.

Before finishing this section we should mention the pros and cons of this choice of the Hamiltonian:

1. It has been shown by Saue *et al.* [60] from the perturbative point of view that single excitation and double excitation amplitudes from the positive-energy to the negative-energy orbitals contribute at O (c^{-3}) and O (c^{-4}), respectively. Therefore, neglecting them would not cause much damage to the whole description.

2. Positronic contribution to the electron density is very minute. Electron correlation contribution due to the positive-energy orbital would therefore be insignificant.

3. For magnetic perturbation, it can be shown that the effect of the coupling is $O(c^0)$. In those cases, it is not a logical choice to ignore the coupling.

We will now very briefly describe some of the developments in relativistic correlation method. In the basic essence of the theory they are closely related to their non-relativistic counterpart. However, there are few aspects where they may differ. We will try to address some of those issues while describing one particular method. The correlation methods can be classified into two categories : Single Reference and Multi Reference. The methods pertaining to each category will be described in the two following sections. However, this list of the methods is not exhaustive by any means, it is to show the present capability of this field.

3.4. Single Reference Methods:

3.4.1. Relativistic CI:

The Configuration Interaction (CI) is one of the earliest methods for the treatment of dynamical electron correlation. In this method ground state configuration is combined

with several excited state configurations for the description of exact wave function of a particular state. In the non-relativistic version two choices are made - the configurations are either the eigenfunctions of specific S_z (Slater determinants) or they are eigenfunctions of both S_z and S^2 (Configuration State Functions or CSFs). In addition, if spatial symmetry is there one can combine the determinants of same spatial symmetry. In the relativistic case neither S_z nor S^2 is a good quantum number. Therefore, in an attempt by Visscher *et.al.* [82] only double group symmetry adapted determinant space has been tried. In order to avoid the factorial scaling of the total number of configurations, restrictions to the configuration space have been tried. The scheme they used is the Restricted Active Space approach [49], where the excitation space is divided into three subspaces : RAS1, RAS2 and RAS3 and electron excitations are allowed only within each subspace. This approach was implemented in conjunction with the group chain technique [83] for the efficient evaluation of coupling coefficients between the determinants. Fleig *et.al.* took another route for the construction of active space namely the Generalized Active Space (GAS) technique [22]. This implementation has been massively parallelized by Knecht et. al. [35, 36]. The GASCI method takes advantage of time-reversal symmetry, that appears in the choice of the excitation operators. The excitation operators for relativistic GASCI are classified according to the number of Kramer's flip (Δm_k) associated with them, thereby it allows coupling between certain classes of determinants. This operator may be thought of as a relativistic analogue of spin-flip (Δm_s) operator. It has been argued, though that this approach does not provide significant savings for a true 4-component calculation, only it helps to adapt spin-free theories much more conveniently in the same framework [75]

3.4.2. Relativistic MP2:

Møller-Plesset perturbation theory is the conceptually simplest approach for the treatment of electron correlation. When "no-pair" projected Hamiltonian is used as in Equation 3.57 we obtain the identical energy expression as in non-relativistic case:

$$E_{MP2} = \frac{1}{4}\frac{|\langle ab||ij\rangle|^2}{\epsilon_i + \epsilon_j - \epsilon_a - \epsilon_b} \tag{3.58}$$

Both Kramer's Restricted [43] and Unrestricted version of the MP2 theory is known. While the Kramer's restricted version is limited only to the closed-shell cases, the unrestricted MP2 in DIRAC [1] can handle simple open-shell references. Another open-shell version of MP2 is known due to Dyall [18] where 2 electrons in 2 open-shell can be treated in Kramer's restricted manner. In terms of application, single reference perturbation theory is preferred in the non-relativistic problems only when one wants to get qualitative accuracy for a large complicated problem (e.g, intermolecular forces). That requires modification of the standard MP2 version, for instance works like Symmetry Adapted Perturbation Theory (SAPT) [57], Z-averaged Perturbation theory (ZAPT) [45] etc. However, in the relativistic domain those theories have never been adapted. Perturbation theory therefore is a method of limited applicability in this domain.

3.4.3. Relativistic Coupled Cluster

The two correlation methods we have discussed so far suffered from the following problems:

1. The CI energy does not scale properly with the increase of system size, if any truncated version of it is used. This is known as the size extensivity problem. The CI method therefore will not be successful except for small to medium sized system.

2. The other one i.e, the MP2 method, inspite being size extensive, misses a large amount of correlation contribution, which can be very significant.

It was required to have a method which can fulfil the size extensivity condition while provides very accurate correlation energy. It has been shown that the Coupled Cluster (CC) theory can satisfy both the criterion.

In the Coupled Cluster theory we define a wave operator of the form $\exp(T)$, which can map a model approximate function to the exact function. If the model function is single determinant in nature, we call that CC technique as Single Reference (SR) CC. In mathematical form:

$$|\Psi\rangle = \exp(T)|\phi_0\rangle \tag{3.59}$$

where, $|\Psi\rangle$ is the exact wave function and $|\phi_0\rangle$ is an approximate N-electronic model function. $|\phi_0\rangle$, in principle, can be any N-electronic configuration (not only ground state). However one should keep in mind that the state it is representing has to be single reference in character. T is a parameter, which by its action on $|\phi_0\rangle$ generates various excited determinants. It is typically represented as

$$T = \sum_l t_l\{E_l\} \tag{3.60}$$

where, $\{E_l\}$ is a string of second quantized operator which generates 'l' - tuple excited function from the model function and t_l is the associated amplitude. In practical purposes, we truncate T at the singles-doubles level i.e, $T = T_1 + T_2$. The Hamiltonian we will be using is already defined in Equation 3.57. To get the correlation energy we need to evaluate the unknown quantity T. The working equation for which is obtained by plugging in the wave function ansatz of Equation 3.59 to the Schrödinger equation and by applying Baker-Campbell-Housdroff (BCH) expansion:

$$[H\exp(T)]_c^S = 0 \tag{3.61}$$

$$[H\exp(T)]_c^D = 0 \tag{3.62}$$

Where $[H\exp(T)]_c$ means various contracted quantities between H and $\exp(T)$ of singles (S) and doubles (D) excitation type. For the second quantization representation of the Hamiltonian matrix elements and T amplitudes, we must specify the MO basis set. Since

the solution of the CC equation unfortunately depends on the underlying perturbative structure we need a set of functions which represents $|\phi_0\rangle$ reasonably well.

Relativistic theory differs from the non-relativistic one in the fact that MO is now a 4 component quantity instead of 2 (spin orbital) or 1 (spatial orbital) component. The choice of 'E' operator is also significantly different in both the cases. Underlying spin symmetry in the non-relativistic Hamiltonian allows one to choose very limited number of spin classes for the Hamiltonian and the amplitudes, if the spin-orbital based formalism is used. Moreover, the use of spin-algebra allows to adapt the amplitudes and the Hamiltonian matrix elements to a particular spin multiplicity. By using those relationships one can show that for the closed-shell singlet cases only one spin class ($t_{i_\alpha j_\beta}^{a_\alpha b_\beta} \equiv t_{i_\beta j_\alpha}^{a_\beta b_\alpha}$) survives for the amplitudes. That helps in saving operation and memory count. In the relativistic case the spin-orthogonality is not there. Therefore the same reduction in the operator class is not possible. However, the use of time reversal symmetry may provide some benefit, though not at all analogous to the spin symmetry. In that case, depending on the specific point group symmetry some of the matrix elements will become zero. The relationship between different classes of integrals are also governed by the time-reversal symmetry, it is not just the equality relationship as in the non-relativistic case (see in Appendix A). Visscher *et al.* [78] proposed a Kramer's adapted coupled cluster scheme for all the symmetry subgroups of d_{2h}^* but C_1^*. Where they define three distinct classes of amplitudes by exploiting the relationship among the integrals. They ended up getting fairly complicated looking algebraic equations. In a follow up paper [80] they gave up that scheme for an unrestricted formalism by stressing on the issue that the latter is better suited not only for the C_1^* symmetry but also for open-shell cases. In the unrestricted formalism the use of double group symmetry allows the Kramer's partners (coming from the SCF calculation) to span different fermionic irreps. That immediately identifies all the zero valued amplitudes and integrals in a Kramer's pair basis. But, of course cannot employ all the relationships invoked in the earlier paper. DIRAC [1] package uses this unrestricted formalism in the RELCCSD module. That is the most widely used DC coupled cluster code. Visscher *et al.* [80] also implemented the CCSD (T) method where 4-th and 5-th order connected triples contributions are added to the CCSD energy equation, under the unrestricted formalism.

3.5. Multi-Configurational Methods:

Major domain of application for the relativistic methods is the lanthanides and actinides chemistry. The ground state of those elements consists of several open-shells. Thus, many realistic application of the relativistic methods needs the formulation and implementation of the multi-configurational methods. Another motivation is that, SOC may strongly couple few states which are otherwise not coupled in the non-relativistic theories due to the spin-symmetry. Therefore strong multi-reference character arises even without the presence of any open-shell. This point has been amply discussed in the book by Dyall and Fægri [20]. We will briefly describe few of the approaches taken for the multi-configurational treatments.

3.5.1. MCSCF

The key to the multi-configurational treatment is the generation of orbitals when the state is described by a combination of determinants. It is a general notion that in the orbital generation step we should keep the symmetry structure intact as much as possible. Thus, the strategy for devising the MCSCF procedure in relativistic domain requires careful treatment of time-reversal symmetry. The detailed theory for it is due to Jensen *et.al.* [32]. They call this method as Kramer's Restricted (KR)-MCSCF. Thyssen *et.al.* [70] implemented that theory in DIRAC by employing double group symmetry. However, that implementation is not computationally very efficient probably because of the construction of explicit Hessain matrix at the orbital optimization step as pointed out by Bates and Shiozaki [12]. They have very recently reported an MCSCF procedure where they alleviate this bottleneck by quasi-second-order optimization procedure (avoid explicit construction of the Hessian). In that work by using density fitting technique and efficient parallelization procedure, they were able to carry out MCSCF calculation with more than 100 atoms.

3.5.2. CASPT2 and NEVPT2

The MCSCF procedure treats static electron correlation adequately, but dynamical correlation is missing in that treatment. The logical step forward is to treat the dynamical correlation by perturbation theory on top of the MCSCF wave function. Those methodologies are called multireference perturbation theory. The major difference among different variance of this theory lies in the choice of zeroth order Hamiltonian which is not unique. Complete Active Space Perturbation Theory (CASPT2) proposed by Anderson *et.al.* [5] adopts a projection operator based definition of the Fock matrix. CASPT2 has been successfully applied for various multi-reference problems. The relativistic version of CASPT2 has been first implemented by Abe *et al.* [4]. More recent implementation of CASPT2 is due to Shiozaki *et al.* [65]. Shiozaki *et al.* uses traditional CASSCF reference state for their CASPT2 implementation whereas Abe *et. al.* used CASCI-Improved Virtual Orbitals (IVO) reference state. Relativistic CASPT2 has been tried for the complicated thallium dimer and Rb-Yb molecule. Various shortcomings of the CASPT2 theory are also well-known namely, the problem of intruder state and size inextensivity. Another MRPT theory, rapidly growing in popularity, the N-electron Valence Perturbation Theory (NEVPT2) by Angeli *et al.* [6] which is immune to all the aforementioned problems of CASPT2. Relativistic NEVPT2 is also known due to the work by Shiozaki *et al.* [65].

3.5.3. DMRG

The Density Matrix Renormalization Group (DMRG) theory has been developed by White *et. al.* [85] for the treatment of strongly correlated systems in condensed matter physics. When DMRG was adapted for the molecular problem, it has been argued that the strong correlation is equivalent to the multi-reference character arises in numerous molecular problems. The construction of a wave function is conceptually much

different from the correlation methods described so far, here one exploits locality of the strong correlation problem. That problem is looked as an one-dimensional lattice chain where only nearest neighbour can interact with each other, and all non-neighbouring ones are coupled in an indirect fashion. This intrinsic one-dimensional nature of the method reduces the problem size to the polynomial. It is thereby possible to carry out a DMRG calculation with very large systems. However, in situations where the one-dimensional nature is not prominent and dynamical electron correlation is significantly large, DMRG is prone to failure. The DMRG method with the DC Hamiltonian has been first implemented by Knecht *et al.* [37] and was applied for a prototype thallium hydride molecule.

3.6. Approximate Correlation methods

4-component DC Hamiltonian based correlation methods can be prohibitively expensive. In the next chapter we have compared the cost of relativistic correlation methods vis-a-vis non-relativistic methods. To keep it computationally tractable several approximate methods have been designed. The approaches can be classified in the following manner:

1. 2-component Hamiltonian based correlation calculations are one of the most common choices. In the two-component approaches the wave-function does not contain any small-component part. Therefore, in the integral transformation step, prior to a correlation method, we need to transform only the large component part of the molecular orbitals. The small component basis being much bigger than the large component one dominates the cost of the integral transformation. Therefore by neglecting the small component we get significant savings at this step in comparison to the full 4-component calculations. However, in the ensuing actual correlation step there is no additional saving in the 2-component approaches since we work with the no-pair projection Hamiltonian and in MO basis anyway. All the 2-component Hamiltonians discussed in the last section are suitable in this purpose.

2. Sometimes Spin-Free DC Hamiltonian based mean-field spinors are used for the subsequent correlation calculation. The motivation is two-fold: the algebra remains real and the spinors obey the spin-orthogonality relation. This has been explained by Dyall [17] himself as a motivation for the spin-separation of the DC Hamiltonian.

   The Spin-Free approaches can also be combined with the machinery for 2-Component approaches, which gives further saving in the integral transformation step.

3. Another route often reported in the literature is to use spin-free/non-relativistic Hamiltonian at the SCF step and treat SO coupling at the correlated level. It has the advantage of using real algebra at the integral transformation step. This approach is very popular, it has been used in the context of Multi-Reference CI [64, 71], MRPT [7], Coupled Cluster[84] etc.

Most of those developments are based on few specific set of applications in mind, they do not generally cover all the aspects of relativistic electronic structure. Thereby application domain of those approaches are also restricted to specific problems.

4. Application of Relativistic Correlation Methods

In the last chapter we have introduced the major theoretical concepts of relativistic electronic structure theory. It is by its very theoretical foundation much more richer than the non-relativistic counterpart. However, there are still some issues in practical aspects of using these methodologies. The non-relativistic counterpart, has been going through stormy developments since the last few years thereby one can carry out very large realistic calculations [48, 38]. Relativistic methodologies are still far from that tremendous breadth of application domain primarily because of its huge inherent computational cost. In this section I will present a comparison between the computational scaling of a relativistic correlation method from that of a non-relativistic one. In view of them quite a few measures have already been taken, which can make it somewhat more tractable. I will describe a few of those approaches. I will keep our discussion focused on the correlation part since that is only of relevance to this thesis. Finally I will show some applications, carried out during the span of this thesis, by applying relativistic correlation methodologies. *et al.*

4.1. Comparison of Computational Cost Between Relativistic and Non-Relativistic Methods:

In the relativistic theory the orbitals are represented as a 4-component quantity (Equation 3.35) in comparison to the 2-component (spin-orbital) or 1-component quantity in non-relativistic domain. Therefore, for the transformation of 2-electron integrals from AO to MO basis we have to consider three type of quantities for the DC Hamiltonian : $(LL|LL)$, $(LL|SS)$ or $(SS|LL)$ and $(SS|SS)$. Among them the quantities involving small components require very high computational cost, since the small component AO basis is roughly double (usually more than double) in size with respect to the large component one (as we use UKB). The integrals (in a scalar basis it is real) and MO coefficients are both complex quantities, any operation between two complex numbers gives a factor of 4 increase in the operation count. We have shown the computational cost for that step in Table 4.1 following Saue and Visscher [60]. Another aspect is that we use scalar un-contracted basis functions, as already explained in section 3.2, that gives us a huge number of unphysical MOs, which we need to transform also. There is no robust way, by which one can eliminate them. This is an additional disadvantage. Furthermore, the spin-integration is not possible for relativistic case.

In the actual correlation step the difference arises first because of the larger size of the

Table 4.1.: Comparison of operation count between various steps of relativistic and non-relativistic correlation calculation. N is the total number of basis functions. N_L and N_S refer to total number of large and small component functions respectively. M is the total number of active spinors. $M = M_o + M_v$ where o refers to occupied and v to virtual. Integral Transformation-1 indicates the first half transformation of AO to MO integrals and Integral Transformation-2 is the corresponding second half transformation.

Step	Non-Relativistic	Relativistic
Integral Transformation-1	$\frac{1}{2}MN^4 + \frac{1}{2}M^2N^3$	$2M(N_L^4 + N_S^2N_L^2 + N_S^4)$ $+8M^2(N_L^3 + N_SN_L^2 + N_S^3)$
Integral Transformation-2	$\frac{1}{2}M^3N^2 + \frac{1}{2}M^4N$	$4M^3(N_L^2 + N_S^2) + 16M^4(N_L + N_S)$
CCSD	$\frac{1}{4}M_o^4M_v^2 + 4M_o^4M_v^2 + \frac{1}{2}M_o^2M_v^4$	$8M_o^4M_v^2 + 128M_o^4M_v^2 + 16M_v^2M_v^4$

virtual orbital space (they would have been the same with the use of contracted basis function), and second due to the lack of spin-orthogonality, which I have discussed in the context of relativistic coupled cluster theory in subsection 3.4.3. The corresponding comparison of cost can be seen in Table 4.1.

4.2. Improvements to the Computational Scheme:

In the integral transformation step Visscher [74] reduced the computational cost by approximating the small component contribution. The total SSSS contribution has been replaced by a Coulombic repulsion term of interatomic small component charge densities. Therefore he got an energy correction:

$$\Delta E = \sum_{AB} \frac{q_A^S q_B^S}{R_{AB}} \tag{4.1}$$

for two atoms A and B, where R_{AB} is the distance between them and q is the charge density. The justification of taking this approximation was small component charge is very much local in the vicinity of the nucleus and spherical in nature. By this way we avoid the costliest part of the integral transformation step.

The lack of spin-integrability can somewhat be overcome by the use of quaternion algebra. In DIRAC[1] with the use of explicit time-reversal symmetry we get our MO coefficients as a quaternion number [1]. Multiplication of two quaternion numbers is also a quaternion. Thereby a two-electron integral can be realized as a product of two quaternion numbers belonging to electron 1 and electron 2. This is identical to the spin-integration, only price we have to pay is to go from real to quaternion algebra. However for the ensuing correlation calculation one quaternion integral is expanded in terms of

[1] A quaternion number is defined as : $q = a + \check{i}b + \check{j}c + \check{k}d$ where, $\check{i} = i\sigma_x; \check{j} = i\sigma_y; \check{k} = i\sigma_z$ and $\check{i}^2 = \check{j}^2 = \check{k}^2 = \check{i}\check{j}\check{k} = -1$

complex integrals in Kramer's pair basis. This has the implication that in the correlation step we do not get any savings equivalent to spin-integration.

In the non-relativistic theories, it is nowadays a common practice to use AO-direct methods in the correlation calculation. Especially in the context of CC theory the integrals which involve four virtual orbitals i.e, $VVVV$-type, are never transformed, that bypasses the cost of integral transformation of that class and avoids the use of large memory space. In relativistic case this choice is questionable since the size of AO basis is much larger than the MO basis and any truncation to the orbital space is also unproductive in that situation.

Now, I will describe two works in which we have applied existing relativistic correlation methodologies, analyzed thoroughly to get better understanding of the interplay between relativity and correlation and implemented new methodologies to facilitate particular kind of studies. Those two works are the substance of two different publications. We will not describe those papers with its entirety, rather first summarize them very briefly, and then will attach them to the end of this chapter.

4.3. Papers

4.3.1. Paper I : A theoretical benchmark study of the spectroscopic constants of the very heavy rare gas dimers

Avijit Shee, Stefan Knecht and Trond Saue, *Phys.Chem.Chem.Phys., 2015, 17, 10978*

Spectroscopic constants for the homonuclear dimers of the very heavy rare gases radon (Rn) and eka-radon (Uuo) are reported. A computational protocol using the eXact 2-Component molecular-mean field Hamiltonian has been established based on extensive calculations of the xenon dimer. We find that reliable results require CCSD(T) calculations at the extrapolated basis set limit. In this limit counterpoise corrected results are closer to experimentally derived values than uncorrected ones. Furthermore, in an attempt to reduce the computational cost while retaining very high accuracy, we studied the performance of range-separated density functional theory. Although we observe a somewhat more favorable basis set convergence and reduced importance of connected triples with range-separated methods compared to pure wave function theory, in practice we have to employ the same computational protocol for obtaining converged results. At the Dirac-Coulomb level we find an almost fourfold increase of binding energy when going from the radon to the eka-radon dimer, but the inclusion of spin-other-orbit interaction reduces the dissociation energy of the heaviest dimer by about 40 %

My contribution in this work was to carry out all the calculations, analyze most of the results and writing the first draft of that article

PCCP

PAPER

View Article Online
View Journal | View Issue

Cite this: *Phys. Chem. Chem. Phys.*, 2015, **17**, 10978

A theoretical benchmark study of the spectroscopic constants of the very heavy rare gas dimers

Avijit Shee,[a] Stefan Knecht[b] and Trond Saue*[a]

Spectroscopic constants for the homonuclear dimers of the very heavy rare gases radon (Rn) and eka-radon (Uuo) are reported. A computational protocol using the eXact 2-Component molecular-mean field Hamiltonian has been established based on extensive calculations of the xenon dimer. We find that reliable results require CCSD(T) calculations at the extrapolated basis set limit. In this limit counterpoise corrected results are closer to experimentally derived values than uncorrected ones. Furthermore, in an attempt to reduce the computational cost while retaining very high accuracy, we studied the performance of range-separated density functional theory. Although we observe a somewhat more favorable basis set convergence and reduced importance of connected triples by range-separated methods compared to pure wave function theory, in practice we have to employ the same computational protocol for obtaining converged results. At the Dirac–Coulomb level we find an almost fourfold increase of binding energy when going from the radon to the eka-radon dimer, but the inclusion of spin-other orbit interaction reduces the dissociation energy of the heaviest dimer by about 40%.

Received 22nd February 2015,
Accepted 18th March 2015

DOI: 10.1039/c5cp01094b

www.rsc.org/pccp

1 Introduction

Rare gas dimers are bound species because of the dispersion interaction, which is generally characterized as an attractive interaction between the induced dipoles of each monomer. In the framework of wave function theory (WFT), the generation of induced dipoles can only be described by adding excited determinants to the ground state Hartree–Fock (HF) determinant. Therefore, the potential energy curves of those dimers at the HF level are repulsive. Consideration of excited determinants, on the other hand, leads to the possibility of various kinds of interactions, namely, Coulombic attraction or repulsion, induction and dispersion at the same time. Careful treatment of all those interactions requires very sophisticated theoretical approaches. It has been demonstrated by Hobza *et al.*[1] that the inclusion of up-to triple excitations in a Coupled Cluster (CC) expansion and extrapolation to the complete basis set limit (CBS) can provide chemical accuracy ($\sim$1 kcal mol^{-1}) for such systems. The overwhelming cost of CC methods at the CBS limit, however, has encouraged the development of various new theoretical techniques to reach the same accuracy with a much cheaper computational setup.[2,3]

Density functional theory (DFT) is undoubtedly the most-used quantum chemistry method.[4] However, it is well-known that standard approximate DFT functionals, with a local *ansatz*, are unable to capture dispersion interaction.[5,6] In recent years there has been intense development in dispersion corrections within the framework of Kohn–Sham theory, mostly by inclusion of explicit dispersion coefficients (C_6 and higher) and the appropriate distance dependence.[7–14] An alternative is provided by range-separated DFT, introduced by Savin,[15] which allows one to graft WFT correlation methods onto DFT without double counting of electron correlation. The resultant long-range WFT-short-range DFT (lrWFT-srDFT) method formally comes with the computational cost of the selected WFT component. However, it has been argued that range-separated methods have a weaker basis set dependence as well as less severe requirements for the size of the correlation space and excitation rank.[16] One of our objectives of the present work is therefore to investigate whether such methods can yield CCSD(T)/CBS-like accuracy for van der Waals dimers at reduced computational cost.

The homonuclear dimers of He, Ne, Ar, Kr and Xe have been studied extensively both theoretically and experimentally by various groups (see ref. 17–28 and references therein). However, the dimers of the heavier elements in this group, that is, Rn (Z = 86) and eka-Rn (Z = 118; ununoctium), have not been studied at all by experiment and very rarely by theory.[29–32] In passing we should note that the chemical exploration of radon is limited due to its price and radioactivity, and it is mostly known

[a] *Laboratoire de Chimie et Physique Quantiques (UMR 5626), CNRS/Université Toulouse III – Paul Sabatier, 118 Route de Narbonne, F-31062 Toulouse cedex, France. E-mail: trond.saue@irsamc.ups-tlse.fr*
[b] *Laboratory of Physical Chemistry, ETH Zürich, Vladimir-Prelog-Weg 2, 8093 Zürich, Switzerland*

as a health hazard,[33–35] whereas (possibly) only three single atoms of the isotope $^{294}118$ have been synthesized.[36–38] The half-life of this isotope is 0.89 ms, which is beyond the limits of present-day techniques for the chemical study of superheavy elements.[39,40]

Runeberg and Pyykkö[29] have reported spectroscopic constants of Rn_2 (and Xe_2) obtained at the CCSD(T) level using relativistic pseudopotentials. Nash, applying a similar computational protocol, has provided corresponding data for Rn_2 and eka-Rn_2.[30] More recently, Kullie and Saue reported spectroscopic constants for the complete series of homoatomic rare gas dimers using MP2-srDFT and the 4-component relativistic Dirac–Coulomb (DC) Hamiltonian.[32] For the heaviest dimers there is, however, a significant discrepancy between results (as shown in the lower parts of Tables 2 and 3). For instance, for Rn_2 Runeberg and Pyykkö obtained a dissociation energy of D_e = 222.6 cm^{-1} and estimated D_e = 276.6 cm^{-1}, which is still far from 323.9 cm^{-1} reported by Kullie and Saue (MP2-srLDA) and from 129.1 cm^{-1}, reported by Nash. Likewise, Kullie and Saue obtained D_e = 1199.1 cm^{-1} for eka-Rn_2, which is more than twice the value 500.1 cm^{-1} reported by Nash. In the present study we therefore carried out 2-component relativistic CCSD(T) as well as CCSD(T)-srLDA calculations in an attempt to provide reference values for the spectroscopic constants of the dimers of the very heavy rare gases and to establish a computational protocol for reliable theoretical studies of the chemistry of the heaviest rare gases. This effort constitutes the very first use of lrCC-srDFT methods with a relativistic Hamiltonian.

Our paper is organized as follows: in Section 2 we discuss our choice of relativistic all-electron Hamiltonian and correlation methods. Computational details are given in Section 3. In Section 4 we present and discuss our results, starting with a calibration study of the xenon dimer. We conclude and provide perspectives in Section 5.

2 Theoretical considerations

2.1 Choice of the Hamiltonian

The selected compounds clearly call for a careful relativistic treatment, including both scalar-relativistic and spin–orbit effects. Starting from the 4-component Dirac Hamiltonian in the molecular field one may add the two-electron Coulomb term, which provides not only the instantaneous two-electron Coulomb interaction, but also two-electron spin-same orbit (SSO) interaction.[41] For very accurate calculations higher-order contributions to the fully relativistic two-electron interaction, notably the spin-other orbit (SOO) interaction, as well as QED corrections may be considered. Formally, WFT-based electron correlation calculations have exactly the same cost using 2- and 4-component relativistic Hamiltonians, to the extent that the latter Hamiltonians are employed within the no-pair approximation (that is, negative-energy orbitals are excluded). This is easily seen from a consideration of the electronic Hamiltonian in second-quantized form

$$H = E^{\mathrm{HF}} + \sum_{p,q} F_p^q \left\{ a_q^\dagger a_p \right\} + \frac{1}{4} \sum_{p,q,r,s} V_{pq}^{rs} \left\{ a_r^\dagger a_s^\dagger a_q a_p \right\}, \qquad (1)$$

where {} denotes normal ordering with respect to the Fermi (HF) vacuum: the number of Fock matrix elements F_p^q and anti-symmetrized two-electron integrals V_{pq}^{rs} will be exactly the same at the 2-component (2c) and 4-component (4c) levels. However, the large prefactor of the 4-index transformation at the 4c level, due to the small-component basis functions, may favor the use of a 2c relativistic Hamiltonian, even though the formal scaling of this computational step is generally lower than the correlated calculation itself. An interesting alternative is provided by the eXact 2-Component (X2C) molecular-mean field (mmf) Hamiltonian,[42] where the converged 4-component Fock operator is subjected to an exact block diagonalization from which only the corresponding 2c Fock operator for positive-energy orbitals is extracted and represented by the large-component basis. The two-electron Coulomb term is thus left untransformed, formally introducing "picture change errors",[43–45] but the resulting $X2C_{mmf}^{DC}$ Hamiltonian has been shown to provide very close agreement with 4c correlated calculations, at least when only valence electrons are correlated.[42] It is also possible to include the Gaunt term, and thereby SOO interactions, in a molecular mean-field manner. We denote this Hamiltonian as $X2C_{mmf}^{DCG}$.

In the present study our correlated calculations have been carried out on top of both HF and short-range Kohn–Sham reference functions, as will be described in the following subsections.

2.2 Wave function theory

We have considered a range of correlation methods: second-order Møller–Plesset perturbation theory (MP2), coupled-cluster singles-and-doubles (CCSD) and CCSD with approximate triples (CCSD(T)). Although MP2 is widely employed to study weak intermolecular interactions, deficiencies have been identified which may lead to a huge overestimation of non-covalent binding energies.[46,47] In particular, Szabo and Ostlund demonstrated that the MP2 energy of a closed-shell diatomic molecule formed by two closed-shell atoms has the correct long-range R^{-6} behavior

$$\lim_{R_{AB}\to\infty} E_{AB}^{MP2} = E_A^{MP2} + E_B^{MP2} + \frac{C_6^{AB}}{R_{AB}^6}, \qquad (2)$$

but with the C_6^{AB} dispersion coefficient calculated at the uncoupled HF level of theory.[48] The CCSD method takes into account all intra-atomic correlation contributions up-to singles and doubles amplitudes, but it has been shown that CCSD can significantly underestimate non-covalent binding energies (see for instance ref. 49 and 50). In contrast, inclusion of connected triples of the inter-atomic type and hence attractive, improves the description vastly. The inclusion of the 4th and 5th orders of connected triples, *i.e.* CCSD(T), is therefore the current reference method for non-covalent interactions.[51–53]

2.3 Range-separated theory

The first implementation of the lrCC-srDFT method was reported by Goll, Werner and Stoll,[16] who also reported the calculated spectroscopic constants of the homoatomic dimers of He, Ne, Ar, Kr and Xe, the latter two rare gas elements described by relativistic

effective core potentials. In the present work we report the first implementation and application of the lrCC-srDFT method at the 2c/4c relativistic level. In this section we briefly outline the theory of the lrCC-srDFT method. Further information can be obtained by consulting ref. 16 and references therein.

One starts from a separation of the two-electron Coulomb term V_{ee} into a short-range part V_{ee}^{sr} and its complement V_{ee}^{lr}. The latter is denoted as the long-range part, although in practice it is non-zero at *all* interelectronic distances r_{12}. Ideally the separation should be such that the long-range part, to be handled by WFT, carries a maximum of static correlation and a minimum of dynamic correlation as well as providing mathematically tractable two-electron integrals. The most common choice is defined in terms of the error function[15]

$$v_{ee}^{lr}(1,2) = \frac{\mathrm{erf}(\mu r_{12})}{r_{12}} \tag{3}$$

where the range-separation parameter μ can take any value between 0 and ∞; $\mu = 0$ defines pure Kohn–Sham DFT and $\mu \to \infty$ corresponds to pure WFT. μ^{-1} has units of length, but one should note that the long-range potential, eqn (3), corresponds to that of a Gaussian charge distribution rather than a hard-sphere model.[32] If one therefore wants to associate the range-separation parameter with a radius R around the reference electron, one should choose $\mu^{-1} = R\sqrt{2/5}$ which provides identical root-mean-square radii for the two models.

The energy functional of lrWFT-srDFT theory

$$E[n] = \min_{\Psi_\mu \to n} \langle \Psi_\mu | T + V_{ee}^{lr} | \Psi_\mu \rangle + E_{Hxc}^{sr}[n] + \int n(1) v_{eN}(1) d1, \tag{4}$$

to be minimized with respect to the (number) density n, is obtained through a generalized adiabatic connection[54] to a fictitious system, defined by μ, with long-range interaction only. The wave equation of the fictitious system is

$$\hat{H}_\mu \Psi_\mu = E_\mu \Psi_\mu; \quad \hat{H}_\mu = T + V_{eff}^{\mu} + V_{ee}^{lr}, \tag{5}$$

where we impose that the local effective potential

$$V_{eff}^{\mu} = v_{eN} + v_{Hxc}^{sr}; \quad v_{Hxc}^{sr}(1) = \frac{\delta E_{Hxc}^{sr}}{\delta n(1)} \tag{6}$$

affords the same electron density as the real interacting system. Analogous to conventional Kohn–Sham theory, the exact form of the short-range Hartree, exchange and correlation (Hxc) energy functional E_{Hxc}^{sr} is not known, but since it is restricted to the short-range part of the total electron interaction (as well as coupling to the long-range part), one may hope that local approximations may be even more effective than in conventional DFT.

A fundamental difference between conventional Kohn–Sham theory and lrWFT-srDFT theory is that the fictitious system of the latter is interacting so that its wave function Ψ_μ cannot be expressed in terms of a single Slater determinant. Approximate methods of WFT are therefore invoked to solve eqn (5). Calculations generally start with a single-determinant *ansatz* HF-srDFT,[55] corresponding to a Kohn–Sham calculation with a range-separated hybrid (RSH),[56] which provides an orbital set for more elaborate correlation calculations. It also defines a partitioning of the Hamiltonian

$$H_\mu = H_{\mu;0} + W_\mu \tag{7}$$

where the zeroth-order Fock-like Hamiltonian

$$H_{\mu;0} = T + V_{eN} + J^{lr}[n_0] + V_{Hxc}^{sr}[n_0] \tag{8}$$

is defined in terms of the zeroth-order density n_0. The perturbation

$$W_\mu = \underbrace{V_{ee}^{lr} - J^{lr}[n_0]}_{\text{lr fluctuation potential}} + \underbrace{V_{Hxc}^{sr}[n] - V_{Hxc}^{sr}[n_0]}_{\text{self consistency correction}} \tag{9}$$

contains a long-range fluctuation potential as well as a short-range self-consistency correction, the latter reflecting the change of the density from the initial HF-srDFT calculation to the final correlated level. The self-consistency correction does not enter the lrMP2-srDFT energy expression,[57,58] but formally enters lrCC-srDFT theory. However, studies by Goll *et al.*[16] indicate that the effect of the density update is quite small, and it will be ignored in the present work.

2.4 Basis set extrapolation

The accuracy of correlation methods also entails that we have to cancel out other sources of errors such as the basis set incompleteness. For pure WFT correlation methods, the two-point extrapolation scheme advocated by Helgaker *et al.*[59,60] provides a convenient means for calculating the energy at the extrapolated basis set limit:

$$E_\infty = E_X^{SCF} + \frac{X^3 E_X^{corr} - (X-1)^3 E_{(X-1)}^{corr}}{X^3 - (X-1)^3}. \tag{10}$$

Here X is the cardinal number of the correlation-consistent basis set.

For range-separated methods the situation is less clear. Very recently, Franck *et al.* have proposed a three-point scheme based on an exponential formula,[61] but we feel that further study is required to settle this issue and have not applied the proposed scheme in the present work.

3 Computational details

We performed all calculations with a development version of the DIRAC-13 quantum chemistry package.[62] Unless otherwise stated all calculations are based on the 2-component relativistic $X2C_{mmf}^{DC}$ Hamiltonian.[42] A Gaussian nuclear model has been chosen for the nuclei.[63] We applied uncontracted large-component basis sets of Dyall-type[64,65] including core-correlating and diffuse functions up to quadruple-ζ quality (the highest available set). The corresponding small component basis set is generated using the restricted kinetic balance condition.

In our range-separated DFT studies a short-range LDA exchange–correlation functional was used for all cases.[66,67] We have chosen a system-independent fixed value $0.4a_0^{-1}$ as our range separation parameter (μ), following the suggestion by Fromager *et al.*[68]

Spectroscopic constants have been derived by a least square fit of the potential energy curve (PEC) to a polynomial using the

TWOFIT utility program available in DIRAC. Throughout this study, we have chosen nine grid points and fitted them against an eighth-degree polynomial. The grid has been generated inside the classical turning points of the PEC. For Xe_2 the grid was generated around the experimental equilibrium bond length, whereas for the heavier dimers we used the best estimate from previous studies.

4 Results and discussion

4.1 Calibration study

We first carried out a calibration study of the xenon dimer with the goal to define a suitable computational protocol in terms of (i) the correlation method, (ii) the number of active occupied orbitals and (iii) the basis set level. We consider the convergence of spectroscopic constants with respect to these parameters rather than their agreement with experimental values in order to avoid getting the right result for the wrong reason. Throughout the calibration study, we compared results of two augmented correlation-consistent basis sets for relativistic calculations provided with the DIRAC package, namely dyall.acv3z (TZ) and dyall.acv4z (QZ).[64] Subsequently, we extrapolated the pure WFT data to the complete basis set limit using eqn (10). The basis set superposition error (BSSE) was addressed by means of the counterpoise correction approach.[69] MP2, CCSD and CCSD(T) have been considered for the correlation treatment and analyzed to ascertain what is sufficient to yield properly converged data. To determine a minimal yet physically accurate active occupied orbital space we have systematically increased our correlation space from valence 5s5p to subvalence 4s4p4d. We used for the xenon dimer an energy cutoff in the virtual space of 40 E_h, but a Mulliken population analysis was carried out in order to ensure that all correlating functions were retained.

Table 1 comprises our results for the equilibrium bond length (r_e), the harmonic frequency (ω_e) and the dissociation energy (D_e) of the xenon dimer. Compared to the QZ basis set calculations with the TZ basis set yield a significant elongation of r_e (>0.1 Å), lowering of harmonic frequencies of $\sim$2–3 cm^{-1} and D_e's reduced by 20%. We are unable to determine to what extent our results are converged at the QZ level, since no Dyall basis sets with a higher cardinal number are available. However, upon basis set extrapolation we find, as summarized in Table 1, that the extrapolated results are significantly different from the results obtained with the QZ basis set. We have therefore systematically performed the same extrapolation technique for the radon and eka-radon dimers in our subsequent pure WFT correlation calculations.

Table 1 further shows that even in the extrapolated basis set limit there is a significant spread in the spectroscopic constants obtained by MP2, CCSD and CCSD(T). In fact, we find that MP2 and CCSD in the best basis indeed over- and underbinds the xenon dimer, respectively, in agreement with previous findings (*cf.* Section 2.2). Therefore, we conclude that we cannot compromise with any lower-level method, but have to use the CCSD(T) method. As shown by Table 1, the deviations of the spectroscopic constants (r_e, ω_e, and D_e) with respect to their values derived from experiments are then (0.017 Å, 0.8 cm^{-1}, and 12 cm^{-1}), respectively, which are quite satisfying.

The effect of correlating sub-valence and outer-core shells can be determined from the CCSD(T)/QZ results outlined in Table 1. Adding the 4d shell to the occupied correlation space of the 5s5p valence shells changes (r_e, ω_e, and D_e) by (−0.04 Å, 0.81 cm^{-1}, and 13.13 cm^{-1}), whereas the addition of the 4s4p shells has hardly any effect. This indicates that saturation with respect to correlated orbitals can to a great extent be reached by including the $(n-1)$d-shell in addition to the $nsnp$ valence shell of a given noble gas. In subsequent calculations we have therefore correlated $(n-1)dnsnp$.

A final issue to be addressed is whether BSSE-corrected results are to be used or not. BSSE typically leads to overbinding in that the atoms in the dimer calculation benefit from the presence of the basis set of the other atom. Counterpoise-corrected interaction energies for homoatomic dimers A_2 are given by

$$\Delta E_{\mathrm{int}} = E^{\mathrm{A}_2}_{\mathrm{A}_2} - 2E^{\mathrm{A}}_{\mathrm{A}} + \Delta\mathrm{BSSE};\ \Delta\mathrm{BSSE} = 2\left(E^{\mathrm{A}}_{\mathrm{A}} - E^{\mathrm{AGh}}_{\mathrm{A}}\right), \quad (11)$$

where atomic energies $E^{\mathrm{AGh}}_{\mathrm{A}}$ have been calculated in the full molecular basis by introducing a ghost (Gh) center at the position of the second atom. The usefulness of the counterpoise correction has been challenged in two recent papers by Baerends and co-workers.[70,71] They have carried out benchmark calculations of the helium and beryllium dimers and find that uncorrected interaction energies overall compare better with (ideally) basis set free reference numbers. They point out that basis set incompleteness is more severe for the dimer than the atom, an imbalance which is aggravated by the improvement of the monomer basis in counterpoise-corrected calculations. Clearly, in a complete basis $E^{\mathrm{A}}_{\mathrm{A}} = E^{\mathrm{AGh}}_{\mathrm{A}}$, but this limit is not ensured by basis set extrapolation, an issue not discussed by Baerends and co-workers. Indeed, by analysis of their data we find that in general ΔBSSE is significantly different from zero in the extrapolated basis set limit. From the expected faster convergence of $E^{\mathrm{AGh}}_{\mathrm{A}}$ with respect to $E^{\mathrm{A}}_{\mathrm{A}}$ one may expect that the correlation contribution to ΔBSSE is positive in the extrapolated limit, but curiously this is not always what we observe. Looking at our own data we find that the CP-uncorrected CCSD(T) results agree best with experiment in any finite basis, but not in the extrapolated basis set limit. We have therefore chosen our computational protocol to be based on counterpoise-corrected CCSD(T) interaction energies extrapolated to the basis set limit.

Let us now turn to the range-separated approach. Table 1 summarizes the performance of lrWFT-srLDA methods for the xenon dimer. The calculated spectroscopic constants are less sensitive with respect to the choice of the basis set as compared to the pure WFT calculations, but the effect is not negligible: the difference between the TZ and QZ basis sets is for either correlation approach on the order of (0.03 Å, 1.2 cm^{-1}, 20 cm^{-1}) for (r_e, ω_e, D_e), respectively. This means in turn that a QZ basis

Table 1 Spectroscopic constants for the xenon dimer. dyall.acv∞z refers to the extrapolated basis using eqn (10) with $X = 4$. CP refers to counterpoise correction. ECP stands for effective core potential. Bold numbers are best numbers for each choice of the Hamiltonian and the method

Method	Correlating orbitals	Hamiltonian	Basis	r_e/Å	ω_e/cm^{-1}	D_e/cm^{-1}	CP
MP2	5s5p	X2C$^{DC}_{mmf}$	dyall.acv3z	4.491	18.01	165.16	x
			dyall.acv4z	4.392	20.76	204.48	x
CCSD			dyall.acv3z	4.673	13.98	98.43	x
			dyall.acv4z	4.564	15.99	120.98	x
CCSD(T)			dyall.acv3z	4.585	15.81	127.20	x
			dyall.acv4z	4.465	18.67	162.62	x
MP2-srLDA			dyall.acv3z	4.431	18.54	173.54	x
			dyall.acv4z	4.404	19.56	189.98	x
CCSD-srLDA			dyall.acv3z	4.440	18.37	171.40	x
			dyall.acv4z	4.408	19.55	190.69	x
CCSD(T)-srLDA			dyall.acv3z	4.429	18.75	179.28	x
			dyall.acv4z	4.396	19.99	200.49	x
MP2	4d5s5p	X2C$^{DC}_{mmf}$	dyall.acv3z	4.375	20.64	213.90	x
				4.349	21.40	230.88	
			dyall.acv4z	4.275	23.87	267.32	x
				4.250	24.68	283.57	
			dyall.acv∞z	4.213	26.21	311.14	x
				4.187	27.16	327.80	
CCSD			dyall.acv3z	4.644	14.19	102.15	x
				4.610	14.96	112.81	
			dyall.acv4z	4.536	16.30	124.95	x
				4.510	16.85	132.95	
			dyall.acv∞z	4.466	17.99	144.53	x
				4.444	18.41	151.01	
CCSD(T)			dyall.acv3z	4.540	16.52	137.53	x
				4.508	17.40	151.13	
			dyall.acv4z	4.421	19.48	175.75	x
				4.396	20.11	186.64	
			dyall.acv∞z	**4.346**	**21.73**	**208.69**	x
				4.324	22.28	217.67	
MP2-srLDA			dyall.acv3z	4.364	20.58	213.29	x
			dyall.acv4z	4.337	21.70	233.59	x
CCSD-srLDA			dyall.acv3z	4.399	19.54	193.04	x
			dyall.acv4z	4.367	20.78	215.03	x
CCSD(T)-srLDA			dyall.acv3z	4.388	19.93	201.65	x
			dyall.acv4z	**4.355**	**21.25**	**225.76**	x
MP2	4s4p4d5s5p	X2C$^{DC}_{mmf}$	dyall.acv3z	4.373	20.71	214.94	x
			dyall.acv4z	4.272	23.94	268.91	x
CCSD			dyall.acv3z	4.646	14.17	101.96	x
			dyall.acv4z	4.537	16.26	124.51	x
CCSD(T)			dyall.acv3z	4.540	16.55	138.01	x
			dyall.acv4z	4.420	19.49	176.17	x
MP2-srLDA			dyall.acv3z	4.362	20.64	214.42	x
CCSD-srLDA			dyall.acv3z	4.398	19.58	193.73	x
CCSD(T)-srLDA			dyall.acv3z	4.386	19.97	202.36	x
CCSD(T)	4d5s5p	X2C$^{DCG}_{mmf}$	dyall.acv4z	4.422	19.49	176.14	x
			dyall.acv∞z	**4.347**	**21.74**	**209.17**	x
MP2-srLDA[32]	4d5s5p	DC	dyall.acv4z	4.337	21.7	233.6	x
CCSD(T)[29]	5s5p	ECP46MWB[78]	"Basis 2"	4.525	17.6	156.5	x
CCSD(T)-srPBE[16]	5s5p	ECP28MDF[84]	aug-cc-pVQZ	4.334	20.5	197.5	x
Exp.[83]				*4.363*	*20.90*	*196.20*	

set is required to achieve sufficient accuracy. We next observe, in agreement with previous findings,[16] that the valence-only results for the range-separated methods are in closer agreement with the experimental references than those of their pure WFT counterparts. However, with the inclusion of the 4d shell in the occupied correlation space numbers change significantly: ($\geq$0.04 Å, $\geq$1.2 cm^{-1}, and $\geq$25 cm^{-1}) for (r_e, ω_e, and D_e), respectively. We therefore conclude that similar to the pure WFT case the addition of the $(n-1)$d shell to the active correlation is required for the WFT-srDFT methods. Also upon correlation of the subvalence we observe a better convergence of the results with regard to the pure WFT correlation model, in particular for CCSD. Still, lrCCSD(T)-srLDA notably outperforms all other methods while showing a consistent behavior with increasing basis set size and correlation space. The lrCCSD(T)-srLDA approach combined with a QZ basis set thus yields

spectroscopic constants within (0.009 Å, 0.5 cm^{-1}, 15 cm^{-1}) for (r_e, ω_e, D_e) of the pure wave function CCSD(T)/CBS reference data. We therefore conclude that lrCCSD(T)-srLDA is indeed a very promising approach for the description of dispersion-bound molecules. We do observe a faster convergence of results with respect to computational parameters, in particular less sensitivity to the inclusion of triple excitations, but not enough to warrant the use of a less expensive computational protocol.

4.2 Rn_2 and Uuo_2

Based on the calibration study discussed in detail in the previous section our computational protocol for the subsequent study of the Rn_2 and Uuo_2 dimers comprises the correlation of the occupied $(n-1)$dnsnp shells using the best basis set available, an augmented correlation-consistent QZ basis set. The energy cutoffs in the virtual space were set to 46 and 40 E_h, respectively, for the radon and eka-radon dimers. In the case of the pure WFT methods we also carry out extrapolation to the basis set limit according to eqn (10).

Table 2 shows our results for the Rn-dimer at the CCSD(T) level, both for the QZ basis set and extrapolated to the basis set limit. The corresponding lrWFT-srDFT/QZ data show very close agreement with the pure WFT CCSD(T)/CBS data. The same conclusion holds for the spectroscopic constants of the eka-radon dimer, which are shown in Table 3. Two remarkable features should be noted: (i) when including the spin-other orbit interaction through the $X2C_{mmf}^{DCG}$ Hamiltonian, the dissociation energy of eka-Rn_2 is reduced by about 40%, whereas the effect of this interaction is almost negligible for the lighter homologues. We would like to stress that whereas previous studies have demonstrated considerable weakening of covalent bonds by spin–orbit interaction,[72–77] the present study concerns bonds arising from London dispersion forces and where a substantial weakening is observed upon introduction of a component of the two-electron interaction often ignored in relativistic molecular calculations, namely the spin-other orbit interaction. This is new and merits further study. (ii) In spite of the very significant weakening of the eka-Rn_2 bond by inclusion of the Gaunt term, the bond is still markedly stronger than for the lighter homologues, as seen in Fig. 1, albeit absent at the HF level.

In Tables 2 and 3 we have listed some results of previous studies. We note that the lrMP2-srDFT spectroscopic constants of Kullie and Saue[32] are in line with the present benchmark values, while this is not the case for the values reported by Runeberg and Pyykkö[29] and by Nash.[30] Runeberg and Pyykkö[29] employed large-core pseudo-potentials,[78,79] calibrated against atomic HF calculations based on the Wood–Boring Hamiltonian[80] using an effective spin–orbit operator. Only valence nsnp electrons were treated explicitly and described by a specially designed basis. By comparison with the all-electron basis sets of Dyall we find that the "Basis 2" of Runeberg and Pyykkö is of augmented correlation-consistent TZ quality. Their results are therefore not converged with respect to the basis set and correlated orbitals. Nash[30] employs small-core pseudopotentials[81,82] calibrated against atomic HF calculations based on the Dirac–Coulomb Hamiltonian. Although Nash correlates with $(n-1)$s$(n-1)$p$(n-1)$dnsnp electrons, his 6sd6p2pf1g valence basis is clearly too small. Runeberg and Pyykkö[29] as well as Nash[30] include spin–orbit interaction in their calculations, but not spin-other orbit interaction, which we have seen is critical for the appropriate description of bonding in eka-Rn_2.

Table 2 Spectroscopic constants for the radon dimer. dyall.acv∞z refers to extrapolated basis using eqn (10) with $X = 4$. CP refers to counterpoise correction. ECP stands for effective core potential. Bold numbers are best numbers for each choice of the Hamiltonian and the method

Method	Correlating orbitals	Hamiltonian	Basis	r_e/Å	ω_e/cm^{-1}	D_e/cm^{-1}	CP
MP2	5d6s6p	$X2C_{mmf}^{DC}$	dyall.acv4z	4.343	20.47	364.40	x
				4.323	21.04	385.70	
			dyall.acv∞z	4.280	22.43	427.31	x
				4.263	23.01	449.82	
CCSD			dyall.acv4z	4.617	13.93	168.56	x
				4.596	14.42	179.55	
			dyall.acv∞z	4.617	15.45	197.25	x
				4.528	15.91	207.22	
CCSD(T)			dyall.acv4z	4.502	16.56	235.56	x
				4.483	17.06	249.70	
			dyall.acv∞z	**4.424**	**18.54**	**282.80**	x
				4.412	18.97	294.95	
MP2-srLDA			dyall.acv4z	4.388	19.06	323.68	x
CCSD-srLDA			dyall.acv4z	4.432	17.87	284.73	x
CCSD(T)-srLDA			dyall.acv4z	**4.418**	**18.31**	**301.02**	x
MP2	5d6s6p	$X2C_{mmf}^{DCG}$	dyall.acv4z	4.346	20.49	363.58	x
			dyall.acv∞z	4.282	22.46	426.99	x
CCSD			dyall.acv4z	4.621	13.91	166.65	x
			dyall.acv∞z	4.547	15.44	195.57	x
CCSD(T)			dyall.acv4z	4.506	16.55	233.82	x
			dyall.acv∞z	**4.427**	**18.53**	**281.41**	x
PBE[31]	All	DC		4.646	15	193.6	
MP2-srLDA[32]	5d6s6p	DC	dyall.acv4z	4.387	19.0	323.9	x
CCSD(T)[29]	6s6p	ECP78MWB[79]	"Basis 2"	4.639	14.9	222.6	x
CCSD(T)[30]	5s5p5d6s6p	RECP60(DC)[81]	6sd6p2pf1g	4.73		129.1	

Table 3 Spectroscopic constants for the eka-radon dimer dyall.acv∞z refers to extrapolated basis using eqn (10) with $X = 4$. CP refers to counterpoise correction. ECP stands for effective core potential. Bold numbers are best numbers for each choice of the Hamiltonian and the method

Method	Correlating orbitals	Hamiltonian	Basis	r_e/Å	ω_e/cm^{-1}	D_e/cm^{-1}	CP
MP2	6d7s7p	X2C$^{DC}_{mmf}$	dyall.acv4z	4.184	26.52	1258.87	x
				4.169	27.60	1286.93	
			dyall.acv∞z	4.136	28.11	1389.73	x
				4.130	28.43	1400.40	
CCSD			dyall.acv4z	4.435	18.85	765.65	x
				4.424	19.55	777.00	
			dyall.acv∞z	4.383	20.13	832.78	x
				4.380	19.87	832.28	
CCSD(T)			dyall.acv4z	4.338	21.70	927.73	x
				4.327	22.51	942.52	
			dyall.acv∞z	**4.280**	**23.39**	**1033.53**	x
				4.280	23.45	1032.71	
MP2-srLDA			dyall.acv4z	4.205	25.51	1198.53	x
CCSD-srLDA			dyall.acv4z	4.254	23.77	1075.93	x
CCSD(T)-srLDA			dyall.acv4z	**4.240**	**24.32**	**1121.05**	x
MP2	6d7s7p	X2C$^{DCG}_{mmf}$	dyall.acv4z	4.223	25.00	840.59	x
			dyall.acv∞z	4.172	26.67	966.61	x
CCSD			dyall.acv4z	4.503	17.02	372.01	x
			dyall.acv∞z	4.445	18.27	434.14	x
CCSD(T)			dyall.acv4z	4.393	19.94	524.18	x
			dyall.acv∞z	**4.329**	**21.74**	**624.24**	x
PBE[31]	All	DC		4.375	20	427.5	
MP2-srLDA[32]	6d7s7p	DC	dyall.acv4z	4.205	26.3	1199.1	x
CCSD(T)[30]	6s6p6d7s7p	RECP92(DC)[82]	6sd6p2pf1g	4.57		500.1	

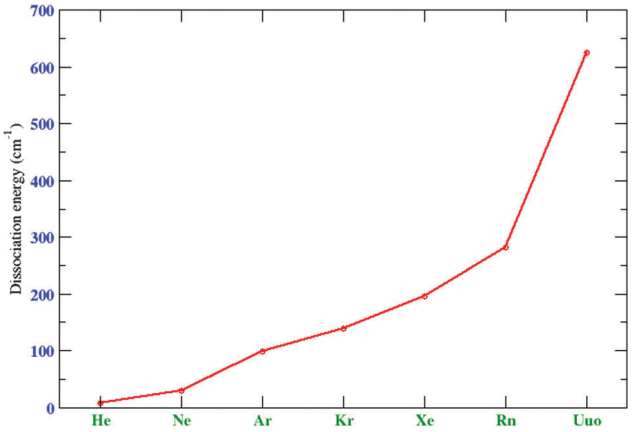

Fig. 1 Dissociation energies D_e (in cm^{-1}) for the homonuclear rare gas dimers. The first five data points are derived from experiment,[83] whereas the final two points correspond to the values obtained in the present work with the X2C$^{DCG}_{mmf}$ Hamiltonian at the CCSD(T) level and extrapolated to the basis set limit.

5 Summary and outlook

We have reported spectroscopic parameters for the homoatomic dimers of xenon, radon and eka-radon obtained with the eXact 2-Component (X2C) molecular-mean field Hamiltonian at the CCSD(T) level and extrapolated to the complete basis set limit, at which counterpoise corrected results seem to be more reliable than uncorrected ones. We also report the very first lrCC-srDFT implementation at the 2-and 4-component relativistic level. The lrCCSD(T)-srLDA/QZ results are in general in rather close agreement with the CCSD(T)/CBS results. Although we observe a somewhat faster convergence of the range-separated results with respect to the number of correlating orbitals, the choice of the basis set and, in particular, inclusion of triples, in practice this does not allow us to proceed with a computationally less expensive protocol.

Our results confirm the previous lrMP2-srDFT numbers reported by Kullie and Saue,[32] notably an almost fourfold increase at the DC level of the binding energy in going from the radon to the eka-radon dimer. However, we also find that the dissociation energy of the eka-Rn_2 dimer is reduced by about 40% upon the inclusion of spin-other orbit interaction. Yet the bonding in the eka-Rn_2 dimer is markedly stronger than in the lighter homologues. This may suggest contributions of covalent bonding to the bonding picture, which clearly deserves further attention, although we find that Uuo_2 is unbound at the HF level. It will therefore be interesting to study the bulk behavior of this superheavy element.

Acknowledgements

This work is financially supported by Indo-French Centre for the Promotion of Advanced Research (IFCPAR). We are thankful to CALMIP (Calcul en Midi-Pyrénées) for the computation time. Helpful discussions with Debashis Mukherjee (Kolkata) and Lucas Visscher (Amsterdam) are acknowledged.

References

1 P. Hobza and R. Zahradnik, *Chem. Rev.*, 1988, **88**, 871–897.
2 M. Pitoňák, P. Neogrády, J. Černý, S. Grimme and P. Hobza, *ChemPhysChem*, 2009, **10**, 282–289.
3 S. Grimme, *J. Chem. Phys.*, 2003, **118**, 9095–9102.

4 K. Burke, *J. Chem. Phys.*, 2012, **136**, 150901.
5 S. Kristyán and P. Pulay, *Chem. Phys. Lett.*, 1994, **229**, 175–180.
6 P. Hobza, J. Šponer and T. Reschel, *J. Comput. Chem.*, 1995, **16**, 1315–1325.
7 E. R. Johnson and A. D. Becke, *J. Chem. Phys.*, 2005, **123**, 024101.
8 A. Tkatchenko and M. Scheffler, *Phys. Rev. Lett.*, 2009, **102**, 073005.
9 T. Sato and H. Nakai, *J. Chem. Phys.*, 2009, **131**, 224104.
10 S. Grimme, J. Antony, S. Ehrlich and H. Krieg, *J. Chem. Phys.*, 2010, **132**, 154104.
11 S. Grimme, *Wiley Interdiscip. Rev.: Comput. Mol. Sci.*, 2011, **1**, 211–228.
12 J. Klimeš and A. Michaelides, *J. Chem. Phys.*, 2012, **137**, 120901.
13 C. Corminboeuf, *Acc. Chem. Res.*, 2014, **47**, 3217–3224.
14 N. Mardirossian and M. Head-Gordon, *J. Chem. Phys.*, 2014, **140**, 18A527.
15 A. Savin, *Recent developments of modern density functional theory*, Elsevier, Amsterdam, 1996, pp. 327–357.
16 E. Goll, H.-J. Werner and H. Stoll, *Phys. Chem. Chem. Phys.*, 2005, **7**, 3917–3923.
17 T. Van Mourik, A. K. Wilson and T. H. Dunning, *Mol. Phys.*, 1999, **96**, 529–547.
18 T. van Mourik and R. J. Gdanitz, *J. Chem. Phys.*, 2002, **116**, 9620–9623.
19 P. Slavek, R. Kalus, P. Paška, I. Odvárková, P. Hobza and A. Malijevský, *J. Chem. Phys.*, 2003, **119**, 2102–2119.
20 R. Hellmann, E. Bich and E. Vogel, *Mol. Phys.*, 2008, **106**, 133–140.
21 B. Jäger, R. Hellmann, E. Bich and E. Vogel, *Mol. Phys.*, 2009, **107**, 2181–2188.
22 A. Tkatchenko, R. A. DiStasio, M. Head-Gordon and M. Scheffler, *J. Chem. Phys.*, 2009, **131**, 094106.
23 M. Przybytek, W. Cencek, J. Komasa, G. Łach, B. Jeziorski and K. Szalewicz, *Phys. Rev. Lett.*, 2010, **104**, 183003.
24 K. Patkowski and K. Szalewicz, *J. Chem. Phys.*, 2010, **133**, 094304.
25 K. Patkowski, *J. Chem. Phys.*, 2012, **137**, 034103.
26 D. Roy, M. Marianski, N. T. Maitra and J. J. Dannenberg, *J. Chem. Phys.*, 2012, **137**, 134109.
27 W. Cencek, M. Przybytek, J. Komasa, J. B. Mehl, B. Jeziorski and K. Szalewicz, *J. Chem. Phys.*, 2012, **136**, 224303.
28 F. Tran and J. Hutter, *J. Chem. Phys.*, 2013, **138**, 204103.
29 N. Runeberg and P. Pyykkö, *Int. J. Quantum Chem.*, 1998, **66**, 131–140.
30 C. S. Nash, *J. Phys. Chem. A*, 2005, **109**, 3493–3500.
31 V. Pershina, A. Borschevsky, J. Anton and T. Jacob, *J. Chem. Phys.*, 2010, **132**, 194314.
32 O. Kullie and T. Saue, *Chem. Phys.*, 2012, **395**, 54–62.
33 V. V. Avrorin, R. N. Krasikova, V. D. Nefedov and M. A. Toropova, *Russ. Chem. Rev.*, 1982, **51**, 12.
34 L. Stein, *Radiochim. Acta*, 1983, **32**, 163–172.
35 B. F. Thornton and S. C. Burdette, *Nat. Chem.*, 2013, **5**, 804.
36 Y. Oganessian, V. Utyonkov, Y. Lobanov, F. Abdullin, A. Polyakov, R. Sagaidak, I. Shirokovsky, Y. Tsyganov, A. Voinov, G. Gulbekian, S. Bogomolov, B. Gikal, A. Mezentsev, S. Iliev, V. Subbotin, A. Sukhov, K. Subotic, V. Zagrebaev, G. Vostokin, M. Itkis, K. Moody, J. Patin, D. Shaughnessy, M. Stoyer, N. Stoyer, P. Wilk, J. Kenneally, J. Landrum, J. Wild and R. Lougheed, *Phys. Rev. C: Nucl. Phys.*, 2006, **74**, 044602.
37 F. P. Heßberger, *ChemPhysChem*, 2013, **14**, 483–489.
38 A. Türler and V. Pershina, *Chem. Rev.*, 2013, **113**, 1237–1312.
39 M. Schädel, *Radiochim. Acta*, 2012, **100**, 579–604.
40 *The Chemistry of Superheavy Elements*, ed. M. Schädel and D. Shaughnessy, Springer, Heidelberg, 2014.
41 T. Saue, *ChemPhysChem*, 2011, **12**, 3077–3094.
42 J. Sikkema, L. Visscher, T. Saue and M. Ilias, *J. Chem. Phys.*, 2009, **131**, 124116.
43 E. J. Baerends, W. H. E. Schwarz, P. Schwerdtfeger and J. G. Snijders, *J. Phys. B: At., Mol. Opt. Phys.*, 1990, **23**, 3225.
44 V. Kellö and A. J. Sadlej, *Int. J. Quantum Chem.*, 1998, **68**, 159–174.
45 K. G. Dyall, *Int. J. Quantum Chem.*, 2000, **78**, 412–421.
46 S. M. Cybulski and M. L. Lytle, *J. Chem. Phys.*, 2007, **127**, 141102.
47 A. Hesselmann, *J. Chem. Phys.*, 2008, **128**, 144112.
48 A. Szabo and N. S. Ostlund, *J. Chem. Phys.*, 1977, **67**, 4351–4360.
49 B. W. Hopkins and G. S. Tschumper, *J. Phys. Chem. A*, 2004, **108**, 2941–2948.
50 A. V. Copan, A. Y. Sokolov and H. F. Schaefer, *J. Chem. Theory Comput.*, 2014, **10**, 2389–2398.
51 K. E. Riley, M. Pitoňák, P. Jurečka and P. Hobza, *Chem. Rev.*, 2010, **110**, 5023–5063.
52 J. Řezáč, K. E. Riley and P. Hobza, *J. Chem. Theory Comput.*, 2011, **7**, 2427–2438.
53 J. Řezáč, K. E. Riley and P. Hobza, *J. Chem. Theory Comput.*, 2011, **7**, 3466–3470.
54 W. Yang, *J. Chem. Phys.*, 1998, **109**, 10107–10110.
55 J. K. Pedersen, PhD dissertation, Department of Chemistry, University of Southern Denmark, 2004.
56 I. C. Gerber and J. G. Ángyán, *Chem. Phys. Lett.*, 2005, **415**, 100–105.
57 E. Fromager and H. J. A. Jensen, *Phys. Rev. A: At., Mol., Opt. Phys.*, 2008, **78**, 022504.
58 J. G. Ángyán, *Phys. Rev. A: At., Mol., Opt. Phys.*, 2008, **78**, 022510.
59 T. Helgaker, W. Klopper, H. Koch and J. Noga, *J. Chem. Phys.*, 1997, **106**, 9639.
60 A. Halkier, T. Helgaker, P. Jörgensen, W. Klopper, H. Koch, J. Olsen and A. K. Wilson, *Chem. Phys. Lett.*, 1998, **286**, 243–252.
61 O. Franck, B. Mussard, E. Luppi and J. Toulouse, *J. Chem. Phys.*, 2015, **142**, 074107.
62 DIRAC, a relativistic *ab initio* electronic structure program, Release DIRAC13 (2013), written by L. Visscher, H. J. Aa. Jensen, R. Bast and T. Saue, with contributions from V. Bakken, K. G. Dyall, S. Dubillard, U. Ekström, E. Eliav, T. Enevoldsen, E. Fahauer, T. Fleig, O. Fossgaard, A. S. P. Gomes, T. Helgaker, J. K. Lrdahl, Y. S. Lee, J. Henriksson,

M. Iliaš, Ch. R. Jacob, S. Knecht, S. Komorovský, O. Kullie, C. V. Larsen, H. S. Nataraj, P. Norman, G. Olejniczak, J. Olsen, Y. C. Park, J. K. Pedersen, M. Pernpointner, K. Ruud, P. Saek, B. Schimmelpfennig, J. Sikkema, A. J. Thorvaldsen, J. Thyssen, J. van Stralen, S. Villaume, O. Visser, T. Winther and S. Yamamoto, see http://www.diracprogram.org.

63 L. Visscher and K. G. Dyall, *At. Data Nucl. Data Tables*, 1997, **67**, 2007.

64 K. Dyall, *Theor. Chem. Acc.*, 2006, **115**, 441–447.

65 K. Dyall, *Theor. Chem. Acc.*, 2012, **131**, 1172.

66 P. M. W. Gill, R. D. Adamson and J. Pople, *Mol. Phys.*, 1996, **88**, 1005.

67 J. Toulouse, A. Savin and H.-J. Flad, *Int. J. Quantum Chem.*, 2004, **100**, 1047–1056.

68 E. Fromager, J. Toulouse and H. J. A. Jensen, *J. Chem. Phys.*, 2007, **126**, 074111.

69 S. Boys and F. Bernardi, *Mol. Phys.*, 1970, **19**, 553–566.

70 X. W. Sheng, L. Mentel, O. V. Gritsenko and E. J. Baerends, *J. Comput. Chem.*, 2011, **32**, 2896–2901.

71 L. M. Mentel and E. J. Baerends, *J. Chem. Theory Comput.*, 2014, **10**, 252–267.

72 P. A. Christiansen and K. S. Pitzer, *J. Chem. Phys.*, 1981, **74**, 1162.

73 P. Hafner, P. Habitz, Y. Ishikawa, E. Wechsel-Trakowski and W. H. E. Schwarz, *Chem. Phys. Lett.*, 1981, **80**, 311.

74 T. Saue, K. Fægri and O. Gropen, *Chem. Phys. Lett.*, 1996, **263**, 360.

75 Y.-K. Han, C. Bae and Y. S. Lee, *J. Chem. Phys.*, 1999, **110**, 8969.

76 Y.-K. Han, C. Bae, S.-K. Son and Y. S. Lee, *J. Chem. Phys.*, 2000, **112**, 2684.

77 K. Faegri and T. Saue, *J. Chem. Phys.*, 2001, **115**, 2456.

78 A. Nicklass, M. Dolg, H. Stoll and H. Preuss, *J. Chem. Phys.*, 1995, **102**, 8942.

79 W. Küchle, M. Dolg, H. Stoll and H. Preuss, *Mol. Phys.*, 1991, **74**, 1245–1263.

80 J. H. Wood and A. M. Boring, *Phys. Rev. B: Solid State*, 1978, **18**, 2701–2711.

81 C. S. Nash and B. E. Bursten, *J. Phys. Chem. A*, 1999, **103**, 402–410.

82 C. S. Nash, B. E. Bursten and W. C. Ermler, *J. Chem. Phys.*, 1997, **106**, 5133–5142.

83 J. Ogilvie and F. Y. Wang, *J. Mol. Struct.*, 1992, **273**, 277–290.

84 K. A. Peterson, D. Figgen, E. Goll, H. Stoll and M. Dolg, *J. Chem. Phys.*, 2003, **119**, 11113–11123.

4.3.2. Paper II : 4-component relativistic calculations of L3 ionization and excitations for the isoelectronic species UO^{2+}, OUN^{+} and UN_2 (manuscript)

Christopher South, Avijit Shee, Debashis Mukherjee, Angela Wilson and Trond Saue

We have studied core-excitation and core-ionization spectra for three isoelectronic compounds of Uranium : UO^{2+}, OUN^{+} and UN_2. For the ionization study, electron removal has been considered from the $2p_{1/2}$ and $2p_{3/2}$ shells of uranium. At the uncorrelated level, we calculate ionization potential using ΔSCF method. For the correlation study, both DFT and ab-initio methods have been considered. Ab-initio study of the core-ionization was very difficult, since one needs to take into account various phenomena very accurately, which may or may not pertain to the present day ab-initio methodologies. Our primary investigation with Coupled Cluster method has lead to divergence of the amplitude equation. We therefore considered a less accurate ΔMP2 method, where optimized orbitals of individual states have been used. It was necessary to employ an open-shell MP2 code for the ionized state. That has been formulated and implemented in the context of DC Hamiltonian. We also analyzed one peculiar behaviour related to core-correlation, where total correlation contribution for a (N-1) elctronic system can be larger than the N electronic system.

The core-excitation spectra we generate is of L_3 edge X-ray absorption near edge structure (XANES) type. It was simulated by Restricted Excitation Window Time-Dependent Density Functional Theory (REW- TDDFT), Complex Polarization Propagator (CPP) and Static Exchange approximation (STEX) methods.

The Dirac-Coulomb Hamiltonian has been used for most of the methods. The contribution of Gaunt interaction has been investigated at the SCF level, which has been huge for these systems.

My major contribution in this work was to formulate, implement and apply the open-shell ΔMP2 method.

PCCP

PAPER

View Article Online
View Journal

Cite this: DOI: 10.1039/c6cp00262e

4-Component relativistic calculations of L_3 ionization and excitations for the isoelectronic species UO_2^{2+}, OUN^+ and UN_2

Christopher South,[a] Avijit Shee,[b] Debashis Mukherjee,[c] Angela K. Wilson[ad] and Trond Saue*[b]

Received 13th January 2016,
Accepted 5th February 2016

DOI: 10.1039/c6cp00262e

www.rsc.org/pccp

We present a 4-component relativistic study of uranium $2p_{3/2}$ ionization and excitation in the isoelectronic series UO_2^{2+}, OUN^+ and UN_2. We calculate ionization energies by ΔSCF at the Hartree–Fock (HF) and Kohn–Sham (KS) level of theory. At the ΔHF level we observe a perfectly linear chemical shift of ionization energies with respect to uranium atomic charges obtained from projection analysis. We have also developed a non-canonical 2nd-order Møller–Plesset code for wave function based correlation studies. We observe the well-known failure of Koopmans' theorem for core ionization due to the dominance of orbital relaxation over electron correlation effects. More unexpectedly, we find that the correlation contribution has the same sign as the relaxation contribution and show that this is due to a strong coupling of relaxation and correlation. We simulate uranium L_3 XANES spectra, dominated by $2p_{3/2} \rightarrow$ U6d transitions, by restricted excitation window time-dependent density functional theory (REW-TDDFT) and the complex polarization propagator (CPP) approach and demonstrate that they give identical spectra when the same Lorentz broadening is chosen. We also simulate XANES spectra by the Hartree–Fock based static exchange (STEX) method and show how STEX excitation energies can be reproduced by time-dependent Hartree–Fock calculations within the Tamm–Dancoff approximation. We furthermore show that Koopmans' theorem provide a correct approximation of ionization energies in the linear response regime and use this observation to align REW-TDDFT and CPP spectra with STEX ones. We point out that the STEX method affords the most detailed assignment of spectra since it employs virtual orbitals optimized for the selected core ionization. The calculated XANES spectra reflect the loss of bound virtual orbitals as the molecular charge is reduced along the isoelectronic series.

1 Introduction

Uranyl compounds are of great interest due to their unique coordination chemistry as well as their potential impact on the environment. Uranium has been shown to readily form a myriad of coordination complexes in three separate oxidation states (IV, V, and VI), though it tends to prefer the IV and VI oxidation states, resulting in its rich chemistry.[1–4] Because uranium (along with thorium, actinium, and protactinium) is one of the few actinide elements that is stable and safe enough to be characterized in a laboratory, this allows for the physical effects of the f orbitals on the electronic structure, geometry and thermochemistry to be determined experimentally, giving much insight on the electronic structure of uranyl coordination complexes.[5–15]

The electronic properties of uranyl coordination complexes, as well as the nature of the compounds themselves, have been determined through electronic spectroscopy and X-ray diffraction methods. X-ray absorbance and photoelectron spectroscopy have been frequently used to provide knowledge about the electronic structure of the deep core, which results in an element-specific electronic spectrum.[7] X-ray absorbance near edge spectroscopy (XANES) has been used to probe low-lying unoccupied core-ionized states of the uranyl complexes, returning energetics of the energy levels of the low-lying virtual orbitals, as well as information on the oxidation state of the molecule.[7,9,14,15] Walshe and coworkers used both high resolution XANES spectroscopy

[a] Department of Chemistry and Center for Advanced Scientific Computation and Modeling (CASCaM), University of North Texas, 1155 Union Circle #305070, Denton, TX 76203-5017, USA
[b] Laboratoire de Chimie et Physique Quantiques, UMR 5626 CNRS – Université Toulouse III-Paul Sabatier, 118 route de Narbonne, F-31062 Toulouse, France. E-mail: trond.saue@irsamc.ups-tlse.fr; Fax: +33 (0)561556031 (Trond Saue); Tel: +33 (0)561556065 (Trond Saue)
[c] Raman Center for Atomic, Molecular and Optical Sciences, Indian Association for the Cultivation of Science, Kolkata 700 032, India
[d] Department of Chemistry, Michigan State University, East Lansing, Michigan 48824-1322, USA

as well as extended X-ray absorbance fine structure (EXAFS) spectroscopy to characterize uranyl peroxides and uranyl oxo-hydroxides in their mineral forms and provided the first experimental crystal structure of metastudtite, as well as subtle differences in the core spectra of the mineral forms studied.[14] Given the highly local nature of the atomic core orbitals, the orbitals will be heavily affected by changes in the local electronic environment, such as relaxation effects which may be caused by changes in the formal oxidation state.

While uranium is not strongly radioactive (an alpha emitter with a half-life of over 44 billion years), it still presents a significant long term health risk, especially in a solvated form such as uranyl.[16] Computational modeling of uranium complexes circumvents this risk and has been used to model the thermochemistry and electronic structure of uranium coordination complexes.[12,17–32]

Analogous to experiment, computational chemistry can be used to calculate electronic transitions, allowing for the creation of electronic spectra from calculated excitation energies. Multi-reference computational methods have been used to directly solve for electronic states and transitions between states in the molecule.[23–25,28] Réal *et al.* compared preexisting CASPT2 electronic transitions of uranyl to intermediate Hamiltonian Fock space coupled cluster (IHFSCC) excitations and found that the two methods perform similarly for low level excitations, but the methods deviate from each other for higher excitation energies.[25] However, multi-reference methods scale unfavorably with the size of the system, and as a result, can only be utilized for the smallest of molecular systems. A commonly used alternative to multi-reference methods for the simulation of molecular spectra is time-dependent DFT (TDDFT), which have been used to great effect to calculate the electronic transitions in uranyl complexes.[23,33–35] Tecmer *et al.* performed TDDFT calculations to simulate the UV-Vis spectrum of uranyl as well as the isoelectronic analogues OUN^+ and UN_2. They found that among the functionals used, CAMB3LYP, M06, and PBE0 gave the lowest mean errors relative to IHFSCC, performing similarly to CASPT2 overall.[34] The complex polarization propagator (CPP) method[36–41] is similar to time-dependent methods, but explicitly accounts for the linewidth of the peaks *via* an imaginary damping factor which, when graphed, generates the spectrum. At the Hartree–Fock level, the static exchange approximation (STEX)[42–44] models core excitations as an electron being acted upon by the core-ionized molecule, the latter of which is optimized separately in order to give a complete account of the orbital relaxation in the molecule.

Accounting for relativistic effects is of great importance in calculations on actinide elements, especially in the calculation of properties of deep core orbitals as spin–orbit is incredibly strong for these orbitals. The most direct means of accounting for relativity is the full four-component Dirac–Coulomb (DC) Hamiltonian. The DC Hamiltonian gives a full account of the one-electron relativistic effects in a molecule, whereas the fully relativistic two-electron interaction is truncated, but includes the instantaneous Coulomb interaction as well as spin–own orbit interaction.[45] It has been used to calculate properties of uranyl and its complexes.[20,24,25] Relativistic effective core potentials (RECPs) are another means of accounting for relativistic effects for heavy atoms, and have been used frequently to recover these effects and to simplify the costly calculations involved.[12,18,23,25,26,32,35,46–49] Dolg and Cao developed a relativistic small core pseudopotential for uranium constructed from Dirac–Coulomb–Breit (DCB) orbitals, compared it to all-electron DKH calculations with perturbative spin–orbit (+BP), and noted that the vertical excitation energies agreed well with the values obtained at the all-electron level, at far reduced computational cost.[46] However, since the chemical core is simplified and treated by a simple function, part of the core-level description is lost and no core-level properties (such as core-ionization energies) can be calculated. The large and small component of the wave function can also be decoupled yielding two (or one) component Hamiltonians for the purpose of reducing computational cost relative to the full four-component calculation.[22,23,25,28,29,33] The eXact 2-Component relativistic Hamiltonian (X2C)[50–52] has been used by Réal *et al.* to calculate relativistic effects for uranyl compounds and has resulted in similar effectiveness to Dirac–Coulomb in the calculation of vertical excitation energies.[25] Klooster *et al.*[53] have reported calculations of X-ray photoelectron spectra, including U^{5+} using the analogous normalized elimination of the small component (NESC) Hamiltonian. Calculations on uranium compounds including scalar relativistic effects through the Darwin and mass-velocity terms have also been reported.[29,31]

Two isoelectronic homologues of uranyl have been synthesized, OUN^+ and UN_2, and have been characterized using experimental and theoretical methods.[23,31,32,34,47,54] Both of these molecules possess uranium in the +VI formal oxidation state and, analogous to uranyl, have also been shown to have linear structures.[17,23,26,29,31,32,34,47,48,55,56] The geometries and valence electronic spectra for these molecules have been determined computationally. However, less is known about the core spectra of these molecules from a theoretical standpoint.

Therefore, to classify and characterize these new molecules, we have in the present work simulated the uranium L_3 edge XANES spectrum for UO_2^{2+}, OUN^+ and UN_2 using restricted excitation window (REW) TDDFT, the CPP method, as well as STEX. We have also investigated the position of the uranium L_3 ionization threshold using both wave function and density functional methods. The paper is outlined as follows: in Section 2 we present the theory behind the methods employed in this work. In Section 3 we provide computational details and then, in Section 4, present and discuss our results. In Section 5 we provide conclusions and perspectives.

2 Theory

2.1 Core ionization

Koopmans' theorem[57] provides a reasonable estimate of valence ionization energies, although it is based on the difference of Hartree–Fock energies between the ionized and the parent state, using the orbitals of the parent state. There are accordingly two major sources of error, that is, (i) lack of orbital

Table 1 Valence and core ionization energies (in eV) of gaseous water obtained using the dyall.ae3z basis set

Method	$1b_1^{-1}$	$1a_1^{-1}$
Exp.[60,61]	12.61	539.7
Koopmans	13.84	560.1
ΔHF	11.05	539.6
ΔMP2	12.75	540.5
Δ_{relax}	−2.79	−20.5
Δ_{corr}	1.70	0.9

relaxation of the core-ionized state and (ii) lack of electron correlation:

$$\text{IP}_i(\text{M}) = -\varepsilon_i(\text{M}) + \Delta_{\text{relax}} + \Delta_{\text{corr}}.$$

The relaxation contribution Δ_{relax} ($-\Delta_{\text{relax}}$ is denoted the contraction error by Koopmans[57]) will be negative since orbital relaxation lowers the energy of the core-ionized state. The correlation contribution Δ_{corr} is, on the other hand, expected to be positive since there is one more electron to correlate in the parent state (see for instance ref. 58). In practice, for valence ionizations, the two contributions are found to be of the same order of magnitude, there by providing fortunate error cancellation, as illustrated for the HOMO ($1b_1$) ionization of the water molecule in Table 1. For core ionizations, on the other hand, the Koopmans estimate is known to be poor[59] since the correlation contribution is typically an order of magnitude smaller than the relaxation contribution, as seen in Table 1 for the $1a_1$ (oxygen 1s) ionization energy.

In the present work the correlation contribution is calculated by ΔMP2. The core-ionized state is first obtained by a Kramers restricted average-of-configuration Hartree–Fock (HF) calculation[62] starting from the orbitals of the parent state. Convergence is straightforward and obtained by first reordering the orbitals such that the target core orbital is in the position of the open shell and then kept there by overlap selection. This method has been used since the molecular ΔSCF calculations of Bagus and Schaefer,[63,64] but has more recently been rediscovered under the name Maximum Overlap Method by Gill and co-workers.[65] For the ΔMP2 calculation we have employed the RELCCSD module of DIRAC[66] which uses a Kramers unrestricted formalism[67] and thereby allows simple open-shell calculations. However, since the incoming molecular orbitals are optimized under Kramers restriction, the reconstructed Fock matrix for the core-ionized state is not diagonal and will have a non-zero occupied-virtual (ov) block. We have therefore extended the MP2 algorithm to handle this case. We start from the electronic Hamiltonian normal-ordered with respect to the Fermi vacuum defined by the current (Kramers restricted) orbital set

$$H_N = \sum_{pq} f_q^p \left\{ a_p^\dagger a_q \right\} + \frac{1}{4} \sum_{pqrs} V_{qs}^{pr} \left\{ a_p^\dagger a_r^\dagger a_s a_q \right\}; \quad V_{qs}^{pr} = \langle pr \parallel qs \rangle.$$

Following Lauderdale *et al.*,[68] we then define the zeroth-order Hamiltonian to be the diagonal blocks (oo and vv) of the Fock matrix. Setting up perturbation theory in a coupled cluster (CC) framework we subsequently derive the non-canonical MP2 energy

$$E^{\text{ncMP2}} = \sum_{ai} f_a^i t_i^{a(1)} + \frac{1}{4} \sum_{ij} \sum_{ab} V_{ab}^{ij} t_{ij}^{ab(1)}. \tag{1}$$

Here and in the following we employ indices i, j, k, l for occupied orbitals, a, b, c, d for virtual orbitals and p, q, r, s for general orbitals. The equations of the first-order CC amplitudes are

$$\sum_b f_b^a t_i^{b(1)} - \sum_j t_j^{a(1)} f_i^j = -f_i^a$$

$$\sum_c \left(f_c^b t_{ij}^{ac(1)} + f_c^a t_{ij}^{bc(1)} \right) - \sum_k \left(f_j^k t_{ik}^{ab(1)} + f_i^k t_{jk}^{ab(1)} \right) = -V_{ij}^{ab}.$$

Starting from these, one may show that the non-canonical MP2 energy is invariant under separate rotation of occupied and virtual orbitals. The equation for the first-order T_1-amplitudes may be recognized as the Sylvester equation and can therefore be solved in a direct fashion, but we have for convenience chosen to use the existing iterative scheme in RELCCSD for the solution of the amplitude equations.

2.2 Core excitation

In this work we are exploring three different methods for the calculation of core excitation spectra: restricted excitation window time-dependent density functional theory (REW-TDDFT), complex polarization propagator (CPP) and the static exchange approximation (STEX). In this section we give a brief presentation and comparison of these methods.

A common starting point for the three methods is the frequency-dependent linear response function which in the exact state formalism[69–71]

$$\langle\langle A; B \rangle\rangle_\omega = -\frac{1}{\hbar} \sum_{m>0} \left\{ \frac{A_m^* B_m}{\omega_m - \omega} + \frac{B_m^* A_m}{\omega_m + \omega} \right\} \tag{2}$$

involves an explicit sum over the excited states $|m\rangle$ of the zeroth-order Hamiltonian. In the above expression $\hbar\omega_m = E_m - E_0$ are excitation energies with respect to the unperturbed ground state $|0\rangle$ and $P_m = \langle m|\hat{H}_P|0\rangle$, ($P = A, B$) the corresponding transition moments with respect to property operator $\hat{H}_P$. In the present work we restrict ourselves to the electric dipole approximation, so that both property operators are limited to components of the electric dipole operator, although the short wave length of X-ray radiation may require the inclusion of terms beyond this approximation.[72,73] It is clear from the above expression that a scan of the linear response function through a frequency window will display poles corresponding to excitations in the range allowed by the property operators $\hat{H}_A$ and $\hat{H}_B$ and whose transition moments can be extracted from the residues. The singularities are unphysical, though, in that they correspond to infinitely long lifetimes of the excited states. This feature may be amended by the introduction of inverse lifetimes γ_m through the substitution $\omega_m \rightarrow \omega_m - i\gamma_m$ in the above expression (2). The response function then becomes generally complex, with the real part corresponding to refractive properties such as polarizabilities and the imaginary part associated with absorption processes.

Within the framework of Hartree–Fock and Kohn–Sham methods we may employ an exponential parametrization of orbitals (and thereby density and energy)

$$\varphi_i(\kappa) = \sum_a \varphi_a \exp[-\kappa]_{ai}; \quad \kappa_{pq} = -\kappa_{qp}^*$$

which allows for unconstrained optimization and straightforward identification of redundancies.[74–77] In the present case we restrict ourselves to closed-shell references in which only rotations between occupied and virtual orbitals, with amplitudes κ_{ai}, are non-redundant; all other amplitudes may therefore be set to zero. At the SCF level of theory the frequency-dependent linear response function may be formulated as

$$\langle\langle A;B\rangle\rangle_\omega = \mathbf{E}_A^{[1]\dagger}\mathbf{X}_B(\omega),$$

where the vector $\mathbf{X}_B(\omega)$ contains the first-order orbital rotation amplitudes

$$\mathbf{X}_B(\omega) = \begin{bmatrix} \mathbf{K}(\omega) \\ \mathbf{K}^*(-\omega) \end{bmatrix}; \quad K_{ai}(\omega) = \kappa_{ai}^{(1)}(\omega).$$

It is a solution of the linear response equation

$$(E_0^{[2]} - \hbar\omega S^{[2]})\mathbf{X}_B(\omega) = -\mathbf{E}_B^{[1]},$$

where appears the property gradient

$$\mathbf{E}_B^{[1]} = \begin{bmatrix} g \\ g^* \end{bmatrix}; \quad g_{ai} = -\langle\varphi_a|\hat{H}_B|\varphi_i\rangle$$

as well as the generalized metric $S^{[2]}$ and the electronic Hessian $E_0^{[2]}$, with structures

$$S^{[2]} = \begin{bmatrix} I & 0 \\ 0 & -I \end{bmatrix}; \quad E_0^{[2]} = \begin{bmatrix} A & B \\ B^* & A^* \end{bmatrix};$$

$$A_{ai,bj} = \left.\frac{\partial^2 E_0}{\partial\kappa_{ai}^*\partial\kappa_{bj}}\right|_{\boldsymbol{\kappa}=0}; \quad B_{ai,bj} = \left.\frac{\partial^2 E_0}{\partial\kappa_{ai}^*\partial\kappa_{bj}^*}\right|_{\boldsymbol{\kappa}=0} \tag{3}$$

Further discussion of the SCF linear response formalism can be for instance be found in ref. 69, 78 and 79. Since the SCF linear response function does not contain any sum over states, its complex extension can not be obtained by the introduction of state-specific inverse lifetimes γ_m. It is therefore common practice to employ a single damping parameter γ which can be interpreted as an imaginary extension of the perturbing frequency $\omega \to \omega + i\gamma$.[36–41] A relativistic implementation of complex response, including spin–orbit interaction, has been reported by Devarajan *et al.*[39] However, it is based on the zeroth order regular approximation (ZORA), which may not be very accurate for core excitations, as pointed out by the authors themselves. In the present contribution we employ the complex response implementation of the DIRAC code,[80] which can be used with the more accurate 4-component Dirac–Coulomb and eXact 2-Component (X2C) Hamiltonians. Working within the electric dipole approximation the isotropic oscillator strength f^{iso}, including a Lorentzian linewidth defined by the damping parameter γ, is obtained directly by a scan of the imaginary part of the isotropic electric dipole polarizability α^{iso} through the desired frequency window

$$f^{\text{iso}}(\omega) = \frac{2m\omega}{\pi e^2}\text{Im}\{\alpha^{\text{iso}}(\omega + i\gamma)\}.$$

Alternatively, excitation energies can be found by TDDFT (or TDHF), that is, by solving the generalized eigenvalue problem

$$(E_0^{[2]} - \hbar\omega_m S^{[2]})\mathbf{X}_m = 0.$$

An inconvenience with this approach is that excitation energies are typically found by a "bottom-up" approach, which becomes highly impractical for core excitations. A solution is to restrict the occupied orbitals entering the orbital rotation amplitudes $\{\kappa_{ai}\}$ to the desired core orbitals. This is referred to as the "restricted excitation window"[81] or "restricted channel"[82] approach. In the present work we employ the relativistic adiabatic TDDFT implementation reported by Bast *et al.*,[71] where restrictions are possible both on occupied and virtual orbitals, such that the extension to REW-TDDFT is straightforward.

Transition moments are found by contracting the eigenvectors $\mathbf{X}_m$ with the corresponding property gradient

$$P_m = \mathbf{X}_m^\dagger(\omega)\mathbf{E}_P^{[1]}.$$

The isotropic oscillator strength associated with excitation m is then obtained as

$$f_m^{\text{iso}} = \frac{2m\omega_m}{3\hbar e^2}\sum_{\alpha=x,y,z}\left|\mu_{m,\alpha}\right|^2. \tag{4}$$

Cumulated isotropic oscillator strengths, including a Lorentzian broadening Δ^{L}, are then obtained as

$$f^{\text{iso}}(\omega) = \sum_m f_m^{\text{iso}}\Delta^{\text{L}}(\omega;\omega_m,\gamma);$$

$$\Delta^{\text{L}}(\omega;\omega_m,\gamma) = \frac{1}{\gamma\pi}\left[\frac{\gamma^2}{(\omega-\omega_m)^2+\gamma^2}\right].$$

The resulting simulated spectra obtained by complex response and REW-TDDFT are expected to be identical to the extent that no other occupied orbitals are involved in the excitation processes with the selected frequency window (channel coupling) and to the extent that the REW-TDDFT calculation includes a sufficient number of excitations to cover the frequency window. In passing we note that upon a change of energy units the Lorentz-broadened oscillator strengths are scaled down by the same factor as the energy is scaled up, in order to conserve the integrated oscillator strength.

A third method investigated in the present work is the static exchange approximation (STEX). The name originated in the context of early theoretical investigations of the scattering of electrons by hydrogen atoms.[83,84] The two-electron wave function of the system was expanded in products of hydrogen atom orbitals and orbitals of the projectile electron.[85] The static exchange approximation was obtained by restricting the atomic orbital in this expansion to the ground state 1s orbital of the target hydrogen atom, thus neglecting polarization of the atomic charge density during collision, yet retaining exchange effects, shown by Morse and Allis in 1933 to have some importance upon scattering with slow electrons.[86] This is apparently the first STEX calculation. A further development was the observation by Hunt and Goddard[87] that the optimal virtual orbital φ_a in the otherwise frozen N-electron singly-excited determinant

Φ_i^a is obtained by diagonalization of the orbital-specific Fock operator

$$\hat{F}^{(N-i)} = \hat{h} + \sum_{j\neq i}^{N} \left(\hat{J}_j - \hat{K}_j\right)$$

where $\hat{J}_j$ and $\hat{K}_j$ are the usual Coulomb and exchange operators, respectively. The diagonalization is carried out in the space of virtual orbitals, thus keeping the occupied orbitals frozen. The assumption that the other occupied orbitals are hardly modified upon excitation is an instance of the STEX approximation, as pointed out by Langhoff.[88–90] The so-called improved virtual orbitals (IVO) generated in this manner contrasts with the canonical virtual HF orbitals generated from the usual Fock operator

$$\hat{F}^{N} = \hat{F}^{(N-i)} + \left(\hat{J}_i - \hat{K}_i\right)$$

and which are more appropriate for the $(N+1)$-electron system. Not surprisingly then, the orbital-specific Fock operator $\hat{F}^{(N-i)}$ is also the conventional Fock operator for the $(N-1)$-electron system obtained by removal of the occupied orbital φ_i from the system. Based on the above observations, Ågren and co-workers[42,43] proposed to extend the IVO approach to core excitations and notably to build the STEX operator $\hat{F}^{(N-i)}$ using the occupied orbitals of the corresponding core-ionized system, thus capturing orbital relaxation essentially missing in TD-DFT/HF. Transition moments are calculated between the parent ground state and the core excited states, the latter built from the core-ionized orbitals. Since two non-orthogonal orbital sets are used, special techniques, such as a cofactor expansion,[91] must be used. In the present work we are using the 4-component relativistic STEX implementation of Ekström *et al.*[92]

The core excitation energies obtained by a STEX calculation can be reproduced by a REW-TDHF calculation using the orbitals of the core-ionized system and invoking the Tamm–Dancoff approximation (TDA), that is, setting $B = 0$ in the electronic Hessian (3). If excitations are restricted to a single (core) orbital φ_i the elements of the remaining A block can be expressed as

$$A_{ai,bi} = \langle\tilde{\Phi}_i^a|\hat{H}^N|\tilde{\Phi}_i^b\rangle - \delta_{ab}\langle\tilde{\Phi}_0|\hat{H}^N|\tilde{\Phi}_0\rangle = \tilde{F}_{ab}^N - \delta_{ab}\tilde{F}_{ii}^N - \langle\tilde{a}\tilde{i}\|\tilde{b}\tilde{i}\rangle = \tilde{F}_{ab}^{N-i} - \delta_{ab}\tilde{F}_{ii}^{N-i},$$

In the above expression we employ the tilde symbol to indicate quantities calculated in the orbitals of the core-ionized system. Upon diagonalization of the A block, we obtain the eigenvalues of the orbital-specific Fock operator $\hat{F}^{(N-i)}$, shifted by $\tilde{F}_{ii}^{N-i}$, which can be recognized as the negative of the core ionization energy, calculated in the frozen orbitals of the core-ionized system, contrary to Koopmans' theorem, who uses the frozen orbitals of the parent system. It is corrected by rather using the ionization energy obtained by ΔSCF.

2.3 Projection analysis

In order to elucidate the electronic structure of the title species as well as to assign the simulated core excitation spectra we have performed projection analysis.[93] This method is akin to Mulliken population analysis, but the strong basis-set dependence of the latter method is avoided by expanding molecular orbitals in pre-calculated orbitals of the atoms constituting the molecule

$$|\psi_i\rangle = \sum_{Aj} \left|\psi_j^A\right\rangle c_{ji}^A + \left|\psi_i^{\mathrm{pol}}\right\rangle, \qquad (5)$$

where indices A and j refer to atoms and atomic orbitals (AOs), respectively. Charges and populations of atoms in the molecule are subsequently calculated in analogous manner to Mulliken population analysis, but starting from molecular orbitals given as linear combinations of true and well-defined atomic orbitals, rather than in terms of atom-centered basis functions. The atoms are calculated in their proper basis and by default in their ground state configuration, either by average-of-configuration at the HF level or by using fractional occupation at the DFT level. In order to make the projection analysis chemically meaningful, the expansion in eqn (5) is normally limited to AOs occupied in the atomic ground state configuration. However, for the assignment of the calculated core excitation spectra these orbitals, in the case of uranium, were supplemented by selected improved virtual orbitals, as discussed in Section 4.3. In either case, the selected set of AOs is not guaranteed to fully span a given molecular orbital. The orthogonal complement $|\psi_i^{\mathrm{pol}}\rangle$, which we denote the polarization contribution, can be eliminated using the Intrinsic Atomic Orbital scheme of Knizia.[94]

3 Computational details

Reference geometries were optimized at the scalar-relativistic CCSD(T) level using the MOLPRO 09[95] package and numerical gradients. For uranium we employed a relativistic small core potential (ECP60MDF) with a (14s13p10d8f6g)/[6s6p5d4f3g] quadruple zeta level valence ANO basis set developed by Dolg and Cao,[46] and the (11s6p3d2f)/[5s4p3d2f] aug-cc-pVTZ basis sets[96,97] for oxygen and nitrogen.

All other calculations were carried out with the DIRAC code[98] and are, unless otherwise stated, based on the 4-component Dirac–Coulomb Hamiltonian using the simple Coulombic correction[99] to avoid the explicit calculation of two-electron integrals involving the small components only. For uranium we employed the dyall.v3z basis set[100] (large component 33s29p20d13f4g2h) and for oxygen and nitrogen the cc-pVTZ basis set[96] (large components 10s5p2d1f). For MP2 calculations we switched to the slightly larger dyall.ae3z basis (large component 33s29p20d13f7g3h) for uranium. All basis sets were uncontracted and the small components generated by restricted kinetic balance. A finite nucleus model in the form of a Gaussian charge distribution was employed.[101]

Uranium 2p ionization energies were calculated by ΔSCF calculations,[59] both at the Kramers-restricted Hartree–Fock and Kohn–Sham level, the latter using the BLYP,[102–104] B3LYP,[105,106] PBE,[107] PBE0[108] and CAM-B3LYP[109] functionals. Convergence of the core excited states was straightforward using initial reordering of orbitals followed by selection of orbitals based on overlap with starting orbitals during the SCF cycles.

The uranium L_3 edge XANES spectrum of the selected molecules was simulated by REW-TDDFT, CPP and STEX calculations, the former two using the CAM-B3LYP[109] functional. Transition moments have been calculated within the electric dipole approximation, more specifically in the length gauge, that is, as integrals over the electric dipole operator. The nature of the excitations was determined from the excitation amplitudes combined with Mulliken and projection analysis[93] of the involved molecular orbitals. In the REW-TDDFT and STEX calculations finite linewidths of the individual peaks were introduced by Lorentzian functions of half-width at half-maximum (HWHM) γ = 0.0367 E_h ($\sim$1 eV). The same value of γ was taken as damping parameter in the CPP calculations.

4 Results and discussions

4.1 Molecular and electronic structures

Prior to the calculation of core ionization and excitation energies we optimized the geometries of the title species and investigated their electronic structures by projection analysis.[93] In Table 2 we report our calculated bond lengths for the isoelectronic series together with selected literature values. Wei *et al.*[23] reported bond lengths for NUO^+ and UN_2 calculated at the CCSD(T) level using the aug-cc-pVTZ basis set[96] for the ligands. For uranium the authors employed the relativistic small core potential ECP60MWB with the accompanying (12s11p10d8f)/[8s7p6d4f] valence basis, although it was developed for SCF calculations.[49] Jackson *et al.*[26] reported bond distances for UO_2^{2+} with the same computational setup, except that they added two g functions to the valence basis. Switching to the larger segmented valence basis set (14s13p10d8f6g)/[10s9p5d4f3g] developed by Cao and co-workers[110,111] and further augmentation by *h* and *i* functions was found to have only a small effect on calculated bond lengths. More recently, Tu *et al.* reported bond lengths for the entire isoelectronic series with basically the same computational setup.[55] They reproduce the uranyl bond length reported by Jackson *et al.*,[26] and get slightly shorter bond distances than reported by Wei *et al.*[23] for the other species. We have optimized bond lengths for the isoelectronic species using the more recent ECP60MDF core potential with the accompanying valence basis[46] and interestingly get somewhat longer bond lengths, closer to those reported by Gagliardi and Roos[48] at the CASPT2 level with ANO basis sets. Particularly noteworthy is that the U–N bond in the nitridooxouranium cation is shorter than the U–O bond, although experiment suggest that that the former is weaker than the latter (bond dissociation energies BDE[OU^+–N] = 4.44 $\pm$ 1.27 eV *vs.* BDE[NU^+–O] = 7.66 $\pm$ 1.70 eV).[31]

We have also investigated the electronic structure of the title compounds by projection analysis[93] at the HF level using the pre-calculated atomic orbitals occupied in the electronic ground state of the constituent atoms. Polarization contributions have been eliminated by polarizing the atomic orbitals in the molecule according to the Intrinsic Atomic Orbital scheme of Knizia,[94] yet conserving overlap between atomic orbitals on different centers. The charge and electronic configuration of uranium in the three molecules are given in Table 3. Concerning the electronic configurations, one in particular notes the 6p-hole,[112] primarily arising from overlap between the $6p_{3/2}$ orbital with the ligands, and which is basically identical for the three species. The calculated atomic charges, which do not suffer from the strong basis set dependence of Mulliken charges, are far from the formal oxidation state +VI of uranium in these molecules, in agreement with previous theoretical and experimental studies.[113] The uranium charge furthermore reduces according to the total molecular charge, as expected. The ligand charge is $-0.42e$ and in $-0.73e$ in UO_2^{2+} and UN_2, respectively. In NUO^+ the charge on oxygen and nitrogen is $-0.63e$ and $-0.49e$, respectively. The calculated dipole moment of NUO^+ is -1.43 D, when the uranium atom is placed at the origin with the nitrogen atom along the positive axis. Interestingly, for certain initial start guesses the HF SCF procedure converges to a solution 0.2 E_h higher in energy and with atomic charges very slightly modified (Q_U = +2.16*e*, Q_O = $-0.70e$, Q_N = $-0.45e$), but enough to switch the sign of the calculated dipole moment (+1.55 D).

Canonical orbitals are quite suitable for the description of electron detachment and excitation processes, such as XPS and XAS, respectively. However, in order to ''see'' chemical bonds one needs to rotate the occupied molecular orbitals to form localized ones,[114,115] although there is no unique localization criterion. In Table 4 we present a projection analysis of bonding orbitals obtained by Pipek–Mezey localization.[116] The bonding orbitals are identified as localized molecular orbitals with significant contributions from both the uranium center and a (single) ligand. Approximate orbital eigenvalues have been calculated as expectation values of the converged Fock operator. For each ligand we find three such bonding orbitals, of which two are almost degenerate and with ω = 1/2 and 3/2, respectively. Based on our analysis we conclude that each ligand is bound to the central uranium atom by triple (σ,π) bonds, where the π bond has been split by spin–orbit interaction into $\pi_{1/2}$ and $\pi_{3/2}$, and where the metal center contributes df hybrid atomic orbitals.

Table 2 Calculated bond lengths (in Å) for the title species

	Bond	CCSD(T)	CCSD(T)	CCSD(T)[55]	CASPT2[48]	PBE[34]
UO_2^{2+}	U–O	1.704	1.6898[26]	1.689	1.705	
OUN^+	U–O	1.748	1.743[23]	1.731	1.746	1.761
	U–N	1.696	1.703[23]	1.681	1.695	1.698
UN_2	U–N	1.736	1.743[23]	1.731	1.735	1.739

Table 3 Charge and electronic configuration of uranium in the title compounds obtained by projection analysis at the HF level

Molecule	Q_U	Atomic configuration
UO_2^{2+}	+2.84	$5f^{2.26}6p^{5.67}6d^{1.20}7s^{0.04}$
NUO^+	+2.12	$5f^{2.52}6p^{5.67}6d^{1.60}7s^{0.10}$
UN_2	+1.45	$5f^{2.68}6p^{5.66}6d^{2.01}7s^{0.23}$

4.2 Uranium 2p binding energy

In Table 5 we report relaxation Δ_{relax} and correlation Δ_{corr} contributions to the uranium 2p ionization energies of the

Table 4 Projection analysis of Pipek–Mezey localized bonding orbitals in the title compounds at the HF level. $\langle\varepsilon\rangle$ refers to the expectation value (in E_h) of the converged Fock operator. X refers to the ligand

	ω	$\langle\varepsilon\rangle$	U6p$_{3/2}$	U5f$_{5/2}$	U5f$_{7/2}$	U6d$_{3/2}$	U6d$_{5/2}$	U7s$_{1/2}$	X	X2s$_{1/2}$	X2p$_{1/2}$	X2p$_{3/2}$
UO_2^{2+}	1/2	−1.487	0.09	0.19	0.18	0.08	0.08	0.00	O	0.10	0.34	0.88
	1/2	−1.078	0.00	0.10	0.12	0.12	0.09	0.00	O	0.00	1.09	0.43
	3/2	−1.075	0.00	0.07	0.16	0.05	0.16	0.00	O	0.00	0.00	1.52
NUO^+	1/2	−1.147	0.06	0.13	0.12	0.09	0.08	0.00	O	0.12	0.35	0.98
	1/2	−0.790	0.00	0.08	0.10	0.11	0.09	0.00	O	0.00	1.16	0.43
	3/2	−0.787	0.00	0.06	0.13	0.04	0.16	0.00	O	0.00	0.00	1.59
	1/2	−1.146	0.19	0.28	0.20	0.11	0.07	0.01	N	0.02	0.23	0.76
	1/2	−0.689	0.01	0.13	0.19	0.20	0.17	0.00	N	0.00	0.94	0.31
	3/2	−0.683	0.01	0.12	0.23	0.09	0.28	0.00	N	0.00	0.00	1.24
UN_2	1/2	−0.826	0.16	0.19	0.16	0.10	0.09	0.03	O	0.03	0.31	0.81
	1/2	−0.427	0.00	0.12	0.14	0.21	0.16	0.00	O	0.00	0.96	0.38
	3/2	−0.425	0.00	0.09	0.19	0.08	0.28	0.00	O	0.00	0.00	1.33

Table 5 Ionization energies (in eV) obtained with dyall.ae3z basis set for uranium

	UO_2^{2+}			OUN^+			UN_2		
Method	2p$_{1/2,1/2}^{-1}$	2p$_{3/2,1/2}^{-1}$	2p$_{3/2,3/2}^{-1}$	2p$_{1/2,1/2}^{-1}$	2p$_{3/2,1/2}^{-1}$	2p$_{3/2,3/2}^{-1}$	2p$_{1/2,1/2}^{-1}$	2p$_{3/2,1/2}^{-1}$	2p$_{3/2,3/2}^{-1}$
Koopmans	21165.33	17321.80	17321.74	21155.86	17312.25	17312.32	21147.87	17304.32	17304.24
ΔHF	21094.94	17257.20	17257.31	21084.79	17247.02	17247.14	21076.27	17238.48	17238.61
ΔMP2	21089.94	17251.82	17251.55	21079.99	17241.85	17241.60	21069.13	17231.16	17230.89
Δ_{relax}	−70.40	−64.60	−64.43	−71.07	−65.23	−65.18	−71.61	−65.84	−65.63
Δ_{corr}	−5.00	−5.38	−5.76	−4.80	−5.17	−5.54	−7.14	−7.32	−7.72

title species, for uranium using the dyall.ae3z basis set which include correlation functions for all occupied orbitals. The calculations are based on the default Hamiltonian of the DIRAC package, that is, the 4-component relativistic Dirac–Coulomb Hamiltonian with a simple Coulomb correction,[99] thus avoiding the calculations of two-electron integrals (SS|SS) containing small component basis functions only. At the HF level the uranium 2p orbitals are split by 3838 eV due to spin–orbit interaction, and the 2p$_{3/2}$ orbital further split by a mere 0.3 eV due to the molecular field. As illustrated by Fig. 1, the ΔHF uranium 2p binding energies are a linear function, all with slope 13.4 eV e^{-1}, of the atomic charges reported in Table 3, thus demonstrating the chemical shift of X-ray photoelectron spectroscopy[117,118] as well as the usefulness of the atomic charges obtained from projection analysis.

We have defined Δ_{corr} as the difference between the ionization energy (IP) obtained at the ΔMP2 and ΔHF level, that is,

$$\Delta_{corr} = \mathrm{IP}(\Delta\mathrm{MP2}) - \mathrm{IP}(\Delta\mathrm{HF}),$$

but it should be emphasized that due to the non-canonical nature of the orbitals of the core-ionized states, there will be non-zero T_1 contributions to the MP2 energy, that are more properly associated with relaxation (see eqn (1)). However, these contributions are negligible in the calculations reported in Table 5, as will be discussed and demonstrated below. Table 5 shows that the correlation contribution Δ_{corr} is an order of magnitude smaller than the relaxation contribution Δ_{relax} and that the Koopmans estimate gives errors on the order of 75 eV. What is striking, though, is that the correlation contribution has the same sign as the relaxation contribution,

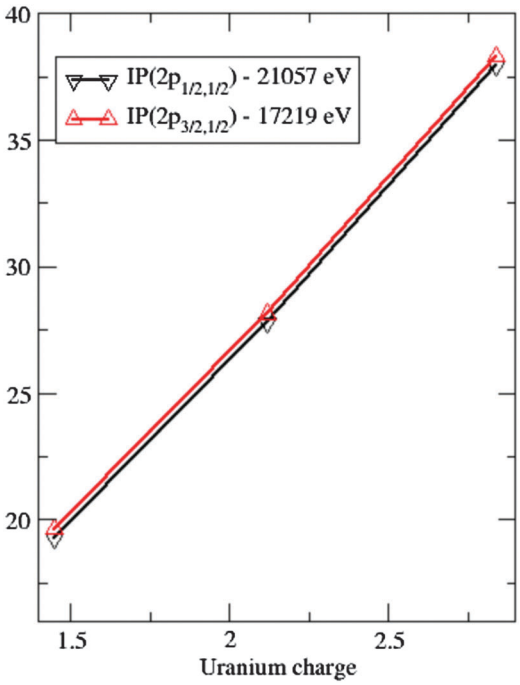

Fig. 1 Shifted ΔHF uranium 2p ionization energies of the title species (in eV) as a function of the uranium charge (in a.u.) from projection analysis.

that is, it is negative. If we consider the canonical MP2 energy expression

$$E^{\mathrm{MP2}} = \sum_{i<j} e_{ij}; \quad e_{ij} = \sum_{a<b} \frac{|\langle ij \parallel ab\rangle|^2}{\varepsilon_i + \varepsilon_j - \varepsilon_a - \varepsilon_b},$$

with N_o occupied and N_v virtual orbitals for the parent state, then the core-ionized state has $(N_o - 1)$ fewer pair energies e_{ij}, all of them negative in the parent state. In addition, the remaining pair energies has N_v new contributions containing the now virtual core orbital, such that denominators may be zero or even positive. Indelicato and co-workers,[119–121] in the framework of many-body perturbation theory, makes a distinction between contributions to the ionization energy for which $|\varepsilon_i + \varepsilon_j| > |\varepsilon_h|$, where ε_h is the energy of the virtual core orbital, say b, and contributions for which $|\varepsilon_i + \varepsilon_j| < |\varepsilon_h|$ and refer to them as core–core and Auger effects, respectively. Core–core contributions only occur if there are core orbitals lower in energy than the ionized one. The denominator is generally negative, but may change sign if the second virtual orbital, say a is bound, which are precisely the orbitals associated with pre-edge structure in X-ray absorption spectroscopy. The denominator of Auger effect contributions, on the other hand, starts off positive with increasing energy of the second virtual orbital, but eventually become negative for sufficiently high-lying virtuals. Such contributions were observed by Nooijen and Bartlett[122] to lead to convergence problems in coupled-cluster calculations of core-ionized states and were therefore ignored. In the present non-canonical MP2 calculations we do not make a distinction between Auger and core–core contributions, but simply monitor contributions to the pair correlation energy of positive sign. For the $1a_1$ ionization energy of water the total contribution is quite small (0.13 eV), whereas we obtain 3.43 eV for the uranium $2p_{3/2,3/2}$ ionization of uranyl.

The above discussion confirms the expectation that the correlation contribution should be positive. However, a negative contribution, arising from a strong coupling of correlation and relaxation, can not be excluded. To investigate this, we carried out non-canonical MP2 calculations on core-ionized uranyl as well as water using the molecular orbitals of the parent state. The results are shown in Table 6. Using the orbitals of the parent state (denoted "frozen" in the table) the relaxation contribution Δ_{relax} is by definition zero, to within numerical noise. The correlation contribution Δ_{corr}, on the other hand, becomes negative for both water and uranyl. However, when decomposing Δ_{corr} further into T_1 and T_2 contributions, according to the non-canonical MP2 expression of eqn (1), one observes that the T_1-contribution, which can be associated with relaxation, is completely dominating. For water the T_2-contribution $\Delta_{corr}(T_2)$ remains positive and is basically the same as when using relaxed orbitals. For uranyl, on the other hand, the T_2-contribution using frozen orbitals is positive, leading us to conclude that the negative correlation contribution obtained with the relaxed orbitals is indeed due to a strong coupling of correlation and relaxation.

Table 6 Relaxation and correlation contributions (in eV) to core ionization energies of water and uranyl. See text for further details

Molecule	IP	Orbital set	Δ_{relax}	Δ_{corr}	$\Delta_{corr}(T_1)$	$\Delta_{corr}(T_2)$
H_2O	$1a_1$	Relaxed	−20.51	0.92	−0.17	1.08
		Frozen	0.00	−34.58	−35.50	0.92
UO_2^{2+}	$2p_{3/2,3/2}$	Relaxed	−64.54	−5.17	−0.28	−4.89
		Frozen	0.06	−103.91	−106.08	2.17

We now turn to the effect of extensions to the default Hamiltonian of the DIRAC package. In Table 7 we report the effect of explicit inclusion of the (SS|SS) class of integrals (ΔΔDOSSSS). Although the effect is sizable, causing a reduction of binding energies on the order of 18 and 6 eV for uranium $2p_{1/2}$ and $2p_{3/2}$ orbitals, respectively, it is constant for all three isoelectronic species, and thus does not contribute to the chemical shift. Even more important is the effect of the inclusion of the Gaunt two-electron interaction, but again the chemical shift is not affected, and so we have ignored these both (SS|SS) integrals and the Gaunt term in the subsequent calculations. In passing we note that the Gaunt term reduces the spin–orbit splitting of the uranium 2p manifold by about 40 eV, which makes sense, since the Gaunt term contains the spin-other-orbit interaction.[45]

We have also investigated the performance of a selection of DFT functionals for the calculation of uranium 2p binding energies of the title species. These are reported in Table 7 relative to the HF binding energies. To the extent that the difference between HF and DFT binding energies can be interpreted as pure correlation contributions, we note that these are significantly larger in magnitude than the correlation contributions extracted from the ΔMP2 calculations. It should be noted that the core-ionized species have been calculated under Kramers restriction such that spin polarization, which is expected to reduce ionization energies, is missing. The GGA functionals PBE and BLYP reduce both uranium $2p_{1/2}$ and $2p_{3/2}$ binding energies, whereas the global hybrid functionals PBE0 and B3LYP, as well as the long-range corrected hybrid CAMB3LYP, decrease the $2p_{3/2}$ binding energies and increase the $2p_{1/2}$ ones. No DFT functional has a performance similar to MP2.

No experimental uranium L_2 or L_3 binding energies are available for the title species. The $2p_{1/2}$ and $2p_{3/2}$ binding energies

Table 7 Ionization energies (in eV) obtained using the dyall.v3z basis set for uranium

	UO_2^{2+}			OUN^+			UN_2		
Method	$2p_{1/2,1/2}^{-1}$	$2p_{3/2,1/2}^{-1}$	$2p_{3/2,3/2}^{-1}$	$2p_{1/2,1/2}^{-1}$	$2p_{3/2,1/2}^{-1}$	$2p_{3/2,3/2}^{-1}$	$2p_{1/2,1/2}^{-1}$	$2p_{3/2,1/2}^{-1}$	$2p_{3/2,3/2}^{-1}$
ΔHF	21095.41	17257.59	17257.71	21085.26	17247.41	17247.54	21076.74	17238.87	17239.01
ΔΔDOSSSS	−18.01	−5.86	−5.86	−18.00	−5.85	−5.86	−18.01	−5.86	−5.86
ΔΔGaunt	−108.73	−68.90	−68.90	−108.73	−68.91	−68.90	−108.74	−68.91	−68.91
ΔΔPBE	−14.41	−59.09	−59.02	−13.90	−58.58	−58.50	−13.53	−58.21	−58.13
ΔΔBLYP	−11.35	−57.03	−56.96	−10.84	−56.51	−56.44	−10.46	−56.12	−56.05
ΔΔPBE0	23.49	−15.91	−15.86	23.83	−15.57	−15.52	24.05	−15.35	−15.29
ΔΔB3LYP	17.89	−22.98	−22.92	18.25	−22.61	−22.55	18.52	−22.34	−22.28
ΔΔCAMB3LYP	18.82	−22.67	−22.62	19.14	−22.35	−22.29	19.37	−22.12	−22.06

of metallic uranium are 20 948 and 17 166 eV, respectively, relative to the Fermi level.[123] If we add the (SS|SS) and Gaunt contributions as corrections, then the MP2 ionization energies for UN_2, in which uranium has the smallest charge, agree to within 10 eV with the cited experimental numbers. If we instead linearly extrapolate the MP2 ionization energies to zero uranium nuclear charge at the HF level and add the cited corrections, we underestimate the experimental numbers by about 30 eV.

4.3 Uranium L_3 edge XANES spectra

In this section we present and analyze simulated uranium L_3 edge XANES spectra of the title species. A good discussion of the electronic structure of actinyls has been given by Denning.[124] Here focus will be on the bound virtual orbitals. We start by considering the calculated uranium L_3 edge XANES spectrum for uranyl obtained by the STEX method. In Fig. 2 we compare the spectra obtained with three different basis sets. These are local Gaussian basis sets which are not appropriate for the description of continuum states,[125] as can be seen from the lack of any convergence of the spectra with respect to basis sets beyond the L_3 edge. Such artifacts have been observed previously, and it was suggested by Ekström and Norman that the meaningful energy range of a simulated spectrum in a local basis can be ascertained by exponent scaling.[126] In the present case, a zoom into the pre-edge region of the spectrum, as shown in Fig. 3 suggests that the spectrum is not fully converged for quasi-bound states in the vicinity of the ionization threshold. Convergence in this region would probably require a rather extensive set of diffuse functions. In the following we shall therefore focus on the first three peaks of the spectrum.

We shall also compare the performance of the three different methods discussed in Section 2.2. We start by demonstrating numerically that the STEX excitation energies can be obtained by using a REW-TDHF calculation within the Tamm–Dancoff approximation and using the orbitals of the core-ionized state. In Fig. 4 the uranium L_3 edge XANES spectrum for uranyl calculated by the two methods is displayed. As discussed in Section 2.2 both

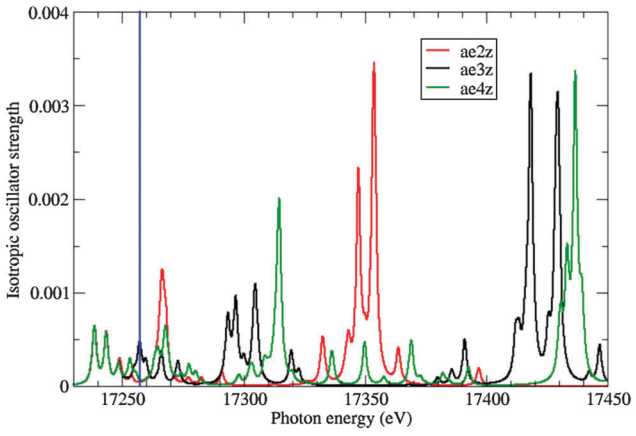

Fig. 2 UO_2^{2+} uranium L_3 edge XANES spectra simulated by STEX using different basis sets and a Lorentzian broadening of ~1 eV. The vertical line indicates the ionization threshold obtained at the ΔHF level (the value changes less than 0.1 eV with the indicated basis sets).

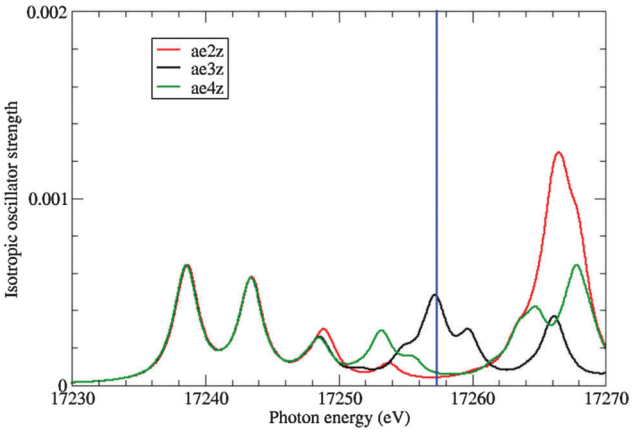

Fig. 3 UO_2^{2+} uranium L_3 edge XANES spectra simulated by STEX using different basis sets and a Lorentzian broadening of ~1 eV: zoom of the pre-edge region.

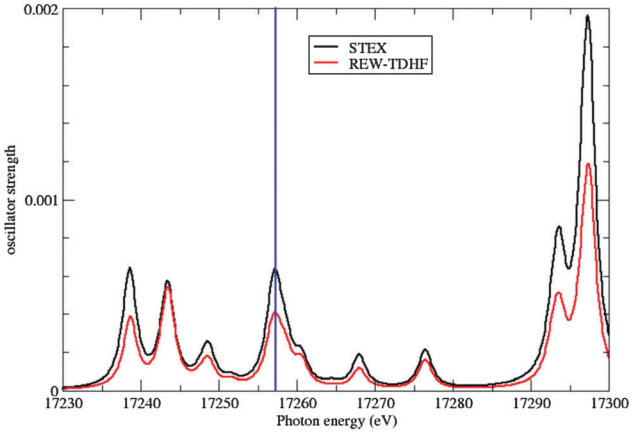

Fig. 4 Comparison of UO_2^{2+} uranium L_3 edge XANES spectra obtained by STEX and REW-TDHF, in both cases adding a Lorentzian broadening of ~1 eV. The REW-TDHF calculations has been carried out within the Tamm–Dancoff approximation and using the orbitals of the core-ionized state. The vertical line indicates the ionization threshold obtained at the ΔHF level. The REW-TDHF and STEX excitation energies are both corrected by the difference between the ground state energy calculated in ground state and core-ionized orbitals.

the STEX and the TDHF/TDA excitation energies have been corrected as

$$\hbar\omega_m \rightarrow \hbar\omega_m + E_0 - \tilde{E}_0$$

where E_0 and $\tilde{E}_0$ are the energies of the parent state calculated in the parent and core-ionized orbitals, respectively. The same correction is applied to the oscillator strengths, eqn (4). The excitation energies are indeed seen to match perfectly, whereas the REW-TDHF/TDA Lorentz-broadened oscillator strengths are systematically smaller than the STEX ones.

A direct comparison of STEX on the one hand and CPP and REW-TDDFT on the other hand is complicated by the fact that the latter spectra are significantly shifted with respect to the experimental L_3 edge due to the combined effect of missing orbital relaxation and self-interaction errors.[127] In order to align

Table 8 Estimated ionization potential of uranium $2p_{3/2}$ orbital (in eV) based on excitation to a tight ghost function placed 100 a_0 away from uranium, compared to the negative orbital energy $-\varepsilon_{2p_{3/2}}$ (averaged over the m_j components). All results have been obtained with the CAMB3LYP functional

Molecule	Estimated IP ($U2p_{3/2}$) in eV	$-\varepsilon_{2p_{3/2}}$ (eV)
UO_2^{2+}	17104.31	17104.41
OUN^+	17095.03	17095.13
UN_2	17087.25	17087.34

the spectra we have therefore considered the position of the L_3 ionization threshold within a linear response regime. We may consider the process of ionization as an extreme case of a charge-transfer excitation in which the separation between donor and acceptor tends towards infinity. Following the arguments of Dreuw *et al.*,[128] it then becomes clear that the excitation energy reduces, for any DFT functional, to the energy difference between the acceptor and donor orbital. Since this excitation energy is also equal to the difference between the ionization potential of the donor and the electron affinity of the acceptor we are led to the conclusion that within TDDFT (and TDHF) the ionization threshold is *de facto* given by Koopmans' theorem, that is, as the negative of the donor orbital. We have tested this conclusion numerically by forcing an excitation from the selected core orbital to a remote tight ghost function placed 100 a_0 away from the uranium atom along the molecular axis and then subtracting the ghost orbital eigenvalue from the resulting excitation energy. The results are given in Table 8 and clearly confirms the validity of our conclusion. On the other hand, it should be emphasized that the meaning of orbital eigenvalues is different in Hartree–Fock and exact Kohn–Sham theory.[129–131]

As a consequence we have shifted the excitation energies obtained with CPP and REW-TDDFT according to

$$\hbar\omega_m \rightarrow \hbar\omega_m + \mathrm{IP}_i(\Delta\mathrm{HF}) + \varepsilon_i^{\mathrm{KS}} \qquad (6)$$

From Fig. 5–7 it is seen that these shifts, on the order of 150 eV, clearly bring the CPP and REW-TDDFT spectra into the same energy region as the STEX one. The CPP and REW-TDDFT spectra agree perfectly, as they should (*cf.* Section 2.2); the slight deviation observed towards higher photon energies in Fig. 6 is simply due to an insufficient number of excitations calculated at the REW-TDDFT level. For uranyl the CPP and REW-TDDFT spectra are seen to match the STEX one very well, but the agreement deteriorates as the molecular charge is reduced along the isoelectronic series. For OUN^+ we note in particular new pre-edge features with respect to STEX. It should be pointed out, however, that the uranium $2p_{3/2}$ natural width is 7.43 eV,[132] although the experimental energy resolution can be reduced down to about 4 eV using partial fluorescence yield techniques.[10,133] This still means that the above-mentioned pre-edge structures of the theoretical spectrum can not be resolved by present-day experiment.

Amongst the three methods STEX offers perhaps the most straightforward assignment of spectra. This is because XANES spectroscopy, in an orbital picture, probes bound virtual

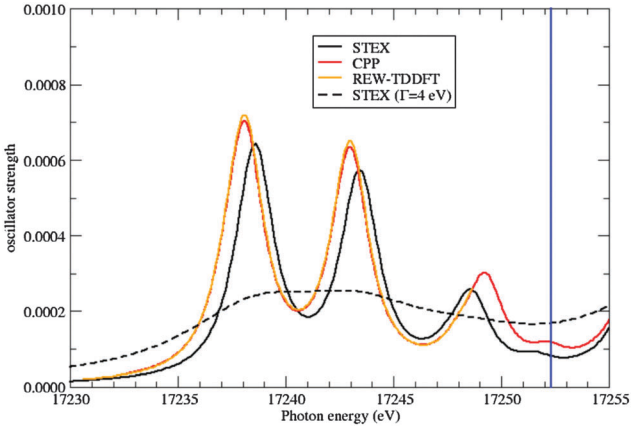

Fig. 5 UO_2^{2+} uranium L_3 edge XANES spectra simulated by STEX, CPP(CAM-B3LYP) and REW-TDDFT(CAM-B3LYP), including a Lorentzian broadening of ~1 eV. The two latter spectra have been shifted by 152.63 eV according to (6).

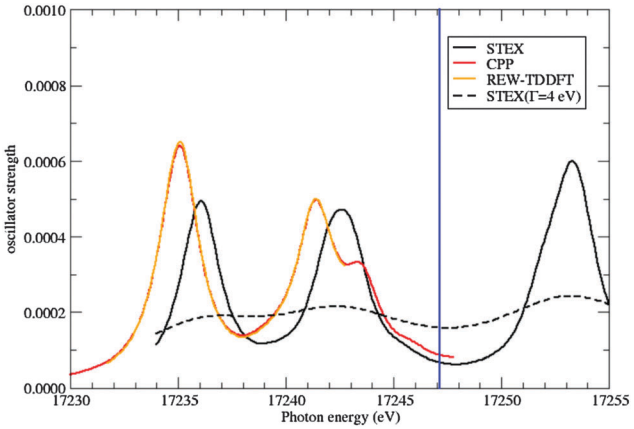

Fig. 6 OUN^+ uranium L_3 edge XANES spectra simulated by STEX, CPP(CAM-B3LYP) and REW-TDDFT(CAM-B3LYP), including a Lorentzian broadening of ~1 eV. The two latter spectra have been shifted by 151.73 eV according to (6).

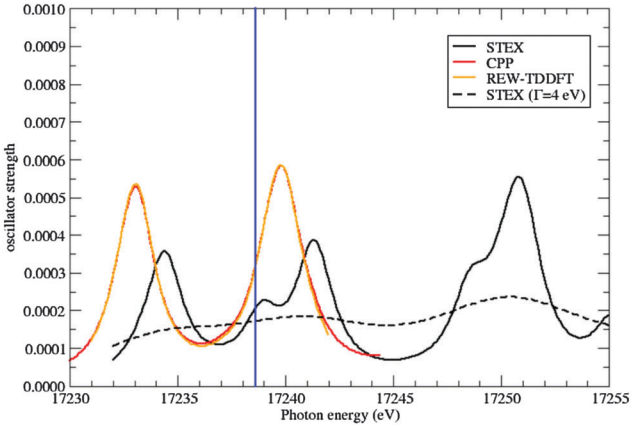

Fig. 7 UN_2 uranium L_3 edge XANES spectra simulated by STEX, CPP(CAM-B3LYP) and REW-TDDFT(CAM-B3LYP), including a Lorentzian broadening of ~1 eV. The two latter spectra have been shifted by 150.98 eV according to (6).

orbitals which, as discussed in Section 2.2, have been optimized by calculating the core-ionized state. As an illustration we may note that in the dyall.v3z basis a HF calculation on the uranyl ground state gives 41 bound also virtual orbitals (Kramers pairs) whereas for OUN^+ this number is reduced to 15 and for UN_2 there are none. In contrast, the corresponding numbers for the uranium $2p_{3/2}$-ionized state are 46, 35 and 15, respectively. We have been able to carry out a detailed assignment of the STEX uranium L_3 XANES spectra using projection analysis.[93] For the ligands we have used the ground state orbitals. For uranium the ground state occupied orbitals were supplemented by the bound improved virtual orbitals generated by freezing the ground state orbitals and then recalculating the virtual orbitals for the $2p_{3/2}$-ionized state. The first peak of the uranyl STEX spectrum (*cf.* Fig. 5) is thereby found to be dominated by excitations to uranium 6d orbitals, but also virtual orbitals of uranium 7s character. These virtual orbitals have essentially no ligand character. The second peak is assigned as excitations to virtual orbitals dominated by uranium 6d, but about 25% ligand character. The third and final peak before the ionization threshold is dominated by excitations to uranium 7d orbitals. Moving to OUN^+ the molecular charge is reduced by one unit and the number of peaks before the ionization threshold to two; both are dominated by excitations to uranium 6d orbitals, but the second peak also has some ligand character (23% nitrogen and 6% oxygen). Finally, for neutral UN_2 there is a single peak before the ionization threshold dominated by excitations to uranium 6d and with no ligand character. The same assignment basically carries over to the CPP and REW-TDDFT spectra, but with less precision since the virtual orbitals are less optimal. The extra features of the second peak of the OUN^+ spectrum (*cf.* Fig. 6) appears to be due to a larger splitting of the $\omega = 3/2$ and $\omega = 5/2$ components of the uranium $6d_{5/2}$ orbitals.

5 Conclusions and perspectives

In the present work we have studied the processes of ionization and excitation out of the uranium $2p_{3/2}$ orbital in the isoelectronic species UO_2^{2+}, OUN^+ and UN_2 at the 4-component relativistic level. Molecular geometries were reoptimized at the CCSD(T) level using small-core scalar relativistic pseudopotentials and correlation-consistent basis sets, and the electronic structure studied by projection analysis in localized orbitals. Using the extracted uranium atomic charges we find a perfectly linear chemical shift of uranium $2p_{3/2}$ ionization energies obtained by ΔHF. We confirm the failure of Koopmans' theorem for core ionization due to the dominance of relaxation contributions over correlation ones. More unexpected is that the correlation contribution Δ_{corr} is negative for all three species, meaning that the parent state has less correlation energy than the core-ionized state. Our analysis suggests that this is due to a strong coupling of relaxation and correlation. Uranium $2p_{3/2}$ ionization energies calculated by ΔSCF using different DFT functionals do not agree very well with our ΔMP2 values, but this situation might improve by the introduction of spin polarization in a Kramers unrestricted formalism.

To describe core excitations we have investigated three methods and shown how they are related. In particular, we show how STEX excitation energies, but not intensities, can be reproduced by TDHF calculations within the Tamm–Dancoff approximation. We also show that for the same Lorentz broadening REW-TDDFT and CPP give identical spectra. The CPP method has a certain ease of application in that the spectrum is directly simulated by scanning the desired frequency region, without any worry about the appropriate number of excitations to include. On the other hand, CPP lacks some flexibility in that spectra are only simulated for one specific damping parameter and would therefore have to be recalculated if another value was chosen. Although Koopmans' theorem fails for core excitations, it is the correct approximation of ionization potentials in the linear response regime, and this observation has allowed us to introduce shifts (*cf.* eqn (6)), on the order of 150 eV, to align REW-TDDFT and CPP uranium L_3 XANES spectra with the STEX ones. Since orbital relaxation dominates over electron correlation for core excitations, the ionization threshold of STEX spectra are in the vicinity of experimental ones. The interpretation of STEX spectra is furthermore more straightforward in that the virtual orbitals of the core-ionized state are optimal. We accordingly obtain a detailed assignment of our calculated STEX spectra using projection analysis, notably with improved virtual orbitals of the uranium atom. On the other hand, it has been claimed (see for instance ref. 134) that REW-TDDFT (and thus CPP) gives better relative peak positions and intensities than STEX compared to experiment due to the inclusion of electron correlation. In the present work no direct comparison with experiment was made. In future work we plan to address this issue in detail. It should also be pointed out that the molecules in the present study are closed shell in their parent state, which is rather the exception in the domain of f-elements. As pointed out by Roemelt *et al.*,[135] TDDFT (and therefore also CPP and STEX) has simply not enough parameters to handle the general open-shell case. A challenge for the future is therefore to develop cost-effective methods for the simulation of X-ray spectra of actinide species.

Acknowledgements

TS and DM acknowledges financial support from the Indo-French Centre for the Promotion of Advanced Research (IFCPAR project No. 4705-3), including the PhD-grant for AS. DM thanks the Science and Engineering Research Board (New Delhi) for conferring on him their Distinguished Fellowship. Computing time from CALMIP (Calcul en Midi-Pyrenées) is gratefully acknowledged. TS would like to acknowledge helpful discussions with Paul Bagus (Denton), Vincenzo Carravetta (Pisa), Ulf Ekström (Oslo), Eva Lindroth (Stockholm), Patrick Norman (Linköping) and Tonya Vitova (Karlsruhe). AKW acknowledges support of the National Science Foundation under Grant No. CHE-1362479. Computing support, in part, was provided by the Computing and Information Technology Center at the University of North Texas. Support is provided by the U.S.

Department of Energy (DOE) for the Center for Advanced Scientific Computing and Modeling (CASCaM) at the University of North Texas. AKW and CS acknowledge support from the Global Research Experiences, Exchange, and Training (GREET) program, a program of the American Chemical Society. We are happy to dedicate this paper to Evert Jan Baerends on the occasion of his 70th birthday.

References

1 J. Selbin and J. D. Ortego, *Chem. Rev.*, 1969, **69**, 657–671.
2 K. A. Kraus, F. Nelson and G. L. Johnson, *J. Am. Chem. Soc.*, 1949, **71**, 2510–2517.
3 K. A. Kraus and F. Nelson, *J. Am. Chem. Soc.*, 1949, **71**, 2517–2522.
4 F. Nelson and K. A. Kraus, *J. Am. Chem. Soc.*, 1951, **73**, 2157–2161.
5 F. R. Livens, M. J. Jones, A. J. Hynes, J. M. Charnock, J. W. Mosselmans, C. Hennig, H. Steele, D. Collison, D. J. Vaughan, R. A. Pattrick, W. A. Reed and L. N. Moyes, *J. Environ. Radioact.*, 2004, **74**, 211–219.
6 E. Bailey, J. Mosselmans and P. Schofield, *Chem. Geol.*, 2005, **216**, 1–16.
7 M. A. Denecke, *Coord. Chem. Rev.*, 2006, **250**, 730–754.
8 N. Belai, M. Frisch, E. S. Ilton, B. Ravel and C. L. Cahill, *Inorg. Chem.*, 2008, **47**, 10135–10140.
9 C. Fillaux, D. Guillaumont, J.-C. Berthet, R. Copping, D. K. Shuh, T. Tyliszczak and C. D. Auwer, *Phys. Chem. Chem. Phys.*, 2010, **12**, 14253–14262.
10 T. Vitova, K. O. Kvashnina, G. Nocton, G. Sukharina, M. A. Denecke, S. M. Butorin, M. Mazzanti, R. Caciuffo, A. Soldatov, T. Behrends and H. Geckeis, *Phys. Rev. B: Condens. Matter Mater. Phys.*, 2010, **82**, 235118.
11 A. Barkleit, H. Foerstendorf, B. Li, A. Rossberg, H. Moll and G. Bernhard, *Dalton Trans.*, 2011, **40**, 9868–9876.
12 R. Atta-Fynn, D. F. Johnson, E. J. Bylaska, E. S. Ilton, G. K. Schenter and W. A. de Jong, *Inorg. Chem.*, 2012, **51**, 3016–3024.
13 F. Poineau, C. Yeamans, G. Silva, G. Cerefice, A. Sattelberger and K. Czerwinski, *J. Radioanal. Nucl. Chem.*, 2012, **292**, 989–994.
14 A. Walshe, T. Prußmann, T. Vitova and R. J. Baker, *Dalton Trans.*, 2014, **43**, 4400–4407.
15 C. J. Nelin, P. S. Bagus and E. S. Ilton, *RSC Adv.*, 2014, **4**, 7148–7153.
16 G. D. Lawrence, K. S. Patel and A. Nusbaum, *Pure Appl. Chem.*, 2014, **6**, 1105–1110.
17 A. Kovács, R. J. M. Konings, J. K. Gibson, I. Infante and L. Gagliardi, *Chem. Rev.*, 2015, **115**, 1725–1759.
18 V. E. Jackson, K. E. Gutowski and D. A. Dixon, *J. Phys. Chem. A*, 2013, **117**, 8939–8957.
19 V. Vallet, U. Wahlgren and I. Grenthe, *J. Phys. Chem. A*, 2012, **116**, 12373–12380.
20 P. Tecmer, R. Bast, K. Ruud and L. Visscher, *J. Phys. Chem. A*, 2012, **116**, 7397–7404.
21 D. Rios, G. Schoendorff, M. J. V. Stipdonk, M. S. Gordon, T. L. Windus, J. K. Gibson and W. A. de Jong, *Inorg. Chem.*, 2012, **51**, 12768–12775.
22 B. B. Averkiev, M. Mantina, R. Valero, I. Infante, A. Kovacs, D. Truhlar and L. Gagliardi, *Theor. Chem. Acc.*, 2011, **129**, 657–666.
23 F. Wei, G. Wu, W. Schwarz and J. Li, *Theor. Chem. Acc.*, 2011, **129**, 467–481.
24 F. Ruipérez, C. Danilo, F. Réal, J.-P. Flament, V. Vallet and U. Wahlgren, *J. Phys. Chem. A*, 2009, **113**, 1420–1428.
25 F. Réal, A. S. P. Gomes, L. Visscher, V. Vallet and E. Eliav, *J. Phys. Chem. A*, 2009, **113**, 12504–12511.
26 V. E. Jackson, R. Craciun, D. A. Dixon, K. A. Peterson and W. A. de Jong, *J. Phys. Chem. A*, 2008, **112**, 4095–4099.
27 J. L. Sonnenberg, P. J. Hay, R. L. Martin and B. E. Bursten, *Inorg. Chem.*, 2005, **44**, 2255–2262.
28 K. Pierloot and E. van Besien, *J. Chem. Phys.*, 2005, **123**, 204309.
29 N. Kaltsoyannis, *Inorg. Chem.*, 2000, **39**, 6009–6017.
30 J. S. Craw, M. A. Vincent, I. H. Hillier and A. L. Wallwork, *J. Phys. Chem.*, 1995, **99**, 10181–10185.
31 C. Heinemann and H. Schwarz, *Chem. – Eur. J.*, 1995, **1**, 7–11.
32 P. Pyykkö, J. Li and N. Runeberg, *J. Phys. Chem.*, 1994, **98**, 4809–4813.
33 K. Pierloot, E. van Besien, E. van Lenthe and E. J. Baerends, *J. Chem. Phys.*, 2007, **126**, 194311.
34 P. Tecmer, A. S. P. Gomes, U. Ekstrom and L. Visscher, *Phys. Chem. Chem. Phys.*, 2011, **13**, 6249–6259.
35 P. Tecmer, N. Govind, K. Kowalski, W. A. de Jong and L. Visscher, *J. Chem. Phys.*, 2013, **139**, 034301.
36 P. Norman, D. M. Bishop, H. J. Aa. Jensen and J. Oddershede, *J. Chem. Phys.*, 2001, **115**, 10323.
37 P. Norman, D. M. Bishop, H. J. Aa. Jensen and J. Oddershede, *J. Chem. Phys.*, 2005, **123**, 194103.
38 J. Autschbach, L. Jensen, G. C. Schatz, Y. C. E. Tse and M. Krykunov, *J. Phys. Chem. A*, 2006, **110**, 2461.
39 A. Devarajan, A. Gaenko and J. Autschbach, *J. Chem. Phys.*, 2009, **130**, 194102.
40 K. Kristensen, J. Kauczor, T. Kjærgaard and P. Jørgensen, *J. Chem. Phys.*, 2009, **131**, 044112.
41 S. Coriani, O. Christiansen, T. Fransson and P. Norman, *Phys. Rev. A: At., Mol., Opt. Phys.*, 2012, **85**, 022507.
42 H. Ågren, V. Carravetta, O. Vahtras and L. G. Pettersson, *Chem. Phys. Lett.*, 1994, **222**, 75–81.
43 V. Carravetta and H. Ågren, in *Computational Strategies for Spectroscopy*, ed. V. Barone, John Wiley & Sons, Inc., 2011, pp. 137–205.
44 H. Ågren, V. Carravetta, L. G. M. Pettersson and O. Vahtras, *Phys. Rev. B: Condens. Matter Mater. Phys.*, 1996, **53**, 16074–16085.
45 T. Saue, *ChemPhysChem*, 2011, **12**, 3077.
46 M. Dolg and X. Cao, *J. Phys. Chem. A*, 2009, **113**, 12573–12581.
47 R. A. Evarestov, A. I. Panin, A. V. Bandura and M. V. Losev, *J. Phys.: Conf. Ser.*, 2008, **117**, 012015.

48 L. Gagliardi and B. O. Roos, *Chem. Phys. Lett.*, 2000, **331**, 229–234.
49 W. Küchle, M. Dolg, H. Stoll and H. Preuss, *J. Chem. Phys.*, 1994, **100**, 7535–7542.
50 M. Iliaš, H. J. A. Jensen, V. Kellö, B. O. Roos and M. Urban, *Chem. Phys. Lett.*, 2005, **408**, 210.
51 W. Kutzelnigg and W. Liu, *J. Chem. Phys.*, 2005, **123**, 241102.
52 M. Iliaš and T. Saue, *J. Chem. Phys.*, 2007, **126**, 064102.
53 R. Klooster, R. Broer and M. Filatov, *Chem. Phys.*, 2012, **395**, 122–127.
54 M. J. Van Stipdonk, M. d. C. Michelini, A. Plaviak, D. Martin and J. K. Gibson, *J. Phys. Chem. A*, 2014, **118**, 7838–7846.
55 T. Zhe-Yan, Y. Dong-Dong, W. Fan and L. Xiang-Yuan, *Acta Phys.-Chim. Sin.*, 2012, **28**, 1707.
56 R. D. Hunt, J. T. Yustein and L. Andrews, *J. Chem. Phys.*, 1993, **98**, 6070–6074.
57 T. Koopmans, *Physica*, 1934, **1**, 104–113.
58 R. S. Mulliken, *J. Chem. Phys.*, 1949, **46**, 497.
59 P. S. Bagus, *Phys. Rev.*, 1965, **139**, A619–A634.
60 K. Siegbahn, C. Nordling, G. Johansson, J. Hedman, P. F. Hedén, K. Hamrin, U. Gelius, T. Bergmark, L. O. Werme and Y. Baer, *ESCA applied to free molecules*, North-Holland, Amsterdam, 1969.
61 K. Siegbahn, *J. Electron. Spectrosc. Relat. Phenom.*, 1974, **5**, 3–97.
62 J. Thyssen, PhD thesis, University of Southern Denmark, 2001.
63 P. S. Bagus and H. F. Schaefer, *J. Chem. Phys.*, 1971, **55**, 1474–1475.
64 J. Almlöf, P. Bagus, B. Liu, D. MacLean, U. Wahlgren and M. Yoshimine, *MOLECULE-ALCHEMY program package*, IBM Research Laboratory, 1972, an on-line manual is found at http://k-sek01.t-komazawa.ac.jp/msekiya/alchemy/.
65 A. T. B. Gilbert, N. A. Besley and P. M. W. Gill, *J. Phys. Chem. A*, 2008, **112**, 13164–13171.
66 DIRAC, a relativistic *ab initio* electronic structure program, Release DIRAC14, written by T. Saue, L. Visscher, H. J. Aa. Jensen and R. Bast, with contributions from V. Bakken, K. G. Dyall, S. Dubillard, U. Ekström, E. Eliav, T. Enevoldsen, E. Faßhauer, T. Fleig, O. Fossgaard, A. S. P. Gomes, T. Helgaker, J. K. Lærdahl, Y. S. Lee, J. Henriksson, M. Iliaš, Ch. R. Jacob, S. Knecht, S. Komorovský, O. Kullie, C. V. Larsen, H. S. Nataraj, P. Norman, G. Olejniczak, J. Olsen, Y. C. Park, J. K. Pedersen, M. Pernpointner, R. di Remigio, K. Ruud, P. Sałek, B. Schimmelpfennig, J. Sikkema, A. J. Thorvaldsen, J. Thyssen, J. van Stralen, S. Villaume, O. Visser, T. Winther and S. Yamamoto, 2014, see http://www.diracprogram.org.
67 L. Visscher, T. J. Lee and K. G. Dyall, *J. Chem. Phys.*, 1996, **105**, 8769–8776.
68 W. J. Lauderdale, J. F. Stanton, J. Gauss, J. D. Watts and R. J. Bartlett, *Chem. Phys. Lett.*, 1991, **187**, 21–28.
69 J. Olsen and P. Jørgensen, *J. Chem. Phys.*, 1985, **82**, 3235.
70 J. Olsen and P. Jørgensen, in *Modern Electronic Structure Theory*, ed. D. R. Yarkoni, World Scientific, 1995.
71 R. Bast, H. J. A. Jensen and T. Saue, *Int. J. Quantum Chem.*, 2009, **109**, 2091.
72 S. Bernadotte, A. J. Atkins and C. R. Jacob, *J. Chem. Phys.*, 2012, **137**, 204106.
73 N. H. List, J. Kauczor, T. Saue, H. J. A. Jensen and P. Norman, *J. Chem. Phys.*, 2015, **142**, 244111.
74 B. Levy, *Chem. Phys. Lett.*, 1969, **4**, 17.
75 P. Joergensen and J. Linderberg, *Int. J. Quantum Chem.*, 1970, **4**, 587.
76 E. Dalgaard and P. Joergensen, *J. Chem. Phys.*, 1978, **69**, 3833.
77 T. Saue and T. Helgaker, *J. Comput. Chem.*, 2002, **23**, 814.
78 O. Christiansen, P. Jørgensen and C. Hättig, *Int. J. Quantum Chem.*, 1998, **68**, 1.
79 T. Saue, in *Relativistic Electronic Structure Theory. Part 1. Fundamentals*, ed. P. Schwerdtfeger, Elsevier, Amsterdam, 2002, p. 332.
80 S. Villaume, T. Saue and P. Norman, *J. Chem. Phys.*, 2010, **133**, 064105.
81 M. Stener, G. Fronzoni and M. de Simone, *Chem. Phys. Lett.*, 2003, **373**, 115–123.
82 U. Ekström, PhD thesis, Linköping universitet, 2007.
83 P. G. Burke and K. Smith, *Rev. Mod. Phys.*, 1962, **34**, 458–502.
84 N. Mott and H. Massey, *The Theory of Atomic Collisions*, Clarendon Press, Oxford, 1965.
85 H. S. W. Massey and C. B. O. Mohr, *Proc. R. Soc. A*, 1932, **136**, 289–311.
86 P. M. Morse and W. P. Allis, *Phys. Rev.*, 1933, **44**, 269–276.
87 W. J. Hunt and W. A. Goddard III, *Chem. Phys. Lett.*, 1969, **3**, 414–418.
88 T. Rescigno and P. Langhoff, *Chem. Phys. Lett.*, 1977, **51**, 65–70.
89 P. W. Langhoff, *Int. J. Quantum Chem.*, 1977, **12**, 301–310.
90 J. A. Sheehy, T. J. Gil, C. L. Winstead, R. E. Farren and P. W. Langhoff, *J. Chem. Phys.*, 1989, **91**, 1796–1812.
91 P.-O. Löwdin, *Phys. Rev.*, 1955, **97**, 1474–1489.
92 U. Ekström, P. Norman and V. Carravetta, *Phys. Rev. A: At., Mol., Opt. Phys.*, 2006, **73**, 022501.
93 S. Dubillard, J.-B. Rota, T. Saue and K. Faegri, *J. Chem. Phys.*, 2006, **124**, 154307.
94 G. Knizia, *J. Chem. Theory Comput.*, 2013, **9**, 4834–4843.
95 H.-J. Werner, P. J. Knowles, R. Lindh, F. R. Manby, M. Schütz, P. Celani, T. Korona, A. Mitrushenkov, G. Rauhut, T. B. Adler, R. D. Amos, A. Bernhardsson, A. Berning, D. L. Cooper, M. J. O. Deegan, A. J. Dobbyn, F. Eckert, E. Goll, C. Hampel, G. Hetzer, T. Hrenar, G. Knizia, C. Köppl, Y. Liu, A. W. Lloyd, R. A. Mata, A. J. May, S. J. McNicholas, W. Meyer, M. E. Mura, A. Nicklass, P. Palmieri, K. Pflüger, R. Pitzer, M. Reiher, U. Schumann, H. Stoll, A. J. Stone, R. Tarroni, T. Thorsteinsson, M. Wang and A. Wolf, *MOLPRO, version 2009.1, a package of ab initio programs*, 2009, see http://www.molpro.net.
96 T. H. Dunning, *J. Chem. Phys.*, 1989, **90**, 1007–1023.
97 R. A. Kendall, T. H. Dunning and R. J. Harrison, *J. Chem. Phys.*, 1992, **96**, 6796.

98 DIRAC, a relativistic *ab initio* electronic structure program, Release DIRAC13, written by L. Visscher, H. J. Aa. Jensen, R. Bast and T. Saue, with contributions from V. Bakken, K. G. Dyall, S. Dubillard, U. Ekström, E. Eliav, T. Enevoldsen, E. Faßhauer, T. Fleig, O. Fossgaard, A. S. P. Gomes, T. Helgaker, J. K. Lærdahl, Y. S. Lee, J. Henriksson, M. Iliaš, Ch. R. Jacob, S. Knecht, S. Komorovský, O. Kullie, C. V. Larsen, H. S. Nataraj, P. Norman, G. Olejniczak, J. Olsen, Y. C. Park, J. K. Pedersen, M. Pernpointner, K. Ruud, P. Sałek, B. Schimmelpfennig, J. Sikkema, A. J. Thorvaldsen, J. Thyssen, J. van Stralen, S. Villaume, O. Visser, T. Winther and S. Yamamoto, 2013, see http://www.diracprogram.org.
99 L. Visscher, *Theor. Chem. Acc.*, 1997, **98**, 68–70.
100 K. G. Dyall, *Theor. Chem. Acc.*, 2007, **117**, 491–500.
101 L. Visscher and K. Dyall, *At. Data Nucl. Data Tables*, 1997, **67**, 207–224.
102 A. D. Becke, *Phys. Rev. A: At., Mol., Opt. Phys.*, 1988, **38**, 3098–3100.
103 C. Lee, W. Yang and R. G. Parr, *Phys. Rev. B: Condens. Matter Mater. Phys.*, 1988, **37**, 785–789.
104 B. Miehlich, A. Savin, H. Stoll and H. Preuss, *Chem. Phys. Lett.*, 1989, **157**, 200–206.
105 P. J. Stephens, F. J. Devlin, C. F. Chabalowski and M. J. Frisch, *J. Phys. Chem.*, 1994, **98**, 11623–11627.
106 A. D. Becke, *J. Chem. Phys.*, 1993, **98**, 5648–5652.
107 J. P. Perdew, K. Burke and M. Ernzerhof, *Phys. Rev. Lett.*, 1996, **77**, 3865–3868.
108 C. Adamo and V. Barone, *J. Chem. Phys.*, 1999, **110**, 6158–6170.
109 T. Yanai, D. P. Tew and N. C. Handy, *Chem. Phys. Lett.*, 2004, **393**, 51–57.
110 X. Cao, M. Dolg and H. Stoll, *J. Chem. Phys.*, 2003, **118**, 487–496.
111 X. Cao and M. Dolg, *THEOCHEM*, 2002, **581**, 139–147.
112 P. Pyykko and L. Laaksonen, *J. Phys. Chem.*, 1984, **88**, 4892–4895.
113 R. Denning, *Complexes, Clusters and Crystal Chemistry*, Springer Berlin Heidelberg, 1992, vol. 79, pp. 215–276.
114 F. Hund, *Z. Phys.*, 1932, **73**, 565–577.
115 R. S. Mulliken, *Science*, 1967, **157**, 13.
116 J. Pipek and P. G. Mezey, *J. Chem. Phys.*, 1989, **90**, 4916.
117 E. Sokolowski, C. Nordling and K. Siegbahn, *Phys. Rev.*, 1958, **110**, 776.
118 S. Hagström, C. Nordling and K. Siegbahn, *Z. Phys.*, 1964, **178**, 439–444.
119 P. Indelicato and E. Lindroth, *Phys. Rev. A: At., Mol., Opt. Phys.*, 1992, **46**, 2426–2436.
120 T. Mooney, E. Lindroth, P. Indelicato, E. G. Kessler and R. D. Deslattes, *Phys. Rev. A: At., Mol., Opt. Phys.*, 1992, **45**, 1531–1543.
121 P. Indelicato, S. Boucard and E. Lindroth, *Eur. Phys. J. D*, 1998, **3**, 29–41.
122 M. Nooijen and R. J. Bartlett, *J. Chem. Phys.*, 1995, **102**, 6735–6756.
123 J. A. Bearden and A. F. Burr, *Rev. Mod. Phys.*, 1967, **39**, 125–142.
124 R. G. Denning, *J. Phys. Chem.*, 2007, **111**, 4125–4143.
125 I. Cacelli, V. Carravetta, A. Rizzo and R. Moccia, *Phys. Rep.*, 1991, **205**, 283–351.
126 U. Ekström and P. Norman, *Phys. Rev. A: At., Mol., Opt. Phys.*, 2006, **74**, 042722.
127 G. Tu, V. Carravetta, O. Vahtras and H. Ågren, *J. Chem. Phys.*, 2007, **127**, 174110.
128 A. Dreuw, J. L. Weisman and M. Head-Gordon, *J. Chem. Phys.*, 2003, **119**, 2943–2946.
129 D. P. Chong, O. V. Gritsenko and E. J. Baerends, *J. Chem. Phys.*, 2002, **116**, 1760–1772.
130 O. V. Gritsenko, B. Braïda and E. J. Baerends, *J. Chem. Phys.*, 2003, **119**, 1937–1950.
131 O. Gritsenko and E. J. Baerends, *Can. J. Chem.*, 2009, **87**, 1383–1391.
132 M. O. Krause and J. H. Oliver, *J. Phys. Chem. Ref. Data*, 1979, **8**, 329–338.
133 K. Hämäläinen, D. P. Siddons, J. B. Hastings and L. E. Berman, *Phys. Rev. Lett.*, 1991, **67**, 2850–2853.
134 Y. Zhang, J. D. Biggs, D. Healion, N. Govind and S. Mukamel, *J. Chem. Phys.*, 2012, **137**, 194306.
135 M. Roemelt, D. Maganas, S. DeBeer and F. Neese, *J. Chem. Phys.*, 2013, **138**, 204101.

Part II.

Molecular properties

5. Molecular Properties with ab-initio Relativistic Methods

In a review article entitled 'Ab Initio Calculation of Molecular Properties' [40] Werner Kutzelnigg commented that:

"Although quantum chemists have spent most of their effort on the construction of wave functions and energies, the final aim of a quantum-chemical calculation is often neither the wave function nor the energy, but rather some physical property, or to phrase it more physically, the response of a system to an external perturbation, e.g. to a magnetic or an electric field or the combination of various fields."

The motivation of studying molecular properties in a relativistic framework is not very much different from a non-relativistic framework. The major difference between those two domains lies in the molecular Hamiltonian and nature of the interaction between the system and the field. The definition of a property operator may differ depending upon that. Notably, magnetic interaction is often envisaged as a pure relativistic phenomena, and the non-relativistic treatment of it is somewhat ad-hoc [58]. In the first section of this chapter we will describe briefly the nature of the Hamiltonian in presence of fields and how various terms enter the Hamiltonian due to that. I will separate out the contribution of spin-dependent terms from scalar relativity in that section. Then the role of Spin Orbit Coupling (SOC) in molecular properties will be theoretically analyzed in section 5.2. For the calculation of properties one needs an accurate wave function or density. Remarkable developments of the wave function methodologies, as described in the first half of the thesis, can be utilized by defining a suitable framework for the molecular property calculation. We will discuss the framework, by which this connection can be established in section 5.4. The accuracy of a calculated molecular property is directly related to the correctness of a wave function. Coupled Cluster (CC) theory is unequivocally considered as one of the most accurate methods for the single reference problems. We will discuss in section 6.3 how one can calculate time-independent molecular properties using the relativistic CC method. The formulation we have used in that section is largely motivated from the non-relativistic theories. However, due to the very nature of the Dirac equation there are some differences namely in the symmetry structure, nature of the orbital relaxation etc., they will be amply clarified in that chapter. This method has been implemented in the DIRAC [1] quantum chemistry package. The principle of this implementation and some theoretical background of symmetry aspects will be provided in chapter 6. I will discuss all the pertinent details of this implementation also in section 6.3. Finally, in the same section 6.3, I will show applications of the present method. Our section 6.3 is the manuscript of an article.

5.1. Molecule Under External field

In the realm of molecular properties a molecule and the interaction of it with the field is treated quantum mechanically, but the electromagnetic field itself is treated classically i.e, by Maxwell equations. The field enters the molecular Hamiltonian by the so-called "minimal substitution" [25]:

$$\vec{p} \rightarrow \vec{p} + e\vec{A} = \vec{\pi} \tag{5.1}$$

$$E \rightarrow E + e\phi \tag{5.2}$$

where, $\vec{A}$ is the vector potential and ϕ is the scalar potential. $\vec{\pi}$ is called the kinetic momentum and $\vec{p}$ is the canonical momentum. This form of the substitution was obtained when it was tried to construct an interaction Lagrangian in Lorentz co-variant form [62]. In the non-relativistic domain, the same form of the substitution is used, in somewhat ad-hoc manner. Though that choice in practice provides good description at that domain as well.

For a uniform electric field in the absence of any magnetic field, the form of the scalar and vector potential is :

$$\phi(r) = -\vec{r}.\vec{E}; \;\; \vec{A} = \vec{0} \tag{5.3}$$

For the magnetic field, specific forms of the vector potential depends on whether the field is external or internal. For a homogeneous external magnetic field in the absence of electric field, the scalar and vector potential is:

$$\phi = 0; \;\; \vec{A}_B(r) = \frac{1}{2}\vec{B} \times \vec{r}, \tag{5.4}$$

and, for the internal nuclear magnetic moments, they are:

$$\phi = 0; \;\; \vec{A}_{m_k}(r) = \frac{1}{c^2}\frac{\vec{m}_k \times \vec{r}_k}{r_k^3} \tag{5.5}$$

where, $\vec{m}_k$ is the point magnetic dipole of nucleus k [1]. In Equation 5.4, $\vec{r}$ should ideally be expressed as $(\vec{r} - \vec{G})$ where $\vec{G}$ is the Gauge origin for the vector potential and for Equation 5.5 gauge origin is customarily chosen at the position of the nucleus for an atom and for an molecule at the centre of mass. In approximate calculations the choice of gauge origin is very problematic issue. In this thesis, though, we are not worried with this problem and henceforth this issue will not be addressed.

After minimal substitution, the one-electronic part of the Dirac Hamiltonian is (we will consider only the vector potential since that will only be the relevant part for the subsequent discussion)

$$H^D = \begin{pmatrix} V & c\vec{\sigma}.(\vec{p} + e\vec{A}) \\ c\vec{\sigma}.(\vec{p} + e\vec{A}) & V - 2mc^2 \end{pmatrix}. \tag{5.6}$$

[1] It is slightly counter-intuitive, since in relativistic theories finite size of the nucleus is considered. It is due to the classical treatment of the field.

To understand the physical content it is often a common practise to decompose Equation 5.6 into spin-free and spin-dependent part. Following the same strategy as in subsection 3.1.1, we express the small-component of a Dirac spinor as:

$$2mc\Psi^S = (\vec{\sigma}.\vec{p})\phi^L \tag{5.7}$$

where, ϕ^L is called the pseudo-large component. It defines a non-unitary transformation matrix to the wave function $\begin{pmatrix}\Psi_L\\ \Psi_S\end{pmatrix}$:

$$W = \begin{pmatrix}\mathbb{I}_2 & \mathbb{O}_2\\ \mathbb{O}_2 & \frac{(\vec{\sigma}.\vec{p})}{2mc}\end{pmatrix}. \tag{5.8}$$

By carrying out a transformation to Equation 5.6 employing the W matrix, we isolate the spin-dependent and the spin-free part:

$$H = H^{sf} + H^{sd} \tag{5.9}$$

where,

$$H^{sf} = \begin{pmatrix}V & T\\ T & \frac{\vec{p}V\vec{p}}{4m^2c^2} - T\end{pmatrix} + \frac{e}{2m}\begin{pmatrix}\mathbb{O}_2 & \vec{A}.\vec{p}\\ \vec{p}.\vec{A} & \mathbb{O}_2\end{pmatrix} \tag{5.10}$$

$$H^{sd} = \begin{pmatrix}\mathbb{O}_2 & \mathbb{O}_2\\ \mathbb{O}_2 & \frac{i\sigma.\vec{p}V\times\vec{p}}{4m^2c^2}\end{pmatrix} + \frac{e}{2m}\begin{pmatrix}\mathbb{O}_2 & i\sigma.(\vec{A}\times\vec{p})\\ i\sigma.(\vec{p}\times\vec{A}) & \mathbb{O}_2\end{pmatrix} \tag{5.11}$$

and, $T = \frac{p^2}{2m}$.

Further manipulation of property term in Equation 5.10 by using the relations $\vec{\nabla}.\vec{A} = 0$ (the Coulomb Gauge condition), $\vec{\nabla}\times\vec{A} = \vec{B}$ and using the definitions of $\vec{A}_B$ and $\vec{A}_{m_k}$ gives us,

$$H^{sf}_{oz} = \frac{e}{4m}\begin{pmatrix}\mathbb{O}_2 & \vec{B}.(\vec{r}\times\vec{p})\\ \vec{B}.(\vec{r}\times\vec{p}) & \mathbb{O}_2\end{pmatrix} \textit{ Orbital Zeeman} \tag{5.12}$$

$$H^{sf}_{PSO} = \frac{e}{2m}\begin{pmatrix}\mathbb{O}_2 & \vec{m}_k.(\frac{\vec{r}_k}{r_k^3}\times\vec{p})\\ \vec{m}_k.(\frac{\vec{r}_k}{r_k^3}\times\vec{p}) & \mathbb{O}_2\end{pmatrix} \textit{ Paramagnetic Spin Orbit} \tag{5.13}$$

Similarly with the property term in Equation 5.11 one gets

$$H^{sd}_{prop} = \frac{ie}{2m}\begin{pmatrix}\mathbb{O}_2 & \vec{\sigma}.(\vec{A}\times\vec{p})\\ \vec{\sigma}.(\vec{A}\times\vec{p}) & \mathbb{O}_2\end{pmatrix} + \frac{e}{2m}\begin{pmatrix}\mathbb{O}_2 & O_2\\ \vec{\sigma}.\vec{B}' & \mathbb{O}_2\end{pmatrix} \tag{5.14}$$

where, $\vec{B}' = \vec{B} + \vec{B}_{hf}$; $\vec{B}_{hf}$ stands for magnetic hyperfine field, which contains

$$H^{sd}_{SZ} = \frac{e}{4m}\begin{pmatrix}\mathbb{O}_2 & \vec{\sigma}\\ \vec{\sigma} & \mathbb{O}_2\end{pmatrix}\left[\begin{pmatrix}\mathbb{O}_2 & \vec{B}.(\vec{\nabla}.\vec{r}) - (B.\vec{\nabla})r\\ \vec{B}.(\vec{\nabla}.\vec{r}) - (\vec{B}.\vec{\nabla})\vec{r} & \mathbb{O}_2\end{pmatrix} + 2\begin{pmatrix}\mathbb{O}_2 & O_2\\ \vec{B} & \mathbb{O}_2\end{pmatrix}\right] \textit{ Spin Zeeman} \tag{5.15}$$

and,

$$H^{sd}_{FC+SD} = \frac{e}{4m}\begin{pmatrix}\mathbb{O}_2 & \vec{\sigma}\\ \vec{\sigma} & \mathbb{O}_2\end{pmatrix} \quad \textit{Fermi-Contact and Spin Dipole} \tag{5.16}$$
$$\times \left[\begin{pmatrix}\mathbb{O}_2 & \vec{m}_k(\vec{\nabla}\frac{\vec{r}_k}{r_k^3}) - \frac{\vec{r}_k}{r_k^3}(\vec{m}_k\vec{\nabla})\\ \vec{m}_k(\vec{\nabla}\frac{\vec{r}_k}{r_k^3}) - \frac{\vec{r}_k}{r_k^3}(\vec{m}_k\vec{\nabla}) & \mathbb{O}_2\end{pmatrix} + 2\begin{pmatrix}\mathbb{O}_2 & O_2\\ B_{hf} & \mathbb{O}_2\end{pmatrix}\right]$$

(in the derivation of Equation 5.16, we have used $\vec{\nabla}\vec{m}_k = 0$, since $\vec{m}_k$ is independent of electronic coordinates.)

In the next section, this spin-separated Hamiltonian will be used to understand the role of SOC for few specific molecular properties.

5.2. Effect of Spin-Orbit coupling on molecular properties

In this section we will show some example of molecular properties, for which inclusion of SOC at the zeroth-order of perturbation has several interesting consequences.

5.2.1. Electronic g-tensor

In Electron Paramagnetic Resonance (EPR) spectroscopy, the g-tensor along with the zero-field splitting tensor provide the essential description of electronic transitions. Energies and intensities of this spectroscopy can be conveniently described by an effective Hamiltonian expressed in terms of magnetic field ($\vec{B}$) and fictitious effective spin operator ($\langle S\rangle$):

$$H^{EPR}_{eff} = \mu_B \vec{B} g \langle S\rangle \tag{5.17}$$

where μ_B is Bohr's magneton and g is a (3×3) tensor depending on the direction of the external magnetic field. The effective spin is used to represent the experimental multiplet splittings. One can easily see that the form of the effective Hamiltonian summarizes the electronic Zeeman effect. From the ab-initio point of view, the electronic g-tensor is a first order property with respect to the external magnetic field. It is expressed as:

$$g_{\mu\nu} = \frac{2c}{\langle S_\nu\rangle}\frac{\partial E}{\partial B_\mu}. \tag{5.18}$$

From the discussion of last section we can see that the contributing perturbation operators for the calculation of g-tensor are : $\frac{\partial H^{sf}_{OZ}}{\partial B_\mu}$ and $\frac{\partial H^{sd}_{SZ}}{\partial B_\mu}$

For clarity, we write the $\frac{\partial H^{sf}_{OZ}}{\partial B_\mu}$ as following:

$$\frac{\partial H^{sf}_{OZ}}{\partial B_\mu} = \frac{e}{2m}\begin{pmatrix}\mathbb{O}_2 & l_\mu\\ l_\mu & \mathbb{O}_2\end{pmatrix}. \tag{5.19}$$

According to the Hellman-Feynman theorem (Equation 5.35) terms in Equation 5.19 will give a zero contribution since the expectation value of angular momentum operator

is vanishing when spin-free hence real wave functions are considered. The other term i.e, $\frac{\partial H_{SZ}^{sd}}{\partial B_\mu}$ will give a constant contribution 2 for each direction of the magnetic field. It does not represent any splitting pattern, therefore not of any interest. However, with the consideration of spin-orbit coupling operator (first term in Equation 5.11) the wave function will no longer be real because of the coupling between spin and orbital degrees of freedom. In that case, both the terms contribute at the same order of hyperfine coupling constant (α). Because of that, in the non-relativistic domain, one needs to consider SO coupling as another perturbation apart from the static magnetic field. It also suggests we need to consider linear response or second order energy derivative technique for its calculation. In the 4c DC level only the consideration of expectation value allows us to calculate g-tensor.

5.2.2. NMR shielding

In Nuclear Magnetic Resonance (NMR) spectroscopy, the nuclei of our interest are shielded from the full external magnetic field, $\vec{B}$, by the very presence of electron shell surrounding them. Nuclear magnetic moments can also couple between themselves by magnetic polarization of the electron system. The connection between this spin-spin coupling tensor, J, and shielding tensor, σ_k of a molecule with its non-relativistic electronic wave function was given by Ramsey [56]:

$$H_{eff}^{NMR} = -\sum_k \vec{B}^T(1-\sigma_k)\vec{m}_k + \frac{1}{2}\sum_{k\neq l}\vec{m}_k^T(D_{kl}+\vec{J}_{kl})\vec{m}_l \tag{5.20}$$

where, D_{KL} is the classical dipolar interaction.

The NMR shielding therefore is a second order molecular property, where derivative is taken both with respect to the external magnetic field (B) and internal magnetic moment ($\vec{m}_k$):

$$\sigma_{k;\mu\nu} = \frac{\partial^2 E}{\partial B_\mu \partial m_{k;\nu}}. \tag{5.21}$$

In the interpretation purpose, the most convenient form of this expression is given by the sum-over-state (SOS) approach [2]:

$$\sigma_{k;\mu\nu} = \langle\psi_0|h^{11}|\psi_0\rangle + \sum_{p>0}\frac{\langle\psi_0|h^{01}|\psi_p\rangle\langle\psi_p|h^{10}|\psi_0\rangle}{E_0-E_p} \tag{5.22}$$

where, ψ_0 is the unperturbed state and ψ_ps are the excited states. h^{01}, h^{10} are the operators for external magnetic field perturbation, nuclear magnetic moment perturbation respectively and h^{11} is a mixture of both.

[2] In practice, the SOS approach is rarely used. For HF wave functions it is analogous to the uncoupled HF equation, meaning electron-electron repulsion term is missing. Much accurate expression is obtained by Coupled Perturbed HF approach where that repulsion term is used to obtain first order response parameters.

We will now show what will happen if we choose ψ_0 as a SF wave function. To do that we will again resort to the spin-separated form of the Hamiltonian. The h^{01} operator contains spin-independent OZ term and spin-dependent SZ term. As ψ_0 preserves spin symmetry, only surviving terms from the SOS expression are those, for which both h^{01} and h^{10} are either spin-free or spin-dependent. If SO coupling is considered, the spin restriction is lifted. Therefore, admixtures between spin-free and spin-dependent terms will also contribute. Any spin-free approach, by this argument, misses contributions from PSO-FC and PSO-SD terms. In heavy elements those missing terms may play very significant role [10]. However, third order perturbation expression considering SO coupling as an additional perturbation operator recovers the contribution due to those terms. The drawback of that treatment is two fold : the third order expansion is computationally much more expensive, requires quadratic response approach and SO coupling in many cases is not at all a perturbation. Here one can notice that the diamagnetic term is missing from our analysis. In the non-relativistic theories the diamagnetic contribution arises from the A^2 part of the perturbation. It is possible to recover that term if we use the relation $\psi^L = \frac{1}{2mc}(\vec{\sigma}.\vec{\pi})\phi^L$ unlike what we have done in Equation 5.7. By using the Dirac identity:

$$(\vec{\sigma}.\vec{\pi}).(\vec{\sigma}.\vec{\pi}) = p^2 + A^2 + [\vec{\sigma}.\vec{p}, \vec{\sigma}.\vec{A}]_+ \tag{5.23}$$

we can clearly see the existence of A^2 term. The same line of argument has been put forward for the construction of small component basis set for studying magnetic properties, instead of Restricted Kinetic Balance (RKB) condition one should have used Restricted Magnetic Balance (RMB) [9].

As a digression here we will try to see what are the terms we get from the original Dirac Hamiltonian. We can see that first by substituting Equation 5.4 and Equation 5.5 into the one-electronic part of the Dirac Equation

$$h_D^B = c(\vec{\alpha}.\vec{p}) + c(\vec{\alpha}.\vec{A}_B(r)) + c(\vec{\alpha}.\vec{A}_{\vec{m}_k}(r)) + \beta mc^2 \tag{5.24}$$

then, by taking derivative with respect to $\vec{B}$ and $\vec{m}_k$

$$\begin{aligned} h^{01} &= \frac{\partial h_D^B}{\partial B_\mu}|_{\vec{B}=0,\vec{m}_k=0} \\ &= \frac{c}{2}(\vec{\alpha} \times \vec{r})_\mu \qquad (5.25) \\ h^{10} &= \frac{\partial h_D^B}{\partial m_{k;\mu}}|_{\vec{B}=0,\vec{m}_k=0} \\ &= \frac{1}{c}(\vec{\alpha} \times \frac{\vec{r}_k}{r_k^3}) \qquad (5.26) \\ h^{11} &= \frac{\partial h_D^B}{\partial B_\mu \partial m_{k;\nu}}|_{\vec{B}=0,\vec{m}_k=0} \\ &= 0 \qquad (5.27) \end{aligned}$$

One should notice that the h^{11} term has no contribution when full Dirac equation is considered. In the non-relativistic case that term gives the diamagnetic contribution. In the context of Dirac Hamiltonian the origin of diamagnetism can be traced in the rotation between positive energy and the negative energy orbitals [58, 41].

5.2.3. Parity Violation

There are ample evidences in the universe for the violation of parity (P-odd effect). Difference of energy between two enantiomers of a molecule is one of such effects. The reason of parity violation is often attributed to the electroweak interaction. The energy shift of this interaction is so small that it is very difficult to measure unambiguously. Though for atoms there are some firm evidences of measuring the parity violation contribution [86], in the molecular domain still it is "unknown". There is continuous search for finding a suitable candidate molecule - both experimentally and theoretically [54, 53, 52, 15]. For theory it is already evident that one needs to employ very sophisticated methodology for this property.

The derivation of the parity-violating Hamiltonian needs tedious recourse to standard model physics, gauge theory and quantum field theory. In the framework of DC Hamiltonian it is given by

$$H_{PV} = \frac{G_F}{2\sqrt{2}} \sum_{i,n} Q_{W,n} \gamma_i^5 \rho_n(\vec{r}_i) \tag{5.28}$$

where $G_F = 1.16637 \times 10^{-11} MeV^{-2} = 2.22255 \times 10^{-14}$ a.u. is the Fermi coupling constant. The summation runs over the nuclei, n and electrons, i. $Q_{W,n} = -N_n + Z_n(1 - 4sin^2\theta_w)$, where N_n and Z_n are the number of neutrons and protons on each nucleus. θ_w is called the Weinberg mixing angle, we have chosen a fixed value of 0.2319 for $sin^2\theta_w$. ρ_n is the normalized nucleon density. γ^5 is the (4×4) chirality operator, which is given by:

$$\gamma^5 = \begin{pmatrix} \mathbb{O} & \mathbb{I} \\ \mathbb{I} & \mathbb{O} \end{pmatrix} \tag{5.29}$$

Nuclear spin-dependent PV effect has been neglected since it has been argued in the literature that for the closed-shell system it is not significant [44].

We will show results of the study of this property in the manuscript.

In spin-free theories the PV operator turns out to be:

$$H_{PV} = \frac{G_F}{4mc\sqrt{2}} \sum_{i,n} \left[Q_{W,n} \begin{pmatrix} \mathbb{O}_2 & \rho_n(\vec{r}_i).(\vec{\sigma}_i.\vec{p}) \\ (\vec{\sigma}_i.\vec{p}).\rho_n(\vec{r}_i) & \mathbb{O}_2 \end{pmatrix} \right] \tag{5.30}$$

Since this is a purely imaginary operator, gives a zero expectation value with real wave function. Non-vanishing contribution for those cases are obtained with the consideration of SO coupling as a first order perturbation. This demonstrates the utility of variational treatment of SO coupling for PV.

5.3. Coupled Relativistic and Correlation Effect on Molecular properties:

In this section I will discuss the importance of correlation in the calculation of molecular properties when relativistic Hamiltonians are used. Let us consider the example of Electric Field Gradient (EFG).

The quadrupolar interaction energy between an electric charge and a nuclear charge is given by :

$$E_{int}^{(2)} = \frac{1}{2}BQ \tag{5.31}$$

where B is the nuclear quadruple moment tensor and Q is called the the Electric Field Gradient tensor.

The operator for EFG at the nucleus position ($\vec{R}$) of an atom in spherical co-ordinate is given by

$$Q_{\alpha\beta}(\vec{r},\vec{R}) = -\frac{3(\vec{r}_\alpha - \vec{R}_\alpha)(\vec{r}_\beta - \vec{R}_\beta) - (\vec{r}-\vec{R})^2\delta_{\alpha\beta}}{|\vec{r}-\vec{R}|^5} \tag{5.32}$$

and the nuclear field gradient contribution is

$$Q_{\alpha\beta}^{nuc}(\vec{R}) = \sum_k Z_k \frac{3(\vec{R}_k - \vec{R}_\alpha)(\vec{R}_k - \vec{R}_\beta) - (\vec{R}_k - \vec{R})^2\delta_{\alpha\beta}}{|\vec{R}_k - \vec{R}|^5} \tag{5.33}$$

where, α, β belong to the x, y and z cartesian components and k belongs to the nuclear co-ordinates, let's say, X, Y, Z. $Q_{\alpha\beta}^{nuc}$ is an additive constant for a fixed geometry of the molecule. We can see that $Q_{\alpha\beta}$ has formal dependence on the parameter - distance from the nucleus, at the inverse cube order. It is therefore called a core property. The core region of a heavy element is subject to very strong relativistic effects. It is indeed numerically shown that relativistic effects are very strong for EFG [33].

In an atom, EFG arises only when open valence shell is present at $j > 0$ orbitals. For $j = 0$, we get an equal charge distribution along each co-ordinate direction. The traceless spherical tensor ($3\alpha\beta - \delta_{\alpha\beta}$) representation of EFG will therefore give a zero contribution. We have to break spherical symmetry to get a non-zero value. Similarly for molecules we find EFG values only when charge distribution deviates from the sphericity [3]. In the core-region of a molecule the charge distribution is largely spherical in nature, whereas in the valence region due to the effect of bonding it is not. As a result, the major contribution of the EFG values comes from the valence region. This point is substantiated numerically by Visscher *et al.* [79], Van Lenthe *et al.* [73] and Neese *et al.* [3]. Due to this valence nature the contribution of correlation methods can be predicted as very high. It is indeed the case and correlation effect is almost equivalent to the total mean-field relativistic effects for several systems [79]. In the correlation treatment apart

[3] Due to this behaviour of EFG, it is a sensitive probe for Jahn-Teller distortions, impurities and defects in solids.

from the valence we should also consider the effect of core to the extent it influences the valence region. What remains to be discussed is the effect of SO coupling on EFG. A First guess is that as EFG is directly related to the bonding, the cases where SO coupling plays significant role in bonding would be substantially important for EFG as well. However, it has been argued by Pyykko *et.al.* [51] through the spin-orbit tilting mechanism [4] that this effect is somewhat smaller than the scalar relativistic one, though not insignificant at all. Aquino *et.al.* [8] has also shown very recently by ZORA-DFT study that this effect is significantly large on the halogen centre of TlI molecule. In the manuscript we will investigate this effect for the molecules containing 6p-block atoms. There are few other allied molecular properties where the central theme is electron density on the nucleus e.g, contact density, which has been used for the study of Mössbauer isomeric shift [34] ; hyperfine interaction, mostly used for NMR J coupling values etc. The major interactions would be very much close to the discussion above.

5.4. Numerical vs Analytical approach

When a molecule is exposed to an external field (X), the total energy can be expressed as a Taylor series expansion around the zero field situation:

$$E(X) = E(0) + \frac{dE}{dX}|_{X=0}X + \frac{1}{2!}\frac{d^2E}{dX^2}|_{X=0}X^2 + \frac{1}{3!}\frac{d^3E}{dX^3}|_{X=0}X^3 + .. \tag{5.34}$$

In the most general situation, there can be arbitrary number of perturbations and then the derivatives of order higher than one can be of mixed type.

The connection between molecular properties with different derivative terms requires to understand the detailed structure of the Hamiltonian in presence of the field as has been described in the last section. One way of connecting them is through the Hellman-Feynman theorem:

$$\frac{dE}{dX}|_{X=0} = \langle\phi_X|\frac{\partial H}{\partial X}|\phi_X\rangle \tag{5.35}$$

Where, ϕ_X is a variationally determined wave function and the perturbation is independent of the molecular parameters. The gradient term of Equation 5.34 can be understood for a simple situation in presence of a static electric field, where the RHS of Equation 5.35 gives the dipole moment of a molecule.

Energy derivatives can very easily be evaluated by applying numerical differentiation formula e.g, symmetric difference formula:

$$\frac{dE}{dX} = \frac{E(+\Delta X) - E(-\Delta X)}{2\Delta X} \tag{5.36}$$

To achieve higher accuracy 5-point and 7-point stencil formulas are also known [30]. Numerically second or higher derivative formulas are also not difficult to obtain and

[4] An p orbital from a scalar relativistic calculation is split into $p_{1/2}$ and $p_{3/2}$ shells in presence of SOC. Valence p is contracted due to the scalar relativistic effects, but SOC allows $p_{3/2}$ shell to expand. That reduces the value of EFG.

the connection of that to the specific properties can be seen by identically extending Equation 5.35 to the higher orders. Despite the ease of implementation, the numerical methods suffer from the following shortcomings:

- Plagued by limited numerical accuracy. The higher the order of derivative, the less accurate it is. Often very rigorous calibration of field-strength, grid-size is necessary for highly sensitive molecular properties.
- Computational cost scales very high if one wants to obtain high accuracy.
- Extension to the time-dependent molecular properties are not possible.

The more rigorous analytical evaluation of the derivatives may alleviate most of the problems mentioned in the above list.

The analytic evaluation of the derivatives requires a much closer look into the dependence of the wave function and the energy on the external perturbation. For our purpose, we will write energy in the following functional form:

$$E = E(X, c_i(X)) \tag{5.37}$$

where, $c_i(X)$ represents a set of wave function parameters.

The gradient formula for Equation 5.37 is

$$\frac{dE}{dX} = \frac{\partial E}{\partial X} + \sum_i \frac{\partial E}{\partial c_i} \frac{dc_i}{dX} \tag{5.38}$$

For a variational method $\frac{\partial E}{\partial c_i}$ vanishes (e.g, in the HF method energy is minimum with respect to the variation of MO coefficients), therefore the gradient of energy takes the simple form:

$$\frac{dE}{dX} = \frac{\partial E}{\partial X} \tag{5.39}$$

which means a simple expectation value implementation will provide us desired properties. To reach Equation 5.39 it is also sufficient that $\frac{dc_i}{dX} = 0$, meaning wave function is free of any perturbation parameter. In most of the cases i.e, in presence of external electromagnetic field that criteria is fulfilled, except for geometrical perturbation. For geometrical perturbation it can be realized by considering Atomic Orbital (AO) as an wave function parameter. They follow the nuclear position therefore geometrical derivative of them are not vanishing. This is a finite basis artefact.

For the non-variational cases, however, the situation is not that straightforward. The energy functional, in that case, depends on more than one wave function parameters of which at least one parameter is not variational. For instance, in the Configuration Interaction (CI) method wave function has a dependence on both the MO coefficients and the coefficient of configurations. The CI energy is minimum only with respect to the variation of configuration coefficients.

In those cases, the equations for determining the non-variational wave function parameters are coupled with the energy functional Equation 5.37, thereby we define a generalized Lagrangian:

$$L(X, c_i, \Lambda) = E(X, c_i, \Lambda) + \Lambda g(X, c_i(X)) \tag{5.40}$$

Where, 'g' is the functional to determine wave function parameters and Λ is the Lagrangian multiplier. Afterwards, by invoking stationarity with respect to all parameters other than the external field,

$$\frac{\partial L}{\partial \Lambda} = 0 \tag{5.41}$$

$$\frac{\partial L}{\partial c_i} = 0 \tag{5.42}$$

we obtain the simple expression as following:

$$\frac{dL}{dX} = \frac{\partial L}{\partial X} \tag{5.43}$$

$$= \frac{\partial E}{\partial X} + \Lambda \frac{\partial g}{\partial X} \tag{5.44}$$

which is a reminiscent of the expectation value like equation for variational theories. We will discuss this point for a more specific case in the next section.

For the higher order analytical derivatives, we need to again start from the energy functional in Equation 5.37 for the variational cases and Equation 5.40 for the non-variational cases and take second derivatives of them. Without going into details we shall state salient features of those derivatives and for more details will refer to the article by Helgaker *et.al.* [26]:

- for the variational cases, we have only wave function parameters, for which we need to calculate the response contribution i.e, $\frac{\partial c}{\partial X}$. They follow the (2n+1) rule of a variational perturbation theory. It is typically solved via Coupled Perturbed Hartree Fock (CPHF) method.

- for the non-variational cases, we need to calculate the response contribution both for the c and Λ parameters. Like variational cases, the response of c would follow the (2n+1) rule and response of Λ follows the (2n+2) rules. That greatly simplifies the higher order derivative expressions.

According to the above formulation, we get extra equations to solve for the analytical evaluation of derivatives. The number of those equations increase with the increase of the order of the derivative. Sometimes, a mixed approach is taken for the higher order derivatives where lowest order derivative is calculated analytically and the higher orders are calculated numerically on top of that. In that way one can minimise the effort of implementing too many new equations.

6. Implementation of the 4c Analytical Coupled Cluster Gradient

In this thesis the major effort was the implementation of analytic gradient code of the 4c relativistic CC theory. The infrastructure we have used, has been provided by the RELCCSD module in DIRAC [1], mostly developed by Lucas Visscher. That module provides an efficient relativistic symmetry scheme, parallel environment. However, that lacks the flexibility of building any single reference coupled cluster code of arbitrary complexity. I should clarify it a bit. In CC coding we need to deal with several binary tensor contractions, the implementation of them require several explicit sorting of integrals, apart from the pivotal contraction step. That module takes care of all those steps for a particular tensor contraction with a hand written explicit code. Moreover it was written for CCSD method, therefore lacks few ingredients of generality. The disadvantage is that adaption of any new CC family of methods e.g, CC analytic gradient, the equation-of-motion coupled cluster where one needs to handle several extra new terms, is tedious and very much error-prone. Therefore we have tried to build a module which can handle tensor contractions related to SRCC theory of arbitrary complexity. The details of that implementation step has been given in the manuscript attached at the end of this chapter.

Another aspect of this work is the implementation of symmetry. In modern day coding practice symmetry is often neglected especially at the correlated step aiming at very large molecules containing huge number of atoms, for which there is no symmetry element. It is advantageous in terms of coding, parallel extension etc. However, when we are dealing with molecules containing not too many atoms, then the symmetry elements are usually there. The relativistic correlation method still has not reached at that level where one can use it for the molecules having large number atoms because of its inherent huge computational cost as discussed in chapter 4. Still the studies are mostly aimed at the investigation of relativistic effects, very specific properties linked to relativistic interaction of the system and the field etc. In that purpose it is very practical to think of having a rigorous symmetry scheme. With the relativistic Hamiltonian we loose the spin-symmetry of the orbitals, also the relativistic electrons don't span spatial point-group symmetry adapted MOs. Instead one can take benefit from the Time Reversal (TR) symmetry and the Double Group (DG) symmetry. Here I shall describe the theoretical aspects of both the symmetries and how they have been used in DIRAC.

6.1. Time Reversal Symmetry

According to the Kramer's degeneracy theorem, in the absence of external magnetic field, for any time-reversal symmetry conserving Hamiltonian, the electronic energy levels are at least doubly degenerate. It allows us to construct a basis of $(\phi, \overline{\phi})$ kind, where the essential relationships between them are:

$$\mathcal{K}\phi = \overline{\phi};\ \ \mathcal{K}^2\phi = -\phi \tag{6.1}$$

where, $\mathcal{K}$ is an antilinear operator i.e, for a complex number 'c', $\mathcal{K}c\phi = c^*\mathcal{K}\phi$. In the 4-component picture the time-reversal symmetry operator is represented by

$$\hat{\mathcal{K}} = i\vec{\Sigma}_y\mathcal{K}_0 \tag{6.2}$$

where,

$$\vec{\Sigma}_y = \begin{pmatrix} \vec{\sigma}_y & 0 \\ 0 & \vec{\sigma}_y \end{pmatrix} \tag{6.3}$$

and $\mathcal{K}_0$ is a complex conjugation operator. It is easy to show by using the relationships in Equation 6.2 that the matrix representation of a time-reversal symmetric one-body operator (let's say Fock Operator F) in the $(\phi, \overline{\phi})$ basis is:

$$\mathbf{F} = \begin{pmatrix} \langle\phi|F|\phi\rangle & \langle\phi|F|\overline{\phi}\rangle \\ -\langle\phi|F|\overline{\phi}\rangle^* & \langle\phi|F|\phi\rangle^* \end{pmatrix} \tag{6.4}$$

For the particular case of Hermition operator this matrix can be diagonalized by using the quaternion unitary matrix:

$$U = \begin{pmatrix} \mathbb{I} & \check{j}\mathbb{I} \\ \check{j}\mathbb{I} & \mathbb{I} \end{pmatrix} \tag{6.5}$$

which gives us two degenerate eigenvectors and they are related by time reversal symmetry. This diagonalization is a very close reminder of the spin-integration in non-relativistic domain. Now, the HF equation can be expressed only in terms of one of those diagonal blocks. In DIRAC this unitary block diagonalization is used, which gives us a suitable Kramer's pair basis to use in the correlation module.

6.2. Double Group Symmetry

As per the prescription of Hans Bethe, double groups always contain an extra element Q (let's say) such that $Q^2 = E$. This Q is envisaged as a rotation by 2π angle about an arbitrary axis. Elements of a double group are represented as a $\{Q, E\} \otimes \{G\}$; where, $\{G\}$ are the elements of a single valued point group. That does not necessarily mean that number of irreducible representations for those groups will be twice in number of that of the single valued group because the extra elements could form a class with other existing elements. For a particular double group all the extra irreducible representations

are for Fermion functions and therefore they will be called Fermion representation and the older ones as Boson representations. We should note here that Q is not an identity operation for a Fermion function rather it will change the sign.

When DGs are coupled with time-reversal symmetry, due to the anti-unitary nature of the time-reversal operator it is not a simple direct-product group. However, there is always a possibility of getting reducible representation for the combined group. They are called co-representation. The Frobenius-Schur test assures that there are three possibilities with that representation:

1. time-reversal partner or Kramer's partners belong to the different rows of same irrep. these are called real groups.

2. Kramer's partners belong to the different irreps. this is complex group

3. Kramer's partners belong to the same one dimensional irrep. this is the case of quaternion group.

For the real and the complex group the time-reversal partners span two different irreps. However, in the case of quaternion groups it is required to do explicit block-diagonalization. Another major advantage of using time-reversal symmetry is that we are able to classify the algebra requires for various groups.

A molecular 4-spinor spans the fermionic irreps. However, each element of the 4-spinor is a scalar basis function, therefore it is possible to relate them to boson irrep. In Appendix A, following the work by [59], I have shown a scheme where integrals in a Kramer's pair basis can be connected to the boson irreps.

All the advantages of time-reversal symmetry are utilized in the most of the modules in DIRAC[1]. However, the RELCCSD module doesn't use the advantage of time-reversal symmetry. It uses only the DG symmetry which allows the spinors to span fermion irrep and the integrals in that case span the boson irreps. The molecular orbitals which are used in that section are Kramer's partners. It has been shown that for the DGs having more that one irrep, the Kramer's partner span the complex conjugate fermion irreps of one to another. In the RELCCSD module apart from the D_2h^* subgroups we use higher dimensional groups like: C_{16}^* and D_{8h}^*. For those higher dimensional groups even some of the boson irreps are complex valued (see the example of C_4^* in Appendix C), that adds substantial complexity to the coding effort. For the CC-type of contraction, the Direct Product Decomposition (DPD) scheme as advocated by Gauss *et al.*[24] for point group symmetries is the most efficient scheme. Here we use the DPD scheme for double groups, where an important part is sorting of integrals in a symmetry-packed manner. In Appendix B I have given an example how we carry out this sorting for the DGs. In the manuscript I have described this double-group symmetry-DPD scheme elaborately.

6.3. Paper III: Analytic Gradient at the 4-component Relativistic Coupled Cluster Level with Inclusion of Spin-Orbit Coupling (manuscript)

Analytic one-electron properties at the 4-component relativistic coupled cluster level with inclusion of spin-orbit coupling

Avijit Shee, Lucas Visscher, and Trond Saue

Citation: J. Chem. Phys. **145**, 184107 (2016); doi: 10.1063/1.4966643
View online: https://doi.org/10.1063/1.4966643
View Table of Contents: http://aip.scitation.org/toc/jcp/145/18
Published by the American Institute of Physics

Analytic one-electron properties at the 4-component relativistic coupled cluster level with inclusion of spin-orbit coupling

Avijit Shee,[1] Lucas Visscher,[2] and Trond Saue[1]
[1]*Laboratoire de Chimie et Physique Quantiques (UMR 5626), CNRS/Université Toulouse III - Paul Sabatier, 118 Route de Narbonne, F-31062 Toulouse Cedex, France*
[2]*Department of Theoretical Chemistry, Faculty of Sciences, Vrije Universiteit Amsterdam, De Boelelaan 1083, 1081 HV Amsterdam, The Netherlands*

(Received 12 June 2016; accepted 17 October 2016; published online 10 November 2016)

We present a formulation and implementation of the calculation of (orbital-unrelaxed) expectation values at the 4-component relativistic coupled cluster level with spin-orbit coupling included from the start. The Lagrangian-based analytical energy derivative technique constitutes the basic theoretical framework of this work. The key algorithms for single reference relativistic coupled cluster have been implemented using routines for general tensor contractions of up to rank-2 tensors in which the direct product decomposition scheme is employed to benefit from double group symmetry. As a sample application, we study the electric field gradient at the bismuth nucleus in the BiX (X = N, P) series of molecules, where the effect of spin-orbit coupling is substantial. Our results clearly indicate that the current reference value for the nuclear quadrupole moment of ^{209}Bi needs revision. We also have applied our method to the calculation of the parity violating energy shift of chiral molecules. The latter property is strictly zero in the absence of spin-orbit coupling. For the H_2X_2 (X = O,S,Se,Te) series of molecules the effect of correlation is found to be quite small. *Published by AIP Publishing.* [http://dx.doi.org/10.1063/1.4966643]

I. INTRODUCTION

Molecular properties are generally defined in terms of the response of a molecule to perturbations, such as electromagnetic fields or geometric displacements. The former are introduced via scalar and vector potentials into the electronic Hamiltonian through the principle of minimal electromagnetic coupling,[1] which expresses a relativistic coupling of particles and fields.[2] The resulting minimal substitution is employed both in the nonrelativistic and relativistic domains. This allows one, for instance, to study magnetic properties in a nonrelativistic framework, although one may argue that magnetic interactions, and in particular magnetic induction, vanish in the nonrelativistic limit.[3]

An important manifestation of magnetic induction is spin-orbit coupling (SOC),[4] which is often treated as a perturbation for efficiency reasons. However, SOC has a profound impact on various molecular properties and may thereby require a non-perturbative treatment. An example is the g-tensor of electron paramagnetic resonance (EPR) spectroscopy which would be strictly twice the 3×3 identity matrix at the nonrelativistic or scalar relativistic level[5] and would not show the dependence on molecular electronic structure that makes EPR such a useful technique. Another example is the parity violation (PV) energy difference between enantiomers of chiral molecules which vanishes if SOC is ignored.[6–8] The spin-orbit interaction may also have a sizable effect on NMR shieldings.[9,10]

The heavy elements, which show the most pronounced relativistic effects, also have many electrons, and electron correlation may therefore also have a significant impact on properties of molecules containing such elements. The electric field gradient (EFG) tensor at a nuclear position is an example; it has been shown for several systems that the correlation effect is almost equivalent to the total mean-field relativistic effect,[11] while the contribution of SOC can be equally significant.[12] This is due to the fact that this molecular property probes the electronic wavefunction both in the valence region and in the vicinity of nuclei. Other examples of properties that sensitively depend on the electronic wave function near the nuclei are the contact density, which has been used for the study of Mössbauer isomer shift,[13] and hyperfine coupling constants.[14] Like the EFG these properties can be used to study the chemical environment, as they primarily depend on the core tails of valence orbitals. The involvement of the valence region which is strongly influenced by electron correlation warrants a careful treatment of correlation.

The above considerations suggest that we in many situations need to consider scalar relativity, spin-orbit coupling, and electron correlation in a combined way.[15] If we restrict ourselves to wavefunction theory, then the second-order Møller-Plesset (MP2) gradient code, based on the 4-component relativistic Dirac-Coulomb (DC) Hamiltonian, by van Stralen *et al.*[16] is one of the few efforts in which both scalar and SOC relativistic effects are included from the outset. Technically easier is to only include scalar relativity in the mean field calculation and then introduce SOC in the subsequent correlation stage. Such a two-step procedure is more efficient in a coupled cluster (CC) framework than a Configuration Interaction (CI) one, since the former method is more efficient at recovering spin-orbit polarization.[17] Wang *et al.*[18] have reported a two-step procedure where an effective

one-electron spin-orbit operator is added at the CC level following a scalar relativistic Hartree–Fock (HF) calculation. An analytic gradient formulation and implementation of that approach has been reported by Wang and Gauss.[19] An alternative approach is to perform scalar relativistic CC energy calculations and then add SOC as an additional perturbation in response theory. Cheng and Gauss have accordingly recently reported CC analytic gradients based on the 4-component spinfree (SF) DC Hamiltonian[20] or the spinfree exact 2-component relativistic Hamiltonian (SF-1sX2C).[21,22] However, for heavy elements the valence electronic structure may be qualitatively altered by SOC and a response theory treatment will need to go through higher orders and can even fail dramatically in a valence-only treatment of electron correlation.[23]

Until now, where the DC coupled cluster based property calculations were deemed to be necessary, a numerical differentiation route was taken.[13,24,25] However, finite-field calculations are plagued by higher computational cost, are more sensitive to numerical noise, and cannot be straightforwardly extended to time-dependent properties. They are, therefore, better replaced by an analytical implementation. The major goal of this work is to provide a fully DC Hamiltonian based CC analytic gradient code that allows us to capture all the essential physics in a consistent way.

The formulation we have used is largely inspired by corresponding nonrelativistic theories. However, due to the very nature of the Dirac equation there are some differences, namely, in the treatment of symmetry and the nature of the orbital relaxation. They will be clarified in Section II. The method has been implemented in the DIRAC quantum chemistry package.[26] All the pertinent details of this implementation will be discussed in Section III. Sample applications of the present method are reported in Section IV. Finally, a summary of our work as well as future prospects will be given in Section V.

II. THEORY

Coupled cluster theory is (in practice) a non-variational theory based on a non-unitary exponential parametrization of the wave function

$$|CC\rangle = \exp(\hat{T})\,|\Phi_0\rangle\,, \quad \hat{T} = \sum_{l=1} t_l \hat{\tau}_l, \tag{1}$$

where t_l and $\hat{\tau}_l$ denote cluster amplitudes and excitation operators, respectively. The reference Φ_0 typically, and in this work, refers to the Hartree–Fock (HF) determinant. Furthermore, in the present work $\hat{T}$ is restricted to single and double excitations,

$$\hat{T} = \hat{T}_1 + \hat{T}_2, \quad \hat{T}_1 = \sum_{ia} t_i^a a_a^\dagger a_i, \quad \hat{T}_2 = \frac{1}{4}\sum_{ijab} t_{ij}^{ab} a_a^\dagger a_b^\dagger a_j a_i. \tag{2}$$

Here and in the following indices $i, j, \ldots, n, o$ refer to occupied (hole) orbitals, indices $a, b, \ldots, f, g$ refer to virtual (particle) orbitals, and p, q, r, s are general orbital indices. A troublesome aspect of 4-component relativistic theory is the presence of negative-energy orbitals which in turn implies that the electronic Hamiltonian, here taken as the Dirac-Coulomb Hamiltonian (see below), has no bound solutions.[27] A solution is provided by the no-pair approximation,[28,29] in which the electronic Hamiltonian is embedded by operators projecting out negative-energy orbitals. In practice, molecular orbitals $\{\varphi_p\}$ are optimized at the HF level and then the negative-energy orbitals are eliminated from the correlated level. The present work is based on this no-pair approximation, hence, unless otherwise stated, orbital indices in the following refer exclusively to positive-energy orbitals.

Equations for the energy and the cluster amplitudes are conveniently given in terms of the similarity-transformed Hamiltonian $\hat{\bar{H}} = \exp(-\hat{T}), \hat{H} \exp(\hat{T})$,

$$\langle\Phi_0|\hat{\bar{H}}|\Phi_0\rangle = E, \tag{3}$$

$$\langle\Phi_l|\hat{\bar{H}}|\Phi_0\rangle = 0, \quad |\Phi_l\rangle = \hat{\tau}_l|\Phi_0\rangle. \tag{4}$$

We now consider the case where the electronic Hamiltonian is extended by perturbations, each characterized by a perturbation strength ε_X, collected in the vector $\boldsymbol{\varepsilon}$,

$$\hat{H} = \hat{H}_0 + \sum_X \varepsilon_X \hat{H}_X. \tag{5}$$

The zeroth-order Hamiltonian will be the 4-component relativistic Dirac-Coulomb Hamiltonian. It has the same generic form,

$$\hat{H}_0 = V_{NN} + \sum_i \hat{h}(i) + \frac{1}{2}\sum_{i\neq j} \hat{g}(i,j), \tag{6}$$

as the nonrelativistic electronic Hamiltonian, including the electrostatic repulsion V_{NN} of clamped nuclei, but the one-electron operator $\hat{h}$ is the Dirac Hamiltonian,

$$\hat{h} = \begin{bmatrix} V_{eN} & c\,(\boldsymbol{\sigma}\cdot\mathbf{p}) \\ c\,(\boldsymbol{\sigma}\cdot\mathbf{p}) & V_{eN} - 2mc^2 \end{bmatrix}, \tag{7}$$

where c is the speed of light ($c = 137.035\,999\,8$ a.u.). The electron–nucleus interaction V_{eN} is expressed in terms of the scalar potential ϕ_A of each nucleus A,

$$V_{eN} = -e\sum_A \phi_A, \quad \phi_A(\mathbf{r}_1) = \frac{1}{4\pi\varepsilon_0}\int \frac{\rho_A(\mathbf{r}_2)}{|\mathbf{r}_1 - \mathbf{r}_2|} d^3\mathbf{r}_2, \tag{8}$$

where we generally employ a Gaussian model for the nuclear charge distribution.[30] The electron-electron interaction $\hat{g}$ is the instantaneous Coulomb interaction which is the zeroth-order term in a perturbational expansion in c^{-2} of the fully relativistic interaction in Coulomb gauge.

Molecular properties may be defined in terms of perturbation (Maclaurin) expansions of expectation values in the framework of response theory.[31–35] For fully variational methods, static molecular properties are conveniently expressed as derivatives of the energy with respect to perturbational strengths at zero field ($\boldsymbol{\varepsilon} = \mathbf{0}$), where the connection to expectation values is assured by the Hellmann-Feynman theorem. Simplifications are then obtained due to Wigner's $2n + 1$ rule.[36,37] Since CC theory is non-variational

we instead consider the Lagrangian[33,38]

$$L^{\mathrm{CC}}(\boldsymbol{\varepsilon},\mathbf{t},\boldsymbol{\lambda},\boldsymbol{\kappa},\overline{\boldsymbol{\kappa}}) = \langle\Phi_0|(1+\Lambda)\hat{\bar{H}}|\Phi_0\rangle + \sum_{ai}\left(\overline{\kappa}_{ai}\frac{\partial E^{HF}}{\partial \kappa_{ai}} + \overline{\kappa}^{*}_{ai}\frac{\partial E^{HF}}{\partial \kappa^{*}_{ai}}\right) \quad (9)$$

where Λ comprise the Lagrangian multipliers for the CC amplitude equations (Eq. (4)), for which a $2n+2$ rule holds.[39–41] The second term represents orbital relaxation and the virtual index a here refers to virtual orbitals of both positive and negative energies. We assume the use of a unitary exponential parametrization of the HF trial function, which assures orthonormality of orbitals throughout optimization.[42–45] κ_{ai} and $\overline{\kappa}_{ai}$ refer to the orbital rotation parameters and the corresponding Lagrange multipliers, respectively. These are elements of anti-Hermitian and Hermitian matrices, respectively, and one may note that only the virtual-occupied blocks are included since all other elements are redundant.[44] In the 4-component relativistic domain the orbital rotation parameters naturally split into two classes: parameters $\{\kappa^{++}_{ai}\}$, involving rotations between the positive-energy occupied and virtual orbitals, and $\{\kappa^{-+}_{ai}\}$, corresponding to rotations between positive-energy occupied orbitals and negative-energy virtual orbitals. The HF energy is minimized with respect to the former set, but maximized with respect to the latter, in accordance with the minmax principle of Talman.[46,47] This corresponds to the implicit use of projection operators embedding the electronic Hamiltonian and reflects the use of the no-pair approximation.[27,28]

In the above approach the redundant orbital rotations are set to zero. This corresponds to an algorithm of least change,[48,49] only assuring that the occupied-virtual blocks of the Fock matrix are zero. For an explicit separation of orbitals of positive and negative energy one may impose canonical orbitals at all perturbation strengths. This can be realized by extension of the CC Lagrangian, Eq. (9),

$$L^{\mathrm{CC}} \rightarrow L^{\mathrm{CC}} + \sum_{pq}\zeta_{pq}\left(F_{pq} - \varepsilon_p\delta_{pq}\right), \quad (10)$$

where $\{\zeta_{pq}\}$ constitutes a new set of Lagrange multipliers.[40,50] In this approach all orbital rotations come into play, including rotations within orbital classes. The two approaches therefore generally give different results when some orbitals are selected as inactive, of which the no-pair approximation is a special case. The canonical approach has the advantage of adhering closer to the usual picture of the Dirac sea, whereas the "minimal" approach allows the extension of the no-pair approximation to situations where orbital energies are not available. For instance, 4-component relativistic MCSCF calculations use second-order optimization based on the Talman minmax principle,[51,52] and allow the complete relaxation of the no-pair projection operators at the correlated level.[29,47] We intend to explore and compare these two approaches in future work.

It may be noted that the Lagrangian formalism can also be used in the case of perturbation-dependent orbitals, as will be the case in geometry optimization or the use of London orbitals[53,54] (also known as gauge-including atomic orbitals (GIAOs)),[55] provided a suitable orbital connection[56] is employed to guarantee orthonormality. However, upon taking derivatives of the Lagrangian, Eq. (9), with respect to perturbations, as we do in the following, further contributions will appear. In the present contribution we therefore limit attention to perturbation-*independent* orbitals.

Since coupled cluster theory is very robust and usually already provides adequate orbital relaxation through the T_1 cluster amplitudes,[57] it is reasonable to ignore it, as we do in the present work. An exception is the calculation of magnetic properties for which the negative-energy (NE) orbitals, which are excluded from the excitation manifold, are essential to get the diamagnetic contribution to magnetic properties.[58,59] For other molecular properties the inclusion of orbital relaxation at the CC level is a matter of debate—for some static first order properties it certainly shows improvement,[60,61] and for others it is not recommended,[62] while for dynamic properties problems arise due to the inaccurate Hartree-Fock poles.[35] For calculations of heavy elements there is the additional complication of the relaxation of core orbitals that are usually left uncorrelated. We plan to come back to these issues in future work. As of now we will work with the reduced Lagrangian appropriate for orbital-unrelaxed calculations,

$$L(\boldsymbol{\varepsilon},\mathbf{t},\boldsymbol{\lambda}) = \langle\Phi_0|\hat{\bar{H}}|\Phi_0\rangle + \sum_{l=1}\lambda_l\langle\Phi_l|\hat{\bar{H}}|\Phi_0\rangle, \quad (11)$$

where we have used a linear parametrization of the Lagrangian multiplier, that is,

$$\Lambda = \sum_{l}\lambda_l\hat{\tau}^{\dagger}_{l}, \quad (12)$$

where "l" indicates the rank of different excited states. Truncation of the Λ operator is dictated by the rank of the T operators. For the coupled-cluster singles-and-doubles (CCSD) analytic gradient method considered in this work, we therefore take up to doubly de-excitation type Λs. In passing, we may note that the appropriate Lagrangian for the calculation of orbital-unrelaxed expectation values at the 4-component relativistic MP2 level is obtained from the above Lagrangian by replacing the similarity-transformed Hamiltonian $\hat{\bar{H}}$ in the first and second term by its second- and first-order component, respectively (assuming optimized orbitals).[40,50,63]

We apply two stationary conditions on the Lagrangian in Equation (11),

$$\frac{\partial L}{\partial \mathbf{t}} = \mathbf{0}, \quad (13)$$

$$\frac{\partial L}{\partial \boldsymbol{\lambda}} = \mathbf{0}. \quad (14)$$

Equation (14) is the already implemented equation to determine the T-amplitudes, whereas Equation (13) defines the Λ-equation used to determine the Lagrange multipliers. Equations (13) and (14) can also be interpreted as equations for the right and left eigenvectors, respectively, of the non-Hermitian similarity-transformed Hamiltonian,[64,65]

$$\begin{aligned}\left(\hat{\bar{H}} - E\right)|\Psi_R\rangle = 0, \quad |\Psi_R\rangle = |\Phi_0\rangle,\\ \langle\Psi_L|\left(\hat{\bar{H}} - E\right) = 0, \quad \langle\Psi_L| = \langle\Phi_0|(1+\Lambda).\end{aligned} \quad (15)$$

This means that the Λ-equation, Equation (13), defines a dual vector of the coupled cluster ket vector, which enables the calculation of molecular properties as an expectation value. In fact, using the stationary conditions, Eqs. (13) and (14), we obtain

$$\left.\frac{dL}{d\varepsilon_X}\right|_{\boldsymbol{\varepsilon}=\mathbf{0}} = \left.\frac{\partial L}{\partial \varepsilon_X}\right|_{\boldsymbol{\varepsilon}=\mathbf{0}} = \langle \Psi_L | \hat{\bar{H}}_X | \Psi_R \rangle, \tag{16}$$

which corresponds to the expectation value of the operator $\hat{H}_X$. Equation (16) thereby constitutes a generalized Hellmann-Feynman theorem. Defining CC density matrices

$$\gamma_p^q = \langle \Psi_L | \exp(-\hat{T}) a_q^\dagger a_p \exp(\hat{T}) | \Psi_R \rangle, \tag{17}$$

$$\Gamma_{pq}^{rs} = \langle \Psi_L | \exp(-\hat{T}) a_r^\dagger a_s^\dagger a_q a_p \exp(\hat{T}) | \Psi_R \rangle, \tag{18}$$

the expectation value can be expressed as a trace between the density and the operator matrix elements,

$$\langle \hat{H}_X \rangle = \sum_{pq} \gamma_p^q h_{X;pq}. \tag{19}$$

All the properties we will be dealing with in the present work are of this expectation value type. The explicit working equations for intermediates and Λ amplitude equations, as well as density matrices, are given in Appendix A.

The size-extensivity of the evaluated properties follows from the following argument: Taking the derivative of the Lagrangian with respect to the amplitudes $\mathbf{t}$ in Equation (13) means from a set of closed terms constructed by H, $\exp(\hat{T})$, and Λ, we take out the amplitude part of $\hat{T}$. The operator part of $\hat{T}$ acts on the ket side of the Lagrangian to generate an excited function which is then connected to the bra side via the de-excitation operators contained in Λ (see Equation (12)). The stationarity condition tells us that the final result will be zero. The total Λ-equation may be written in the following algebraic form:[66]

$$\frac{\partial L}{\partial t_m} = \left\langle \Phi_0 | \hat{\bar{H}} | \Phi_m \right\rangle + \left\langle \Phi_0 \right| \left[\Lambda, \hat{\bar{H}} \right] \left| \Phi_m \right\rangle + \sum_{k \neq 0} \langle \Phi_0 | \hat{\bar{H}} | \Phi_k \rangle \langle \Phi_k | \Lambda | \Phi_m \rangle = 0, \tag{20}$$

where the sum over the complete excitation manifold in the final term is limited by the de-excitations contained in Λ. The above equation can be analyzed by diagrammatic techniques[67,68] which reveals a connected quantity[63,69] $\hat{\bar{H}}$, an explicit connected quantity between $\hat{\bar{H}}$ and Λ, and a third disconnected term containing Λ and $\hat{\bar{H}}$. The evaluated Λs are therefore not connected quantities. However, if we write Equation (16) more explicitly as follows

$$\frac{\partial L}{\partial \epsilon_X} = \left\langle \Phi_0 \right| \left[\Lambda, \hat{\bar{H}}_X \right] + \hat{\bar{H}}_X | \Phi_0 \rangle, \tag{21}$$

we see that it contains an explicitly connected quantity between Λ and $\hat{\bar{H}}_X$, where $\hat{\bar{H}}_X$ is a connected quantity since our converged T amplitudes are connected. Now the completely contracted nature of Equation (21) ensures that only the connected part of Λ can contribute to the final property value, which in turn ascertains the size-extensivity of the evaluated properties.

III. IMPLEMENTATION

The RELCCSD module in DIRAC[26] provides 2- and 4-component relativistic CCSD, CCSD(T), and Fock-space coupled cluster methods.[70–72] In the present work, we have extended this module in such a way that it can handle any arbitrary tensor contraction. Any implementation along this line generally hinges on an efficient tensor contraction routine where the tensor can be of arbitrary rank. Recently, there has been considerable focus on the development of general purpose tensor contraction routines, such as the "Tensor Contraction Engine,"[73] Cyclops,[74] SIAL,[75] libtensor,[76] and TiledArray.[77] In this work, our target is to achieve almost the same flexibility without yet focusing on the parallel efficiency of the algorithm. By flexibility is meant that we want to employ tensors of arbitrary operator structure and rank. It will, in turn, facilitate the implementation of the methods pertaining to both energy and molecular properties at the Single Reference Coupled Cluster (SRCC) level.

A. General structure of the implementation

The pivotal operation in the CC family of methods is the binary tensor contraction,

$$A_{ij..}^{k'l'..} * B_{kl..}^{i'j'..} = C_{ij...kl..}^{k'l'...i'j'..}. \tag{22}$$

Following the Einstein summation convention whenever the upper primed (bra) and lower unprimed (ket) indices are the same, they define a contraction. For each contraction, the rank of the product tensor is reduced by 1. All tensors — A, B, and C — are anti-symmetrized tensors of arbitrary rank.

There are no readily available library routines which are able to perform such tensor operations. However, one can take advantage of Basic Linear Algebra Subroutines (BLAS)[78] by conveniently mapping a tensor contraction onto a matrix-matrix multiplication,

$$A(free, contractable) * B(contractable, free) \rightarrow C(free, free). \tag{23}$$

In the present work we have generalized binary tensor contractions by "contraction_xyz" FORTRAN 90+ subroutines, where x and y are the ranks of the left and right input tensors, respectively, and z is the rank of the output tensor. For the theories which incorporate up to singles and doubles excitation operators, we have written the subroutines corresponding to contraction classes xyz = 222, 242, 422, 444, 244, and 424 to be able to carry out every possible tensor contraction. These routines identify the permutational and double group symmetry built into a tensor and preserve the optimal symmetry structure after the contraction. Reshaping of the tensors is implicit in these routines from the placement of indices. Furthermore, we need to provide information only from a diagrammatic expression, therefore they can easily be coupled with an automatic expression generator. We illustrate the use of these routines in Appendix B.

B. Sparsity and blocking of tensors by using double group symmetry

Use of molecular symmetry provides dense and blocked structure to the tensors used in a coupled cluster contraction. This has been exploited most efficiently by Stanton *et al.*[79] in their Direct Product Decomposition (DPD) scheme for the spatial symmetry groups.

For the relativistic molecular Hamiltonian we cannot work with simple spatial point group symmetry due to spin-orbit coupling, which couples the spin and spatial degrees of freedom. Rather we shall work with the corresponding double groups, obtained by the introduction of a rotation 2π about an arbitrary axis.[80] These groups contain more irreps than the regular single group, but not necessarily twice the number. The extra irreps are called fermion irreps and the pre-existing ones boson irreps. Spinors span fermion irreps, whereas spinor products, operators, and integrands span boson irreps.

In the present work, we use double groups of D_{2h} and its subgroups. However, not all of them are Abelian since the direct product between the 2π rotation and other elements of the point group may generate elements which belong to the same class as some other element. In that case, we consider the highest Abelian subgroup of that double group. For example, the D^*_{2h} double group contains one two-dimensional irrep, therefore we work with the Abelian subgroup C^*_{2h} instead. For linear systems we have exploited the advantage of going beyond D^*_{2h} symmetry by using double groups C^*_{8h} and C^*_{16} for molecules with and without inversion symmetry, respectively. For the spin-free cases, we use the direct product group between the point group and the SU(2) group. These extensions provide very significant computational savings in realistic applications. This Abelian double group scheme, which is analogous to DPD, builds on the symmetry handling in the CCSD implementation by Visscher *et al.*[71] In Appendix C we present that scheme in a bit more generalized perspective while recapitulating the essential details from that work.

Further symmetry reductions are possible by exploiting time reversal symmetry.[70] However, in the present code Kramers-restriction is not imposed at the CC level. On the other hand, presently the initial HF calculations are carried out using a quaternion symmetry scheme[81] that exploits both spatial and time reversal symmetry such that the input orbitals for the CC module form a Kramers basis. As a consequence, the input one- and two-electron integrals are real for certain point groups, a feature that is exploited in our calculations by defining an xGEMM subroutine that wraps around either the DGEMM or ZGEMM BLAS primitives, depending on the algebra of the point group (real or complex).

C. Construction of expectation values

The steps involved in a coupled cluster gradient calculation can be written down succinctly as follows:

1. iterative HF solution to get the MO basis;
2. transforming integrals in AO basis to the MO basis;
3. iterative solution of the CCSD amplitude equation to get the T_1 and T_2 amplitudes;
4. construction of the fixed intermediates, Eqs. (A4)–(A14), using V, F, T_1 and T_2;
5. iterative solution of the Λ-equations, Eqs. (A1) and (A2);
6. construction of one-particle density matrix, Eq. (A17), at the CC level with the help of converged T- and Λ-amplitudes;
7. back-transformation of the CC density matrix from the MO basis to the AO basis;
8. tracing the density matrix with the AO derivative integrals to get the desired property values.

Steps (4) and (5) use the contraction scheme described in the Section III A. Some intermediates involve integrals over four virtual orbital indices (VVVV). Because of the very high memory scaling of those terms, we have implemented them in a distributed fashion. The RELCCSD module in DIRAC distributes the VOVV (three virtual and one occupied) and VVVV type integrals on several nodes. In the present work, we gather all the distributed VOVV integrals on each node and continue with the distributed VVVV integrals. The intermediate which contains four virtual orbitals, that is, W^{ef}_{ab} in Equation (A11) is calculated only with the locally available integrals on each node. Furthermore, when those intermediates are used in Equations (A10) and (A2) we use only the local contribution on each node. At the end we synchronise the δ^{ij}_{ab} and W^{ef}_{am} arrays to the master.

Step (6) in the above scheme needs careful consideration since the AO property matrices are generated in the framework of the quaternion symmetry scheme[81] operating at the SCF level in the DIRAC program. Presently the input MOs to the CC module form a Kramer's basis, such that the 1-particle CC density matrix (${}^{MO}\gamma$) is expressed in terms of Kramer's pairs,

$$\begin{pmatrix} A & B \\ C & D \end{pmatrix}, \quad \begin{aligned} A_{pq} &= \gamma_{pq}, & B_{pq} &= \gamma_{p\bar{q}}, \\ C_{pq} &= \gamma_{\bar{p}q}, & D_{pq} &= \gamma_{\bar{p}\bar{q}}. \end{aligned} \tag{24}$$

In the closed-shell case, this matrix has a time-symmetric structure

$$\begin{pmatrix} A & B \\ -B^\star & A^\star \end{pmatrix} \tag{25}$$

and can be block-diagonalized by quaternion unitary transformation[81]

$$U = \begin{pmatrix} \mathbb{I} & \check{j}\mathbb{I} \\ \check{j}\mathbb{I} & \mathbb{I} \end{pmatrix}, \tag{26}$$

where $\mathbb{I}$ is the 2×2 unit matrix. One then proceeds with the upper block of the quaternion block-diagonalized matrix, with elements

$${}^{Q}\gamma_{PQ} = Re(\gamma_{pq}) + \check{i}Im(\gamma_{pq}) + \check{j}Re(\gamma_{p\bar{q}}) + \check{k}Im(\gamma_{p\bar{q}}). \tag{27}$$

Based on spatial symmetry the matrix may be further compressed to complex or real form.

The ${}^{Q}\gamma$ density matrix is next back-transformed to the AO basis

$${}^{Q}\gamma_{\mu\nu} = \sum_{PQ} {}^{Q}c_{\mu P}\, {}^{Q}\gamma_{PQ}\, {}^{Q}c^*_{\nu Q}. \tag{28}$$

In the final step the resulting AO CC density matrix is traced with the appropriate AO property matrix.

As mentioned the RELCCSD module of DIRAC does not exploit time reversal symmetry and can also be invoked to handle a single open shell (one unpaired electron). In that case the CC density matrix can be separated into a time symmetric and a time antisymmetric part, the latter allowing the calculation of expectation values of time antisymmetric operators such as the magnetic dipole or the hyperfine operator. This will be exploited in future work.

IV. SAMPLE APPLICATIONS

In this section we will show two pilot applications of the DC-CCSD analytic gradient code. We first consider parity violation (PV) of chiral molecules which, as already mentioned, is a property that is strictly zero in the absence of SOC and for which we would like to benchmark a currently employed computational protocol based on density functional theory (DFT).[82] Presently we have studied PV in the H_2X_2 (X = O, S, Se, Te) series of molecules. For the first two members of that series orbital-relaxed finite-field 4-component relativistic CC calculations are available.[83] We next consider the electric field gradient (EFG) at nuclear positions in the BiN and BiP diatomic molecules, which were already studied by Teodoro and Haiduke[84] using a finite-field CC approach.

A. Parity violation

Upon extension of the conventional electromagnetic formulation of quantum chemistry to the electroweak regime a minute energy difference,

$$\Delta E_{PV} = E_{PV}(L) - E_{PV}(R) = 2E_{PV}(L), \tag{29}$$

is induced between the left (L)- and right (R)-handed enantiomers of chiral molecules.[6,8,85,86] At the 4-component relativistic level the iterapairs violating (PV) energy E_{PV} can be calculated as an expectation value of the nuclear spin-independent P-odd operator[87]

$$H_{PV} = \sum_A H_{PV;A}, \quad H_{PV;A} = \frac{G_F}{2\sqrt{2}} Q_{W,A} \sum_i \gamma_i^5 \rho_A(r_i), \tag{30}$$

where $G_F = 1.166\,37 \times 10^{-11}$ MeV^{-2} $= 2.222\,55 \times 10^{-14}$ $E_h a_0^3$ is the Fermi coupling constant. The summation runs over the nuclei, A, and electrons, i. The weak charge $Q_{W,A} = -N_A + Z_A(1 - 4\sin^2\theta_w)$, where N_A and Z_A is the number of neutrons and protons on each nucleus. θ_w is the Weinberg mixing angle; we have chosen a fixed value of 0.2319 for $\sin^2\theta_w$. ρ_A is the normalized nucleon density. γ^5 is the 4×4 chirality operator, which is given by

$$\gamma^5 = \begin{pmatrix} \mathbb{O} & \mathbb{I} \\ \mathbb{I} & \mathbb{O} \end{pmatrix}. \tag{31}$$

The nuclear spin-dependent PV contribution has been neglected since it is zero for a closed-shell system.[87]

There is at present no experimental observation of the effect of parity violation in chiral molecules, but several experiments are in preparation.[7,88–90] The present role of theory is to guide experiment towards suitable candidate molecules, but a successful observation would call for a direct confrontation between theory and experiment and allow to probe the standard model of the universe in the low-energy regime.[91] Most present-day molecular PV calculations are carried out using DFT. As a first step towards benchmarking of this computational protocol we have investigated the H_2X_2 (X = O, S, Se, Te) series of molecules using our newly implemented CC gradient code. These are not ideal candidate molecules for actual experiments, but have been widely employed for calibration and analysis.[8,83,87,92–107] In our study with the first candidate of that series, that is, H_2O_2, the O–O, and H–O bond lengths as well as the O–O–H angles have been kept fixed, and the dihedral angle τ_e has been varied from 0° to 180° with a grid of 20° to generate an E_{PV} vs τ_e curve. The fixed structure parameters for H_2O_2 and the heavier homologues have been taken from the article by Laerdahl and Schwerdtfeger.[87] We have considered a series of basis sets to estimate the minimal size which provides good accuracy. The smallest basis set has been taken from the work by Laerdahl and Schwerdtfeger,[87] who considered several basis sets in their work. From these we have chosen the basis type1, which is slightly better than double zeta quality. Then we systematically improved the size by using the Dyall-type all-electron basis sets, that is, dyall.ae3z and dyall.ae4z[108] (a higher cardinal number is presently not available). We will employ the optimal cardinal number obtained form this study to the other molecules of this series. The Gaussian model of nuclei has been employed for all the molecules in this series.[30] We have chosen an approximate version of the DC Hamiltonian, with the $(SS|SS)$ class of integrals neglected. Our choice of correlation space consists of all the occupied orbitals, but the virtual orbital space has been truncated by choosing an energy threshold of 100 E_h.

In Figure 1 E_{PV} is traced as a function of dihedral angle at both the HF and CCSD levels of theory, using the cc-pVDZ+3p basis set,[87] to demonstrate the effect of correlation. The curve we obtained is of sinusoidal type, in agreement with previous studies.[8,93–95,97,98,100] The effect of correlation gives a negative vertical shift to the E_{PV} value throughout the

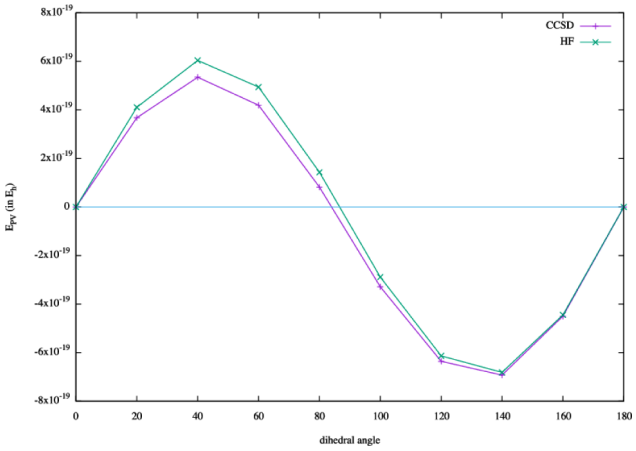

FIG. 1. Total parity violating energy E_{PV} as a function of torsional angle curve for H_2O_2 at the HF and CCSD level of theory using the cc-pVDZ+3p basis set.[87]

TABLE I. Parity violating energies E_{PV} for P enantiomers of H_2X_2 molecules at various levels of theory. We have considered 45° torsional angle for all the molecules. Finite-field results (orbital-relaxed) are marked as ff; all other numbers are analytical.

Molecule	Hamiltonian	Method	Basis set for X	$E_{PV}/10^{-20}E_h$
H_2O_2	DC	CCSD[a]	cc-pVDZ+3p	−61.26
			dyall.ae3z	−53.23
			dyall.ae4z	−55.83
		HF[a]	cc-pVDZ+3p	−67.90
			dyall.ae3z	−60.51
			dyall.ae4z	−63.76
		CCSD(ff)[b]	cc-pVDZ+3p	−61.80
		MP2[c]	cc-pVDZ+3p	−57.88
	NR	CCSD[d]	cc-pVQZ	−51.69
H_2S_2	DC	CCSD[a]	cc-pCVTZ	−1821.03
			cc-pVDZ+2p	−2088.76
		HF[a]	cc-pCVTZ	−1825.86
			cc-pVDZ+2p	−2078.20
		CCSD(ff)[b]	cc-pVDZ+2p[e]	−2165.23
		MP2[c]	cc-pVDZ+2p	−2112.0
	NR	CCSD[d]	cc-pVQZ	−2248.6

[a]This study.
[b]Thyssen *et al.*[83]
[c]van Stralen *et al.*[16]
[d]Horný and Quack.[107]
[e]The authors report cc-pVDZ+3p, but this appears to be incorrect.

curve. We have obtained a maximum correlation contribution at 60° torsional angle, and minimum is at 160° torsional angle. Table I gives CCSD and HF values of E_{PV} at 45° torsional angle and indicates the convergence of E_{PV} with respect to the basis set. Clearly, there is a significant difference in values when the double-zeta basis is compared with the triple-zeta one, whereas the effect of further increasing the cardinal number is quite small. We will prefer triple zeta quality basis set for our calculations on the heavier homologues of H_2O_2. We have also compared our findings with previous studies in Table I. Our analytical number matches very well the orbital-relaxed finite-field numbers reported by Thyssen *et al.*[83] when the basis set is exactly the same.[109] The slight discrepancy in value may be attributed to orbital relaxation in the latter case, which is accordingly quite small. The difference with the MP2 value, when we use the same basis set, is not very large, as has been seen earlier.[83]

For the next candidate in this series, that is, H_2S_2, we apply the cc-pCVTZ basis. Here we freeze the 1s2s orbitals of the sulfur atoms, as motivated by the MP2 study by van Stralen *et al.*[16] For the virtual orbital space we again choose 100 E_h as the energy threshold. We vary the torsional angle from 0° to 180° with a fixed grid size of 15°. We observe the same sinusoidal behaviour of the E_{PV} vs τ_e curve (Figure 2) as seen for H_2O_2. However, the effect of correlation is less dominant for this molecule, and correlation contributions have both negative and positive signs along the curve.

When we compare our cc-pCVTZ results at 45° torsional angle for H_2S_2 with previous findings in Table I, we see a significant difference in values. In order to directly compare with the CCSD orbital-relaxed finite field number of Thyssen *et al.*,[83] we calculated the parity violating energy in the

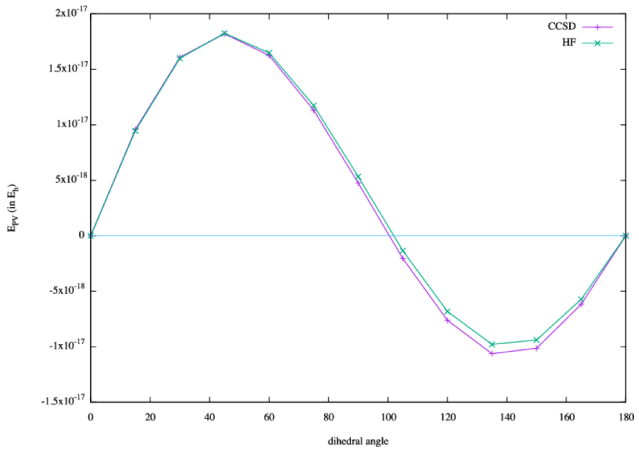

FIG. 2. Total parity violating energy E_{PV} as a function of torsional angle curve for H_2S_2 at the HF and CCSD level of theory using the cc-pCVTZ basis.

cc-pVDZ+2p basis with all electrons correlated. The discrepancy is now reduced to 76×10^{-20} E_h (3.5%), which is essentially due to orbital relaxation. At the orbital-unrelaxed MP2 level, switching off orbital relaxation in the implementation of van Stralen *et al.*,[16] we obtain -2013.89×10^{-20} E_h, whereas using the orbital-relaxed MP2 code[16] the result is -2113.83×10^{-20} E_h. The effect of orbital relaxation at the MP2 level is thus more important. The latter number agrees well with that reported by van Stralen *et al.*,[16] with the 1s2s2p orbitals of sulfur frozen.

In Table I we also included recent CCSD results reported by Horný and Quack.[107] However, direct comparison with our values is less straightforward. Not only are basis sets and geometries different, but the parity-violating energy has been calculated as a linear response function by introducing a one-electron spin-orbit operator with effective nuclear charge as a perturbation in an otherwise nonrelativistic calculation. We note, however, that with the triple zeta basis set we obtain very good agreement with the value reported for H_2O_2 by Horný and Quack, whereas a more significant discrepancy is observed for H_2S_2, probably mostly due to scalar relativistic effects.

For H_2Se_2 and H_2Te_2 we have chosen (n-1)d$ns$$np$ as the active occupied orbital space, where n is the principal quantum number of the valence shell. The energy cutoff for the virtual orbitals was set to 40 E_h. In Table II, we report our calculated E_{PV} values at 45° torsional angle for the complete series H_2X_2 (X = O, S, Se, Te) of molecules. An interesting observation is that the correlation contribution is on the order of 10% for H_2O_2, but is reduced by one order of magnitude or

TABLE II. Total parity violating energy shift (in E_h) at the CCSD level for the H_2X_2 (X = O, S, Se, Te) molecules at 45° dihedral angle. Basis sets employed (both atoms): dyall.ae3z (H_2O_2), cc-pCVTZ (H_2S_2) and dyall.cv3z (H_2Se_2, H_2Te_2). ΔE_{PV}^{corr} corresponds to the energy shift (in E_h) at the CCSD level with respect to the HF method.

	H_2O_2	H_2S_2	H_2Se_2	H_2Te_2
E_{PV}	-53.23×10^{-20}	-18.21×10^{-18}	-21.15×10^{-16}	-32.89×10^{-15}
ΔE_{PV}^{corr}	7.4×10^{-20}	4.8×10^{-20}	2.4×10^{-17}	2.8×10^{-16}

more for the heavier homologues. There has been a previous analysis for that by Berger *et al.*,[101] where they have compared the ZORA-DFT numbers of theirs with the DC Hamiltonian based MP2 numbers by van Stralen *et al.*[16] Their conclusion was that while MP2 numbers underestimate the correlation contribution of a DFT calculation, it overestimates that of a CCSD(T) calculation. Our numbers also corroborate with the overestimation of correlation by MP2, for which we have not carried out any calculation, but have observed the qualitative trend in the work by van Stralen *et al.*[16] However, it should be pointed out that it is possible to provide a definite benchmark number only when an analytic CCSD(T) energy gradient implementation will be available.

B. Electric field gradient

We next consider the interplay between SOC and electron correlation by calculating the electric field gradient (EFG) at the ^{209}Bi nucleus (nuclear spin I = 9/2) in the BiX (X = N,P) series of molecules, for which spin-orbit effects may be expected to be prominent. The corresponding nuclear quadrupole coupling constant (NQCC; in MHz) may be expressed as

$$\mathrm{NQCC}(^{209}\mathrm{BiX}) = 234.9647 \times Q(^{209}Bi) q_{zz}(\mathrm{Bi}), \quad (32)$$

where Q is the nuclear quadrupole moment of ^{209}Bi in barns (b) and q_{zz} is the electric field gradient (in atomic units E_h/ea_0^2) along the molecular axis at the position of the bismuth nucleus.

The basis set for Bi has been taken from the work by Teodoro and Haiduke,[84] where they have incremented the Relativistic Adapted Gaussian Basis Set (RAGBS), previously developed by Haiduke and Da Silva.[110] For the lighter atom in those molecules, that is, for N and P, we have chosen the cc-pVTZ basis set.[111,112] An approximate version of the DC Hamiltonian was used, where the $(SS|SS)$ class of integrals is neglected and a simple Coulombic correction added to the energy.[113] To estimate the contribution from SOC, we have also employed the Spin-Free (SF)-DC Hamiltonian[23,114] which allows us to define the SOC contribution as the difference between the results obtained with the full DC Hamiltonian and with the SF Hamiltonian. The correlating orbital space has been restricted by selecting all the orbitals between −6 and 20 E_h, following the suggestion by Teodoro and Haiduke.[84]

We have summarized our results in Table III. For the BiN molecule at the SF level, electron correlation gives a 16.31% negative shift to the absolute value of q_{zz}. At the DC level, on the other hand, we get a huge positive shift of 57.2% to the absolute value of q_{zz}. This immediately shows that the SOC and correlation cannot be treated independently and that both are important to obtain a quantitatively correct total EFG value. With further analysis we can see that SOC reduces the absolute value of q_{zz} by 7.01 E_h/ea_0^2 at the mean-field level, in line with other previous studies of different molecules.[117,118] The extent of coupling between SOC and correlation can be singled out by subtracting the mean field ΔSOC contribution from that at the CCSD level, which is a significantly large value −5.62 E_h/ea_0^2. For BiP the role of SOC is less dramatic, and our simple analysis tells us that the role of coupling between correlation and SOC is 2.47 E_h/ea_0^2 in that case.

TABLE III. Calculated electric field gradient q_{zz} at the Bi nucleus of the BiN and BiP molecules. Only electronic contributions are given in the table. The nuclear contribution is 0.2864 and 0.3685 E_h/ea_0^2 for BiN and BiP, respectively. Bond lengths for BiN and BiP are chosen as 1.9349 Å[115] and 2.2934 Å,[116] respectively. We used a 31s24p18d12f2g basis set for Bi and cc-pVTZ for N and P. ΔSOC refers to the spin-orbit coupling contribution at the indicated level of theory.

Molecule	Hamiltonian	Method	q_{zz} (in E_h/ea_0^2)	%correlation	ΔSOC
BiN	SF-DC	HF	−13.0961	−16.31	7.0121
		CCSD	−10.9596	...	1.3958
	DC	HF	−6.0840	+57.20	...
		CCSD	−9.5638	...	...
BiP	SF-DC	HF	−13.6345	−21.06	3.5969
		CCSD	−10.7626	...	1.1318
	DC	HF	−10.0376	−4.05	...
		CCSD	−9.6308	...	...

If we combine our DC-CCSD EFG value with the NQCC data from Cooke *et al.*,[84,116] we obtain a nuclear quadrupole moment of −415.1 mb for ^{209}Bi, in line with Teodoro and Haiduke (CCSD: −420(8) mb).[84] This clearly indicates that the present literature value of −516(15) mb[119,120] needs revision, in particular since the triples contribution to the EFG is rather modest, on the order of 5 mb.[84] One further interesting point is that if we compare our orbital unrelaxed analytical NQM value with the relaxed numerical value by Teodoro and Haiduke,[84] we see a difference of 5 mb. Therefore, for this particular case the effect of orbital relaxation is minor.

V. SUMMARY AND FUTURE OUTLOOK

In this article we have reported the first formulation and implementation of 4-component DC Hamiltonian based coupled cluster analytic derivative technique. The present implementation allows first-order energy derivative calculations of one-electron properties. We have used full permutational and double group symmetry of the integrals in the coupled cluster contraction section. This method has been applied to the calculation of zz-component of EFG tensors at the Bi centre of BiN and BiP molecules. We have demonstrated a strong coupling between SOC and correlation for those molecules. In future work we plan to investigate the spin-orbit effect on the EFG in more detail. We have also calculated the total parity violating energy contribution for H_2X_2 (X = O,S,Se,Te) molecules and compared that with the previous studies. For the selected molecules the effect of electron correlation on the parity-violating energy is rather modest, but we would like to extend our benchmark study to more realistic candidate molecules where for instance the difference between HF and DFT results are more prominent (see for instance Ref. 82).

In the present implementation we have not included the (T) correction to the calculated molecular properties. The main bottleneck of that implementation is the high

memory requirements, which becomes particularly severe in the relativistic case due to the large prefactor caused by spin-orbit coupling. A viable implementation should include parallelization techniques. We are presently exploring suitable algorithms in that direction. In this implementation we have so far avoided the consideration of orbital relaxation via the Z-vector technique. For the calculation of geometrical derivatives and magnetic properties it is, however, mandatory to incorporate that contribution. The main bottleneck for the relativistic case arises because of the rotation between positive energy and negative energy orbitals, which will possibly require transformed negative energy MO integrals. Nevertheless, in view of the theoretical importance of that technique we are planning to implement it as well.

This work provides a generalized framework for tensor contraction in the relativistic single reference coupled cluster regime. We therefore plan to use this framework for the implementation of coupled cluster linear response. The response implementation will allow the calculation of excited state energies and higher-order molecular properties, most notably the NMR shielding tensor and indirect spin-spin coupling tensor.

An open-shell extension of this work will increase the scope of this work for magnetic properties such as the EPR g-tensor. In the spinor-based coupled cluster implementation one can calculate relaxed density matrix for simple open-shell systems. We are planning to use that benefit as outlined in Section III C.

ACKNOWLEDGMENTS

A.S. acknowledges his Ph.D. fellowship from the Indo-French Centre for the Promotion of Advanced Research (IFCPAR) and would like to thank Debashis Mukherjee (Kolkata), Lan Cheng (John Hopkins), Andre Gomes (Lille), and Sangita Sen (Oslo) for many fruitful discussions. A.S. would also like to acknowledge computing time on the Linux clusters of Laboratoire de Chimie et Physique Quantiques (LCPQ, Toulouse) and Laboratoire de Physique des Lasers, Atomes et Molécules (PhLAM, Lille).

APPENDIX A: WORKING EQUATIONS FOR Λ EQUATIONS, INTERMEDIATES, AND DENSITY MATRICES

The Λ amplitudes have been expressed in terms of a limited number of intermediates, where we have largely followed the work of Gauss *et al.*[121] The Λ_1 amplitude equation is given by

$$\begin{aligned} 0 = \overline{F}^i_a &+ \sum_e \lambda^i_e \overline{F}^e_a - \sum_m \lambda^m_a \overline{F}^i_m + \sum_{m,e<f} \lambda^{im}_{ef} * W^{ef}_{am} \\ &- \sum_{e,f} G^f_e * W^{ei}_{fa} - \sum_{mn} G^n_m * W^{mi}_{na} \\ &+ \sum_{me} \lambda^m_e * W^{ie}_{am} - \sum_{m>n,e} \lambda^{mn}_{ae} * W^{ie}_{mn}, \end{aligned} \tag{A1}$$

whereas the Λ_2-equation is

$$\begin{aligned} 0 = V^{ij}_{ab} &+ P(ab) \sum_e \lambda^{ij}_{ae} * \overline{F}^e_b - P(ij) \sum_m \lambda^{im}_{ab} * \overline{F}^j_m + \sum_{m>n} \lambda^{mn}_{ab} * W^{ij}_{mn} + P(ij)p(ab) \sum_{me} \lambda^{im}_{ae} * W^{je}_{bm} \\ &+ P(ab) \sum_e V^{ij}_{ae} * G^e_b - \sum_m \lambda^m_a * W^{ij}_{mb} - P(ij) \sum_m V^{im}_{ab} * G^j_m + P(ij) \sum_{m,e} V^{mj}_{ab} * (\lambda^i_e * t^e_m) \\ &+ P(ij) \sum_e \lambda^i_e * V^{ej}_{ab} + P(ij)P(ab) \lambda^i_a \overline{F}^j_b + \sum_{e>f} \lambda^{ij}_{ef} * W^{ef}_{ab}, \end{aligned} \tag{A2}$$

where the permutation operator

$$P(pq)f(p,q) = f(p,q) - f(q,p), \tag{A3}$$

appears. Most of the intermediates are constructed from the known Hamiltonian matrix elements and the already solved T amplitudes; we will hence call them fixed intermediates. The one-body fixed intermediates are

$$\overline{F}^i_m = f^i_m + \sum_e f^i_e * t^e_m + \sum_{en} V^{in}_{me} * t^e_n + \sum_{n,e>f} V^{in}_{ef} * \tau^{ef}_{mn}, \tag{A4}$$

$$\overline{F}^e_a = f^e_a - \sum_m f^m_a * t^e_m - \sum_{mf} V^{me}_{fa} * t^f_m - \sum_{m>n,f} V^{mn}_{af} * \tau^{ef}_{mn}, \tag{A5}$$

$$\overline{F}^m_e = f^m_e + \sum_{nf} v^{mn}_{ef} * t^f_n, \tag{A6}$$

whereas the two-body fixed intermediates are

$$W^{ij}_{mn} = V^{ij}_{mn} + P(mn) \sum_e V^{ij}_{en} * t^e_m + \frac{1}{2} \sum_{e>f} V^{ij}_{ef} * \tau^{ef}_{mn}, \tag{A7}$$

$$\begin{aligned} W^{mb}_{ej} = V^{mb}_{ej} &+ \sum_f V^{mb}_{ef} * t^f_j - \sum_n V^{mn}_{ej} * t^b_n \\ &+ \sum_{nf} V^{mn}_{ef} * (t^{fb}_{jn} - t^f_j t^b_n), \end{aligned} \tag{A8}$$

$$\begin{aligned} W^{ie}_{mn} = V^{ie}_{mn} &+ \sum_f \overline{F}^i_f * t^{ef}_{mn} - \sum_o W^{io}_{mn} * t^e_o \\ &+ \sum_{f>g} V^{ie}_{fg} * \tau^{fg}_{mn} + P(mn) \sum_f \overline{W}^{ie}_{fn} * t^f_m \\ &+ P(mn) \sum_{of} V^{io}_{mf} * t^{ef}_{no}, \end{aligned} \tag{A9}$$

$$W_{am}^{ef} = V_{am}^{ef} + P(ef)\sum_{ng} V_{ag}^{en} * \tau_{mn}^{gf} + \sum_{g} W_{ag}^{ef} * t_m^g + \sum_{n} \overline{F}_a^n * t_{mn}^{ef} + \sum_{n>o} V_{am}^{no} * \tau_{no}^{ef} - P(ef)\sum_{n} \overline{W}_{am}^{nf} * t_n^e, \quad \text{(A10)}$$

$$W_{ab}^{ef} = V_{ab}^{ef} - P(ef)\sum_{m} V_{ab}^{mf} * t_m^e + \sum_{m>n} V_{ab}^{mn} * \tau_{mn}^{ef}, \quad \text{(A11)}$$

$$\overline{W}_{ej}^{mb} = V_{ej}^{mb} - \sum_{nf} V_{ef}^{mn} * t_{nj}^{bf}, \quad \text{(A12)}$$

$$W_{ie}^{mn} = V_{ie}^{mn} + \sum_{f} t_i^f * V_{fe}^{mn}, \quad \text{(A13)}$$

$$W_{ef}^{am} = V_{ef}^{am} - \sum_{n} V_{ef}^{nm} * t_n^a. \quad \text{(A14)}$$

To avoid higher than two-body intermediates we furthermore define two intermediates of mixed Λ and T type,

$$G_a^e = -\sum_{m>n,f} \lambda_{af}^{mn} * t_{mn}^{ef}, \quad \text{(A15)}$$

$$G_m^i = \sum_{m,e>f} \lambda_{ef}^{in} * t_{mn}^{ef}. \quad \text{(A16)}$$

The density matrices are evaluated by using the converged T and Λ as follows:

$$\gamma_i^{'j} = -\sum_{m,e>f} t_{im}^{ef} * \lambda_{ef}^{jm} - \sum_{e} t_i^e * \lambda_e^j, \quad \text{(A17)}$$

$$\gamma_b^{'a} = \sum_{m>n,e} t_{mn}^{ae} * \lambda_{be}^{mn} + \sum_{m} t_m^a * \lambda_b^m, \quad \text{(A18)}$$

$$\gamma_i^{'a} = t_i^a + \sum_{me} \lambda_e^m (t_{im}^{ae} - t_i^e t_m^a) - \sum_{m>n,e>f} \lambda_{ef}^{mn} (t_{in}^{ef} * t_m^a + t_i^e * t_{mn}^{af}), \quad \text{(A19)}$$

$$\gamma_a^{'i} = \lambda_a^i, \quad \text{(A20)}$$

$$\gamma_p^q = \frac{1}{2}(\gamma_p^{'q} + \gamma_q^{'p}).$$

APPENDIX B: USE OF THE TENSOR CONTRACTION ROUTINES

As an illustration of the use of our implemented tensor contraction routines we consider a representative term from the Λ-equation,

$$\delta\lambda_{ab}^{ij} + P(ij)P(ab)\sum_{me} \lambda_{ae}^{im} * W_{bm}^{je} \rightarrow \delta\lambda_{ab}^{ij}. \quad \text{(B1)}$$

In the above equation, we are contracting a rank-4 tensor λ_{ae}^{im} with a rank-4 tensor W_{bm}^{je} to generate another rank-4 tensor $\delta\lambda_{ab}^{ij}$. Therefore, it belongs to the contraction class 444. In the code the corresponding subroutine is called as

```
call contraction_444((/"o1","o3","p1","p3"/),(/"o2","p3","p2","o3"/), &
 & (/"o1","o2","p1","p2"/),ResL2, 1.0d0,1.0d0,nrep,RightTensor=w_voov, &
 & LeftTensor=L2).
```

The first three arguments to the subroutine are orbital strings for the input and output tensors in the order they appear from a diagram. Indices are numbered with "o" and "p" referring to occupied (hole) and virtual (particle) orbitals, respectively. Then, we provide the name of the output tensor (or arrays), the diagram factor, the scaling factor of the product tensor, the number of irreducible representations (nrep), and finally the names of the input tensors (or arrays). In this example (Eq. (B1)) the input tensors would be reshaped to

$$\lambda(i,m,a,e) \rightarrow \lambda'(i,a,e,m), \quad \text{(B2)}$$

$$W(j,e,b,m) \rightarrow W'(j,b,e,m). \quad \text{(B3)}$$

Thereafter the BLAS matrix-matrix multiplication routine is employed to the tensors mapped onto matrices, e.g.,

$$\lambda'(ia,em) * W'^{T}(em,jb) = \delta\lambda'(ia,jb) \rightarrow \delta\lambda(i,j,a,b), \quad \text{(B4)}$$

followed by a reshaping (sort) of the resultant tensor, as above. When explicit anti-symmetrization of the final tensors is needed (as it is in the present example), we first generate the full product tensor, and then perform the explicit anti-symmetrization and pack them in triangular fashion. Again, this is also implicit in the placement of the orbital indices.

APPENDIX C: USE OF DOUBLE GROUP SYMMETRY IN TENSOR CONTRACTION

The DPD scheme is applicable to all possible contractions in coupled cluster theory and entails nested loops over irreps to skip contributions that are zero by symmetry. A particular challenge in the relativistic framework is that the irrep of the complex conjugate of a quantity, e.g., an orbital appearing in the bra position of an two-electron integral, is typically not equal to the irrep of the original quantity. This is symbolically indicated by $\Gamma_p \neq \Gamma_p^*$ and may occur for both fermion and boson irreps. An example are the irreps of the groups C_n^* $(n > 1)$.

Using the equation for generic tensor contraction (Equation (22)), we get

$$A((\Gamma_{k'}^* \otimes \Gamma_{l'}^* \ldots) \otimes (\Gamma_i \otimes \Gamma_j ..) \equiv \Gamma_0) B((\Gamma_{i'}^* \otimes \Gamma_{j'}^*) \otimes (\Gamma_k \otimes \Gamma_l ..) \equiv \Gamma_0) = C((\Gamma_{K_f'}^* \otimes \Gamma_{I_f'}^*) \otimes (\Gamma_{I_f} \otimes \Gamma_{K_f}) \equiv \Gamma_0) \quad \text{(C1)}$$

when the explicit symmetry label of each index is considered. In that equation K'_f represents a set of uncontracted or free indices coming from the $(k',l'..)$ orbital set and $\Gamma^*_{K'_f}$ is the direct product of all these indices. Likewise, I'_f stands for all the free indices from the $(i',j'..)$ set, I_f is for the $(i,j..)$ set, and K_f is for the $(k,l..)$ set. Γ_0 is the totally symmetric irrep. The remaining orbitals which do not belong to the sets K'_f, I'_f, I_f, and K_f are contracted, and the direct product irreps of them within A and B are the same.

As we have already mentioned, every contraction is mapped onto Equation (23). For this case the symmetry restrictions entails that

$$A \rightarrow A' : (\Gamma^*_{K'_f} \otimes \Gamma_{I_f}) \otimes (\Gamma^*_{K'_c} \otimes \Gamma_{I_c}) = \Gamma'_{f_1} \otimes \Gamma'_{c_1} = \Gamma_0, \quad \text{(C2)}$$

$$B \rightarrow B' : (\Gamma^*_{I'_c} \otimes \Gamma_{K_c}) \otimes (\Gamma^*_{I'_f} \otimes \Gamma_{K_f}) = \Gamma'_{c_2} \otimes \Gamma'_{f_2} = \Gamma_0, \quad \text{(C3)}$$

$$C \leftarrow C' : (\Gamma^*_{K'_f} \otimes \Gamma_{I_f}) \otimes (\Gamma^*_{I'_f} \otimes \Gamma_{K_f}) = \Gamma'_{f_1} \otimes \Gamma'_{f_2} = \Gamma_0, \quad \text{(C4)}$$

where the subscript "f" stands for free indices and subscript "c" stands for contractable indices. Equations (C2)–(C4) define the symmetry structure of the tensors after employing the sorting step. We have introduced a new symmetry label Γ' to indicate that the sorted indices can originate from the ket (that is, Γ) or bra (that is, Γ^*) position or from both of them. Consequently, multiplication tables have been set up for the direct products $(\Gamma_p \otimes \Gamma_q)$ and $\left(\Gamma_p \otimes \Gamma^*_q\right)$, where Γ_p and Γ_q may refer to both fermion and boson irreps.

Now, with a specific example as in Equation (B1), the input tensor λ appears as an array (i,m,a,e,Γ_{ae}) containing only elements for which

$$\left(\Gamma^*_i \otimes \Gamma^*_m\right) \otimes (\Gamma_a \otimes \Gamma_e) = \Gamma^*_{im} \otimes \Gamma_{ae} = \Gamma_0, \quad \text{(C5)}$$

where Γ_0 is the totally symmetric irrep. Upon sorting it will be reshaped to an array (i,a,e,m,Γ'_{em}), where $\Gamma'_{em} = \Gamma_e \otimes \Gamma^*_m$. The arrays W and $\delta\lambda$ will undergo similar treatment.

Finally, one contraction with explicit symmetry labelling can be written as

$$A'(\Gamma'_{f_1},\Gamma'_{c_1}) \otimes B'(\Gamma'_{c_2},\Gamma'_{f_2}) = C'(\Gamma'_{f_1},\Gamma'_{f_2}). \quad \text{(C6)}$$

In this step we make sure that $\Gamma'_{c_1} = \Gamma'_{c_2}$ and all other symmetry restrictions follow from Equations (C2)–(C4). In our specific example, we multiply λ and W in the matrix form $\lambda(ia,em:\Gamma'_{em})$ and $W(jb,em:\Gamma'_{em})$ by using a BLAS matrix-matrix multiplication routine. Notice that we need to transpose the array W for carrying out the multiplication. Finally the product array $\delta\lambda(ia:\Gamma'_{ia},jb:\Gamma'_{jb})$ is reshaped to $\delta\lambda(i,j,a,b)$, where $\Gamma^*_{ij} = \Gamma_{ab}$.

These sorting steps are at most of order N^4 (with N the number of orbitals) and should be insignificant relative to the N^6 order contractions. Due to the higher speed of the latter it is in practice, however, necessary to also consider optimization of these sorting steps as they often require non-contiguous memory access.

[1]M. Gell-Mann, Il Nuovo Cimento **4**, 848 (1956).
[2]K. Schwarzschild, Gött. Nach., Math.-Phys. Kl. 126 (1903).
[3]T. Saue, Adv. Quantum Chem. **48**, 383 (2005).
[4]T. Saue, ChemPhysChem **12**, 3077 (2011).
[5]H. Bolvin, ChemPhysChem **7**, 1575 (2006).
[6]R. Berger, "Parity-violation effects in molecules," in *Relativistic Electronic Structure Theory, Part 2, Applications*, edited by P. Schwerdtfeger (Elsevier, Netherlands, 2004), pp. 188–288.
[7]M. Quack, J. Stohner, and M. Willeke, Annu. Rev. Phys. Chem. **59**, 741 (2008).
[8]R. Bast, A. Koers, A. S. P. Gomes, M. Ilias, L. Visscher, P. Schwerdtfeger, and T. Saue, Phys. Chem. Chem. Phys. **13**, 864 (2011).
[9]Y. Nomura, Y. Takeuchi, and N. Nakagawa, Tetrahedron Lett. **10**, 639 (1969).
[10]I. Morishima, K. Endo, and T. Yonezawa, J. Chem. Phys. **59**, 3356 (1973).
[11]L. Visscher, T. Enevoldsen, T. Saue, and J. Oddershede, J. Chem. Phys. **109**, 9677 (1998).
[12]F. Aquino, N. Govind, and J. Autschbach, J. Chem. Theory Comput. **6**, 2669 (2010).
[13]S. Knecht, S. Fux, R. van Meer, L. Visscher, M. Reiher, and T. Saue, Theor. Chem. Acc. **129**, 631 (2011).
[14]P. O. Lipas, P. Pyykkö, and E. Pajanne, J. Chem. Phys. **58**, 3248 (1973).
[15]P. Pyykkö, Chem. Rev. **88**, 563 (1988).
[16]J. N. van Stralen, L. Visscher, C. V. Larsen, and H. J. A. Jensen, Chem. Phys. **311**, 81 (2005).
[17]I. Kim, Y. C. Park, H. Kim, and Y. S. Lee, Chem. Phys. **395**, 115 (2012).
[18]F. Wang, J. Gauss, and C. van Wüllen, J. Chem. Phys. **129**, 064113 (2008).
[19]F. Wang and J. Gauss, J. Chem. Phys. **129**, 174110 (2008).
[20]L. Cheng and J. Gauss, J. Chem. Phys. **134**, 244112 (2011).
[21]L. Cheng and J. Gauss, J. Chem. Phys. **135**, 084114 (2011).
[22]L. Cheng and J. Gauss, J. Chem. Phys. **135**, 244104 (2011).
[23]L. Visscher and T. Saue, J. Chem. Phys. **113**, 3996 (2000).
[24]S. Knecht and T. Saue, Chem. Phys. **401**, 103 (2012).
[25]I. S. Lim and P. Schwerdtfeger, Phys. Rev. A **70**, 062501 (2004).
[26]DIRAC, a relativistic *ab initio* electronic structure program, Release DIRAC15 (2015), written by R. Bast, T. Saue, L. Visscher, and H. J. Aa. Jensen, with contributions from V. Bakken, K. G. Dyall, S. Dubillard, U. Ekstroem, E. Eliav, T. Enevoldsen, E. Fasshauer, T. Fleig, O. Fossgaard, A. S. P. Gomes, T. Helgaker, J. Henriksson, M. Ilias, Ch. R. Jacob, S. Knecht, S. Komorovsky, O. Kullie, J. K. Laerdahl, C. V. Larsen, Y. S. Lee, H. S. Nataraj, M. K. Nayak, P. Norman, G. Olejniczak, J. Olsen, Y. C. Park, J. K. Pedersen, M. Pernpointner, R. Di Remigio, K. Ruud, P. Salek, B. Schimmelpfennig, J. Sikkema, A. J. Thorvaldsen, J. Thyssen, J. van Stralen, S. Villaume, O. Visser, T. Winther, and S. Yamamoto, see http://www.diracprogram.org.
[27]G. E. Brown and D. G. Ravenhall, Proc. R. Soc. A **208**, 552 (1951).
[28]J. Sucher, Phys. Rev. A **22**, 348 (1980).
[29]A. Almoukhalalati, S. Knecht, H. J. A. Jensen, K. G. Dyall, and T. Saue, J. Chem. Phys. **145**, 074104 (2016).
[30]L. Visscher and K. G. Dyall, At. Data Nucl. Data Tables **67**, 2007 (1997).
[31]J. Olsen and P. Jørgensen, J. Chem. Phys. **82**, 3235 (1985).
[32]O. Christiansen, P. Jørgensen, and C. Hättig, Int. J. Quantum Chem. **68**, 1 (1998).
[33]J. Gauss, in *Modern Methods and Algorithms of Quantum Chemistry*, edited by J. Grotendorst (John von Neumann–Institute for Computing, Jülich, 2000), see http://webarchiv.fz-juelich.de/nic-series//Volume1/Volume1.html.
[34]T. Saue, in *Relativistic Electronic Structure Theory. Part 1. Fundamentals*, edited by P. Schwerdtfeger (Elsevier, Amsterdam, 2002), p. 332.
[35]T. Helgaker, S. Coriani, P. Jørgensen, K. Kristensen, J. Olsen, and K. Ruud, Chem. Rev. **112**, 543 (2012).
[36]E. A. Hylleraas, Z. Phys. **65**, 209 (1930).
[37]E. Wigner, Math. Natur. Anz. (Budapest) **53**, 477 (1935).
[38]H. Koch, H. J. A. Jensen, P. Jørgensen, T. Helgaker, G. E. Scuseria, and H. F. Schaefer, J. Chem. Phys. **92**, 4924 (1990).
[39]T. Helgaker and P. Jørgensen, Theor. Chim. Acta **75**, 111 (1989).
[40]P. Jørgensen and T. Helgaker, J. Chem. Phys. **89**, 1560 (1988).
[41]T. Helgaker and P. Jørgensen, in *Methods in Computational Molecular Physics*, edited by S. Wilson and G. H. F. Diercksen (Plenum, New York, 1992), p. 353421.
[42]B. Levy, Chem. Phys. Lett. **4**, 17 (1969).
[43]P. Jørgensen and J. Linderberg, Int. J. Quantum Chem. **4**, 587 (1970).
[44]E. Dalgaard and P. Jørgensen, J. Chem. Phys. **69**, 3833 (1978).
[45]T. Helgaker, P. Jørgensen, and J. Olsen, *Molecular Electronic Structure Theory* (John Wiley & Sons, Ltd., Chichester, 2000).
[46]J. Talman, Phys. Rev. Lett. **57**, 1091 (1986).
[47]T. Saue and L. Visscher, in *Theoretical Chemistry and Physics of Heavy and Superheavy Elements*, edited by S. Wilson and U. Kaldor (Kluwer, Dordrecht, 2003), p. 211.

7. Summary and Future Perspective

This thesis covers two major domains of Relativistic Quantum Chemistry - electronic structure and molecular properties. While in the first part our main objective was to study the existing relativistic correlation methodologies, in the second part it was to develop and implement new theory.

In our first work we tried to provide benchmark spectroscopic constants of Radon and eka-Radon dimers. To achieve the best accuracy, we calibrated all the major parameters associated with an ab-initio calculation - the Hamiltonian, the basis sets, the method of correlation against experiment for the lighter homologue Xenon. We applied long range Coupled Cluster corrected short range DFT method for the same systems, which has been the very first reported number for the relativistic variety of that method. Our study asserted that the Gaunt interaction is very important in the bonding of eka-Radon. However, we treated Gaunt interaction at the mean-field level. It will be worthwhile to study the interplay between Gaunt interaction and correlation. Lastly eka-Radon exhibits surprisingly strong bonding behaviour. It will not at all be irrational to think it as a liquid or a solid!

In the next work we simulated Xray Spectra for the Actinide compounds. We found that ab-initio study of the X-ray spectroscopy is very challenging, few of the effects one needs to deal with are somewhat unreachable by the present day ab-initio methods. In our experience, even the "most" accurate ab-initio method, the CC theory is not adequate in that purpose. We contained ourselves with the less accurate MP2 method which in a way bypasses numerical divergence. Nevertheless, that led us to implement a new Open-Shell MP2 method.

In the second part of this thesis we have implemented coupled cluster analytic gradient module in DIRAC [1]. This being a DIRAC-code, have access to different varieties of Hamiltonian - spin-free, 2-component (one must be aware of the picture change error for using it) etc. We have so far performed some pilot calculations to validate the code. It is of course a method of very wide scope. We are optimistic to be able to show large number of applications of this method in near future.

The parallel version of this code is not completely debugged. We hope to get that very very soon. Besides, the (T) version of this code is yet to implement. The implementation of that method is very much memory intensive, it scales as N^6. In the relativistic case, with its added pre-factor, serial implementation is not likely to work satisfactorily. We are trying to frame a suitable parallel algorithm for that method. With these two implementation the scope of this work will be widened up very significantly.

Our implementation of this method has been designed in a way that other non-relativistic SRCC methods can very conveniently be adapted to the relativistic domain. The first method we can name is the Equation-of-motion coupled cluster theory, which

is used very widely, very routinely for the low-lying excited states of closed-shell ground state system. In the motivation section of our work we have mentioned the NMR spectroscopy. That will only be possible to study by implementing Linear Response coupled cluster theory. We are aiming to implement that one too.

Open-shell extension of the relativistic CC gradient code is not completely trivial. It is somewhat hindered by the strict time-reversal symmetry adaption in the most part of the code. Nevertheless, it is of very high importance, it will open up the possibility of studying several magnetic properties. We will soon try to make a strategy of dealing with that problem.

Theoretical chemists trust the accuracy of coupled cluster method. Therefore, we hope to see a large number of applications in near future, not only from our group but also from others.

Part III.

Appendices

A. Integrals in Kramer's Pair Basis

In this appendix I will show how we can connect the integrals represented in a Kramer's pair basis to the boson irreps of a Double Group. In the matrix form the DIrac Hamiltonian can be written down as:

$$H = \begin{pmatrix} V & c(\sigma.p) \\ c(\sigma.p) & V - 2mc^2 \end{pmatrix} \tag{A.1}$$

For the simplicity of analysis we will consider V as totally symmetric i.e, devoid of any vector potential. This implies the diagonal part of the Hamiltonian is totally symmetric. Let us, write down the Hamiltonian in Eqn.A.1 in the following manner, so that symmetry information for individual parts will be clear:

$$H = \begin{pmatrix} A(\Gamma_0) & B(\Gamma) \\ B(\Gamma) & A'(\Gamma_0) \end{pmatrix} \tag{A.2}$$

To get the explicit symmetry content in each part we will analyze the B matrix in terms of irreps

$$B(\Gamma) = c. \begin{pmatrix} p_z & p_x - ip_y \\ p_x + ip_y & -p_z \end{pmatrix} \equiv \begin{pmatrix} -i\Gamma(z) & -i\Gamma(x) + \Gamma(y) \\ -i\Gamma(x) - \Gamma(y) & i\Gamma(z) \end{pmatrix} \tag{A.3}$$

Now, operating the Hamiltonian in Eqn. A.2 on four component wave function we get the following result.

$$\begin{aligned} \begin{pmatrix} A(\Gamma_0) & B(\Gamma) \\ B(\Gamma) & A'(\Gamma_0) \end{pmatrix} \cdot \begin{pmatrix} \Phi_L \\ \Phi_S \end{pmatrix} &= \begin{pmatrix} A.\Phi_L + B.\Phi_S \\ B.\Phi_L + A'.\Phi_S \end{pmatrix} \\ &= \begin{pmatrix} \Phi'_L \\ \Phi'_S \end{pmatrix} \end{aligned} \tag{A.4}$$

For generality purpose Φ_L should be expressed as:

$$\begin{aligned} \Phi_L &= \begin{pmatrix} \Phi_{Re}^{L,\alpha} + i\Phi_{Im}^{L,\alpha} \\ \Phi_{Re}^{L,\beta} + i\Phi_{Im}^{L,\beta} \end{pmatrix} \\ &\equiv \begin{pmatrix} \Gamma_{Re}^{L,\alpha} + i\Gamma_{Im}^{L,\alpha} \\ \Gamma_{Re}^{L,\beta} + i\Gamma_{Im}^{L,\beta} \end{pmatrix} \end{aligned} \tag{A.5}$$

This is applicable for Φ_S also. i.e,

$$\begin{aligned} \Phi_S &= \begin{pmatrix} \Phi_{Re}^{S,\alpha} + i\Phi_{Im}^{S,\alpha} \\ \Phi_{Re}^{S,\beta} + i\Phi_{Im}^{S,\beta} \end{pmatrix} \\ &\equiv \begin{pmatrix} \Gamma_{Re}^{S,\alpha} + i\Gamma_{Im}^{S,\alpha} \\ \Gamma_{Re}^{S,\beta} + i\Gamma_{Im}^{S,\beta} \end{pmatrix} \end{aligned} \tag{A.6}$$

Using the relations of Eqns.A.5 and A.6 in Eqn.A.4 we get:

$$\begin{aligned}
\Gamma'^{\alpha}_{Re} &= \Gamma_0 \otimes \Gamma^{L,\alpha}_{Re} + \Gamma(z) \otimes \Gamma^{S,\alpha}_{Im} + \Gamma_x \otimes \Gamma^{\beta}_{Im} - \Gamma_y \otimes \Gamma^{\beta}_{Re} \\
\Gamma'^{\alpha}_{Im} &= \Gamma_0 \otimes \Gamma^{L,\alpha}_{Im} - \Gamma_z \otimes \Gamma^{S,\alpha}_{Re} + \Gamma_x \otimes \Gamma^{\beta}_{Re} - \Gamma_y \otimes \Gamma^{\beta}_{Im} \\
\Gamma'^{\beta}_{Re} &= \Gamma(0) \otimes \Gamma^{\beta}_{Re} + \Gamma_x \otimes \Gamma^{S,\alpha}_{Im} + \Gamma_y \otimes \Gamma^{S,\alpha}_{Re} - \Gamma_z \otimes \Gamma^{\beta}_{Im} \\
\Gamma'^{\beta}_{Im} &= \Gamma_0 \otimes \Gamma^{\beta}_{Im} - \Gamma_x \otimes \Gamma^{S,\alpha}_{Re} + \Gamma_y \otimes \Gamma^{S,\alpha}_{Im} + \Gamma_z \otimes \Gamma^{\beta}_{Re}
\end{aligned} \tag{A.7}$$

For small components we will get the identical relations just by replacing L by S and vice versa in the above equations:

$$\begin{aligned}
\Gamma'^{\alpha}_{Re} &= \Gamma_0 \otimes \Gamma^{S,\alpha}_{Re} + \Gamma_z \otimes \Gamma^{L,\alpha}_{Im} + \Gamma_x \otimes \Gamma^{\beta}_{Im} - \Gamma_y \otimes \Gamma^{\beta}_{Re} \\
\Gamma'^{\alpha}_{Im} &= \Gamma_0 \otimes \Gamma^{S,\alpha}_{Im} - \Gamma_z \otimes \Gamma^{L,\alpha}_{Re} + \Gamma_x \otimes \Gamma^{\beta}_{Re} - \Gamma_y \otimes \Gamma^{\beta}_{Im} \\
\Gamma'^{\beta}_{Re} &= \Gamma_0 \otimes \Gamma^{\beta}_{Re} + \Gamma_x \otimes \Gamma^{L,\alpha}_{Im} + \Gamma_y \otimes \Gamma^{L,\alpha}_{Re} - \Gamma_z \otimes \Gamma^{\beta}_{Im} \\
\Gamma'^{\beta}_{Im} &= \Gamma_0 \otimes \Gamma^{\beta}_{Im} - \Gamma_x \otimes \Gamma^{L,\alpha}_{Re} + \Gamma_y \otimes \Gamma^{L,\alpha}_{Im} + \Gamma_z \times \Gamma^{\beta}_{Re}
\end{aligned} \tag{A.8}$$

Now, our objective is to define the representation of the all components in the transformed wave function with respect to the IRR of $\Phi^{L,\alpha}_{Re}$. We have also noticed that all the combinations of IRRs in Eqns.A.7 and A.8 will be equivalent to a fixed representation because of the structure of the wave function will be of the same form as A.5 and A.6.

$$\begin{pmatrix} \Phi'_L \\ \Phi'_S \end{pmatrix} = \Gamma^{L,\alpha}_{Re} \begin{pmatrix} (\Gamma_0, \Gamma_x \otimes \Gamma_y) \\ (\Gamma_x \otimes \Gamma_z, \Gamma_z \otimes \Gamma_y) \\ (\Gamma_x \otimes \Gamma_y \otimes \Gamma_z, \Gamma_z) \\ (\Gamma_y, \Gamma_x) \end{pmatrix} = \Gamma^{L,\alpha}_{Re} \begin{pmatrix} (\Gamma_0, \Gamma_{R_z}) \\ (\Gamma_{R_y}, \Gamma_{R_x}) \\ (\Gamma_{xyz}, \Gamma_z) \\ (\Gamma_y, \Gamma_x) \end{pmatrix} \tag{A.9}$$

For all point groups without inversion symmetry we will consider $\Gamma^{L,\alpha}_{Re}$ as Γ_0. For inversion symmetry containing point groups we will consider Γ_0 for 'gerade' type irreducible representations and Γ_{xyz} for 'ungerade' type irreducible representation.

Symmetry of Overlap and One Electronic Integrals

In the relativistic domain spin is not a good quantum number. Therefore, unlike non-relativistic cases 'Kramers degeneracy' is absent here. But time reversal symmetry helps us to recover some sort of above mentioned degeneracy between the partner wave functions. Here we will call them as time reversal partner of one another or 'Kramers Pair'. They are related by the following equations:

$$\Phi_{\overline{p}} = T\Phi_p \tag{A.10}$$

$$T\Phi_{\overline{p}} = -\Phi_p \tag{A.11}$$

where,

$$T = -i \begin{pmatrix} \sigma_y & 0 \\ 0 & \sigma_y \end{pmatrix} \kappa_0 \tag{A.12}$$

In the 'Kramers Pair' basis general overlap matrix will look like as follow:

$$\Omega_{PQ} = \begin{pmatrix} \Omega_{pq} & \Omega_{p\bar{q}} \\ \Omega_{\bar{p}q} & \Omega_{\bar{p}\bar{q}} \end{pmatrix} \tag{A.13}$$

For the present situation we will consider two component wave function only. But this is easily generalizable in terms of 4-component. Our wave-function will generally look like:

$$\Phi_p = \begin{pmatrix} \Phi_p^{\alpha} \\ \Phi_p^{\beta} \end{pmatrix} \tag{A.14}$$

$$\Phi_{\bar{p}} = \begin{pmatrix} -\Phi_p^{*\beta} \\ \Phi_p^{*\alpha} \end{pmatrix} \tag{A.15}$$

case I

$$\begin{aligned} \langle \Phi_p | \Phi_q \rangle &= \begin{pmatrix} \Phi_p^{*\alpha} & \Phi_p^{*\beta} \end{pmatrix} \times \begin{pmatrix} \Phi_q^{\alpha} \\ \Phi_q^{\beta} \end{pmatrix} \\ &= \Phi_p^{*\alpha}\Phi_q^{\alpha} + \Phi_p^{*\beta}\Phi_q^{\alpha} \\ &= A \end{aligned} \tag{A.16}$$

case II

$$\begin{aligned} \langle \Phi_p | \Phi_{\bar{q}} \rangle &= \begin{pmatrix} \Phi_p^{*\alpha} & \Phi_p^{*\beta} \end{pmatrix} \times \begin{pmatrix} -\Phi_q^{*\beta} \\ \Phi_q^{*\alpha} \end{pmatrix} \\ &= -\Phi_p^{*\alpha}\Phi_q^{*\beta} + \Phi_p^{*\beta}\Phi_q^{*\alpha} \\ &= B \end{aligned} \tag{A.17}$$

case III

$$\begin{aligned} \langle \Phi_{\bar{p}} | \Phi_q \rangle &= \begin{pmatrix} -\Phi_p^{\beta} & \Phi_p^{\alpha} \end{pmatrix} \times \begin{pmatrix} \Phi_q^{\alpha} \\ \Phi_q^{\beta} \end{pmatrix} \\ &= \Phi_p^{\beta}\Phi_q^{\alpha} - \Phi_p^{\alpha}\Phi_q^{\beta} \\ &= -B^* \end{aligned} \tag{A.18}$$

case IV

$$\begin{aligned} \langle \Phi_{\bar{p}} | \Phi_{\bar{q}} \rangle &= \begin{pmatrix} \Phi_p^{*\alpha} & \Phi_p^{*\beta} \end{pmatrix} \times \begin{pmatrix} \Phi_q^{\alpha} \\ \Phi_q^{\beta} \end{pmatrix} \\ &= \Phi_p^{*\alpha}\Phi_q^{\alpha} + \Phi_p^{*\beta}\Phi_q^{\beta} \\ &= A^* \end{aligned} \tag{A.19}$$

Therefore, the final form of the matrix Ω_{PQ} is:

$$\Omega_{PQ} = \begin{pmatrix} A & B \\ -B^* & A^* \end{pmatrix} \tag{A.20}$$

Now, we will elucidate the symmetry content of each parts:
First, I will consider the case for which the symmetry of our reference function is Γ_0:

$$\begin{aligned} A(\Gamma) &= \begin{pmatrix} (\Gamma_0, \Gamma_{R_z}) & (\Gamma_{R_y}, \Gamma_{R_x}) \end{pmatrix} \times \begin{pmatrix} (\Gamma_0, \Gamma_{R_z}) \\ (\Gamma_{R_y}, \Gamma_{R_x}) \end{pmatrix} \\ &= (\Gamma_0, \Gamma_{R_z}) \end{aligned}$$

$$\begin{aligned} B(\Gamma) &= \begin{pmatrix} (\Gamma_0, \Gamma_{R_z}) & (\Gamma_{R_y}, \Gamma_{R_x}) \end{pmatrix} \times \begin{pmatrix} -(\Gamma_{R_y}, \Gamma_{R_x}) \\ (\Gamma_0, \Gamma_{R_z}) \end{pmatrix} \\ &= (\Gamma_{R_y}, \Gamma_{R_x}) \end{aligned} \tag{A.21}$$

Next, we will consider the situation where instead of Γ_0, the symmetry for the reference state will be considered as Γ_{xyz}. The symmetry structure of the matrix elements will be same for this irreps also since $\Gamma_{xyz} \otimes \Gamma_{xyz} = \Gamma_0$.

At this point we can argue that, one-elctronic part of the Hamiltonian being totally symmetric, the symmetry structure for the matrix elements will be same as the overlap integral. H being invariant under all operation of the group, only totally symmetric matrix elements will have non-zero value. This clearly suggests further simplification in the matrix element structure of the one electronic operator in Kramer's basis e.g, in D_{2h} symmetry we can see that A is only real and B is zero.

Two-electron Coulomb Integrals

This analysis can be extended to the two-electronic part of the Hamiltonian even. If we consider Mulliken notation for the integrals then, matrix element for the two-electronic part of the Hamiltonian is nothing but the direct product of overlap integrals. Again, this is possible because of the fact two-electronic Hamiltonian belongs to the totally symmetric representation. Let us write two electronic integrals in the following way:

$$\Omega_{PQRS} = \Omega_{PQ} \otimes \Omega_{RS} \tag{A.22}$$

$$= \begin{pmatrix} \Omega_{pqrs} & \Omega_{pqr\bar{s}} & \Omega_{p\bar{q}rs} & \Omega_{p\bar{q}r\bar{s}} \\ \Omega_{pq\bar{r}s} & \Omega_{pq\bar{r}\bar{s}} & \Omega_{p\bar{q}\bar{r}s} & \Omega_{p\bar{q}\bar{r}\bar{s}} \\ \Omega_{\bar{p}qrs} & \Omega_{\bar{p}qr\bar{s}} & \Omega_{\bar{p}\bar{q}rs} & \Omega_{\bar{p}\bar{q}r\bar{s}} \\ \Omega_{\bar{p}q\bar{r}s} & \Omega_{\bar{p}q\bar{r}\bar{s}} & \Omega_{\bar{p}\bar{q}\bar{r}s} & \Omega_{\bar{p}\bar{q}\bar{r}\bar{s}} \end{pmatrix} \tag{A.23}$$

$$= \begin{pmatrix} AC & AD & BC & BD \\ -AD^* & AC^* & -BD^* & BC^* \\ -B^*C & -B^*D & A^*C & A^*D \\ B^*D^* & -B^*C^* & -A^*D^* & A^*C^* \end{pmatrix} \tag{A.24}$$

One can easily see that, it is sufficient to consider only the upper half of this matrix and the lower part can be generated merely by complex conjugation and changing the sign. So, for the symmetry content we have to analyze only 8 unique upper half entries of Ω_{PQRS}. This gives the following structure of the resultant matrix in terms of symmetry:

$$\Omega_{PQRS} = \begin{pmatrix} (\Gamma_0, \Gamma_{R_z}) & (\Gamma_{R_y}, \Gamma_{R_x}) & (\Gamma_{R_y}, \Gamma_{R_x}) & (\Gamma_0, \Gamma_{R_z}) \\ (\Gamma_{R_y}, \Gamma_{R_x}) & (\Gamma_0, \Gamma_{R_z}) & (\Gamma_0, \Gamma_{R_z}) & (\Gamma_{R_y}, \Gamma_{R_x}) \end{pmatrix} \tag{A.25}$$

If we consider particle exchange symmetry in the situation where both particle 1 and 2 span the same orbital space then, between AD and BC only one class is unique and so also between AD^* and BC^*. That reduces the number of unique classes of matrix elements to 6 among the 16 possibilities.

For the Hamiltonian matrix elements in D_{2h} symmetry we will get non-zero values for real part in AC, BD, AC^* and BD^* class of integrals. It is very apparent from this analysis that consideration of point group symmetry gives a considerable reduction in the number of non-zero integrals. Now we will classify the integrals

Two electron Gaunt Integral

The operator form of the Gaunt term is:

$$G^{gaunt} = -\frac{\vec{\alpha}_1.\vec{\alpha}_2}{r_{12}} \tag{A.26}$$

In Mulliken notation the gaunt integral is generally expressed as: $(\Phi_p \vec{\alpha} \Phi_q | \Phi_r \vec{\alpha} \Phi_s)$. Now to explore the symmetry content of the Gaunt integral we will follow the same strategy as above.
step1:

$$\Phi_p \vec{\alpha} \Phi_q = \begin{pmatrix} \phi_p^{L\dagger} & \phi_p^{S\dagger} \end{pmatrix} . \begin{pmatrix} 0 & \sigma \\ \sigma & 0 \end{pmatrix} \begin{pmatrix} \phi_q^L \\ \phi_q^S \end{pmatrix} = \phi_p^{L\dagger} \sigma \phi_q^S + \phi_p^{S\dagger} \sigma \phi_q^L \tag{A.27}$$

step2 : So, the total Gaunt Integral is:

$$(\Phi_p \vec{\alpha} \Phi_q | \Phi_r \vec{\alpha} \Phi_s) = (\phi_p^{L\dagger} \sigma \phi_q^S + \phi_p^{S\dagger} \sigma \phi_q^L | \phi_r^{L\dagger} \sigma \phi_s^S + \phi_r^{S\dagger} \sigma \phi_s^L) \tag{A.28}$$

Our next task is to construct the matrix representation of the current density term in the 'Kramer's pair' basis. Our considered form of the wave function is same as Eqns. A.15 and A.14. Following the same strategy, the individual components are:

1)

$$\begin{aligned}\langle\Phi_p|\sigma_x|\Phi_q\rangle &= \begin{pmatrix}\Phi_p^{*\vec{\alpha}} & \Phi_p^{*\beta}\end{pmatrix}.\begin{pmatrix}0 & 1\\ 1 & 0\end{pmatrix}.\begin{pmatrix}\Phi_q^{\vec{\alpha}}\\ \Phi_q^{\beta}\end{pmatrix} \\ &= \Phi_p^{*\vec{\alpha}}.\Phi_q^{\beta} + \Phi_p^{*\beta}.\Phi_q^{\vec{\alpha}} \\ &= A_x^{gaunt}\end{aligned} \tag{A.29}$$

$$\begin{aligned}\langle\Phi_p|\sigma_y|\Phi_q\rangle &= \begin{pmatrix}\Phi_p^{*\vec{\alpha}} & \Phi_p^{*\beta}\end{pmatrix}.\begin{pmatrix}0 & -i\\ i & 0\end{pmatrix}.\begin{pmatrix}\Phi_q^{\vec{\alpha}}\\ \Phi_q^{\beta}\end{pmatrix} \\ &= -i.\Phi_p^{*\vec{\alpha}}.\Phi_q^{\beta} + i.\Phi_p^{*\beta}.\Phi_q^{\vec{\alpha}} \\ &= A_y^{gaunt}\end{aligned} \tag{A.30}$$

$$\begin{aligned}\langle\Phi_p|\sigma_z|\Phi_q\rangle &= \begin{pmatrix}\Phi_p^{*\vec{\alpha}} & \Phi_p^{*\beta}\end{pmatrix}.\begin{pmatrix}1 & 0\\ 0 & -1\end{pmatrix}.\begin{pmatrix}\Phi_q^{\vec{\alpha}}\\ \Phi_q^{\beta}\end{pmatrix} \\ &= \Phi_p^{*\vec{\alpha}}.\Phi_q^{\vec{\alpha}} - \Phi_p^{*\beta}.\Phi_q^{\beta} \\ &= A_z^{gaunt}\end{aligned} \tag{A.31}$$

2)

$$\begin{aligned}\langle\Phi_p|\sigma_x|\Phi_{\overline{q}}\rangle &= \begin{pmatrix}\Phi_p^{*\alpha} & \Phi_p^{*\beta}\end{pmatrix}.\begin{pmatrix}0 & 1\\ 1 & 0\end{pmatrix}.\begin{pmatrix}-\Phi_q^{*\beta}\\ \Phi_q^{*\alpha}\end{pmatrix} \\ &= \Phi_p^{*\alpha}\Phi_q^{*\alpha} - \Phi_p^{*\beta}\Phi_q^{*\beta} \\ &= B_x^{gaunt}\end{aligned} \tag{A.32}$$

$$\begin{aligned}\langle\Phi_p|\sigma_y|\Phi_{\overline{q}}\rangle &= \begin{pmatrix}\Phi_p^{*\alpha} & \Phi_p^{*\beta}\end{pmatrix}.\begin{pmatrix}0 & -i\\ i & 0\end{pmatrix}.\begin{pmatrix}-\Phi_q^{*\beta}\\ \Phi_q^{*\alpha}\end{pmatrix} \\ &= -i.\Phi_p^{*\alpha}\Phi_q^{*\alpha} - i.\Phi_p^{*\beta}\Phi_q^{*\beta} \\ &= B_y^{gaunt}\end{aligned} \tag{A.33}$$

$$\begin{aligned}\langle\Phi_p|\sigma_x|\Phi_{\overline{q}}\rangle &= \begin{pmatrix}\Phi_p^{*\alpha} & \Phi_p^{*\beta}\end{pmatrix}.\begin{pmatrix}1 & 0\\ 0 & -1\end{pmatrix}.\begin{pmatrix}-\Phi_q^{*\beta}\\ \Phi_q^{*\alpha}\end{pmatrix} \\ &= \Phi_p^{*\alpha}\Phi_q^{*\beta} - \Phi_p^{*\beta}\Phi_q^{*\alpha} \\ &= B_z^{gaunt}\end{aligned} \tag{A.34}$$

3)

$$\begin{aligned}\langle\Phi_{\overline{p}}|\sigma_x|\Phi_q\rangle &= \begin{pmatrix}-\Phi_p^\beta & \Phi_p^\alpha\end{pmatrix}.\begin{pmatrix}0 & 1\\ 1 & 0\end{pmatrix}.\begin{pmatrix}\Phi_q^\alpha\\ \Phi_q^\beta\end{pmatrix} \\ &= -\Phi_p^\beta.\Phi_q^\beta + \Phi_p^\alpha.\Phi_q^\alpha \\ &= B_x^{*gaunt}\end{aligned} \tag{A.35}$$

$$\begin{aligned}\langle\Phi_{\overline{p}}|\sigma_y|\Phi_q\rangle &= \begin{pmatrix}-\Phi_p^\beta & \Phi_p^\alpha\end{pmatrix}.\begin{pmatrix}0 & -i\\ i & 0\end{pmatrix}.\begin{pmatrix}\Phi_q^\alpha\\ \Phi_q^\beta\end{pmatrix} \\ &= i.\Phi_p^\beta.\Phi_q^\beta - i\Phi_p^\alpha.\Phi_q^\alpha \\ &= B_y^{*gaunt}\end{aligned} \tag{A.36}$$

$$\begin{aligned}\langle\Phi_{\overline{p}}|\sigma_z|\Phi_q\rangle &= \begin{pmatrix}-\Phi_p^\beta & \Phi_p^\alpha\end{pmatrix}.\begin{pmatrix}1 & 0\\ 0 & -1\end{pmatrix}.\begin{pmatrix}\Phi_q^\alpha\\ \Phi_q^\beta\end{pmatrix} \\ &= -\Phi_p^\beta.\Phi_q^\alpha - \Phi_p^\alpha.\Phi_q^\beta \\ &= B_z^{*gaunt}\end{aligned} \tag{A.37}$$

4)

$$\begin{aligned}\langle\Phi_{\overline{p}}|\sigma_x|\Phi_{\overline{q}}\rangle &= \begin{pmatrix}-\Phi_p^\beta & \Phi_p^\alpha\end{pmatrix}.\begin{pmatrix}0 & 1\\ 1 & 0\end{pmatrix}.\begin{pmatrix}-\Phi_q^{*\beta}\\ \Phi_q^{*\alpha}\end{pmatrix} \\ &= -\Phi_p^\beta.\Phi_q^{*\alpha} - \Phi_p^\alpha.\Phi_q^{*\beta} \\ &= -A_x^{*gaunt}\end{aligned} \tag{A.38}$$

$$\begin{aligned}\langle\Phi_{\overline{p}}|\sigma_y|\Phi_{\overline{q}}\rangle &= \begin{pmatrix}-\Phi_p^\beta & \Phi_p^\alpha\end{pmatrix}.\begin{pmatrix}0 & -i\\ i & 0\end{pmatrix}.\begin{pmatrix}-\Phi_q^{*\beta}\\ \Phi_q^{*\alpha}\end{pmatrix} \\ &= i.\Phi_p^\beta.\Phi_q^{*\alpha} - i.\Phi_p^\alpha.\Phi_q^{*\beta} \\ &= -A_y^{*gaunt}\end{aligned} \tag{A.39}$$

$$\begin{aligned}\langle\Phi_{\overline{p}}|\sigma_z|\Phi_{\overline{q}}\rangle &= \begin{pmatrix}-\Phi_p^\beta & \Phi_p^\alpha\end{pmatrix}.\begin{pmatrix}1 & 0\\ 0 & -1\end{pmatrix}.\begin{pmatrix}-\Phi_q^{*\beta}\\ \Phi_q^{*\alpha}\end{pmatrix} \\ &= \Phi_p^\beta.\Phi_q^{*\beta} - \Phi_p^\alpha.\Phi_q^{*\alpha} \\ &= -A_z^{*gaunt}\end{aligned} \tag{A.40}$$

The Gaunt integrals can be constructed by considering the direct product between the current density matrices in Mulliken notation.

$$\begin{aligned}\Omega^{gaunt}_{PQRS} &= \Omega^{gaunt}_{PQ} \otimes \Omega^{gaunt}_{RS} \\ &= \begin{pmatrix} A^g & B^g \\ B^{*g} & -A^{*g} \end{pmatrix} \otimes \begin{pmatrix} C^g & D^g \\ D^{*g} & -C^{*g} \end{pmatrix} \\ &= \begin{pmatrix} AC & AD & BC & BD \\ AD^* & -AC^* & BD^* & -BC^* \\ B^*C & B^*D & -A^*C & -A^*D \\ B^*D^* & -B^*C^* & -A^*D^* & A^*C^* \end{pmatrix}\end{aligned} \tag{A.41}$$

So, like the Coulomb term we will gain the same advantage in terms of time reversal symmetry for the Gaunt terms also. Only exception is that the equality between different integrals will differ by a sign factor, though, it will not affect the symmetry structure. Therefore, the conclusions regarding Bosonic symmetries will also remain unchanged for this case.

B. Sorting of Integrals in Double Group Symmetry-DPD Scheme

We will show an example of sorting, in which symmetry-packed triangular anti-symmetrized integrals in Dirac notation are sorted to the full symmetry-packed list on Mulliken form

$$\langle I > J \,||\, K > L; \Gamma_{KL} \rangle \quad \rightarrow \quad \left(IK|JL; \widetilde{\Gamma}_{JL} \right)$$

The integral sort uses the Direct Product Decomposition Scheme to skip contributions that are zero due to symmetry. The integrand must be totally symmetric which amounts to

$$\Gamma_I^* \otimes \Gamma_J^* \otimes \Gamma_K \otimes \Gamma_L = 1 \tag{B.1}$$

Note that we use the complex conjugates of the irreps of functions I and J since they are in ket position. Generally we have

$$\Gamma_I^* \otimes \Gamma_I = 1.$$

The DPD scheme leads to nested loops over symmetries. In the particular case the starting list of integrals are orded on

$$\Gamma_{KL} = \Gamma_K \otimes \Gamma_L; \quad \rightarrow \quad KLREP = MULTB(KREP, LREP, 1)$$

Here, MULTB(KREP,LREP,1) is a function to generate the product symmetry between two Γ type or Γ^* type irreps. However, the two outer loops are over Γ_{KL} and Γ_L and we now want to find, for a given Γ_L the matching Γ_K such that

$$\Gamma_L \otimes \Gamma_K = \Gamma_{KL}$$

We achieve this by multiplying with the complex conjugate irrep of Γ_L on both sides to obtain

$$\Gamma_K = \Gamma_L^* \otimes \Gamma_{KL}; \quad \rightarrow \quad KREP = MULTB(LREP, KLREP + NREP, 2).$$

MULTB(KREP,LREP,2) is a function to generate the product symmetry between a Γ type and Γ^* type irrep. Note that in the algorithm $KLREP$ is shifted by $NREP$ since it is a boson irrep (and they come after the $NREP$ fermion irreps).

We now want to find possible Γ_I and Γ_J. We start by looping over Γ_J and now want to find the matching Γ_I such that

$$\Gamma_J \otimes \Gamma_I \otimes \Gamma_{KL}^* = 1$$

This is re-arranged by manipulating the above expression to

$$\Gamma_I = \Gamma_J^* \otimes \Gamma_{KL}; \quad \rightarrow \quad IREP = MULTB(JREP, KLREP + NREP, 2)$$

Now we have defined a batch of integrals in terms of matching Γ_L, Γ_K, Γ_J and Γ_I and we will distribute these integrals into the second list. Here we have to take into account the triangular packing, which means that we also get contributions from $\langle IJ \,||\, KL\rangle$

$$\langle IJ \,||\, KL\rangle \quad \rightarrow \quad \begin{cases} \left(IK|JL; \tilde{\Gamma}_{JL} = \Gamma_J^* \otimes \Gamma_L\right) \\ \left(JK|IL; \tilde{\Gamma}_{IL} = \Gamma_I^* \otimes \Gamma_L\right) \\ \left(IL|JK; \tilde{\Gamma}_{JK} = \Gamma_J^* \otimes \Gamma_K\right) \\ \left(JL|IK; \tilde{\Gamma}_{IK} = \Gamma_I^* \otimes \Gamma_K\right) \end{cases}$$

The corresponding symmetries are calculated as

```
JLREP = MULTB(JREP,LREP,2)
IKREP = MULTB(IREP,KREP,2)
ILREP = MULTB(IREP,LREP,2)
JKREP = MULTB(JREP,KREP,2)
```

From (B.1) we deduce the relations

$$\tilde{\Gamma}_{JL} = \tilde{\Gamma}_{IK}^* \quad \text{and} \quad \tilde{\Gamma}_{IL} = \tilde{\Gamma}_{JK}^*$$

The loop structures we have set up runs over the integrals of the first list. In order to place integrals correctly in the second list we have to think about how we would loop through this list. Let us now take the specific example of the sorting $\langle V_I V_J(\Gamma_{IJ} = \Gamma_{KL})|O_K O_L(\Gamma_{KL})\rangle \rightarrow \left(V_I O_K\left(\tilde{\Gamma}_{IK} = \tilde{\Gamma}_{JL}^*\right)|V_J O_L\left(\tilde{\Gamma}_{JL}\right)\right)$. To find the first element in the list for given $\tilde{\Gamma}_{JL}$ we use the offset

$$J2_{VOVO}(\tilde{\Gamma}'+1) = \sum_{\tilde{\Gamma}=1}^{\tilde{\Gamma}'} M_{VO}(\tilde{\Gamma}) * M_{VO}(\tilde{\Gamma}^*); \quad M_{VO}(\tilde{\Gamma}_{IJ}) = \sum_{\left\{(\Gamma_I,\Gamma_J)|\Gamma_I^* \otimes \Gamma_J = \tilde{\Gamma}_{IJ}\right\}} N_V(\Gamma_I) * N_O(\Gamma_J)$$

Note that the offset is given by he accumulated product $M_{VO}(\hat{\Gamma}) * M_{VO}(\tilde{\Gamma}^*)$, whereas our integrals in the second list are on the form $\left(V_I O_K\left(\tilde{\Gamma}_{IK} = \tilde{\Gamma}_{JL}^*\right)|V_J O_L\left(\tilde{\Gamma}_{JL}\right)\right)$. For given $\tilde{\Gamma}_{JL}$ we therefore use $J2_{VOVO}(\tilde{\Gamma}_{JL}^* = \tilde{\Gamma}_{IK})$. We now enter the section of integrals characterized by a particular $\tilde{\Gamma}_{JL}$ and we want to find the beginning of a set characterized by particular values of Γ_L and Γ_J. That offset is given by $M_{VO}(\tilde{\Gamma}_{IK}) * JJ_{VO}(\Gamma_J, \Gamma_L)$, where the variable refers to the number of pairs (I, K) of each index (J, L), and the second is the contribution to $M_{VO}(\tilde{\Gamma}_{JL})$ from pairs $\left\{(\Gamma_I, \Gamma_J)|\Gamma_I^* \otimes \Gamma_J = \tilde{\Gamma}_{IJ}\right\}$ prior to the actual one. We have accordingly entered the section of integrals characterized by $\left(\tilde{\Gamma}_{JL}, \Gamma_L, \Gamma_J\right)$. From the first list we have also specified indices of K and L. The offset

to the particular value of index L will be $M_{VO}(\tilde{\Gamma}_{IK}) * (L-1) * N_V(\Gamma_J)$. In the subroutine the sum of offsets so far is expressed as

```
IKJL0 = OFF(IKREP)+(OFF2(JREP,LREP)+(L-1)*JFIE(JREP)) * NPAIR(IKREP)
```

where OFF=J2VOVO, OFF2=JJVO, NPAIR=MVO and JFIE=NV. The index $J = 1$ within its symmetry. We now need the offset to the particular values of (Γ_I, Γ_K). It is given by $JJ_{VO}(\Gamma_I,\Gamma_K)$. Finally we need the offset to our particular value of index K. It is given by $(K-1) * N_V(\Gamma_I)$. These additional offsets are in the code expressed as

```
IKJL0 = IKJL0 + OFF1(IREP,KREP) + (K-1)*IFIE(IREP)
```

where OFF1=JJVO and IFIE=NV.

We now start a loop over J. If I is in the same symmetry we have $I > J$ and so we may copy $N = N_V(\Gamma_I) - J$ elements. If I is not in the same symmetry we may copy $N = N_V(\Gamma_I)$ elements. We may combine these two case as $N = N_V(\Gamma_I) - I_{min} + 1$. The copy position in the first listis given by the variable `IJKL`, updated at the end of each cycle over J, and in the second list by

```
IKJL = IKJL0 + IMIN-1
```

The copy statement in the code is

```
CALL XCOPY (N,BUF1(IJKL),1,BUF2(IKJL+1),1)
```

The offset `IKJL0` is updated at the end of each cycle over J by

```
IKJL0 = IKJL0 + NPAIR(IKREP)
```

We see that the copy is over N contiguous elements of the array (I, J, K, L) since I is the inner index. Contiguous copying is also possible for $\langle IJ \,||\, KL\rangle \rightarrow (IL|JK)$. Here we build the offset

```
ILJK0 = OFF(ILREP)+(OFF2(JREP,KREP)+(K-1)*JFIE(JREP)) * NPAIR(ILREP)
ILJK0 = ILJK0 + OFF1(IREP,LREP) + (L-1)*IFIE(IREP)
```

completely analogous to the first case, and for the copy we use, inside the loop over J

```
ILJK = ILJK0 + IMIN-1
CALL XCOPY (N,BUF1(IJKL),1,BUF2(ILJK+1),1)
```

For the remaining two cases

$$\begin{aligned} \langle IJ \,||\, KL\rangle &\rightarrow (JK|IL) \\ \langle IJ \,||\, KL\rangle &\rightarrow (JL|IK) \end{aligned}$$

the copy has to proceed with strides since the inner index is now J. The initial offsets are as before

```
JKIL0 = OFF(JKREP)+ (OFF2(IREP,LREP)+(L-1)*IFIE(IREP)) * NPAIR(JKREP)
JKIL0 = JKIL0 + OFF1(JREP,KREP) + (K-1)*JFIE(JREP)
JLIK0 = OFF(JLREP) + (OFF2(IREP,KREP)+(K-1)*IFIE(IREP)) * NPAIR(JLREP)
JLIK0 = JLIK0 + OFF1(JREP,LREP) + (L-1)*JFIE(JREP)
```

For the case $\langle IJ \,||\, KL\rangle \rightarrow (JK|IL)$ the offset will be `NPAIR(JKREP)`, and for the case $\langle IJ \,||\, KL\rangle \rightarrow (JL|IK)$ the stride will be `NPAIR(JLREP)`. The copy statements are accordingly

```
NP = NPAIR(JKREP)
CALL XCOPY(N,BUF1(IJKL),1,BUF2(JKIL+1),NP)
NP = NPAIR(JLREP)
CALL XCOPY (N,BUF1(IJKL),1,BUF2(JLIK+1),NP)
```

C. C_4^* Character Table

For the C_4^* double group the extra elements from the C_4 are following:
$\overline{C}_2 = C_2 * \overline{E}$, $\overline{C}_4 = C_4 * \overline{E}$, $\overline{C}_4^{-1} = C_4^{-1} * \overline{E}$, $\omega = \exp(\frac{i\pi}{4})$
In Table C, Γ_1 to Γ_4 are the boson irreps and Γ_5 to Γ_8 are the fermion irreps.

Table C.1.: Character Table of C_4^* double group.

C_4^*	E	C_4	C_2	C_4^{-1}	$\overline{E}$	$\overline{C}_2$	$\overline{C}_4$	$\overline{C}_4^{-1}$
Γ_1	1	1	1	1	1	1	1	1
Γ_2	1	-1	1	-1	1	1	-1	-1
Γ_3	1	i	-1	-i	1	-1	i	-i
Γ_4	1	-i	-1	i	1	-1	-i	i
Γ_5	1	ω	i	$-\omega$	-1	-i	$-\omega$	ω^3
Γ_6	1	$-\omega^3$	-i	ω^3	-1	i	ω^3	$-\omega$
Γ_7	1	$-\omega$	i	ω	-1	-i	ω	$-\omega^3$
Γ_8	1	ω^3	-i	$-\omega^3$	-1	i	$-\omega^3$	ω

Part IV.

Additional Paper

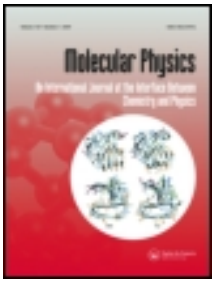

Molecular Physics: An International Journal at the Interface Between Chemistry and Physics

Publication details, including instructions for authors and subscription information:
http://www.tandfonline.com/loi/tmph20

A study of the ionisation and excitation energies of core electrons using a unitary group adapted state universal approach

Sangita Sen [a] , Avijit Shee [a b] & Debashis Mukherjee [a]

[a] Raman Centre for Atomic, Molecular and Optical Sciences , Indian Association for the Cultivation of Science , Kolkata , India

[b] Laboratoire de Chimie et Physique Quantique (UMR 5626) , CNRS/Université de Toulouse , Toulouse , France

Accepted author version posted online: 17 May 2013.Published online: 05 Jun 2013.

To cite this article: Molecular Physics (2013): A study of the ionisation and excitation energies of core electrons using a unitary group adapted state universal approach, Molecular Physics: An International Journal at the Interface Between Chemistry and Physics, DOI: 10.1080/00268976.2013.802384

To link to this article: http://dx.doi.org/10.1080/00268976.2013.802384

Molecular Physics, 2013
http://dx.doi.org/10.1080/00268976.2013.802384

Taylor & Francis
Taylor & Francis Group

RESEARCH ARTICLE

A study of the ionisation and excitation energies of core electrons using a unitary group adapted state universal approach

Sangita Sen[a], Avijit Shee[a,b] and Debashis Mukherjee[a,*]

[a]*Raman Centre for Atomic, Molecular and Optical Sciences, Indian Association for the Cultivation of Science, Kolkata, India;* [b]*Laboratoire de Chimie et Physique Quantique (UMR 5626), CNRS/Université de Toulouse, Toulouse, France*

(*Received 12 March 2013; final version received 29 April 2013*)

The unitary group adapted state universal multi-reference coupled cluster (UGA-SUMRCC) theory, recently developed by us using a normal-ordered multi-exponential wave operator Ansatz with spin-free excitations in the cluster operators, has the twin advantages of generating a spin-adapted coupled-cluster (CC) function and having a terminating expression of the so-called 'direct term' at the quartic power of cluster amplitudes. Not having any valence spectators, it also has the potentiality to describe orbital- and correlation-relaxation effectively. We illustrate this aspect by applying our formalism to study ionised/excited state energies involving core electrons. The high degree of orbital relaxation attendant on removal of a core electron and the consequent correlation relaxation of the ionised state are demonstrated to be captured very effectively with the Hartree–Fock orbitals for the neutral ground state.Three different formalisms have been used: (1) the ionisation potential/excitation energies (IP/EE) are computed as difference between state energies of the concerned states; (2) a quasi-Fock extension of the UGA-SUMRCC theory, which computes IP/EE directly and (3) use of a special model space to describe both the ground and the excited states such that EE is obtained directly. The model spaces for EE are incomplete and we have indicated the necessary modifications needed to have extensive energies. The results obtained by all the three approaches are very similar but they usually outperform the current CC-based allied theories with roughly the same computational effort.

Keywords: spin-free MRCC; normal ordering; core ionisation/excitation; unitary group; incomplete model space

1. Introduction

Theories for accurately modelling energy differences of spectroscopic interest involving ionised/excited states relative to a ground state continues to be a challenging task. When the ground state is predominantly a closed shell, there are various coupled-cluster-based methods, which address this problem in a compact manner. Such methods include the now widely accepted symmetry-adapted-cluster configuration interaction (SAC-CI) [1–3], the coupled-cluster-based linear response theories (CC-LRT) [4–7] and the coupled-cluster-based equation of motion method (CC-EOM/EOM-CC) [8–10] where the ground state energy is modelled using an exponential single reference (SR) coupled-cluster Ansatz and the excited state is modelled as a product of the wave operator for the ground state in exponential form and a linear ionisation/excitation operator acting on the ground state. Such a factorised Ansatz cleanly separates out the correlated ground state energy from the correlated energy of the ionised/excited states (to be henceforth generically called excited states), providing the desired energy difference. For low-lying excited states dominated by h–p excited determinants, such methods have been widely used with success. The most commonly used approximation for the excitation operator of the excited state is a singles and doubles truncation. For the ionised state, a similar approximation for the ionisation operators would be $1h$ and $2h$–$1p$ excitations for the cationic state and $1p$ and $1h$–$2p$ excitations for the anionic state. For higher accuracy, perturbative triples are also invoked both for the ground state operators and the ionisation/excitation operators and several schemes are described in the literature [11–14] using such extended schemes. Similar choice of excitation manifolds were also invoked in the analogous SAC-CI strategy [15]. When the orbital relaxation is high, as in the core excited or core ionised states, the use of Hartree–Fock (HF) orbitals of the ground state to model the ionised/excited states is beset by the linear structure of the excitation operator: a better strategy would have been to use an exponential representation of single excitations to take care of the orbital relaxation via Thouless parameterisation [16]. However, this warrants a full cluster expansion of the wave operator to model the excited state also. Nevertheless, in the spirit of the linear response, CC-EOM and SAC-CI, suitable extensions were suggested by the expansion of the excitation manifold to account for the relaxation effects with varying degrees of success [15,17–20]. For excited states with strong orbital relaxations relative to a ground sate, such a stratagem is somewhat

*Corresponding author. Email: pcdm@iacs.res.in

artificial and one should use multi-reference formalisms capable of treating relaxations via Thouless-like parameterisation, involving appropriate model spaces for computing ionisation/excitation energies. The multi-reference valence universal (VU) coupled-cluster theory (also called, the Fock space multi-reference coupled cluster (FS-MRCC) [21–24]) uses an exponential or a normal-ordered exponential of the wave operator for the correlated excited state. The normal-ordered wave operator in VUMRCC always has valence destruction operators and this precludes a full Thouless parameterisation. Thus, VUMRCC only partially takes care of the orbital relaxation inherent in the linearised structure for the CC-LRT or SAC-CI. The VUMRCC theory for energy differences has also been used for describing low-lying ionised and excited states where it was demonstrated that for the cationic and anionic states the working equations for the CC-LRT and FS-MRCC are equivalent [25], while for the excitation energies they are different. In fact, the CC-LRT provide energies, which are only core extensive [26], while the FS-MRCC gives fully extensive excited state energies [26]. Possibility of intruders in FS-MRCC can be obviated to a large extent by casting the FS-MRCC equations into a set of eigenvalue equations via what is known as an eigenvalue independent partitioning technique (EIP) [25,27–30] and a very similar strategy has also been invoked in the similarity transformed equation of motion CC (STEOM-CC) [31–33] with the proviso of an approximation. In the state universal MRCC (SUMRCC) setting [34,35], an idea of a factorised cluster Ansatz on top of a Jeziorski–Monkhorst (JM) representation of the excited state was also invoked for excitation energy using the *h–p* excited determinants as spanning the appropriate model space for excitation energy [36]. Unlike a valence-universal Ansatz employed in FS-MRCC, model-function-dependent cluster operators were used in this variant of SUMRCC using the JM Ansatz. Since the factorised Ansatz is designed for computing energy differences for a given mh–np valence sector with the (0,0) sector as the HF function of the ground state, the orbital relaxation and differential correlation effects accompanying successive addition/deletion of electrons are modelled by an inclusion of valence cluster operators all the way from (1,0), (0,1) and (1,1) up to the (*m*,*n*) sector in FS-MRCC. In contrast, in the factorised cluster Ansatz of this variant of SUMRCC, the intermediary cluster operators for the lower valence sectors are not included at all but are subsumed in the cluster operators for the mh–np target space. This is why this variant has been called quasi-Fock (QF) MRCC [36]. It should be noted that the model space containing *h–p* excited determinants is an incomplete space, and one requires special care about the normalisation of the valence part of the wave operator to maintain size extensivity of the excited state energies. Size extensive theories abandoning intermediate normalisation (IN) were developed both in the context of FS-MRCC [37–40] and the SUMRCC [36,41,42].

In recent years, state specific multi-reference coupled-cluster (SSMRCC) theories have been put forward to bypass the problem of intruders. Notable among them are SSM-RCC (also known as Mk-MRCC) [43–45], BW-MRCC [46,47] and MR expT [48,49]. There is also the closely related JM-inspired dressed MRCI formalism of Malrieu *et al.* [50,51]. A multi-reference extension of the EOM-CC [52–54] and a state-selective variant [55,56] were also formulated and applied. Methods of references [43–49,52–54] are designed for computation of state energies *per se* for a variety of states including a multi-reference ground state. Because of the use of the JM Ansatz in methods of references [43–49], the use of model-function-dependent cluster representation of the wave operator takes care of the orbital relaxation because of the complete exponentiation and this can serve as a good model for cases where the orbital relaxation is rather large. One difficulty of the JM Ansatz is that the cluster operator T_μ is represented as various mh–np excitations out of the model determinant ϕ_μ it acts on which necessitates the use of spin orbital representation of the cluster amplitudes. This generally leads to *spin broken solutions for non-singlet cases*. Very recently, spin-free formulations for both SS- and SU-MRCC have been proposed using normal ordered exponential Ansatz, inspired by the original JM parameterisation, in terms of spin-free unitary generators for the cluster operators T_μ and unitary group adapted (UGA) configuration state functions (CSFs) for the model functions ϕ_μ. Such theories have been termed UGA-SSMRCC [57] and UGA-SUMRCC [58]. Preliminary applications have indicated the potentiality of the methods. In particular, energy differences with respect to a closed shell ground state are found to be superior to those from EOM-CC and allied methods in the same truncation scheme. This Ansatz provides full exponential parameterisation for all the inactive excitations, thereby providing an opportunity to induce major orbital relaxation and correlation relaxation subsumed in the differential correlation. Due to the normal ordering, excitation involving the active orbitals terminates after a finite power although it has been numerically found that such incomplete exponentiation has only a modest effect on the accuracy because of appearance of certain compensating 'exclusion principle violating' (EPV) contributions from the so-called coupling terms [57]. Another spin-free coupled-cluster Ansatz for treating orbital- and correlation-relaxation effects has been suggested from our group, which mimics the physics embedded in the spin-orbital-based JM Ansatz to the closest extent. The Ansatz, called the combinatoric open-shell CC (COS-CC) [59,60], uses a modified polynomial where each nth power of the cluster operator connected by valence lines is accompanied by the inverse of the automorphic factor, rather than the customary $\frac{1}{n!}$ as in the exponential representation. The COS-CC has been proposed and applied to study both valence ionisation and core ionisation in VU, SU and SS variants and in each case the performance of the method has been found

to be highly satisfactory. The Mk-MRCC in the spin orbital based form has also been used recently to study core excitation where the ground and the excited state energies were separately calculated using the Mk-MRCC Ansatz with different active spaces chosen for the ground and core-excited states [61]. The model spaces for all three approaches using $1h$–$1p$ CSFs are incomplete, and ensuring extensivity of the excited state energies requires careful analyses.

In this paper, we shall develop and explore a spin-adapted MRCC for computation of energy differences like core excitation and core ionisation energies where the full orbital relaxation and correlation relaxation are going to be vitally important. In our applications, we will always consider molecular states whose corresponding ground state is predominantly SR in character, while a quasi-Fock like strategy will be employed (vide infra) to compute ionisation and excitation energies directly. We will employ the apparatus of UGA-MRCC theories for incomplete active spaces to study excitation energies. Three distinct strategies will be explored: (1) the excited state energies are computed directly and the ground state energy is subtracted explicitly to compute the energy difference, (2) the energy differences are computed directly by invoking a QFMRCC with a model space of h–p excited CSFs and (3) the energy differences are computed directly by invoking a special incomplete active space (isolated incomplete model space (IMS)), which in our case is a union of both the HF function of the ground state and the h–p excited states in the model space.

The paper is organised as follows: In Section 2 we discuss the theoretical underpinnings of the methods to be used by us, their inter-relations and necessary modifications for their generalisation to encompass incomplete active spaces. Section 3 deals with the issue of size extensivity. Section 4 discusses the extent of orbital- and correlation-relaxation incorporated in the theories used by us vis-a-vis the current coupled-cluster-based theories used to compute core ionisation and core excitation energies. Section 5 presents the molecular applications. Section 6 includes the summarising remarks and our future outlook.

2. Theoretical developments

We proceed by providing a brief background of the unitary group adapted CC methods for simple open shell and multi-reference cases. Automatic implementation of the UGA-exponential parameterisation for simple open shell cases were suggested by Jansen and Schaefer [62]. Because of the non-commutativity of the cluster operators, the Baker–Hausdorff expansion of the similarity transformed Hamiltonian does not terminate at quartic power and up to octic commutator expansion is required to reach natural termination. A more comprehensive approach was proposed by Li and Paldus and others [63–66] who formulated not only the open shell CC theory using exponential parameterisation for the single CSF reference, but also sketched a general adaptation for a multi-reference case in the SUMRCC framework [64]. Again, due to the non-commutativity of the cluster operators, there was no termination of the Baker–Hausdorff expansion at the quartic commutator. For simple open shell cases, Szalay and Gauss [67,68] proposed both spin-restricted and spin-adapted spin-orbital-based CC theory. The spin adaptation generated a plethora of complicated terms. What will obviously be more satisfactory is to use a cluster Ansatz of the JM type but which does not use pure exponential parameterisation to avoid non-termination of most of the terms at quartic powers. One such formulation, termed as the COS-MRCC has been developed by Datta and Mukherjee, both for SU [59]and for SS [60] versions. It allows specific contractions via spectator valence lines between the various cluster operators and the various composites so obtained are given weights, which are inverses of the corresponding automorphic factors, unlike that in an exponential Ansatz. A simpler formulation is possible if one invokes an Ansatz $\Omega_\mu = \{\exp T_\mu\}$ where T_μs are written in terms of unitary generators which will act on the CSFs, ϕ_μ and the normal ordering is with respect to a closed-shell core state common to all the ϕ_μs. As we shall discuss in Section 2.1, this Ansatz leads to exact termination of the so-called 'direct term' at the quartic power of the cluster operators and termination at a finite power for the 'coupling term' (depending on the number of active electrons) for both the SS and SU theories.

The UGA-SSMRCC [57] approach using the normal-ordered Ansatz was used for computing energies of multi-reference states, potential energy surfaces and singlet–triplet splittings. Just like in a spin-orbital-based SSMRCC, UGA-SSMRCC requires the use of sufficiency conditions, which leads to the inclusion of redundant excitation operators in the cluster manifold. A related theory where the inactive double excitations were treated in an internally contracted manner (Internally Contracted for Inactive Doubles, ICID) called UGA–ICID–SSMRCC [69] was also developed, which greatly reduces the computational cost and incorporates more coupling in the excited function space. The UGA-SUMRCC [58] has been used for computing ionised and excited state energies. A QF variant of the UGA-SUMRCC, UGA-QFMRCC [70], has been developed very recently and has been used to compute excitation energies relative to a closed-shell ground state.

A summary of the UGA-SUMRCC and UGA-QFMRCC will be presented in Sections 2.1 and 2.2 to give the readers the relevant background of the methodologies adopted by us for core ionisation and core excitation energies. Modifications necessary for application of these theories in the context of IMS, as in the case of excitation energies, are discussed in Section 2.3. The aspects of size extensivity of these theories and the relation to the normalisation of wave operator is quite involved and has been presented in Section 3.

2.1. *Summary of UGA-SUMRCC for complete active spaces (CAS)*

The Ansatz, for $\Omega = \sum_\mu \Omega_\mu |\phi_\mu\rangle\langle\phi_\mu|$ in UGA-SUMRCC is a normal-ordered exponential of spin-free cluster operators, which are generators of a unitary group and hence implicitly maintain the spin of any starting wave function they act upon. A normal ordering with respect to a core function common to all the model functions, $\{\phi_\mu\}$, is invoked to ensure the commutativity of the cluster operators, T_μ among themselves as well as between model functions (say, ϕ_μ and ϕ_ν),

$$\Omega_\mu = \{\exp(T_\mu)\}. \tag{1}$$

In our scheme, the model functions $\{\phi_\mu\}$ are unitary group adapted CSFs in the direct product space of the unitary groups of n_c core orbitals and n_v active (equivalently valence) orbitals, $U(n_c) \bigotimes U(n_v)$. Specifically, our ϕ_μs are taken to be Gel'fand–Tsetlin states [66]. Each ϕ_μ is defined by the occupancies of each active orbital (to be denoted by a string of n_v active orbitals) and the component k of the M^{th} irreducible representation of $U(n_v)$ to which ϕ_μ belongs. Thus, every ϕ_μ has descriptors k and $\Gamma_M^{n_v}$: $\phi_\mu(k, \Gamma_M^{n_v})$. Each ϕ_μ is generated from the core function $|0\rangle$ by a Gel'fand adapted creator Y_k^M,

$$\phi_\mu \equiv \phi_\mu\left(k, \Gamma_M^{n_v}\right) = Y_k^M|0\rangle. \tag{2}$$

However, the excited CSFs in our scheme are not Gel'fand adapted. They span a space identical to the Gel'fand adapted CSF space of excited functions reachable by the excitation operators considered in our Ansatz but do not bear a one-to-one correspondence. Moreover, we must distinguish an excited space of functions reachable by upto two-body operators and that reached by single and double orbital substitution. We work in the former space but our operators are such that the excited space functions of the former is a self-complete subset of the latter such that the sub-space is exactly equivalent to a set of spin-adapted functions,

$$\left|\chi_\mu^l\right\rangle = \left\{\epsilon_\mu^l\right\}|\phi_\mu\rangle, \tag{3}$$

where the excitation unitary group generator $\{\epsilon_\mu^l\}$ is in normal order with respect to $|0\rangle$ and forms a linearly independent (LIN) set. The selection of a LIN manifold is not unique and our choice of combinations of unitary group generators for LIN excitations for open shells of specific spin multiplicity are tabulated in Table 1. The effect of choice of LIN combinations of cluster operators on stability of solution and accuracy of results has been carefully analysed by Szabados *et al.* [71] in the perturbative version of the SSMRCC, i.e. state specific multi-reference perturbation theory (SSMRPT) [72–74].The final working equations involve matrix elements between ϕ_μs wherein reduced density matrices (RDM) appear, which incorporate the spin information of the target state.

Table 1. Choices of Ts for $1h$–$1p$ states in UGA-SUMRCC and UGA-QFMRCC.

Singlet excitation	Combination for singlet states	Triplet excitation	Combination for triplet state
T_i^I	$t_i^I\{E_i^I\}$	T_i^I	$t_i^I\{E_i^I\}$
T_i^A	$t_i^A\{E_i^A\}$	T_i^A	$t_i^A\{E_i^A\}$
T_I^a	$t_I^a\{E_I^a\}$	T_I^a	$t_I^a\{E_I^a\}$
T_A^a	$t_A^a\{E_A^a\}$	T_A^a	$t_A^a\{E_A^a\}$
$^1T_i^a$	$^1t_i^a\{E_i^a\}$	T_i^a	$t_i^a\{E_i^a\}$
$^2T_i^a$	$^2t_i^a[\{E_{iA}^{Aa}\} - \{E_{iI}^{Ia}\}]$	T_{iI}^{Ia}	$t_{iI}^{Ia}\{E_{iI}^{Ia}\}$
		T_{iA}^{Aa}	$t_{iA}^{Aa}\{E_{iA}^{Aa}\}$
T_I^A	$t_I^A\{E_I^A\}$		
T_A^I	$t_A^I\{E_A^I\}$		
$T_{ij}^{\bullet\bullet}$	$t_{ij}^{\bullet\bullet}[\{E_{ij}^{IA}\} + \{E_{ij}^{AI}\}]$	$T_{ij}^{\bullet\bullet}$	$t_{ij}^{\bullet\bullet}[\{E_{ij}^{IA}\} - \{E_{ij}^{AI}\}]$
$T_{\bullet\bullet}^{ab}$	$t_{\bullet\bullet}^{ab}[\{E_{IA}^{ab}\} + \{E_{AI}^{ab}\}]$	$T_{\bullet\bullet}^{ab}$	$t_{\bullet\bullet}^{ab}[\{E_{IA}^{ab}\} - \{E_{AI}^{ab}\}]$
$\tilde{T}_i^a$	$^1\tilde{t}_i^a[\{E_{iI}^{aA}\} - 0.5\{E_{iI}^{Aa}\}]$	T_{iI}^{Aa}	$t_{iI}^{Aa}\{E_{iI}^{Aa}\}$
	$^2\tilde{t}_i^a[\{E_{iA}^{aI}\} - 0.5\{E_{iA}^{Ia}\}]$	T_{iA}^{Ia}	$t_{iA}^{Ia}\{E_{iA}^{Ia}\}$
T_{ij}^{aI}	$t_{ij}^{aI}\{E_{ij}^{aI}\}$	T_{ij}^{aI}	$t_{ij}^{aI}\{E_{ij}^{aI}\}$
T_{ij}^{aA}	$t_{ij}^{aA}\{E_{ij}^{aA}\}$	T_{ij}^{aA}	$t_{ij}^{aA}\{E_{ij}^{aA}\}$
T_{iI}^{ab}	$t_{iI}^{ab}\{E_{iI}^{ab}\}$	T_{iI}^{ab}	$t_{iI}^{ab}\{E_{iI}^{ab}\}$
T_{iA}^{ab}	$t_{iA}^{ab}\{E_{iA}^{ab}\}$	T_{iA}^{ab}	$t_{iA}^{ab}\{E_{iA}^{ab}\}$
T_{ij}^{ab}	$t_{ij}^{ab}\{E_{ij}^{ab}\}$	T_{ij}^{ab}	$t_{ij}^{ab}\{E_{ij}^{ab}\}$

Note: i, j, ..., etc. denote inactive hole orbitals.
a, b, ..., etc. denote inactive particle orbitals.
I, A denote active hole and active particle orbital respectively.
The amplitude, 't', and the unitary generators, 'E', together constitute the cluster operators, 'T'. Where a common amplitude is associated with a combination of two or more operators differing in their active orbital indices, the active orbital indices of the amplitude have been suppressed and replaced with a symbol, $\bullet$, $\tilde{}$ etc. For excitations of the same rank (in terms of changes in occupancy of inactive orbitals), the different classes of excitation amplitudes (differing in changes of occupancy of active orbitals) are denoted by ^{1}T, ^{2}T, etc.

Using our proposed Ansatz, $\Omega_\mu = \{\exp(T_\mu)\}$ in the Bloch equation we arrive at Equation (4). For detailed derivations, we refer to our earlier papers [58,70],

$$G_\mu|\phi_\mu\rangle \equiv \{\overline{H}_\mu\}|\phi_\mu\rangle - \sum_\nu \{\exp -(T_\mu)\exp(T_\nu) \times \exp\overbrace{(T_\nu)W_{\nu\mu}}\}|\phi_\mu\rangle = 0, \tag{4}$$

where

$$\{\overline{H}_\mu\} = \{\overbrace{H\exp(T_\mu)}\} \tag{5}$$

and

$$W_{\nu\mu}|\phi_\mu\rangle = |\phi_\nu\rangle\langle\phi_\nu|H_{eff}|\phi_\mu\rangle. \tag{6}$$

$W_{\nu\mu}$ is an operator labelled by all active orbitals distinguishing ϕ_μ and ϕ_ν. However, the rank of $W_{\nu\mu}$ may be higher than the number of orbitals by which ϕ_μ and ϕ_ν differ as it may also contain components with spectator scatterings involving creation and destruction of common active orbitals of ϕ_μ and ϕ_ν. The spectators need not all be diagonal, it is

only essential for the labels of the spectators to be one of the common orbitals of ϕ_μ and ϕ_ν. The expression for $W_{\nu\mu}$, or equivalently for $H_{\rm eff}$ requires that we specify the 'closed' components of Ω. For a CAS, the customary and the simplest choice is to use intermediate normalisation (IN) for Ω: $\langle\phi_\lambda|\Omega|\phi_\mu\rangle = \delta_{\lambda\mu}$.With this proviso, it is straightforward to show from the vanishing value of the closed components of the Bloch equation, $[G_\mu]_{\rm cl}$, coming from G_μ, acting on $|\phi_\mu\rangle$,

$$[G_\mu]_{\rm cl}|\phi_\mu\rangle = \{\overline{H}_\mu\}_{\rm cl}|\phi_\mu\rangle - \sum_\nu \{\exp -(T_\mu)\exp(T_\nu) \times \exp(\overbrace{T_\nu)W_{\nu\mu}}\}_{\rm cl}|\phi_\mu\rangle = 0, \quad (7)$$

that if we project Equation (7) with ϕ_ν,

$$[H_{\rm eff}]_{\nu\mu} = \langle\phi_\nu|\{\overline{H}_\mu\}_{\rm cl}|\phi_\mu\rangle. \quad (8)$$

The equations for determining the cluster amplitudes of T_μ are obtained by equating the excitation components of Equation (4) on both sides denoted by $[G_\mu]_{\rm ex}$.

$$[G_\mu]_{\rm ex}|\phi_\mu\rangle \equiv \{\overline{H}_\mu\}_{\rm ex}|\phi_\mu\rangle - \sum_\nu \{\exp -(T_\mu)\exp(T_\nu) \times \exp(\overbrace{T_\nu)W_{\nu\mu}}\}_{\rm ex}|\phi_\mu\rangle = 0. \quad (9)$$

Projecting with the virtual functions, χ^l_μ, reached by the various components of T_μ, we have

$$\langle\chi^l_\mu|\{\overline{H}_\mu\}_{\rm ex}|\phi_\mu\rangle - \langle\chi^l_\mu|\sum_\nu \{\exp(-T_\mu)\exp(T_\nu) \times \exp(\overbrace{T_\nu)W_{\nu\mu}}\}_{\rm ex}|\phi_\mu\rangle = 0. \quad (10)$$

As emphasised in Section 1, the normal ordering of our Ansatz, ensures the termination of the first term, called the 'direct term' at quartic power in all situations while the truncation of the second, so-called, 'coupling term', will be controlled by the rank of the valence sector under consideration.

The detailed content of our working equations and consequently the size extensivity becomes clearer if we express our working equation in terms of specific excitation components of G_μ, say $[G_\mu]^{(n)}_{\rm ex}$. $[G_\mu]^{(n)}_{\rm ex}$ is defined as the n-body composite containing both direct and coupling terms exciting from ϕ_μ to virtual functions. The working equations can thus be alternatively written as

$$\langle\chi^l_\mu|[G_\mu]_{ex}|\phi_\mu\rangle \equiv \langle\chi^l_\mu|\sum_n [G_\mu]^{(n)}_{ex}|\phi_\mu\rangle = 0. \quad (11)$$

Writing $|\chi^l_\mu\rangle = \{\varepsilon^l_\mu\}|\phi_\mu\rangle$, with suitable excitation operators,$\{\varepsilon^l_\mu\}$, Equation (11) can be written as sums of products of the amplitudes of various $[G_\mu]^{(n)}_{\rm ex}$, $[g_\mu]^{(n)}_{\rm ex}$, and active RDM, Γ of various ranks.

The combining coefficients, $c_{\mu k}$, for the state, k, is obtained by solving the eigenvalue equation involving $H_{\rm eff}$. This is obtained from the closed projection of $G_\mu|\phi_\mu\rangle$, $[G_\mu]_{cl}|\phi_\mu\rangle$ and using the IN for Ω,

$$\sum_\nu [\overline{H}_{\rm eff}]_{\mu\nu}c_{\nu k} \equiv \sum_\nu \langle\phi_\mu|W_{\mu\nu}|\phi_\nu\rangle c_{\nu k} = E_k c_{\mu k}. \quad (12)$$

Clearly, $H_{\rm eff}$ is a 'closed' operator by construction involving unitary generators with active orbitals only.

The $1h$ and $1p$ valence sectors are by construction complete and ionisation energies and electron affinities have been computed using the above strategy in an earlier paper [58]. As it turns out, for obtaining excited state energies or excitation energies, the corresponding active spaces are usually dominated by h–p excited CSFs from the HF function, ϕ_0. Such functions span an *incomplete model space*, even when all the hole and all the particle orbitals are included in the h–p model space. It has been known for quite some time that the naive use of IN for Ω involving incomplete active space entails size inextensivity of the computed energies. However, by defining appropriate excitation operators in the wave operator and abandoning IN, a size extensive formulation can be obtained [75–78]. Size extensive formulations for general incomplete spaces for both VU- [37–40,79–80] and SU-MRCC [36,41,42] theories have been suggested where definition of $H_{\rm eff}$ gets non-trivially modified because of the lack of IN. One may thus imagine that the equations for UGA-SUMRCC and the expression for $H_{\rm eff}$ will have to be appropriately modified for obtaining excited state energies and excitation energies. The major modification would be in the definition of $H_{\rm eff}$, which should be obtained, just as for the CAS, from the closed projection, $[G_\mu]_{\rm cl}|\phi_\mu\rangle$, but without using IN. The definition of a 'closed' operator also needs to be modified when an IMS is used [36–42,79–80]. We would discuss the pertinent issues for IMS in Section 2.3 wherein we will show how one may design an algorithm such that very little programmatic modification would be necessary to convert an implementation of a CAS theory to the corresponding IMS theory within the realm of Bloch equation based theories. We discuss the essentials of these observations and the necessary modifications thereof in Section 2.3.

2.2. *Summary of UGA-QFMRCC*

The UGA-SUMRCC is a theory for computation of state energies where the T_μs are parameters for describing the target state, be it the ground, ionised or excited state. It is possible to envisage an Ansatz which parameterises the wave function in such a manner that solution of the energy equation yields energy differences directly, vis. ionisation energies

and excitation energies. Assuming that the ground state is well described by a SR theory namely SR coupled-cluster theory, $\exp(T)$ is sufficient to parameterise the ground state wave function. Excited states are treated by a state universal Ansatz, $\{\exp(S_\mu)\}$, where the S_μ amplitudes are differential correlation amplitudes, which parameterise the correlation of the target state over and above that of the ground state parameterised by $\exp(T)$. Thus our choice of Ansatz for UGA-QFMRCC should be of the form

$$\Omega_\mu = \exp(T)\{\exp(S_\mu)\}. \tag{13}$$

We must distinguish carefully between the commonly used T_μ and S_μ in the context of theories based on the use of the JM Ansatz where the wave operator is dependent on the model function it acts on, i.e. Ω_μ acting on ϕ_μ. The actual correlation of the target state contributed by the excitations from ϕ_μ to χ_μ^l is quantified by the amplitudes of T_μ as in the parent UGA-SUMRCC theory. The S_μs, on the other hand, represent the *change* in correlation and relaxation incident on ionisation or excitation, i.e. the difference in the correlation contribution of T_μ of the target state and the subduced valence sector. Thus, UGA-QFMRCC is a two-state computation yielding directly the energy difference between the two. We once again emphasise here that UGA-QFMRCC is different from VUMRCC [21–24] in that sequential computation of all valence sectors from closed shell, (0,0), upwards is not necessary.

The coupled-cluster equation for the SR ground state is first solved to obtain the T amplitudes, which are used to transform the Hamiltonian as in Equation (14).

Having solved for T, a dressed Hamiltonian is defined as

$$\widetilde{H} = \exp(-T)H\exp(T). \tag{14}$$

$\widetilde{H}$ and H_{eff} are now partitioned to separate out the ground state energy,

$$\widetilde{H} = E_{\text{gr}} + \overline{H}, \tag{15}$$

$$H_{\text{eff}} = E_{\text{gr}} + \overline{H}_{\text{eff}}, \tag{16}$$

$$[\overline{H}_{eff}]_{v\mu} = \langle\phi_v|\overline{W}_{v\mu}|\phi_\mu\rangle. \tag{17}$$

$\overline{W}_{v\mu}$ may be considered as the operator whose matrix element with respect to $\langle\phi_v|$ and $|\phi_\mu\rangle$ corresponds to $[\overline{H}_{\text{eff}}]_{v\mu}$.

The corresponding Bloch equation yielding energy differences for the μth model function ϕ_μ, on using the definitions, Equations (15)–(17), takes the form,

$$\bar{G}_\mu|\phi_\mu\rangle = \{\overline{\overbrace{H\exp(S_\mu)}}\}|\phi_\mu\rangle - \sum_v\{\exp(S_v)\exp(-S_\mu) \times \overbrace{\exp(S_v)\overline{W}_{v\mu}}\}|\phi_v\rangle = 0, \tag{18}$$

$$\langle\chi_l\{\overline{\overline{H}}\}|\phi_\mu\rangle - \sum_v\langle\chi_l|\{\exp(S_v)\exp(-S_\mu) \times \overbrace{\exp(S_v)\overline{W}_{v\mu}}\}|\phi_v\rangle = 0. \tag{19}$$

Equation (18) is the QF analogue of the parent Bloch equation, Equation (4). Equations for the S_μ are obtained by taking the excitation part of $\bar{G}_\mu$, $[\bar{G}_\mu]_{\text{ex}}$ and projecting the Bloch equation, Equation (18) above, on to the virtual functions $\langle\chi_\mu^l|$.

After solving for the amplitudes of $\{S_\mu\}$, we evaluate the energy difference of interest, ΔE_k and the associated coefficients, $\{c_{\mu k}\}$ from the following eigenvalue equation:

$$\sum_v[\overline{H}_{\text{eff}}]_{v\mu}c_{vk} \equiv \sum_\mu\langle\phi_v|\overline{W}_{v\mu}|\phi_\mu\rangle c_{\mu k} = \Delta E_k c_{vk}, \tag{20}$$

obtained from the projection of the closed part of $\bar{G}_\mu$, $[\bar{G}_\mu]_{cl}|\phi_\mu\rangle$ on to the various model CSFs. The expression for $[\overline{H}_{\text{eff}}]_{v\mu}$ is simply $\langle\phi_v|\{\overline{\overline{S}}_\mu\}_{cl}|\phi_\mu\rangle$ for a CAS, while it will have to be appropriately modified for an IMS.

2.3. *Necessary modifications for the use of incomplete model space in the theories for excited state energies and energy differences*

A physically motivated choice of the model space for the case of excited states is a set of h–p excited CSFs, ϕ_μ, for a selection of hole and particle orbitals taken as active. The active spaces for such choices are called quasi-complete model spaces. As Mukherjee has shown [75–77], the simplest way to achieve size extensivity for an incomplete model space is to abandon IN for the wave operator. The essential difficulty of maintaining size extensivity in an incomplete model space is that it is not enough to have an H_{eff} which is connected, since the eigenvalues obtained on diagonalisation would lead to disconnected terms and hence size inextensive energies. The situation is entirely analogous to the diagonalisation of a CI matrix in an IMS where each element of the CI matrix is connected due to the connectedness of H but diagonalisation leads to size inextensive energies. Mukherjee analysed this issue and concluded that the operator H_{eff} to be diagonalised in the IMS should not only be connected, but should also be *closed* in a very special sense. For an IMS, a closed operator should be chosen as one which by construction can never lead to excitation outside the IMS by its action on any ϕ_μ. We cannot go into the details here, but refer to a paper by Mukherjee *et al.* [78] where the reason behind such a definition to ensure extensivity of the roots of H_{eff} is analytically demonstrated.

In the most general situation, it is conceivable that an operator labelled by active lines only can lead to a transition from a ϕ_μ to a ϕ_ν but it would not be closed *if there is at least one function* ϕ_λ for which the same operator leads to excitation outside the IMS. They are called *quasi-open* operators [39] and since all operators of H_{eff} are labelled by active lines only, one should impose the constraint that the quasi-open components of H_{eff} are zero by construction: this is achieved via the inclusion of quasi-open operators in the set $T_\mu \forall \phi_\mu$ and this ensures that the matrix of H_{eff} in the IMS would generally have zero entries connecting the pair (μ, ν) if the corresponding excitation is a quasi-open operator. It is to be emphasised here that once an operator is identified as quasi-open, it should be included in a T_μ for every ϕ_μ even if its action on that ϕ_μ would lead to another model function ϕ_ν. Of course, one should delete those quasi-open operators in T_μ whose action on ϕ_μ is trivially zero because of Pauli principle.

For the special case of *h–p* model spaces, the quasi-open and the closed operators are clearly of different types: any quasi-open operator must involve changes in occupancies of holes and particles and hence, transfer of electrons between active holes and active particles, while the closed operators would scatter a *h–p* function to another *h–p* function of the *h–p* model space. These have been termed as 'quasi-complete' by Lindgren [81]. For theories involving the *h–p* IMS having the same symmetry as that of the ground state, a *h–p* de-excitation operator acting on a ϕ_μ would lead to the HF function, ϕ_0 which is outside the model space, thus these operators are quasi-open. Also, the *h–p* excitation operators lead from the model space to 2*h*–2*p* virtual functions and these could be quasi-open. Thus, in the $\{\exp T_\mu\}$, there could be a quadratic power ($\{\frac{1}{2}T_\mu^2\}$) where there could be a closed component of the quadratic term arising from the situation where one of the components of T_μ is a de-excitation and the other is an excitation. The simplest choice of achieving a connectedness of $\{T_\mu\}$ and H_{eff} is *not* to impose the IN: but allow the closed part of normal-ordered exponential $\{T_\mu\}$ to have the value it should have if Bloch equations are solved without imposing IN. We should mention that a very comprehensive book-keeping procedure for classifying the various Fock-space operators where this concept of quasi-open [39] and closed are defined by alternative symbols was suggested by Kutzelnigg *et al.*, which provides additional insight into the aspects of connectivity by classifying operators in the Fock space [79,80]. A connected formulation of H_{eff} was achieved first in the FS-MRCC [37–40], while the corresponding SUMRCC formulation for IMS was proposed a few years later [36,41,42],

$$T_\mu = [T_\mu]_{\text{op}} + [T_\mu]_{q-\text{op.}} \tag{21}$$

Since the IN is not satisfied because the powers of quasi-open operators might be closed, we have the relation: $\{\exp T_\mu\}_{\text{cl}} = \{\exp[T_\mu]_{q-\text{op}}\}_{\text{cl}}$. For the quasi-open components of T_μ, we have to project Equation (4) onto those functions, which are reachable by the action of quasi-open operators acting on ϕ_μ. They may, depending on the type of excitation and the ϕ_μ, either belong to the IMS itself or may belong to the 'complementary active space'. The union of the model space and the complementary active space is a complete active space. Defining all such functions reachable by the action of quasi-open operators on ϕ_μ as $\{\bar{\phi}_\mu^\lambda\}$ we would have the corresponding equations for determining the quasi-open operators of T_μ by projecting on to $\langle\bar{\phi}_\mu^\lambda|$. The corresponding residuals for the open and quasi-open *T*-operators would thus be defined as

$$\begin{aligned} R_{l\mu} &= \langle \chi_\mu^l | [G_\mu]_{op} | \phi_\mu \rangle \equiv \langle \chi_\mu^l | \{\overline{H}_\mu\}_{op} | \phi_\mu \rangle \\ &\quad - \langle \chi_\mu^l | \sum_\nu \{\exp(-T_\mu)\exp(T_\nu)\exp(\overbrace{T_\nu) W_{\nu\mu}}\}_{op} | \phi_\mu \rangle, \end{aligned} \tag{22}$$

$$\begin{aligned} R_{\bar{\lambda}\mu} &= \langle \bar{\phi}_\mu^\lambda | [G_\mu]_{q-op} | \phi_\mu \rangle \equiv \langle \bar{\phi}_\mu^\lambda | \{\overline{H}_\mu\}_{q-op} | \phi_\mu \rangle \\ &\quad - \langle \bar{\phi}_\mu^\lambda | \sum_\nu \{\exp(-T_\mu)\exp(T_\nu)\exp(\overbrace{T_\nu) W_{\nu\mu}}\}_{q-op} | \phi_\mu \rangle. \end{aligned} \tag{23}$$

Equations (22) and (23) are used to determine $[T_\mu]_{\text{op}}$ and $[T_\mu]_{q-\text{op}}$, respectively, by the usual updating procedure for the open and the quasi-open amplitudes of T_μ. However, they require the knowledge of $W_{\nu\mu}$. This must be obtained from the equation for H_{eff}. We note that the closed component of the residual may be analogously defined as

$$\begin{aligned} R_{\lambda\mu} &= \langle \phi_\lambda | [G_\mu]_{\text{cl}} | \phi_\mu \rangle = \langle \phi_\lambda | \{\overline{H}_\mu\}_{\text{cl}} | \phi_\mu \rangle \\ &\quad - \langle \phi_\lambda | \sum_\nu \{\exp(-T_\mu)\exp(T_\nu)\exp(\overbrace{T_\nu) W_{\nu\mu}}\}_{\text{cl}} | \phi_\mu \rangle, \end{aligned} \tag{24}$$

which should be equated to zero to get H_{eff}. This is where the theories for IMS differ from those for CAS. For defining the $W_{\nu\mu}$, we now have to make explicit use of the fact that there is a closed component of $\{\exp T_\mu\}$: $\{\exp T_\mu\}_{\text{cl}}$. From the vanishing values of the closed projection of the residual, $R_{\lambda\mu}$ via Equation (24), we can have a recursive definition for W^{i+1} with $W_{\nu\mu}^{i+1}$ (i+1)th iteration. We may initiate the iteration with $W_{\lambda\mu}^0$,

$$W_{\lambda\mu}^0 |\phi_\mu\rangle = |\phi_\lambda\rangle\langle\phi_\lambda|\{\overline{H}_\mu\}_{\text{cl}}|\phi_\mu\rangle. \tag{25}$$

We then have

$$\begin{aligned} W_{\lambda\mu}^{i+1}|\phi_\mu\rangle &= |\phi_\lambda\rangle\langle\phi_\lambda|\{\overline{H}_\mu\}_{\text{cl}}|\phi_\mu\rangle - \sum_\nu |\phi_\lambda\rangle \\ &\quad \times \langle\phi_\lambda|\{[\exp -(T_\mu)\exp(T_\nu) - 1]\exp(\overbrace{T_\nu) W_{\nu\mu}^i}\}_{\text{cl}}|\phi_\mu\rangle \\ &\quad - \sum_\nu |\phi_\lambda\rangle\langle\phi_\lambda|\{\exp -(T_\mu)\exp(T_\nu) \\ &\quad \times [\exp(\overbrace{T_\nu) - 1] W_{\nu\mu}^i}\}_{\text{cl}}|\phi_\mu\rangle, \end{aligned} \tag{26}$$

$$W^{i+1}_{\lambda\mu}|\phi_\mu\rangle = \{G_\mu\}^{i+1}_{\lambda\mu}|\phi_\mu\rangle - W^{i}_{\lambda\mu}|\phi_\mu\rangle. \quad (27)$$

Thus, in principle, we solve for H_{eff} without assuming IN but the structure of our residuals is such as to allow us to use the same programmatic machinery that we had used for a CAS with IN. For situations where IN holds good there is no need to update W recursively using Equation (26) but we have instead $W_{\lambda\mu}|\phi_\mu\rangle = |\phi_\lambda\rangle\langle\phi_\lambda|\{\bar{H}_\mu\}|\phi_\mu\rangle$. Of course, we need to update $\{\bar{H}_\mu\}$ after the updating of T_μs. By the same arguments as is adduced to prove the connectivity of Equation (10) one can infer the connectivities of Equations (22) and (23) as elaborated in Section 3. When IN is abandoned, implicit iteration of $W_{\nu\mu}$ along with the iteration for T-amplitudes leads to convergence of $W_{\nu\mu}$ and hence, equivalently H_{eff}.

Sinha *et al.* [25] have shown quite some time ago that, in the context of VUMRCC theory for IMS, if only the computation of excitation energy is our target then it is possible, operationally speaking, to ignore the de-excitation quasi-open operators in $\{T_\mu\}$ since the equations for such de-excitation amplitudes are completely decoupled from those of the excitation amplitudes in the sense that in the equations for excitation amplitudes there are no terms containing the de-excitation cluster operators. In effect, this implies that H_{eff} for the h–p IMS does not involve the de-excitation operators at all and we may simply diagonalise H_{eff} in this model space to get excitation energies/excited state energies, depending on the formulation, without the knowledge of the de-excitation cluster amplitudes. Applications of the VUMRCC in this setting have been studied by others as well [82–84]. However, the analysis of Sinha *et al.* is not valid for the SUMRCC for the h–p IMS. Thus, we have proceeded by abandoning IN, though we have shown that the structure of our equations is such as to implicitly handle the normalisation of the wave operator in a way operationally not different from our treatment of the UGA-SUMRCC equations for CAS [70].

For computing excitation energies, we can think of two more strategies. Instead of using the Ansatz, $\Omega_\mu = \{\exp T_\mu\}$ we can introduce a factorised cluster Ansatz $\Omega_\mu = \exp T\{\exp S_\mu\}$ where T contains the ground state cluster operator and $S_\mu s$ are the valence cluster operators bringing in orbital relaxation and differential correlation accompanying excitation. Clearly, for studying core excited states, this formulation neatly factors out the correlated ground state energy and focuses entirely on the orbital relaxation, correlation relaxation and differential correlation effects induced via S_μ. We have very recently formulated such a theory for direct computation of excitation energies and have called it the unitary group adapted QF-MRCC (UGA-QFMRCC) [70]. The QF-MRCC formulation leads to working equations for S_μ which are strikingly similar to those of T_μ except that a 'ground state dressed' effective operator $\tilde{H} = \exp(-T)H\exp(T)$ plays the role of the Hamiltonian for excitation energies. Pilot calculations using QF-MRCC indicates the potentiality of the method for computing excitation energies (EE) [70]. We shall make use of this formalism too for core excitation energy in this paper.

In another formalism, we choose our incomplete model space as comprising of the HF function, ϕ_0 and a set of h–p excited functions ϕ_μ. Such kind of model spaces were first introduced and studied by Kutzelnigg *et al.* [79,80] who termed them as 'isolated incomplete model spaces' (IIMS). The IIMS has the interesting property that all quasi-open operators are of excitation type. The de-excitation operators for the h–p model space inducing transitions to the HF ground state function, ϕ_0, in either UGA-SUMRCC or UGA-QFMRCC, do not appear in $\{T_\mu\}$ since this now becomes a closed rather than quasi-open operator. Thus, for such IIMS, powers of T_μ inducing closed operator excitation do not then appear at all and the customary IN holds good. In this paper, we shall study all the three methods, vis. UGA-SUMRCC, UGA-QFMRCC and UGA-IIMS-SUMRCC in the context of core excitation energies.

3. Size extensivity

For complete model spaces, h–p quasi-complete model spaces and IIMS the IN of the wave operator may be retained and connectivity of the working equations must be demonstrated to establish size extensivity of our proposed theories. The size extensivity of both UGA-SUMRCC and UGA-QFMRCC may be analysed in similar fashion at two levels: the connectivity of the G-blocks defined in Equations (9) and (19) and the connectivity of the working equations in Equation (11).

The detailed proof of extensivity is delineated in our previous paper [70]. However, we mention the salient features here for completeness.

3.1. *Connectivity of G_μ*

The cluster amplitudes being connected the connectivity of the components of the G-blocks is as follows: The G-blocks in Equations (9) and (19) are composed of the so-called 'direct term' and the 'coupling term'. $\bar{H}_\mu$, is an explicitly connected quantity if T_μs are connected. Hence, the direct terms are unambiguously connected. The coupling term presents a more complicated situation involving more than one model function and requires consideration of two main issues.

(1) Connectivity of $\exp(\overline{T_\nu})W_{\nu\mu}$: $W_{\nu\mu}$ is defined as the closed component of $\bar{H}_\mu$ which scatters ϕ_μ to ϕ_ν and is explicitly connected. The next connection involves T_ν s in $\exp(\overline{T_\nu})W_{\nu\mu}$, which is explicitly connected to $W_{\nu\mu}$. We will henceforth use the compact notation $X_{\nu\mu}$ for $\exp(\overline{T_\nu})W_{\nu\mu}$.

(2) Connectivity of $\{\exp-(T_\mu - T_\nu)X_{\nu\mu}\}$: Two situations that arise in this case are (a) ϕ_ν and ϕ_μ differ by at least one orbital (Case 2a) and (b) ϕ_μ and ϕ_ν have the same orbital occupancy such that either $\mu \equiv \nu$ or the spin coupling scheme of the active orbitals in ϕ_μ and ϕ_ν are different (Case 2b).

In Case 2a, $X_{\nu\mu}$ is explicitly dependent on all the active orbitals by which ϕ_μ and ϕ_ν differ since $X_{\nu\mu}$ contains $W_{\nu\mu}$. The functional dependence of the cluster amplitudes on the active orbitals is the same for all the model functions since they are all treated on the same footing. Hence, the difference of the amplitudes $t_\mu - t_\nu$ for the same excitation depends implicitly on one or more of the active orbitals by which ϕ_μ and ϕ_ν differ. Thus $\{\exp-(T_\mu - T_\nu)$ must have implicitly at least one common active orbital label with $X_{\nu\mu}\}$ leading to connectivity between the two. We also note here that our arguments subsume the case where the action of some components of T_ν on ϕ_μ is invalid because of the occupancy restrictions of the active orbitals. The T_μ involved must then be labelled by those orbitals by which ϕ_μ and ϕ_ν differ.

For Case 2b, if ϕ_μ and ϕ_ν are the same, the composite in the coupling term reduces simply to $X_{\nu\mu}$ which is obviously connected. If ϕ_μ and ϕ_ν have the same orbital occupancy but differ in their spin coupling schemes, then the quantity $X_{\nu\mu}$ would depend on one or more of the same orbitals involved in the different spin couplings for ϕ_μ and ϕ_ν. In such a situation, the difference $t_\mu - t_\nu$ will have implicit dependence on all active orbitals involved in the segments in which the spin couplings of ϕ_μ and ϕ_ν are different.

3.2. Connectivity of the working equations

The proof of the connectivity of the working equation is much more involved since it involves RDM along with the *G*-blocks of which the former are not connected quantities. Thus, it is essential to analyse all possibilities of occurrence of disconnected terms in our working equations and to demonstrate unambiguously that these components either do not occur on account of some limitations imposed by the nature of our problem or cancel out analytically due to the internal structure of the RDMs in terms of lower body RDMs and cumulants.

The interplay of two facts helps us establish the connectivity of our working equations. Firstly, the RDM used in our amplitude equations are those between the same model functions. Thus, they are necessarily diagonal (each pair of creation-annihilation has the same labels) or quasi-diagonal (set of creations have the same labels as the set of annihilations) which ensures that common labels occur between the projection, $\langle 0|\epsilon_l^\mu$, and the *G*-block leading to connected quantities. Thus, several apparently disconnected entities are connected by diagonality or quasi-diagonality. Secondly, there are some situations like in Figure 1 where

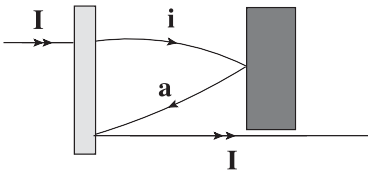

Figure 1. Occurrence of disconnected RDM in a projection with valence spectator in exchange mode.

the former argument is not applicable. In this situation, one must recognise that our set of equations is such that there exist lower body equations containing the same G-blocks for every higher body equation where the RDM may arise entirely from the projection. Furthermore, it is possible to decompose the higher rank RDM in the latter equation and algebraically manipulate it such that the lower body equation in its entirety occurs as a part of the higher body equation and may be deleted by invoking the former. The decomposition rules which need to be adopted for the RDMs is the standard spin-free cumulant decomposition of spin-free RDMs proposed by Kutzelnigg and Mukherjee [85–87]. An important issue we should mention here is that, in order to be able to carry out this algebraic manipulation it is necessary to start out with *all possible* RDMs in the higher body equations, including those which are of EPV type and are thus, zero in value. The corresponding EPV-type cumulants, unlike the Γs, are non-zero and should be retained. Once, the lower body equation is eliminated from the higher body equation, it is found that no disconnected pieces remain. The residual terms are either such, that the RDMs or cumulants have common indices with the G-blocks or only single cumulants occur, which are extensive by construction. For further details and an illustrative example we refer to our recent publication [70].

4. Treatment of orbital relaxation and correlation relaxation effects in UGA-SUMRCC and UGA-QFMRCC theories

One major focus of this paper is to explore the extent of incorporation of orbital relaxation and correlation relaxation in our UGA-SUMRCC [58] and UGA-QFMRCC [70] in the context of core electron ionisation and excitation as against SU-COS-CC [59] which is known to be highly successful for core-ionisation potentials (IPs) and the more widely applied EOM-CC [8–10,88–90]. We believe the latter does not have sufficient compactness and flexibility for handling such situations. Another allied and widely applied theory is SAC-CI [1–3], which uses an exponential Ansatz for describing the correlation of the ground state adapted to the correct spin and spatial symmetry and a linear, CI-like Ansatz for generating the ionised/excited states of interest. One of its variants, SAC-CI (R) [15], uses orbitals of the ground state HF function. Another variant, SAC-CI

(OR) [91], takes the orbitals of the core-ionised state in a similar setting. The SAC-CI for core ionised/excited states require higher order operators for reasonable accuracy. These higher body operators simulate the powers of *h–p* excitations, which are absent in an SD truncation scheme of a linearised ionisation/excitation operator. The corresponding higher order IP- and EA-EOM-CC theories have also been studied [92,93].

Our UGA-SUMRCC and UGA-QFMRCC have three common salient features. Firstly, the theories are spin-free such that the final wave function is an eigen-function of S^2 and thus, open-shell states of different spin multiplicity may be accurately handled. This is achieved by unitary group adaptation of the *T* operators, which must be labelled by spatial orbitals of a common closed shell vacuum. This creates two hurdles. Firstly, the *T*-operators become non-commuting as they may now contain annihilation operators of active holes and particles and secondly, the orbitals to be used are for one function, which may not be one of the model functions or even of the same valence sector making it essential to have a mechanism for correction of orbitals in the wave operator Ansatz as advocated in Thouless theorem [16]. The first hurdle is overcome by normally ordering our exponential Ansatz with respect to a common closed shell vacuum, which restores commutativity of the operators but in doing so sacrifices some part of the clustering but without loss of size extensivity. If the non-commutativity is retained and the *T*-operators are allowed to contract among themselves with suitable evaluation of combinatoric factors as in COS-CC [59,60], the second hurdle is not a significant problem at all, since the evaluation of the chains of one-body excitation inducing operators results in full clustering analogous to a spin orbital based theory and a high degree of Thouless relaxation is possible. However, the evaluation of chains of operators and the determination of the corresponding combinatoric factors is more involved than a theory using the normal-ordered cluster Ansatz in UGA-SUMRCC theory. The μ-dependence of the operators T_μ and S_μ allows us to delete valence spectator excitations and thus allows full exponential structure of the wave operator for all those excitations, which do not involve valence destructions. This feature alone makes the UGA-SUMRCC theory worth exploring. Assuming we are to use the normal ordered Ansatz, we can overcome the second hurdle to a considerable extent by clubbing together certain operators such that the valence destruction containing operators, which are proportional to lower body operators do not occur explicitly but their effect is implicitly taken to all powers of the lower body operator. For example, G_i^a and G_{iA}^{aA} are added together and the sum contributes to the equation for T_i^a. The operator T_{iA}^{aA} is discarded. However, operators like T_{iA}^{Aa},T_i^I and T_A^a terminate at linear power due to their inability to contract with each other unlike in COS-CC.

On the other hand, in Fock-space theories like STEOM-CC [31–33] and VUMRCC [21–24], for the mh–np valence sector, all operators containing mh, np or mh–np valence destructions terminate at linear power. They thus would be unable to fully take care of the orbital relaxation and differential correlation effects involving inactive excitations ($i \rightarrow a$ for orbital relaxation and $ij \rightarrow ab$ for differential correlation incorporating relaxation). The normal order Ansatz precludes inclusion of complete relaxation effects, since the valence operator inducing $i \rightarrow a$ will have to be accompanied by operators of the type $iI \rightarrow aI$, $iA \rightarrow aA$, etc., which leads to incomplete exponentiation. Similarly, $ij \rightarrow ab$ excitation inducing differential correlation would need operators like $ijI \rightarrow abI$, $ijA \rightarrow abA$, etc. which again would preclude full exponentiation. In our formalism, in contrast, the corresponding operators are both of the same rank as the ground state T, and do not contain spectator excitation. There is thus a trade-off between having CSF-independent valence operators as in FS-MRCC etc. and the explicit use of μ-dependence in UGA-SUMRCC/UGA-QFMRCC without spectator lines. We have elaborated on this in Section 5.

The SAC-CI, by virtue of its Ansatz also adopts a linear expression for the excitation operators even though the ground state correlated function is described by an exponential Ansatz. SAC-CI (R) is a SAC-CI theory using the closed shell HF function as a reference function where higher excitation manifolds are included in the excitation operators to simulate the relaxation effects. The method is allied to ours, though we have a normal ordered exponential parameterisation. Comparative results for core ionised states are provided in Section 5. It is documented [91,94] that for a reasonable description of core electron ionisation and excitation using SAC-CI (R), it is necessary to use at least triple excitation operators. This requirement has been attributed to the high degree of orbital relaxation and correlation change accompanying core processes. Our results show that, using only up to double excitations we have been able to match or even supercede the accuracy of SAC-CI (R) using up to triple excitation operators.

5. Molecular applications

In this section, we will present results for core ionised states of H_2O, CH_4, HF, NH_3 and CO with suitable comparisons with COS-CC, SAC-CI and EOM-CC and core excited states of H_2O, N_2 and CH_4 with comparisons with spin orbital based Mk-MRCCSD (Mukherjee's SSMRCC under singles-doubles, SD, approximation), Brillouin-Wigner(BW)-MRCCSD and EOM-CC. In all cases we have presented the relevant experimental values. Our results are presented in Tables 2–7. We have made use of three closely allied methods: (1) A straightforward use of the UGA-SUMRCC method with the SD truncation to describe the core-ionised/core-excited states and the ground state energy computed by the usual SRCCSD is subtracted to generate the corresponding energy differences. The model space is

Table 2. Adiabatic core ionisation energies for H_2O.

Basis	Ionisation	ΔUGA-SUMRCC	QF-Type COS-CC [98]	ΔCOS-CC [98]	EOM-CCSD [99]	Expt. [100]
cc-pVDZ	O 1s$^-$1	541.97	542.29	542.11	543.27	539.78
cc-pVTZ	O 1s$^-$1	539.02	539.36	539.14	540.66	
cc-pCVTZ	O 1s$^-$1	539.24	539.55	539.34	541.06	

Note: Geometry: R (O–H) = 0.9772 Å Θ (H–O–H) = 104.52°.
Energies are in eV.

Table 3. Diabetic core ionisation energies for CH_4, HF and NH_3.

Molecule	Basis	Ionisation	ΔUGA-SUMRCC	SAC-CI (R) [94]	EOM-CCSD [99]	Expt. [94]
CH_4	cc-pCVTZ	C 1s$^-$1	290.50	290.50	290.83	290.86
HF	cc-pCVTZ	F 1s$^-$1	693.40	693.89	695.42	693.80
NH_3	cc-pCVTZ	N 1s$^-$1	405.22	405.15	405.71	405.52

Note: Geometries for G.S.:
R (C–H) = 1.087Å, Θ (H–C–H) = 104.3°; R (H–F) = 0.917Å ; R (N–H) = 1.014Å, Θ (H–N–H) = 107.2°.
Geometries for ionised state:
R (C–H) = 1.039Å, Θ (H–C–H) = 104.3°; R (H–F) = 0.995Å ; R (N–H) = 0.981Å, Θ (H–N–H) = 113.6°.
Energies are in eV.

Table 4. Adiabatic core ionisation energies for CO.

Basis	Ionisation	ΔUGA-SUMRCC	ΔCOS-CC	SAC-CI (R) [94]	EOM-CCSD [99]	Expt. [101]
cc-pVTZ	C 1s$^-$1	295.25	295.28	296.13	297.02	296.2
cc-pCVTZ	C 1s$^-$1	295.67	295.71	–	297.55	

Note: Geometry: R (C-O) = 1.1283 Å.
Energies are in eV.

Table 5. Adiabatic core excitation energies for H_2O.

Basis	Excitation	ΔUGA-SUMRCC	ΔUGA - IIMS-SUMRCC	UGA-QFMRCC	EOM-CCSD [99]	Mk-MRCCSD [61]	BW-MRCCSD [61]	Expt. [61]
cc-pVDZ	$1a_1 \rightarrow 4a_1$	537.43	537.70	537.50	538.40	537.62	537.56	534.0
	$1a_1 \rightarrow 2b_1$	539.33	539.33	539.42	540.21	539.55	539.49	535.9
cc-pCVDZ	$1a_1 \rightarrow 4a_1$	536.58	536.86	536.66	537.65	–	-	
	$1a_1 \rightarrow 2b_1$	538.50	538.50	538.58	539.44	–	-	
aug-cc-pCVDZ	$1a_1 \rightarrow 4a_1$	536.24	536.61	536.24	537.55	–	-	
	$1a_1 \rightarrow 2b_1$	538.05	538.05	538.05	539.35	–	-	
cc-pVTZ	$1a_1 \rightarrow 4a_1$	534.15	534.40	534.15	535.34	534.30	534.26	
	$1a_1 \rightarrow 2b_1$	536.05	536.05	536.05	537.13	536.20	536.15	
Sadlej-pVTZ	$1a_1 \rightarrow 4a_1$	536.50	536.85	536.50	537.92	536.56	536.47	
	$1a_1 \rightarrow 2b_1$	538.27	538.27	538.27	539.60	538.34	538.35	

Note: Geometry: R (O–H) = 0.9772 Å Θ H-O-H = 104.52°.
Energies are in eV.

comprised of certain h–p excited CSFs involving the core and some low-lying virtual orbitals as active orbitals; (2) using a factorised cluster Ansatz, $\Omega_\mu = \exp(T)\{\exp S_\mu\}$, with T as the ground state cluster operator, we can model the orbital relaxation and correlation relaxation for ϕ_μ relative to the corresponding amplitudes of T of the ground state. Since, apart from $0h$–$0p$ valence sector $|\phi_0\rangle$ we deliberately subsume all the differential relaxation effects in S_μ characterising the $1h$–$1p$ model space spanned by ϕ_μ, we call this a quasi-fock version: UGA-QFMRCC. It provides us a direct access to core-IP/core-EEs. (3) By invoking a model space containing ϕ_0 and the h–p excited CSFs involving the core orbitals as the hole we may generate excitation energies directly by dropping the vacuum energy $\langle\phi_0|\overline{H\exp(T)}|\phi_0\rangle$ completely from the diagonal elements of the matrix of the effective Hamiltonian. The three approaches have been denoted, respectively, as UGA-SUMRCC, UGA-QFMRCC and UGA-IIMS-SUMRCC. The excitation energies calculated by Kowalski *et al.* [61] using Mk-MRCCSD and BW-MRCCSD consider a multi-reference description of both

Table 6 Adiabatic core excitation energies for N_2.

Basis	Excitation	Δ UGA-SUMRCC	UGA-QFMRCC	EOM-CCSD [99]	Mk-MRCCSD [61]	BW-MRCCSD [61]	Expt. [61]
6-311G**	$1\Sigma_u \rightarrow 1\Pi_g$	402.53	402.48	402.20	402.37	402.52	401.2
	$1\Sigma_g \rightarrow 1\Pi_g$	402.58	402.53	402.26	402.42	402.57	400.0
cc-pVDZ	$1\Sigma_u \rightarrow 1\Pi_g$	407.67	404.75	404.38	–	–	(1.8-2 eV
	$1\Sigma_g \rightarrow 1\Pi_g$	404.83	404.80	404.43	–	–	resolution)
cc-pVTZ	$1\Sigma_u \rightarrow 1\Pi_g$	401.82	401.79	401.62	401.81	401.66	
	$1\Sigma_g \rightarrow 1\Pi_g$	401.88	401.84	401.68	401.86	401.72	
Sadlej-pVTZ	$1\Sigma_u \rightarrow 1\Pi_g$	404.66	404.63	404.05	–	–	
	$1\Sigma_g \rightarrow 1\Pi_g$	404.73	404.68	xxx	–	–	

Note: Geometry: R (N–N) = 2.068 au.
Energies are in eV.
xxx: Did not converge.

Table 7. Diabatic core excitation energies for CH_4.

Basis	Excitation	ΔUGA-SUMRCC	SAC-CI (R) [94]	Expt. [94]
cc-pCVTZ	C 1s → LUMO(A_1)	287.80	288.50	287.99

Note: Geometry of G.S.: R (C–H) = 1.087 Å.
Geometry of Excited State.: R (C–H) = 1.032 Å.
Energies are in eV.

the excited and ground state using different CASs and the comparisons are thus, not exactly on the same footing with ours. HF orbitals of the ground state are used in all cases so that the phenomenon of orbital relaxation may be amply demonstrated. The spin adaptation of the wave function in our theories also modifies the computed excitation energies but due to the interplay of several factors at the same time, the role of spin adaptation itself is not immediately apparent. A study of properties sensitive to the spin of the wave function may be expected to demonstrate this aspect more conclusively. Moreover, it must be mentioned here that BW-MRCCSD is not size extensive.

There are several issues which must be discussed in relation to core electron phenomena. Firstly, core electron phenomena are accompanied by strong orbital relaxation and correlation changes which are taken care of by Thouless-effects in coupled-cluster theories. As explained in Section 4, theoretically speaking, our theories account for more relaxation than EOM-CC and our results should reflect this fact. Moreover, spin orbital based Mk-MRCCSD and BW-MRCCSD contain a complete clustering of single excitation inducing operators and therefore incorporate as much Thouless relaxation as feasible under a CCSD scheme. The closeness of our core excitation energies with Mk-MRCCSD and BW-MRCCSD to within a few tenths of an electronvolt is an indicator of this. The spin contamination of the wave function in Mk-MRCCSD and BW-MRCCSD is another matter unrelated to the relaxation of orbitals and and we do not discuss this here. They will have spin contamination only for core IPs and not for core EEs (singlet). The SAC-CI (R) results presented here use upto triple excitation operators and are hence not suitable for theoretical comparison. However, the fact that our numbers using SD truncation for core ionised states are very similar to SAC-CI (R) with three-body operators and also approaches high accuracy experimental results is a clear sign of incorporating appropriate physics at low truncation in UGA-SUMRCC and UGA-QFMRCC theories. The comparisons with EOM-CC are somewhat erratic as EOM-CC itself gives erratic levels of accuracy with change in basis and across different molecules doing remarkably well in certain cases and failing entirely in others. Our studies indicate that for core excitations, all three variants of our theory perform consistently better than EOM-CC in different bases and for different states presumably due to better mechanism for relaxation of orbitals and correlation. However, for diabatic core ionisation energies of CH_4 and NH_3, EOM-CC outperforms our theories and SAC-CI (R). It must be noted that our benchmark numbers are experimental and meaningful comparison would necessitate much involved study using the same basis in the full CI limit to have the proper comparison. This has not been undertaken at this preliminary stage of development of our theories. In view of this, the quality of the EOM-CC numbers for CH_4 and NH_3 may just as well be due to a cancellation of errors as it might be an indication that relaxation through higher powers of one body excitations is insignificant for these molecules. The latter reason seems unlikely as then, theories with better mechanism for Thouless-relaxation, viz. our UGA theories and SAC-CI (R) would have yielded equally accurate results. The ionisation energies computed using our UGA-SUMRCC closely mirror COS-CC to within a few tenths of an electronvolt indicating how closely we approach the effect of full exponentiation in a JM-like COS-CC Ansatz.

Secondly, the choice of basis should be such as to provide the function space for accurate description of core ionised and core excited states. Core ionised states only require the addition of core correlation functions such that the loss in correlation may be adequately modelled. Core excited states present a much bigger challenge since core electrons are often excited to loosely bound Rydberg states which are not well described by standard bases. Thus, experimental excitation energies are difficult to reproduce and interpretation of core excitation spectra remain challenging. We present high accuracy experimental data for both core ionisation and excitation and observe that while core ionisation energies are closely reproduced and improve systematically with improvement in bases, experimental and computed core excitation energies vary significantly. More detailed studies using Rydberg orbitals and special manipulation of contraction coefficients of the Gaussian basis have succeeded to approach the experimental values. In this paper, we present preliminary applications of our newly developed theoretical formulations and thus, such details have not been considered. However, care has been taken to clarify the extent of comparison with other theories.

Thirdly, geometry considerations are crucial depending on the nature of the experiment we wish to compare with. We specifically mention in each case if the energy computed is diabatic (different geometries for ground and excited/ionised state taken from experiment or as used in the computations presented for comparison) or adiabatic (excitation/ionisation at ground state experimental geometry). Where spectral data has been analysed, the (0,0) vibrational band is considered for comparison with our computed energies. The geometries considered are mentioned as footnotes to the respective tables. Vibrational corrections have not been undertaken. All integrals were obtained from GAMESS-US [95].

There is a close correspondence between the IP/EE values for the example molecules studied by us as computed by the three theories, indicating that the essential physics incorporated by these theories are more or less similar. We ascribe such closeness of the results to the full exponential structure of all operators of T_μ/S_μ, where valence destruction is not involved. Such is not the case for the VUMRCC approach. In fact, even for the core-ionisation in the VUMRCC, the effective wave operator for a ϕ_μ is just $\exp T\{1 + S_\mu\}$ whereas for most of the components of S_μ the effective wave operator for the UGA-QFMRCC is $\exp(T + S_\mu)$ with a full exponential structure. Thus, it does not really matter much whether a separation of the ground state cluster operator is made as above or one simply uses $T_\mu = T + S_\mu$ as the variable.

6. Summarising remarks and future outlook

In this paper, we have explored the efficacy of a suite of inter-related theories built around the UGA-SUMRCC approach. The UGA-SUMRCC approach utilises a multi-component state-universal Ansatz of the form $\Omega|\Psi_{0k}\rangle = \sum_\mu \Omega_\mu|\phi_\mu\rangle c_{\mu k}$, with $\{\phi_\mu\}$ as the set of unitary group adapted Gel'fand CSFs spanning the model space of the components of Ω acting on ϕ_μ: $\Omega_\mu = \{\exp(T_\mu)\}$ where $\{\}$ denotes the normal-ordering with respect to the doubly occupied core state, $|0\rangle$, taken as the vacuum. T_μs are composed of suitable excitation operators inducing transitions from the model function ϕ_μ to various virtual functions χ^l_μ, with the excitation operators expressed as various spin-free unitary generators. The entire formalism is spin-free and preserves the total spin rigorously. For a CAS, the T_μs consist of excitations with at least one occupancy change of inactive orbitals. We have focussed our attention in this paper on two specific aspects of the UGA-SUMRCC where the formalism works at its best. (1) For all excitations from the model space where the operators do not involve the destruction of the active quasi-particles, the associated components of T_μ allow full exponentiation as the parent spinorbital based JM Ansatz. They thus are able to relax the orbitals almost as fully as in the JM Ansatz but retaining spin symmetry. (2) For the corresponding two-body inactive excitations and those not involving destruction of active quasi-particles, the Ansatz again allows full exponentiation, thereby affording very compact representation of the relaxation of correlation attendant on ionisation and excitation. (3) It provides an easy access to both ionised/excited state energies *per se* and of the energy difference with respect to a ground state which is predominantly SR. More concretely using the HF orbitals for the ground state, ϕ_0, the one-body operators of T_μ relaxes the orbitals fully on ionisation/excitation and the two-body operators involving inactive orbitals induce correlations appropriate to the CSF, ϕ_μ and embodies correlation relaxation via relaxed orbitals by their coupling with the one-body T_μs. For ionised/excited states involving removal of a core electron the orbital relaxation of the HF orbitals of the ground state is severe, and such effects are not normally accessible to the commonly used methods like SAC-CI, CC-LRT/CC-LR, EOM-CC or VUMRCC in the singles–doubles (SD) truncation schemes. While belabored formulations are certainly feasible via inclusion of higher body cluster operators, even a simple truncation scheme of our UGA-SUMRCC Ansatz would suffice to incorporate the essential physics because of its redeeming features (1)–(3) above.

We have emphasised in the paper that a model space of *h–p* CSFs is incomplete (actually, quasi-complete as defined by Lindgren [81]) and we must abandon the customary IN for Ω to maintain size extensivity of the ionised/excited states. The necessary modifications for defining H_{eff} have been discussed in the paper and the appropriate equations have been presented. It has also been emphasised that for our method, (3), the incomplete model space has the interesting property that the IN for Ω holds good and no modifications are necessary.

Our results amply demonstrate that core-IPs are very well described by our methods. The results are somewhat inferior to those obtained from the COS-CC method, which uses a richer Ω of Datta and Mukherjee [59,60]. We still get very good quality results, but at a considerably reduced cost. The numbers require enhanced operator space for SAC-CI or CC-LRT or EOM to match our accuracy. Because of the presence of valence destruction operators in all the valence operators of VUMRCC or its equivalent STEOM-CC, we presume that a normal ordered exponential representation of Ω would not perform as well as the UGA-SUMRCC or UGA-QFMRCC.

Since the UGA-SUMRCC theory is based on effective Hamiltonians, it is prone to intruder problems [96,97] if the active space is not energetically well separated from the virtual space. Also, to get the core-hole satellites in core excitations, one needs a model space with another ladder of *h–p* excitations, such generalisations are obviously wanted if high precision spectroscopic results are to be predicted or interpreted. In a way reminiscent of the EIP technique [25,27–30] (or as in the STEOM-CC [31–33]) it is possible to cast the system of Bloch equations into a dressed CI eigen problem. This strategy would not only obviate the intruder problem by homing into the set of desired eigenvalues in a numerically robust manner, but would also allow the well developed machinery of the direct-CI to automate the computational organisations. Research along these lines are in progress for both core- and valence-ionisation/excitation and would be reported in one of our future publications.

Acknowledgements

DM acknowledges the Humboldt Award, the J. C. Bose Fellowship, the Indo-EU grant and the Indo-French project for research support. SS thanks the SPM fellowship of the CSIR (India) and AS thanks the DST (India) and CEFIPRA for generous financial support. It gives us great pleasure to dedicate this paper to Werner Kutzelnigg on the occasion of his 80th birthday. DM wishes Werner Kutzelnigg many more years of creative pursuit and excellent health, and cherishes many happy moments in the long and intense collaborations with him and his warm friendship.

References

[1] H. Nakatsuji and K. Hirao, J. Chem. Phys. **68**, 2053 (1978).
[2] H. Nakatsuji, Chem. Phys. Lett. **67**, 329 (1979).
[3] H. Nakatsuji, Chem. Phys. Lett. **67**, 334 (1979).
[4] H.J. Monkhorst, Int. J. Quantum Chem. **S11**, 421 (1977); E. Dalgaard and H.J. Monkhorst, Phys. Rev. A **28**, 1217 (1983).
[5] D. Mukherjee and P.K. Mukherjee, Chem. Phys. **39**, 325 (1979); B. Datta and D. Mukherjee, Chem. Phys. Lett. **176**, 468 (1991); B. Datta, P. Sen, and D. Mukherjee, J. Phys. Chem. **99**, 6441 (1995).
[6] H. Koch and P. Jorgensen, J. Chem. Phys. **93**, 3333 (1990).
[7] H. Koch, H.J.A. Jensen, P. Jorgensen, T. Helgaker, G.E. Scuseria, and H.F. Schaefer III, J. Chem. Phys. **92**, 4924 (1990).
[8] H. Sekino and R.J. Bartlett, Int. J. Quantum Chem. Symp. **18**, 255 (1984).
[9] J. Geertsen, M. Rittby, and R.J. Bartlett, Chem. Phys. Lett. **164**, 57 (1989).
[10] J.F. Stanton and R.J. Bartlett, J. Chem. Phys. **98**, 7029 (1993).
[11] K. Raghavachari, G.W. Trucks, J.A. Pople, and M. Head-Gordon, Chem. Phys. Lett. **157**, 479 (1989).
[12] N. Oliphant and L. Adamowich, J. Chem. Phys. **94**, 1229 (1991).
[13] P. Piecuch and L. Adamowich, J. Chem. Phys. **100**, 5792 (1994).
[14] P. Piecuch and L. Adamowich, J. Chem. Phys. **100**, 5857 (1994).
[15] H. Nakatsuji, Chem. Phys. Lett. **177**, 331 (1991); M. Ehara and H. Nakatsuji, Chem. Phys. Lett. **282**, 347 (1998).
[16] D.J. Thouless, Nucl. Phys. **21**, 225 (1960).
[17] N. Oliphant and L. Adamowicz, Int. Rev. Phys. Chem. **12**, 339 (1993).
[18] P. Piecuch, N. Oliphant, and L. Adamowicz, J. Chem. Phys. **99**, 1875 (1993).
[19] K. Kowalski and P. Piecuch, J. Chem. Phys. **113**, 8490 (2000).
[20] M. Kállay, P.G. Szalay, and J. Gauss, J. Chem. Phys. **117**, 980 (2002).
[21] D. Mukherjee, R.K. Moitra, and A. Mukhopadhyay, Mol. Phys. **33**, 955 (1977).
[22] I. Lindgren, Int. J. Quantum Chem. **S12**, 33 (1978).
[23] D. Mukherjee, R.K. Moitra, and A. Mukhopadhyay, Mol. Phys. **30**, 1861 (1975).
[24] I. Lindgren and D. Mukherjee, Phys. Rep. **151**, 93 (1987).
[25] D. Sinha, S.K. Mukhopadhyay, R. Chaudhuri, and D. Mukherjee, Chem. Phys. Lett. **154**, 544 (1989).
[26] D. Mukherjee and S. Pal, Adv. Quantum Chem. **20**, 291 (1989).
[27] D. Mukhopadhyay, B. Datta, and D. Mukherjee, Chem. Phys. Lett. **197**, 236 (1992).
[28] M. Musial and R.J. Bartlett, J. Chem. Phys. **129**, 244111 (2008).
[29] R. Chaudhuri, D. Mukhopadhyay, and D. Mukherjee, Chem. Phys. Lett. **162**, 394 (1989).
[30] B. Datta, R. Chaudhuri, and D. Mukherjee, J. Mol. Struct. (Theochem) **361**, 21 (1996).
[31] M. Nooijen and R.J. Bartlett, J. Chem. Phys. **106**, 6441 (1997).
[32] M. Nooijen and R.J. Bartlett, J. Chem. Phys. **106**, 6449 (1997).
[33] M. Nooijen and R.J. Bartlett, J. Chem. Phys. **107**, 6812 (1997).
[34] B. Jeziorski and H.J. Monkhorst, Phys. Rev. **A 24**, 1668 (1981).
[35] B Jeziorski and J. Paldus, J. Chem. Phys. **88**, 5673 (1988).
[36] D. Mukhopadhyay, Jr, and D. Mukherjee, Chem. Phys. Lett. **163**, 171 (1989).
[37] D. Mukherjee, Chem. Phys. Lett. **125**, 207 (1986).
[38] D. Mukherjee, Int. J. Quantum Chem. **S20**, 409 (1986).
[39] D. Mukherjee, in *Condensed Matter Theories*, edited by J. Arponen, R.F. Bishop, and M. Manninen (Plenum Press, New York, 1988).
[40] D. Mukhopadhyay and D. Mukherjee, Chem. Phys. Lett. **163**, 171 (1989).
[41] L. Meissner, S.K. Kucharski, and R.J. Bartlett, J. Chem. Phys. **91**, 6187 (1989).
[42] L. Meissner and R.J. Bartlett, J. Chem. Phys. **92**, 561 (1990).
[43] U.S. Mahapatra, B. Datta, B. Bandyopadhyay, and D. Mukherjee, Adv. Quantum Chem. **30**, 163 (1998).

[44] U.S. Mahapatra, B. Datta, and D. Mukherjee, Mol. Phys. **94**, 157 (1998).
[45] U.S. Mahapatra, B. Datta, and D. Mukherjee, J. Chem. Phys. **110**, 6171 (1999).
[46] I. Hubac and P. Neogrady, Phys. Rev. A **50**, 4558 (1994).
[47] J. Masik and I. Hubac, Adv. Quantum Chem. **31**, 75 (1998).
[48] M. Hanrath, J. Chem. Phys. **123**, 84102 (2005).
[49] M. Hanrath, Chem. Phys. Lett. **420**, 426 (2006).
[50] I. Nebot-Gil, J. Sanchez-Martin, J.P. Malrieu, J.L. Heully, and D. Maynau, J. Chem. Phys. **103**, 2576 (1995).
[51] J. Meller, J.P. Malrieu, and R. Caballol, J. Chem. Phys. **104**, 4068 (1996).
[52] L. Kong, K.R. Shamasundar, O. Demel, and M. Nooijen, J. Chem. Phys. **130**, 114101 (2009).
[53] D. Datta, L. Kong, and M. Nooijen, J. Chem. Phys. **134**, 214116 (2011).
[54] D. Datta and M. Nooijen, J. Chem. Phys. **137**, 204107 (2012).
[55] M. Nooijen and V. Lotrich, J. Mol. Struc. (Theochem) **547**, 253 (2001).
[56] M. Nooijen, Int. J. Mol. Sci. **3**, 656 (2002).
[57] R. Maitra, D. Sinha, and D. Mukherjee, J. Chem. Phys. **137** 024105 (2012).
[58] S. Sen, A. Shee, and D. Mukherjee, J. Chem. Phys. **137**, 074104 (2012).
[59] D. Datta and D. Mukherjee, J. Chem. Phys. **131**, 044124 (2009).
[60] D. Datta and D. Mukherjee, J. Chem. Phys. **134**, 054122 (2011).
[61] J. Brabec, K. Bhaskaran-Nair, N. Govind, J. Pittner, and K. Kowalski, J. Chem. Phys. **137**, 171101 (2012).
[62] C.L. Jansen and H.F. Schaefer, Theor. Chim. Acta **79**, 1 (1991).
[63] X. Li and J. Paldus, J. Chem. Phys. **102**, 8897 (1995); Mol. Phys. **94**, 41 (1998) (and references therein).
[64] X. Li and J. Paldus, J. Chem. Phys. **101**, 8812 (1994);
[65] U.S. Mahapatra, B. Datta and D. Mukherjee, in *Recent Advances in Computational Chemistry*, edited by R.J. Bartlett (World Scientific, Singapore, 1997), p. 155.
[66] B. Jeziorski, J. Paldus, and P. Jankowski, Int. J. Quant. Chem. **56**, 129 (1995).
[67] P.G. Szalay and J. Gauss, J. Chem. Phys. **107**, 9028 (1997).
[68] M. Heckert, O. Heun, J. Gauss, and P.G. Szalay, J. Chem. Phys. **124**, 124105 (2006).
[69] D. Sinha, R. Maitra, and D. Mukherjee, J. Chem. Phys. **137**, 094104 (2012).
[70] A. Shee, S. Sen, and D. Mukherjee, J. Chem. Theory Comput. (In press). <http://dx.doi.org/10.1021/ct3011024>
[71] P. Jeszenszki, P.R. Surjn, and Szabados, J. Chem. Phys. **138**, 124110 (2013).
[72] U.S. Mahapatra, B. Datta, and D. Mukherjee, J. Phys. Chem. A. **103**, 1822 (1999).
[73] S. Mao, L. Cheng, W. Liu, and D. Mukherjee, J. Chem. Phys. **136**, 024105 (2012).
[74] S. Mao, L. Cheng, W. Liu, and D. Mukherjee, J. Chem. Phys. **136**, 024106 (2012).
[75] D. Mukherjee, Chem. Phys. Lett. **125**, 207 (1986).
[76] D. Mukherjee, Int. J. Quantum Chem. **S20**, 409 (1986).
[77] D. Mukherjee, in *Condensed Matter Theories*, edited by J. Arponen, R.F. Bishop, and M. Manninen (Plenum Press, New York, 1988).
[78] R. Chaudhuri, D. Sinha, and D. Mukherjee, Chem. Phys. Lett. **163**, 165 (1989).
[79] W. Kutzelnigg, D. Mukherjee, and S. Koch, J. Chem. Phys. **87**, 5902 (1987).
[80] W. Kutzelnigg, D. Mukherjee, and S. Koch, J. Chem. Phys. **87**, 5911 (1987).
[81] I. Lindgren, Phys. Scr. **32**, 611 (1985).
[82] S. Pal, M. Rittby, R.J. Bartlett, D. Sinha, and D. Mukherjee, Chem. Phys. Lett. **137**, 273 (1987).
[83] S. Pal, M. Rittby, R.J. Bartlett, D. Sinha, and D. Mukherjee, J. Chem. Phys. **88**, 4357 (1988).
[84] U. Kaldor, J. Chem. Phys. **88**, 5248 (1988).
[85] D. Mukherjee, in *Recent Progress in Many Body Theories*, edited by E. Schachinger, H. Mitter, and H. Sormann (Plenum, New York, 1995), p. 127.
[86] U.S. Mahapatra, B. Datta, B. Bandopadhyay, and D. Mukherjee, Adv. Quantum Chem. **30**, 163 (1998).
[87] W. Kutzelnigg and D. Mukherjee, J. Chem. Phys. **107**, 432 (1997).
[88] J. Stanton, J. Chem. Phys. **99**, 8840 (1993).
[89] J. Stanton and J. Gauss, J. Chem. Phys. **100**, 4695 (1994).
[90] J. Stanton and J. Gauss, J. Chem. Phys. **103**, 8931 (1995).
[91] M. Ehara, J. Phys. Conf. Series **194**, 012006 (2009).
[92] S. Hirata, M. Nooijen, and R.J. Bartlett, Chem. Phys. Lett. **328**, 459 (2000).
[93] S. Hirata, M. Nooijen, and R.J. Bartlett, Chem. Phys. Lett. **326**, 255 (2000).
[94] M. Ehara and H. Nakatsuji, Collect. Czech. Chem. Commun. **73**, 771 (2008).
[95] GAMESS, J. Comp. Chem. **14**, 1347 (1993).
[96] T.H. Schucan and H.W. Widenmueller, Ann. Phys. **73**, 108 (1972).
[97] T.H. Schucan and H.W. Widenmueller, Ann. Phys. **76**, 483 (1973).
[98] D. Datta, Ph.D. thesis, Jadavpur University, 2009.
[99] CFOUR, a quantum chemical program package written by J.F. Stanton, J. Gauss, M.E. Harding, P.G. Szalay with contributions from A.A. Auer, R.J. Bartlett, U. Benedikt, C. Berger, D.E. Bernholdt, Y.J. Bomble, O. Christiansen, M. Heckert, O. Heun, C. Huber, T.-C. Jagau, D. Jonsson, J. Juslius, K. Klein, W.J. Lauderdale, D.A. Matthews, T. Metzroth, D.P. O'Neill, D.R. Price, E. Prochnow, K. Ruud, F. Schiffmann, S. Stopkowicz, A. Tajti, J. Vzquez, F. Wang, J.D. Watts and the integral packages MOLECULE (J. Almlf and P.R. Taylor), PROPS (P.R. Taylor), ABACUS (T. Helgaker, H.J. Aa. Jensen, P. Jrgensen, and J. Olsen), and ECP routines by A.V. Mitin and C. van Wllen. For the current version, <http://www.cfour.de.>.
[100] Y. Ohtsuka and H. Nakatsuji, J. Chem. Phys. **124**, 054110 (2006).
[101] J. Stohr, *NEXAFS Spectroscopy: Springer Series in Surface Sciences*, (Springer, New York, 1992) Vol. 25.

Bibliography

[1] DIRAC, a relativistic ab initio electronic structure program, Release DIRAC14 (2014), written by T. Saue, L. Visscher, H. J. Aa. Jensen, and R. Bast. with contributions from V. Bakken, K. G. Dyall, S. Dubillard, U. Ekström, E. Eliav, T. Enevoldsen, E. Faßhauer, T. Fleig, O. Fossgaard, A. S. P. Gomes, T. Helgaker, J. K. Lærdahl, Y. S. Lee, J. Henriksson, M. Iliaš, Ch. R. Jacob, S. Knecht, S. Komorovský, O. Kullie, C. V. Larsen, H. S. Nataraj, P. Norman, G. Olejniczak, J. Olsen, Y. C. Park, J. K. Pedersen, M. Pernpointner, R. di Remigio, K. Ruud, P. Sałek, B. Schimmelpfennig, J. Sikkema, A. J. Thorvaldsen, J. Thyssen, J. van Stralen, S. Villaume, O. Visser, T. Winther, and S. Yamamoto (see http://www.diracprogram.org).

[2] On the Interaction of Two Electrons. *Proceedings of the Royal Society A: Mathematical, Physical and Engineering Sciences*, 208(1095):552–559, sep 1951.

[3] Calculation of electric-field gradients based on higher-order generalized Douglas-Kroll transformations. *Journal of Chemical Physics*, 122:1–10, 2005.

[4] M. Abe, T. Nakajima, and K. Hirao. The relativistic complete active-space second-order perturbation theory with the four-component Dirac Hamiltonian. *The Journal of chemical physics*, 125(23):234110, dec 2006.

[5] K. Andersson, P. A. Malmqvist, B. O. Roos, A. J. Sadlej, and K. Wolinski. Second-order perturbation theory with a CASSCF reference function. *The Journal of Physical Chemistry*, 94(14):5483–5488, jul 1990.

[6] C. Angeli, R. Cimiraglia, S. Evangelisti, T. Leininger, and J.-P. Malrieu. Introduction of n-electron valence states for multireference perturbation theory. *The Journal of Chemical Physics*, 114(23):10252, jun 2001.

[7] F. Aquilante, L. De Vico, N. Ferré, G. Ghigo, P.-Å. Malmqvist, P. Neogrády, T. B. Pedersen, M. Pitoňák, M. Reiher, B. O. Roos, et al. MOLCAS 7: The next generation. *Journal of computational chemistry*, 31(1):224–247, 2010.

[8] F. Aquino, N. Govind, and J. Autschbach. Electric field gradients calculated from two-component hybrid density functional theory including spin-orbit coupling. *Journal of Chemical Theory and Computation*, 6(9):2669–2686, 2010.

[9] G. A. Aucar, T. Saue, L. Visscher, and H. J. A. Jensen. On the origin and contribution of the diamagnetic term in four-component relativistic calculations of magnetic properties. *The Journal of Chemical Physics*, 110(13):6208, apr 1999.

[10] J. Autschbach and S. Zheng. Relativistic computations of nmr parameters from first principles: theory and applications. *Annual Reports on NMR Spectroscopy*, 67:1–95, 2009.

[11] M. Barysz and A. J. Sadlej. Two-component methods of relativistic quantum chemistry: from the DouglasKroll approximation to the exact two-component formalism. *Journal of Molecular Structure: THEOCHEM*, 573(1-3):181–200, oct 2001.

[12] J. E. Bates and T. Shiozaki. Fully relativistic complete active space self-consistent field for large molecules: quasi-second-order minimax optimization. *The Journal of chemical physics*, 142(4):044112, jan 2015.

[13] K. Beloy and A. Derevianko. Application of the dual-kinetic-balance sets in the relativistic many-body problem of atomic structure. *Computer Physics Communications*, 179(5):310–319, Sept. 2008.

[14] C. Chang, M. Pelissier, and P. Durand. Regular Two-Component Pauli-Like Effective Hamiltonians in Dirac Theory. *Physica Scripta*, 34(5):394–404, nov 1986.

[15] J. Crassous, C. Chardonnet, T. Saue, and P. Schwerdtfeger. Recent experimental and theoretical developments towards the observation of parity violation (PV) effects in molecules by spectroscopy. *Organic & biomolecular chemistry*, 3(12):2218–24, jun 2005.

[16] M. Douglas and N. M. Kroll. Quantum electrodynamical corrections to the fine structure of helium. *Annals of Physics*, 82(1):89–155, 1974.

[17] K. G. Dyall. An exact separation of the spin-free and spin-dependent terms of the Dirac-Coulomb-Breit Hamiltonian. *The Journal of Chemical Physics*, 100(3):2118, 1994.

[18] K. G. Dyall. Second-order Møller-Plesset perturbation theory for molecular Dirac-Hartree-Fock wavefunctions. Theory for up to two open-shell electrons. *Chemical Physics Letters*, 224(1-2):186–194, jul 1994.

[19] K. G. Dyall. A question of balance: Kinetic balance for electrons and positrons. *Chem. Phys.*, 395:35, 2012.

[20] K. G. Dyall and K. Faegri Jr. *Introduction to Relativistic Quantum Chemistry*. Oxford University Press, USA, 2007.

[21] K. G. Dyall, I. P. Grant, and S. Wilson. Matrix representation of operator products. *Journal of Physics B: Atomic and Molecular Physics*, 17(4):493–503, feb 1984.

[22] T. Fleig, J. Olsen, and C. M. Marian. The generalized active space concept for the relativistic treatment of electron correlation. I. Kramers-restricted two-component configuration interaction. *The Journal of Chemical Physics*, 114(11):4775, mar 2001.

[23] L. L. Foldy and S. A. Wouthuysen. On the Dirac Theory of Spin 1/2 Particles and Its Non-Relativistic Limit. *Physical Review*, 78(1):29–36, apr 1950.

[24] J. Gauss, W. J. Lauderdale, J. F. Stanton, J. D. Watts, and R. J. Bartlett. Analytic energy gradients for open-shell coupled-cluster singles and doubles (CCSD) calculations using restricted open-shell HartreeFock (ROHF) reference functions. *Chemical Physics Letters*, 182(3-4):207–215, Aug. 1991.

[25] M. Gell-Mann. The interpretation of the new particles as displaced charge multiplets. *Il Nuovo Cimento (1955-1965)*, 4(2):848–866, 1956.

[26] T. Helgaker and P. Jørgensen. *Methods in Computational Molecular Physics*, volume 293 of *NATO ASI Series*. Springer US, Boston, MA, 1992.

[27] B. A. Hess. Applicability of the no-pair equation with free-particle projection operators to atomic and molecular structure calculations. *Physical Review A*, 32(2):756–763, aug 1985.

[28] B. A. Hess. Relativistic electronic-structure calculations employing a two-component no-pair formalism with external-field projection operators. *Physical Review A*, 33(6):3742–3748, jun 1986.

[29] B. A. Heß, C. M. Marian, U. Wahlgren, and O. Gropen. A mean-field spin-orbit method applicable to correlated wavefunctions. *Chemical Physics Letters*, 251(5-6):365–371, mar 1996.

[30] F. B. Hildebrand. *Introduction to numerical analysis*. Courier Corporation, 1987.

[31] M. Ilias and T. Saue. An infinite-order two-component relativistic Hamiltonian by a simple one-step transformation. *The Journal of chemical physics*, 126(6):064102, feb 2007.

[32] H. Jorgen Aa. Jensen, K. G. Dyall, T. Saue, and K. Fægri. Relativistic four-component multiconfigurational self-consistent-field theory for molecules: Formalism. *The Journal of Chemical Physics*, 104(11):4083, 1996.

[33] V. Kellö and A. J. Sadlej. Relativistic contributions to molecular electric-field gradients in hydrogen halides. *Chemical Physics Letters*, 174(6):641–648, Nov. 1990.

[34] S. Knecht, S. Fux, R. van Meer, L. Visscher, M. Reiher, and T. Saue. Mössbauer spectroscopy for heavy elements: a relativistic benchmark study of mercury. *Theoretical Chemistry Accounts*, 129(3-5):631–650, mar 2011.

[35] S. Knecht, H. J. A. Jensen, and T. Fleig. Large-scale parallel configuration interaction. I. Nonrelativistic and scalar-relativistic general active space implementation with application to (Rb-Ba)+. *The Journal of chemical physics*, 128(1):014108, jan 2008.

[36] S. Knecht, H. J. A. Jensen, and T. Fleig. Large-scale parallel configuration interaction. II. Two- and four-component double-group general active space implementation with application to BiH. *The Journal of chemical physics*, 132(1):014108, jan 2010.

[37] S. Knecht, Ö. Legeza, and M. Reiher. Communication: four-component density matrix renormalization group. *The Journal of chemical physics*, 140(4):041101, jan 2014.

[38] K. Kristensen, M. Ziłkowski, B. Jansík, T. Kjærgaard, and P. Jørgensen. A Locality Analysis of the Divide–Expand–Consolidate Coupled Cluster Amplitude Equations. *Journal of Chemical Theory and Computation*, 7(6):1677–1694, 2011.

[39] W. Kutzelnigg. The relativistic many body problem in molecular theory. *Physica Scripta*, 36(3):416, 1987.

[40] W. Kutzelnigg. Ab initio calculation of molecular properties. *Journal of Molecular Structure: THEOCHEM*, 202:11–61, dec 1989.

[41] W. Kutzelnigg. Diamagnetism in relativistic theory. *Physical Review A*, 67(3):032109, mar 2003.

[42] W. Kutzelnigg. Solved and unsolved problems in relativistic quantum chemistry. *Chemical Physics*, 395:16–34, Feb. 2012.

[43] J. K. Laerdahl, T. Saue, and K. Faegri Jr. Direct relativistic MP2: properties of ground state CuF, AgF and AuF. *Theoretical Chemistry Accounts: Theory, Computation, and Modeling (Theoretica Chimica Acta)*, 97(1-4):177–184, oct 1997.

[44] J. K. Laerdahl and P. Schwerdtfeger. Fully relativistic ab initio calculations of the energies of chiral molecules including parity-violating weak interactions. *Physical Review A*, 60(6):4439–4453, dec 1999.

[45] T. J. Lee and D. Jayatilaka. An open-shell restricted Hartree–Fock perturbation theory based on symmetric spin orbitals. *Chemical Physics Letters*, 201(1-4):1–10, jan 1993.

[46] W. Liu and D. Peng. Infinite-order quasirelativistic density functional method based on the exact matrix quasirelativistic theory. *The Journal of Chemical Physics*, 125(4), 2006.

[47] M. Mittleman. Theory of relativistic effects on atoms: Configuration-space Hamiltonian. *Physical Review A*, 24(3):1167–1175, Sept. 1981.

[48] F. Neese, A. Hansen, and D. G. Liakos. Efficient and accurate approximations to the local coupled cluster singles doubles method using a truncated pair natural orbital basis. *The Journal of chemical physics*, 131(6):064103, 2009.

[49] J. Olsen, B. O. Roos, P. Jorgensen, and H. J. A. Jensen. Determinant based configuration interaction algorithms for complete and restricted configuration interaction spaces. *The Journal of Chemical Physics*, 89(4):2185, aug 1988.

[50] P. Pyykko. Relativistic effects in structural chemistry. *Chemical Reviews*, 88(3):563–594, may 1988.

[51] P. Pyykkö and M. Seth. Relativistic effects in nuclear quadrupole coupling. *Theoret. Chem. Acc.*, 96:92, 1997.

[52] M. Quack. On the measurement of the parity violating energy difference between enantiomers. *Chemical physics letters*, 132(2):147–153, 1986.

[53] M. Quack. How important is parity violation for molecular and biomolecular chirality? *Angewandte Chemie (International ed. in English)*, 41(24):4618–30, dec 2002.

[54] M. Quack, J. Stohner, and M. Willeke. High-resolution spectroscopic studies and theory of parity violation in chiral molecules. *Annual review of physical chemistry*, 59:741–69, jan 2008.

[55] H. M. Quiney, H. Skaane, and I. P. Grant. Relativistic calculation of electromagnetic interactions in molecules. *Journal of Physics B: Atomic, Molecular and Optical Physics*, 30:829–834, 1997.

[56] N. F. Ramsey. Magnetic Shielding of Nuclei in Molecules. *Physical Review*, 78(6):699–703, jun 1950.

[57] S. Rybak, B. Jeziorski, and K. Szalewicz. Many-body symmetry-adapted perturbation theory of intermolecular interactions. H2O and HF dimers. *The Journal of Chemical Physics*, 95(9):6576, nov 1991.

[58] T. Saue. Spin-Interactions and the Non-relativistic Limit of Electrodynamics. *Advances in Quantum Chemistry*, 48:383–405, 2005.

[59] T. Saue and H. J. A. Jensen. Quaternion symmetry in relativistic molecular calculations: The DiracHartreeFock method. *The Journal of Chemical Physics*, 111(14):6211, oct 1999.

[60] T. Saue and L. Visscher. *Theoretical Chemistry and Physics of Heavy and Superheavy Elements*, volume 11 of *Progress in Theoretical Chemistry and Physics*. Springer Netherlands, Dordrecht, 2003.

[61] B. Schimmelpfennig, L. Maron, U. Wahlgren, C. Teichteil, H. Fagerli, and O. Gropen. On the combination of ECP-based CI calculations with all-electron spin-orbit mean-field integrals. *Chemical Physics Letters*, 286(3-4):267–271, apr 1998.

[62] K. Schwarzschild. Zur Elektrodynamik: I. Zwei Formen des Princips der kleinsten Action in der Elektrontheorie. *Gött. Nach., Math.-Phys. Kl.*, page 126, 1903.

[63] V. M. Shabaev, I. I. Tupitsyn, V. A. Yerokhin, G. Plunien, and G. Soff. Dual Kinetic Balance Approach to Basis-Set Expansions for the Dirac Equation. 93:130405, Sep 2004.

[64] R. Shepard, I. Shavitt, R. M. Pitzer, D. C. Comeau, M. Pepper, H. Lischka, P. G. Szalay, R. Ahlrichs, F. B. Brown, and J.-G. Zhao. A progress report on the status of the COLUMBUS MRCI program system. *International Journal of Quantum Chemistry*, 34(S22):149–165, 1988.

[65] T. Shiozaki and W. Mizukami. Relativistic Internally Contracted Multireference Electron Correlation Methods. *Journal of chemical theory and computation*, 11(10):4733–9, oct 2015.

[66] J. Sikkema, L. Visscher, T. Saue, and M. Ilias. The molecular mean-field approach for correlated relativistic calculations. *The Journal of chemical physics*, 131(12):124116, sep 2009.

[67] R. E. Stanton and S. Havriliak. Kinetic balance: A partial solution to the problem of variational safety in Dirac calculations. *The Journal of Chemical Physics*, 81(4):1910, 1984.

[68] J. Sucher. Foundations of the relativistic theory of many-electron atoms. *Physical Review A*, 22(2):348–362, aug 1980.

[69] J. Talman. Minimax principle for the Dirac equation. *Physical review letters*, 57(9):1091–1094, sep 1986.

[70] J. Thyssen, T. Fleig, and H. J. A. Jensen. A direct relativistic four-component multiconfiguration self-consistent-field method for molecules. *The Journal of chemical physics*, 129(3):034109, 2008.

[71] V. Vallet, L. Maron, C. Teichteil, and J.-P. Flament. A two-step uncontracted determinantal effective Hamiltonian-based SO–CI method. *The Journal of Chemical Physics*, 113(4):1391–1402, 2000.

[72] E. van Lenthe, E. J. Baerends, and J. G. Snijders. Relativistic regular two-component Hamiltonians. *The Journal of Chemical Physics*, 99(6):4597, sep 1993.

[73] E. van Lenthe and E. Jan Baerends. Density functional calculations of nuclear quadrupole coupling constants in the zero-order regular approximation for relativistic effects. *The Journal of Chemical Physics*, 112(19):8279–8292, 2000.

[74] L. Visscher. Approximate molecular relativistic Dirac-Coulomb calculations using a simple Coulombic correction. *Theoretical Chemistry Accounts*, 98(2-3):68–70, 1997.

[75] L. Visscher. The Dirac equation in quantum chemistry: strategies to overcome the current computational problems. *Journal of computational chemistry*, 23(8):759–66, June 2002.

[76] L. Visscher, P. J. C. Aerts, O. Visser, and W. C. Nieuwpoort. Kinetic balance in contracted basis sets for relativistic calculations. *International Journal of Quantum Chemistry*, 40(S25):131–139, 1991.

[77] L. Visscher and K. Dyall. Relativistic and correlation effects on molecular properties. I. The dihalogens F_2, Cl_2, Br_2, I_2, and At_2. *The Journal of chemical physics*, 104(22):9040–9046, 1996.

[78] L. Visscher, K. G. Dyall, and T. J. Lee. Kramers-restricted closed-shellCCSD theory. *International Journal of Quantum Chemistry*, 56(S29):411–419, feb 1995.

[79] L. Visscher, T. Enevoldsen, T. Saue, and J. Oddershede. Molecular relativistic calculations of the electric field gradients at the nuclei in the hydrogen halides. *The Journal of Chemical Physics*, 109(22):9677, 1998.

[80] L. Visscher, T. J. Lee, and K. G. Dyall. Formulation and implementation of a relativistic unrestricted coupled-cluster method including noniterative connected triples. *The Journal of Chemical Physics*, 105(19):8769, nov 1996.

[81] L. Visscher and T. Saue. Approximate relativistic electronic structure methods based on the quaternion modified Dirac equation. *The Journal of Chemical Physics*, 113(10):3996, sep 2000.

[82] L. Visscher, T. Saue, W. C. Nieuwpoort, K. Faegri, and O. Gropen. The electronic structure of the PtH molecule: Fully relativistic configuration interaction calculations of the ground and excited states. *The Journal of Chemical Physics*, 99(9):6704, nov 1993.

[83] L. Visscher, O. Visser, P. Aerts, H. Merenga, and W. Nieuwpoort. Relativistic quantum chemistry: the MOLFDIR program package. *Computer Physics Communications*, 81(1-2):120–144, jun 1994.

[84] F. Wang, J. Gauss, and C. van Wüllen. Closed-shell coupled-cluster theory with spin-orbit coupling. *The Journal of Chemical Physics*, 129(6):064113, 2008.

[85] S. White. Density matrix formulation for quantum renormalization groups. *Physical review letters*, 69(19):2863–2866, nov 1992.

[86] C. S. Wood. Measurement of Parity Nonconservation and an Anapole Moment in Cesium. *Science*, 275(5307):1759–1763, mar 1997.

[87] T. Yanai, T. Nakajima, Y. Ishikawa, and K. Hirao. A highly efficient algorithm for electron repulsion integrals over relativistic four-component Gaussian-type spinors. *The Journal of Chemical Physics*, 116(23):10122, may 2002.